MECHANISMS OF SENSITIZATION TO CHEMOTHERAPY IN NON-SMALL CELL LUNG CANCER

APPROVED BY SUPERVISORY COMMITTEE

John D. Minna, M.D. (Mentor)

Jef DeBrabander, Ph.D. (Chair)

Melanie Cobb, Ph.D.

Michael A. White, Ph.D.

DEDICATION

For Martha, Charles C., James, Wanda, Michelle, James Jr, Charles T., and Manwe.

MECHANISMS OF SENSITIZATION TO CHEMOTHERAPY IN NON-SMALL CELL LUNG CANCER

by

RACHEL MARIE GREER

DISSERTATION

Presented to the Faculty of the Graduate School of Biomedical Sciences

The University of Texas Southwestern Medical Center at Dallas

In Partial Fulfillment of the Requirements

For the Degree of

DOCTOR OF PHILOSOPHY

The University of Texas Southwestern Medical Center at Dallas

Dallas, Texas

November, 2011

ACKNOWLEDGEMENTS

For me to get this point in my scientific career has taken considerable time and a large amount of effort on the part of many individuals, who I will now attempt to thank. Without the endless support and encouragement from my mentor, John Minna, I would have never made it this far. I am grateful for the mentorship he has given me during my time in graduate school. I would also like to thank Dr. Adi Gazdar, one of Dr. Minna's long time collaborators, who has given me endless advice and support during my time in graduate school.

I am most grateful for the time and effort my committee members, Dr. Jef de Brabander, Dr. Michael White, and Dr. Melanie Cobb have put into my project and growth as a scientist. I could always count on lively discussions when we would meet.

Then there are all of the members of the Minna Lab both past and present without whom these works would have been infinitely harder to accomplish. Dr. Michael Peyton has always given me help when I asked for it, and was very helpful throughout my SMAC mimetic project. Dr. David Shames, who obtained his PhD under the mentorship of Dr. Minna during my early years in the lab has been both a big brother and mentor for me both while he was in the Minna Lab and since his departure. Drs. Di Cai and James Sullivan were both my classmates who joined the Minna Lab with me and graduated before me, they were great companions on the journey through graduate school. Dr. Jill Larsen has been

immensely helpful since her arrival in the Minna lab and has managed to keep me smiling through some of the roughest times. My time in graduate school would have been drastically different if it were not for my bay-mate and partner in science Robin Frink, there aren't enough words to express my how much I appreciate her friendship and help.

I sincerely thank Dr. Xiaodong Wang, who was my committee chair until he left UTSW, Dr. Rolf Brekken, and Dr. Lai Wang for their help and discussions about the manuscript they helped me to produce. My collaborators have been so good to me, giving me ideas and suggestions of where to take a given project next.

I also need to thank my family and friends that have supported me through thick and thin. My parents James and Wanda Greer always made me believe that I could do anything I put my mind to. My sister Michelle, and brothers James and Charles helped to keep me motivated. Mike Dodge, one of my classmates has been my friend throughout my time at UTSW even after he switched from the Minna lab to the Lum lab, and was my partner in crime when we went rafting on the north campus creeks, first for passing quals, and then for finishing our dissertations. All of those tough days in the lab were balanced out by going home to the adoring faces of my dogs Manwë and Aston and my sister's dog Penfold.

Finally these works were done in the memory of Martha Rowe, my grandmother who passed away in 1997 from metastatic lung cancer. And this

dissertation inspired by my grandfather Charles C Rowe, who like me, struggled with dyslexia all of his life, but always believed that I would not be hindered by it. I'm not sure if he ever knew just how much that meant to me.

MECHANISMS OF SENSITIZATION TO CHEMOTHERAPY IN NON-SMALL CELL LUNG CANCER

RACHEL MARIE GREER, Ph.D.

The University of Texas Southwestern Medical Center at Dallas, 2011

JOHN D. MINNA, M.D.

Lung cancer is the leading cause of cancer-related deaths world-wide for men and women, due in part to late detection of disease and inherent resistance to treatment. This body of work focuses on resistance to treatment, specifically chemotherapy and understanding ways to sensitize non-small cell lung cancers to existing chemotherapies. Using a large panel of non-small cell lung cancers, response to common platinum-based doublet chemotherapy was tested, and compared in a statistical fashion to each chemotherapy as a single agent, to understand the breadth of responses, and have a baseline of response to improve

upon. The rest of this work endeavors to make chemotherapies more effective at tumor kill by targeting tumor specific alterations. One such targeted approach focused on miR337, and its ability to influence paclitaxel sensitivity through introduction of miR337 mimics and antagomiRs was evaluated using MTS based assays; increasing miR337 levels in moderately paclitaxel-sensitive or completely paclitaxel resistant cells sensitized the cells at least ten-fold to paclitaxel. Non-small cell lung cancers have frequent mutations in p53 (>80%). Targeting of the p53 promoter region with agRNAs, in p53-mutant containing cell lines induces cytotoxicity that is reminiscent of wild type p53 activity and is associated with large increases of the non-coding RNA lincRNAp21, and can cause large sensitizations to p53-dependent chemotherapies such as doxorubicin, indicating that these agRNAp53s could be of therapeutic importance in p53-mutant lung cancers. Re-engagement of the apoptotic pathway by a small molecule (JP1201) sensitizes non-small cell lung cancers to a variety of chemotherapies. Anti-mitotic chemotherapies have the most frequent sensitization across a large panel of non-small cell lung cancers, and the largest degree of sensitization by combination with JP1201, and this sensitization is dependent on activation of the ER stress pathway. Xenograft models using cell lines recapitulate the ability of JP1201 to sensitize non-small cell lung cancers to chemotherapy, indicating that combinations with JP1201 might be effective in patients.

TABLE OF CONTENTS

PRIOR PUBLICATIONS

Dineen S.P., Roland C.L., **Greer R.**, Carbon J.G., Toombs J.E., Gupta P., Bardeesy N., Sun H., Williams N., Minna J.D., and Rolf A. Brekken (2010). Smac Mimetic Increases Chemotherapy Response and Improves Survival in Mice with Pancreatic Cancer. *Cancer Research* 70, 2852-61.

Greer, R.M., Peyton, M., Larsen, J.E., Girard, L., Xie, Y., Gazdar, A.F., Harran, P., Wang, L., Brekken, R.A., Wang, X., and John D. Minna (2011). SMAC mimetic (JP1201) sensitizes non-small cell lung cancers to multiple chemotherapy agents in an IAP dependent but TNFα independent manner. *Cancer Research* (In Press)

LIST OF FIGURES

LIST OF TABLES

LIST OF APPENDICES

LIST OF DEFINITIONS

Abl	Abelson murine leukemia viral oncogene homolog
AC	Adenocarcinoma
agRNA	anti-gene ribonucleic acid
ALK	Anaplastic lymphoma kinase
ALL	Acute Lymphocytic Leukemia
AML	Acute Myeloid Leukemia
ANOVA	Analysis of variance
APAF	Apoptotic protease activating factor 1
ASK1	Apoptosis signaling kinase
ATCC	American Type Culture Collection
AUC	area under the curve
AVPF	alanine-valine-proline-phenylalalnine
BAD	BCL2-associated agonist of cell death
BAK	BCL2 antagonist/killer 1
BAX	BCL2-associated X protein
BCL2	B-cell lymphoma 2
BCL-XL	B-cell lymphoma extra large
BCR	Breakpoint cluster region
BH3	BCL2 homology domain 3
BID	BH3 interacting death domain agonist

BIM	BCL2-interacting mediator
BIR	Baculovirus inhibitor of apoptosis protein repeat
C. elegans	*Caenorhabditis elegans*, nematode
CDKN1A	Cyclin depdendent kinase inhibitor 1A (p21)
cDNA	complementary deoxyribonucleic acid
CI	Combination Index
cIAP1	cellular inhibitor of apoptosis 1
cIAP2	cellular inhibitor of apoptosis 2
CT	X-ray computed tomography
CTP	cytadine triphosphate
DBD	deoxyribonucleic acid binding domain
DBTSS	database of transcription start sites
DISC	death inducing signaling complex
DMSO	dimethyl sulfoxide
DNA	deoxyribonucleic acid
EGFR	epidermal growth factor receptor
ELISA	enzyme-linked immunosorbent assay
EML4	Echinoderm microtubule-associated protein-like 4
ER	endoplasmic reticulum
ERK	extracellular signal-regulated kinase
ETS	environmental tobacco smoke

FACS	fluorescent-activated cell sorting
FADD	Fas-associated death domain
FBS	fetal bovine serum
FDA	Food and Drug Administration
FDG-PET	fludeoxyglucose-positron emission tomography
FITC	fluorescein isothiocyanate
G12V	glycine to valine mutation at residue 12
GAPDH	glyceraldehyde 3-phosphate dehydrogenase
GDP	guanosine diphosphate
GI	gastrointestinal
GTP	guanosine triphosphate
GTPase	family of hydrolase enzymes that can bind to GTP and catalyze its conversion to GDP
HBEC	Human bronchial epithelial cell
HSP90	heat shock protein 90
hTERT	Human telomerase enzyme
IACUC	Institutional Animal Care and Use Committees
IAP	inhibitor of apoptosis protein
IC_{50}	inhibitory concentration that kills 50% of the population
ICAD	inhibitor of caspase activated DNase
IRB	Internal Review Board

IRE1	inositol requiring enzyme 1
JNK	c-Jun N-terminal kinase
KSFM	keratinocyte serum free media
LCC	large cell carcinoma
lincRNA	long non-coding ribonucleic acids
LKB1/STK11	liver kinase b1 also known as serine/threonine-protein kinase 11
LOH	loss of heterozygosity
MDM2	murine double minute oncogene
miRNA	micro-ribonucleic acid
mRNA	messenger-ribonucleic acid
MTS	3-(4,5-dimethylthiazol-2-yl)-5-(3-carboxymethoxyphenyl)-2-(4-sulfophenyl)-2H-tetrazolium, inner salt
NF-κB	nuclear factor kappa-light-chain-enhancer of activated B-cells
NOD/SCID	non-obese diabetic/severe combined immunodeficient mouse
Noxa	Latin for “an injury” BH3 only pro-apoptotic protein
NSAID	non-steroidal anti-inflammatory drug
NSCLC	non-small cell lung cancer
PAGE	poly-acrylamide gel electrophoresis

PARP	poly-ADP ribose polymerase
PDGFR	platelet-derived growth factor receptor
pri-miRNA	completely un-processed precursor miRNA directly transcribed from DNA
PUMA	p53 upregulated modulator of apoptosis
qPCR	quantitative polymerase chain reaction
Ras	homologue of Rat-sarcoma viral protein, small GTPase
Rb	retinoblastoma gene/protein
RIPK1	receptor interacting protein kinase 1
RISC	RNA-induced silencing complex
RNAi	RNA interference
RPMI	Roswell park memorial institute medium
SCC	squamous cell carcinoma
SCLC	small cell lung cancer
SDS	sodium dodecyl-sulfate
SEM	standard error of the mean
shRNA	short hairpin-RNA
siRNA	small-interfering RNA
SMAC	second mitochondrial-derived activator of caspases
SPARC	secreted protein acidic and rich in cysteine
TGFb	transforming growth factor beta

TKI	tyrosine kinase inhibitor
TNF	tumor necrosis factor
TNFR	tumor necrosis factor receptor
TNFSFL	tumor necrosis factor super family of ligands
TNM	tumor, node, metastasis classification of malignant tumors
TP53	tumor protein 53 kilodaltons
TP63	tumor protein 63 kilodaltons
TP73	tumor protein 73 kilodaltons
TRADD	TNF receptor associated death domain
TRAF	TNF receptor associated factor
TRAIL	TNF-associated apoptosis inducing ligand
TSS	transcription start site
TUNEL	terminal deoxynucleotidyl transferase dUTP nick end labeling
UPR	unfolded protein response
UTSW	University of Texas Southwestern Medical Center
VEGF	vascular endothelial growth factor
VEGFR	vascular endothelial growth factor receptor
VIM	vimentin
WRAP53	WD repeat containing, antisense to *TP53*
XIAP	X-linked inhibitor of apoptosis protein

CHAPTER ONE

INTRODUCTION

1.1 CANCER

Contrary to popular belief, cancer has been a problem facing humans since antiquity. The first descriptions of cancer are from ancient Egypt, where women had growths in their breasts which ultimately was a death sentence for these women (Diamandopoulus, 1996). Hippocrates termed malignant tumors carcinos, Greek for crab or crayfish, owing to the appearance of the cut surface of a solid tumor with the veins stretched out on all sides as the crab has its feet (Karpozilos & Pavlidis, 2004). He later added the Greek suffix –oma for swelling giving rise to the term carcinoma, which is now used to describe cancers arising from epithelial cell origin (Karpozilos & Pavlidis, 2004).

The history of cancer treatments is also very ancient. Tales of treatments of breast cancer in Ancient Egypt with a tool called a fire drill, used to cauterize the ulcerated tumors abound. Hippocrates was well known for treating ailments according to the four humors (yellow bile, black bile, phlegm, blood), and cancer treatment was no different, depending on the humor of the patient, treatment consisted of diet, bloodletting, laxatives, and or plasters (Diamandopoulus, 1996; Karpozilos & Pavlidis, 2004). Actually, this type of treatment for cancers was very popular until the discovery of cells.

Cancer remains a large problem, despite it affecting individuals for many centuries, one out of two men, and one out of three women in the US will be diagnosed with cancer in their lifetime. In fact, cancer is the number one cause of death in people under 85 years of age, and in people over 85 cancer is only second to heart disease in cause of death (Siegel, Ward, Brawley, & Jemal, 2011).

There are many different terms used to describe cancers, such as malignant neoplasm, or tumor. Tumors are given specific names that are descriptive in a clinical or pathological fashion. Sarcomas are tumors that arise from mesenchymal tissues. Carcinoma is a term given to tumors arising from epithelial cell origin, with the exception of melanomas. An adenocarcinoma is a tumor of epithelia cell origin that has features resembling glands or ducts, while a squamous cell carcinoma is a tumor of epithelial cell origin that resembles differentiated squamous cell type. Lymphomas are tumors arising in the lymph system, usually in lymph nodes.

Leukemias are tumors that arise in blood precursor cells in bone marrow, there are two cell types that give rise to leukemias, lymphocytic or myeloid cells. Lymphocytes are a granular white blood cells, typically NK cells, T cells, B cells, and common precursor cells. Granular white blood cells; eosinophils, basophils, neutrophils, macrophages, dendritic cells; red blood cells, and platelets make up the cell types covered in the myeloid classification. Typically myeloblastic leukemias are characterized by accumulation of abnormal granulocytes in either

the blood or bone marrow. Most patients with CML (chronic mylogenous leukemia) have a (9;22) translocation with fusion of the Bcr and Abl genes which is often called the Philadelphia Chromosome. One of the great success stories of targeted therapy is CML with (9;22) translocation being treated with imatinib which can inhibit the progression of CML and in some patients lead to regrowth of normal bone marrow (Beran et al., 1998). CML is now treated with three different targeted therapies that all target the BCR-ABL fusion, imatinib, dasatinib, and nilotinib (Kimura, Ashihara, & Maekawa, 2010).

1.2 Lung Cancer

Lung cancer is the leading cause of cancer related deaths, with over 200,000 deaths in 2009 (Ahmedin, Rebecca, Jiaquan, & Elizabeth, 2010), lung cancer is the second most commonly diagnosed cancer in both men and women (Figure 1.1). The overall life time risk for being diagnosed with lung cancer in the United States is 1 out of 13 men will be diagnosed, and 1 in 16 women will be diagnosed in their lifetime with lung cancer (Ahmedin, et al., 2010; Jemal et al., 2009; Siegel, et al., 2011).

Smoking is a well-known factor associated with lung cancer development, because of this there have been many campaigns to warn the public of the harmful effects of smoking (Cardenas et al., 1997). With the decline in smoking due to these campaigns, there has been a decline in the incidence rate in men, there is still an increase in the incidence rate of women (Cardenas, et al., 1997; Pao et al.,

2004; Rudin et al., 2009; S. Sun, Schiller, & Gazdar, 2007). There is no clear reason as to the increase in incidence in women; however, some possible causes will be discussed in the next section. Despite advances in both detection and treatment of cancer, the 5-year survival rate of lung cancer remains near 15% of those diagnosed with the disease (Siegel, et al., 2011). This cause of this low survival rate can be attributed to at least two causes; late detection, and resistance to treatment.

One of the problems in detecting lung cancer at an early stage is there are no early screening procedures like there are for breast and prostate cancer; however, the National Lung Cancer Screening Trial has recently found that in a population of current and former heavy smokers that using low dose spiral CT as a screening technique results in a 20% decrease in lung cancer mortality from when the trial began in 2002 as compared to current and former heavy smokers that were screened with chest x-ray alone (Team). While this trial is promising, there are many factors that should be considered when evaluating this study, firstly is the large increase in false positive findings with CT screening, the less sophisticated CTs used on the trial than are routinely used across the country, this will likely result in a further increase in false positive rate with CT screening. Additionally, the trial only used three CT measurements in the study, but if people are routinely screened with CT every year, or two years or however often it is decided to do this, the long term effects of chronic exposure to X-rays on cancer

development is not known at this time. Additionally, who should be screened regularly was not addressed by this study. The NLCST only screened individuals that had smoked at least 30-pack years within the last fifteen years without a previous lung cancer diagnosis, so only high-risk patients were being screened. The utility of CT screening across non-smokers is not addressed even though never smokers account for at least 20% of lung cancer cases per year (S. Sun, et al., 2007).

1.2.1 ETIOLOGY

Smoking is one of the best characterized risk factors for developing lung cancer. In fact 85% of lung cancer in men world wide and 47% of cases of lung cancer in women is attributable to smoking (Parkin, Bray, Ferlay, & Pisani, 2005). Smoking increases the risk of developing lung cancer by 10-20 fold (Parkin, et al., 2005). Studies done by the Environmental Protection Agency and others have shown that environmental tobacco smoke (ETS) accounts for roughly 3,000 lung cancer deaths per year in the US, and increases risk of developing lung cancer by 20-25% (Cardenas, et al., 1997). However, most lung cancers that are not directly attributable to smoking cannot be explained by ETS alone. The other known risk factors for lung cancer include radioactive radon, cooking oil vapors, indoor coal and wood burning, genetic factors (Table 1.1), asbestos, and viral factors (S. Sun, et al., 2007). Other factors such as chromium, arsenic, cadmium,

silica, nickel, outdoor air pollutants, previous lung disease, and dietary factors have also been implicated in increasing risk of lung cancer (S. Sun, et al., 2007). Epidemiological studies from China, Taiwan, and Singapore have shown that cooking oil fumes, especially in the absence of fume extractors is significantly associated with increased risk of lung cancer in female never-smokers (S. Sun, et al., 2007).

1.2.2 PATHOLOGY

Lung cancer develops in the epithelium of the respiratory system, including bronchi, bronchioles, all the way to alveoli, which is distinct from mesotheliomas and sarcomas (stromal tumors). There are four major histological classes of lung cancer; however, lung cancer is usually broken into two classes, small cell lung cancer (SCLC) and non-small cell lung cancer (NSCLC). SCLC is mainly associated with smoking, and it is characterized by small tumor cells that express neuroendocrine markers. NSCLC is a group of all the other kinds of lung cancer that cannot be classified as SCLC. There are at least three histologically distinct cancers within NSCLC, squamous cell carcinomas (SCC), adenocarcinomas (AC), and large cell carcinomas (LCC). Tumors that cannot be definitively identified as one particular type of NSCLC are generally called poorly differentiated, undifferentiated, or just NSCLC. It has recently been realized that not only are these histologically distinct tumors, but they respond

differently to different treatment regimens (Triano, Deshpande, & Gettinger, 2010).

SCLC and SCC tend to occur in the central airways of the lung, while ACs tend to occur in the peripheral lung (S. Sun, et al., 2007). While all histological types of lung cancer are associated with smoking, the strongest associations are for SCLC or SCC. Adenocarcinomas are the prevalent form of lung cancer in never smokers. A rare global trend has been seen in lung cancer histological patterns in the recent history, with AC increasing while SCC has been decreasing. It has been postulated that this trend is due to the majority of cigarettes having a lower tar and nicotine content than was found in cigarettes of the past (S. Sun, et al., 2007). In theory smokers then compensate for the reduced nicotine by consuming more cigarettes, resulting in changes in the anatomic location and histological type of lung cancer. It has been shown in rodents that a nicotine-derived carcinogen, NKK, readily induces KRAS mutation-associated adenocarcinomas, which supports the theory that changes in cigarettes leading to changes in smoking behavior (Hecht, 1999).

1.2.3 Tumor Staging

One important prognostic factor in cancer is the tumor stage at diagnosis. Tumor stage takes into account three factors, the size of the primary tumor, the extent to which lymph nodes are involved, and if the tumor has spawned distant metastases, and follows modified TNM classifications (Table 1.2) (Greene, 2004;

Ihde & Minna, 1991a). When determining the stage of a non-small cell lung cancer (NSCLC) patient history, physical examination, routine laboratory evaluations, chest x-ray, and chest computed tomography scan with contrast media, are used. The added utility of FDF-PET in stage determination is being explored in clinical trials (Sieren, Ohno, Koyama, Sugimura, & McLennan, 2010). Once the existence of a primary tumor has been established, further methods such as bronchoscopy, bronchial biopsy, medianoscopy for node biopsy, or fine needle aspiration guided by CT scan are used to obtain nodal samples for determining nodal involvement. Using all of these data, the tumor is then staged between stage 0 and stage IV (Table 1.2) which then helps determine the course of treatment. For SCLC a simple two stage system has been used; limited stage disease when the tumor is limited to one hemi thorax and regional lymph nodes, or extensive stage disease when the tumor is found beyond these boundaries.

1.2.4 TREATMENT

Treatments are generally based upon the staging criteria. Stage 0 is carcinoma in situ for which the suggested treatment options include surgical resection, or other endobronchial therapies. Stage I lung cancer is optimally treated with surgical resection of the primary lesion alone (Ihde & Minna, 1991b). There have been three large randomized studies exploring the possibilities for benefit of adjuvant chemotherapy in early stage lung cancer (stage I – IIB), the summary of all three studies shows that there is no benefit to patients with stage

IA tumors, and marginal benefit (2-3%) for patients with stage IB tumors due to limited risk of recurrence (Non-small Cell Lung Cancer Collaborative, 1995), for inoperable or where patients refused surgery with stage I disease, radiation with curative intent, clinical trials involving adjuvant chemotherapy, or endobronchial therapies are suggested as alternative treatment options. Stage II disease is still considered early stage lung cancer and as such the primary suggested therapy is surgery or surgery with adjuvant chemotherapy, curative radiotherapy, or experimental therapy in the setting of a clinical trial. Patients with surgically resectable stage IIIA disease are most often treated with surgery and adjuvant chemotherapy or can participate in clinical trials for which they are eligible. In some cases pre-operative chemotherapy may be used to make the tumor smaller for more effective surgical outcomes. In stage IIIA patients where surgery is not suggested and patients with stage IIIB disease, chemoradiation, radiation therapy, or enrollment into available clinical trials are the treatments used. Forty percent of newly diagnosed NSCLC patients present with stage IV disease, most of these patients will not benefit from surgery; instead chemotherapy, chemoradiation therapy, radiation therapy, or available clinical trials are the preferred treatment regimens for these patients.

1.2.5 Molecular oncogenic changes in Lung Cancer

Mutations leading to cancer tend to occur in two gene types, proto-oncogenes and tumor suppressor genes. Proto-oncogenes are genes which when activated, by point mutations, over expression, or chromosomal translocation that results in deregulation of activation or localization, lead to cancer formation. Some of the most famous oncogenes are Ras, Myc, EGFR, BCR-ABL, and the HPV encoded proteins E6/E7. Tumor suppressor genes are genes which act to control the development of cancer, these genes can directly regulate an oncogene, i.e. PTEN negatively regulates PI3K, are involved in DNA repair mechanisms, i.e. BRCA1, regulate the cell cycle, i.e. Rb or p53. p53, Kras, STK11/LKB1, and EGFR are some of the most commonly mutated genes in NSCLC (Figure 1.3) (Ding et al., 2008). Most TSG follow the two hit hypothesis in which both alleles of the gene must be inactivated whether by methylation, LOH coupled to inactivating mutation, or homozygous deletions. However, not all mutations that occur in cancer are necessary for the formation of cancer as will be discussed in the following section on Ras because sometimes Kras mutations are driver mutations and other times just passenger mutations. More detailed information follows for some of the most prevalent mutations found in lung cancer with emphasis for mutations that affect treatment either positively or negatively.

1.2.5.1 *TP53*

TP53 is the single most commonly mutated gene in human cancers, 50% of all cancers, and as such it is most likely the most heavily studied tumor

suppressor gene (Mitsudomi, Steinberg, et al., 1992). In lung cancer p53 is mutated in around 80% of tumors. *TP53* encodes a basally transcribed inducible transcription factor. Many types of cellular stresses are known to activate p53, such as irradiation, hypoxia, oxidative stress, osmotic shock, oncogene activation, and an array of chemotherapeutic agents. Upon activation, which consists of stabilization, post-translational modification, and binding to p53 response elements within the genome, p53 can activate apoptosis, senescence, or reversible cell cycle arrest by activating genes, such as CDKN1A, or repressing genes, such as VIM, gene transcription (Table 1.3). The majority of mutations in *TP53* occur within the DNA binding domain (DBD), which can then be divided into two groups; those that affect direct interaction of p53 with DNA, or those that affect tertiary structure (Weisz, Oren, & Rotter, 2007). Mutations in p53 not only result in the loss of wild type p53 transcriptional activity, dominant negative effects on wild type p53, but also gain of function activity that is through inhibition of p63 and p73 (Dittmer et al., 1993; Strano et al., 2007).

p53 also activates MDM2 which is responsible for keeping p53 levels low by promoting degradation of p53 by ubiquitination (Fesik, 2005). The regulation of p53 is very complex, and occurs at many levels. *TP53* is located on chromosome 17p13.1 and shares exon 1 with that of another gene, WRAP53, that is transcribed from the opposite strand (Mahmoudi et al., 2009). WRAP53 RNA binds to p53 mRNA and stabilizes the mRNA, which provides another layer of

control, not to mention the large promoter region and long list of transcription factors that have been found bound to the promoter of *TP53* (Table 1.4). In addition to ubiquitination, p53 can be acetylated or phosphorylated as well which can modulate both transcriptional and non-transcription activities of p53 (Van Dyke, 2007). Frequent LOH of 17p13 accompanied by point mutation of the other allele of p53 combined with the paucity of homozygous deletions of p53 when compared to other tumor suppressors suggests that mutations in p53 provides a dominant oncogenic activity that is important during tumorigenesis (Weisz, et al., 2007). Mutations in p53 not only lead to decreased ability to activate target genes, but also interferes with proper p63 and p73 signaling (S. W. Lowe, Cepero, & Evan, 2004). Mutant p53 also has gain of function activity and was initially thought to be an oncogene instead of tumor suppressor.

In addition to uncoupling DNA damage from the cell cycle, mutations in p53 confer cancer cells with resistance to some chemotherapy because p53 can directly activate apoptosis through transcriptional activation of NOXA and PUMA as discussed in 1.4.3.

1.2.5.2 RAS

The RAS proto-oncogene family includes Kras, Nras, and Hras, which encode membrane bound small GTPases involved in signaling cascades controlling diverse cellular processes (Bos, 1989). Ras exists in two forms, inactive which is characterized by Ras being bound to GDP, or active which is

characterized by binding to GTP; mutations in codons 12, 13, 59, or 61 abolishes the ability of Ras to bind GTP/GDP but also leads to intrinsic activation of Ras and thus oncogenic potential (Bos, 1989; Mitsudomi, Oyama, et al., 1992; Wennerberg, Rossman, & Der, 2005). The best characterized (and well known) Ras pathway is activation of Ras downstream of EGFR, which leads to recruitment and activation of Raf and thereby activating the ERK1/2 kinase cascade (Wennerberg, et al., 2005). Mutations in Ras gives cancer cells a growth advantage in that they no longer require growth signals such as EGF binding to EGFR to cause activation of the ERK kinase cascade, other downstream genes such as Braf can acquire mutations in place of Ras, as a result Ras and Raf mutations are mutually exclusive (Brose et al., 2002; Gandhi et al., 2009; Suzuki et al., 2006; Tam et al., 2006). If mutant Kras is expressed in normal immortalized HBECs it causes senescence in these cells, most likely through a p53 dependent mechanism; however, if p53 is first knocked down or neutralized by overexpression of mutant p53 then mutant Kras can be successful expressed in HBECs and confers a growth advantage to them (Sato et al., 2006).

Mutations in Ras not only remove the dependence of GTP for Ras signaling, but they also preclude the GTP binding pocket from being targeted by small molecules to inhibit mutant Ras signaling, as a result, a targeted therapeutic approach to mutant Ras tumors has as of yet been unsuccessful.

1.2.5.3 CDKN2A

The CDKN2A locus encodes three different tumor suppressor proteins, p16, p14, and p15. While these proteins are encoded by the same gene, alternative splicing results in proteins with very different functions. Both p16 and p15 act as cell cycle regulators by inhibiting activity of CDK4 which prohibits progression into S phase. p14ARF however acts to stabilize p53 by interacting with both p53 and MDM2 and preventing degradation of p53 via the ubiquitin proteolysis pathway. The CDKN2A locus is often hypermethylated in NSCLC (Minna, Fong, Zochbauer-Muller, & Gazdar, 2002; Sato, et al., 2006; Toyooka et al., 2003).

1.2.5.4 STK11/LKB1

Serine/Threonine kinase 11 (STK11) which is also referred to as liver kinase B (LKB1) is a very frequent mutation in NSCLC (~10%). STK11 activates by phosphorylation a number of targets such as adenine monophosphate-activated protein kinase (AMPK). Not only does STK11 exert its tumor suppressive role by suppressing growth and proliferation while energy stores are low, but also regulating polarity of the cell (Gao, Ge, & Ji, 2011).

1.2.5.5 EGFR

In the early part of the last decade mutations in EGFR were shown to be important not only in terms of response to treatment but also in defining a subtype of NSCLC, female never-smokers (Amann et al., 2005). EGFR is the receptor for epidermal growth factor (EGF), that is part of a normal kinase cascade that

includes Ras, Raf, and ERK, for this reason, mutations in EGFR, Ras, and Raf are all mutually exclusive, as it gives a cell no growth advantage to have multiple members of the same pathway mutated. EGFR is also a member, the founding member, of the ErbB receptors which also includes Her2/ErbB2, Her3/ErbB3, and Her4/ErbB4. Her2 is well known for being involved in breast cancer, and breast tumors with high Her2 levels are identified from initial biopsy and these patients then receive anti-Her2 therapy (trastuzamab, see section 1.5.4.2). There is increasing evidence that Her2, which has a non-functional ligand binding domain so, must heterodimerize with another ErbB family member, dimerizes with EGFR, and can provide EGFR-TKI mediated resistance.

1.2.5.6 PTEN

Another pathway that is often activated downstream of growth factor receptors such as EGFR is the PI3K pathway, and PTEN is a negative regulator of said pathway. PTEN mutations are quite common as well in lung cancer (Forgacs et al., 1998). Activating mutations are also found in lung cancers, suggesting that activation of the PI3K either by activating mutations or by loss of PTEN are oncogenic, and PI3K inhibitors are being developed.

1.3 HALLMARKS OF CANCER

Hanahan and Weinberg classify the major alterations that differentiate cancer cells from normal cells by the ten hallmarks of cancer (Figure 1.4) (Hanahan & Weinberg, 2011). The first hallmark discovered by cancer

researchers was that cancer cells no longer rely on supply of growth signals from other tissues, cancer cells were able to secrete the growth signals that were necessary for them to continue to grow. Cancer cells also become insensitive to antigrowth signals, these can be both secreted signals, such as TGFβ, or signals embedded within the surrounding stroma, such as SPARC. Antigrowth signals usually affect cells within the G1 phase, and as such the pathways that regulate insensitivity to antigrowth signals are involved in the cell cycle. Tumor suppressor genes such as Rb or $p15^{INK4B}$ are inactivated to allow for this insensitivity. Consequently these mutations as well as others, such as expression of hTERT that is normally not expressed except in stem cell populations, confer upon cancers the ability to have limitless replicative potential. Additionally, in order to keep up with the high metabolic needs of tumors which have the ability to grow indefinitely, cancers also develop the ability to recruit nearby blood vessels to sprout new growth of smaller blood vessels to the tumor in a process known as angiogenesis, additionally cancer cells have deregulated cellular energetics usually by increased glycolysis and decreased mitochondrial function often referred to the Warburg effect (Warburg, 1956). An effect of limitless growth potential is that eventually the tumors overgrow the space they originated in, which leads to invasion of normal tissues, and eventually metastasis. And the final hallmark of cancer is the evasion of apoptosis.

Cancers have developed multiple strategies for evading apoptosis, primarily by over expression of the various anti-apoptotic proteins that have been previously described. Over expression of BCL-2 and BCL_{XL} makes it much less probably that the mitochondria will release the pro-apoptotic proteins that have become sequestered by high BCL-2 levels. Cancer also over express many of the IAP family members including (but not limited to) XIAP, cIAP1, cIAP2, and survivin (Nachmias, Ashhab, & Ben-Yehuda, 2004; Richter & Duckett, 2000; Salvesen & Duckett, 2002; Srinivasula & Ashwell, 2008; Y. Wei, Fan, & Yu, 2008). XIAP inhibits apoptosis most directly through its regulation of caspase activity. cIAP1 and 2 are also known to localize to the TNFR and promote the pro-survival signaling and inhibit pro-apoptotic signaling through the TNFR (Kuai et al., 2003; Samuel et al., 2006; Wang, Mayo, Korneluk, Goeddel, & Baldwin, 1998). Survivin is probably the most studied member of the IAP family; however, its role in binding caspases is completely unknown. Survivin does have a clear role in mitosis, and in cancer has been shown to allow cells to pass through mitosis that would normally trigger cell cycle checkpoints.

Cancers also avoid apoptosis through less direct means. *TP53* is the most commonly mutated gene across all cancers because of its key role as a central hub for sensing damage to the genome. Mutations in *TP53* that affect the DNA binding domain of p53, alter the ability of p53 to activate downstream targets

which includes proteins such as NOXA and PUMA, which are members of the BH3 only proteins (S. Lowe & Lin, 2000).

1.4 APOPTOSIS

Apoptosis is an evolutionarily conserved process that was originally described by a series of distinct morphological events (Kerr, Wyllie, & Currie, 1972). Characteristic features of apoptosis include cell shrinkage, nuclear fragmentation, loss of membrane architecture, membrane blebbing, as well as changes in plasma membrane lipid composition(Figure 1.5) (Kerr, et al., 1972). Our understanding of the biochemical processes involved in apoptosis comes from genetic studies in *C. elegans*. During development of *C. elegans*, it is critical for excess cells to die, a mutation in a gene called *ced3* casuses accumulation of these excess cells in the adult animal, they also saw that *ced3* shared homology with human IL-1β converting enzyme (ICE) (Yuan, Shaham, Ledoux, Ellis, & Horvitz, 1993). These two proteins were the first to be discovered in a family of cysteine-dependent aspartate-directed proteases (caspases). The discovery of *ced3* as a caspase was critical in bringing the field of apoptosis into mainstream science. Currently there are twelve caspases in the human genome; however, not all are known to be involved in apoptosis (caspase-1, caspase-4, caspase-5, and caspase-11) (Yigong, 2004).

There are two classes of apoptogenic caspases, initiator caspases and effector/executioner caspases. Caspases are produced as inactive zymogens, and

most require processing for maximal enzymatic activity. Initiator caspases (caspase-2, -8, -9, and -10) rely on upstream signals for activation, which requires being a part of a large protein complex and auto proteolysis. Effector caspases (caspase-3, -6, and -7) require proteolytic cleavage by initiator caspases for maximal enzymatic activity, these caspases go on to cleave a number of proteins which facilitates the death of the cell such as PARP and ICAD (Figure 1.2).

Currently there are two well elucidated pathways that initiate apoptosis, the intrinsic and extrinsic pathways, and two less well understood pathways that are thought to initiate apoptosis, granzyme b initiated apoptosis and ER stress induced apoptosis.

1.4.2 Extrinsic Apoptotic Pathway

The extrinsic pathway or death receptor pathway is initiated when pro-death cytokines, the tumor necrosis factor super family ligands (TNFSFL) bind to their cognate receptors initiating a signaling cascade that results in caspase activation (Figure 1.3). Ligand binding occurs in a trimeric fashion, similarly for efficient receptor activation, the receptors also trimerize. In the case of FasL and TRAIL, ligand binding induces recruitment of fas-associated death domain (FADD). Recruitment of FADD induces recruitment of pro-caspase-8; these two proteins along with the receptor constitute the major components of the death inducing signaling complex (DISC). cFLIP can be a member of the DISC that acts in an inhibitory fashion, but is dispensable.

In the case of TNFα, again ligands bind in a trimeric fashion, and studies have shown that there is equilibrium of trimerization of un-bound receptor, binding of TNFα results in the greatest down-stream signaling when the receptors are trimerized before ligand binding. Studies have also shown that in some cell types these pre-assembled trimers of TNFR are localized to lipid rafts, and that this localization also enhances downstream signaling. Upon ligand binding, the adaptor molecule tumor necrosis factor receptor associated death domain protein (TRADD) is recruited to the receptor, which causes recruitment of tumor necrosis factor receptor associated factor, TRAF1 and TRAF2, and receptor interacting protein kinase 1 (RIPK1). TRAF2 interacts with and helps to localize cIAP1 and cIAP2 to the TNFR complex. TRAF2, cIAP1, and cIAP2 all have RING domains, which allow them to act as ubiquitin E3 ligases. RIPK1 becomes ubiquitinated which allows RIPK1 to serve as a scaffold for TAB and TAK1 leading to downstream JNK activation, and is also involved in NF-κB signaling by activation of NIK. If RIPK1 does not become ubiquitinated, then TRADD as well as RIPK1 are allowed to dissociate from the active receptor, and form a secondary complex with FADD and caspases-8 which can lead to downstream activation. Regulation of the ability of TRADD and RIPK1 to dissociate from the receptor is a key switch between TNFα pro-survival signaling and TNFα apoptotic signaling.

1.4.3 Intrinsic Apoptotic Pathway

The intrinsic pathway is regulated by the mitochondria of a cell (Figure 1.4). Inside of the mitochondria are many key factors that are involved in both energy production and death induction, such as cytochrome c. Cytochrome c is not only a component of the electron transport chain, but when released into the cytosol, it binds with APAF1, together these act as scaffolds for caspases-9 and all three components are known as the apoptosome, and leads to activation of downstream executioner caspases. Activation of mitochondrial apoptosis is regulated by a family of both pro- anti-apoptotic proteins named for the founding member, BCL-2. There is a fine balance between the pro-apoptotic and anti-apoptotic BCL-2 family members, and that balance regulates how a cell will respond to an intrinsic apoptogenic stress. Classification as a BCL-2 super family member relies on homology of BCL-2 homology (BH) domains. There are four distinct BH domains, BH1, BH2, BH3, and BH4. Anti-apoptotic BCL-2 family members (BCL-2, BCL_{XL}, BCL-W, A1, MCL-1) contain all four BH domains. The pro-apoptotic proteins BAX and BAK contain BH1-3, and the pro-apoptotic BH3 only family members (BAD, BID, BIM, NOXA, PUMA) only contain the BH3 domain (P. Li, Nijhawan, & Wang, 2004). BAX and BAK are required to initiate mitochondrial-induced apoptosis, and BCL-2, BCL_{XL} antagonize the ability of BAX and BAK to lead to mitochondrial release of cytochrome c as well as other pro-apoptotic proteins (M. C. Wei et al., 2001). The BH3 only proteins serve as upstream mediators of apoptosis, they sit and wait for a pro-apoptotic

signal, whether it's by cleavage (BID), phosphorylation (BAD), or transcriptional activation (PUMA and NOXA), and then they antagonize the ability of the anti-apoptotic BCL-2 family members to bind BAX and BAK. The second mitochondrial activator of caspases (SMAC) is the natural antagonist of IAP inhibition of caspases by binding to IAPs in a competitive fashion to caspases. SMAC is localized in mitochondria, within the inter membrane space, and is released along with cytochrome c when BAX and BAK signal for initiation of apoptosis to ensure that apoptosis occurs (Du, Fang, Li, Li, & Wang, 2000).

1.4.4 INHIBITORS OF APOPTOSIS

The inhibitor of apoptosis proteins (IAPs) are key players in the activation of apoptosis. IAPs are characterized by containing between one and three repeats of a zinc binding baculovirus IAP repeat (BIR) domains that bind to caspases, and are required for anti-apoptotic function. The human IAP family contains eight proteins, ML-IAP, ILP2, survivin, BRUCE, NIAP, cIAP1, cIAP2, and XIAP (Figure 1.5) (Nachmias, et al., 2004; Richter & Duckett, 2000; Salvesen & Duckett, 2002; Srinivasula & Ashwell, 2008). XIAP, cIAP1, cIAP2, and survivin have been studied the most out of this family. While survivin contains one BIR domain, its role in direct caspase inhibition is controversial; however, survivin does regulate mitosis by direct interaction with tubulin, and is up-regulated in many cancers (Danial & Korsmeyer, 2004; Salvesen & Duckett, 2002). X-chromosome encoded IAP (XIAP) binds to caspases-3 and -7 inhibiting each of

their catalytic activity through binding of BIR2 and the linker region between BIR1-BIR2 of XIAP to caspases-3 or -7 (Shi, 2004; Yuan, 2006). XIAP also binds to caspase 9 through its BIR3 domain and prevents its activation by cytochrome c. cIAP1 and cIAP2 can also bind to the same caspases but lack the ability to robustly inhibit enzymatic activity (Eckelman & Salvesen, 2006; Holcik, Gibson, & Korneluk, 2001). cIAP1 and cIAP2 were first identified for their ability to interact with tumor necrosis factor associated factors (TRAFs), most notably TRAF2 and TRAF1.

1.5 CHEMOTHERAPY

1.5.1 HISTORY

The first modern chemotherapeutic was isolated from nitrogen mustards as a result of chemical warfare used in World War I, and was further developed by Louis Goodman and Alfred Gilman (Brunton, Lazo, & Parker, 2006; Chabner & Roberts, 2005), which became a standard treatment for lymphomas. The next major advance came with Sydney Farber who was studying the effects of folic acid on leukemias. With the help of others he was the first to delve into rational drug design, making structural analogues of folic acid that could not be metabolized but could block enzymes that required folate, this drug is now commonly referred to as methotrexate, and is commonly used in the clinic as are other more recently designed folate analogues, see pemetrexed in next section.

Both academics and pharmaceutical companies have taken up the search for better treatments for cancer.

1.5.2 Single Agent Chemotherapies used to treat NSCLC

Platinum compounds are standard agents used to treat a variety of cancers. The oldest, cisplatin is a mainstay of doublet chemotherapy used to treat NSCLC, carboplatin is structurally very similar to cisplatin with the exception that the platinum atom is covalently linked to a cyclobutane 1,1 dicarboxylate ligand in place of two chlorines. As a result, DNA binding kinetics of carboplatin are slower than cisplatin, but the same DNA adducts are formed. Due to the decrease in reactivity, carboplatin has less severe side effects compared to cisplatin, with respect to nephrotoxicity and GI effects, but more severe myelosuppressive effects.

In the latter part of the 20th century many new chemotherapies were found to exhibit single agent activity in NSCLC including vinorelbine, paclitaxel, docetaxel, gemcitabine, irinotecan, and pemetrexed (Kosmidis, 2002). Most of these agents are derivatives of older agents; however, these newer formulations are more selective in target binding leading to reduced toxicity.

Vinorelbine, a tubulin depolymerizing agent, is a semi-synthetic vinca alkaloid, and shows more selectivity for mitotic tubules compared to axonal tubules resulting in fewer dose limiting toxicities such as myelosuppression (granulocytopenia or thrombocytopenia) and mild neurotoxicity. Vinorelbine has

been used as a single agent to treat NSCLC and was a particularly good treatment for elderly patients; however, it is now rarely used as a single agent (Brunton, et al., 2006).

Paclitaxel and docetaxel are structurally related tubulin polymerizing agents that belong to the taxane group of anti-mitotics, and have similar toxicity profiles, neutropenia, mucositis, peripheral neuropathy, asthenia, peripheral edema, hair loss, cardiac toxicity (Brunton, et al., 2006). Paclitaxel is a natural product extracted from the rare Pacific Yew Tree, is administered to patients in an excipient known as cremaphor, a polyoxyethylated castor oil that causes some of the side effects felt by patients receiving paclitaxel such as severe anaphylactic hypersensitivity reactions, hyperlipidemia, abnormal lipoprotein patterns, aggregation of erythrocytes and peripheral neuropathy (Gelderblom, Verweij, Nooter, & Sparreboom, 2001; McAuliffe, Roberts, & Roberts, 2002). Docetaxel is a semi-synthetic analogue that is synthesized from precursor molecules extracted from the readily available and renewable European Yew Tree, and is administered in polysorbate 80, ethanol, and citric acid which are not known to cause as severe of side effects as cremaphor (Gelderblom, et al., 2001).

Gemcitabine is a cytosine analogue, as such it can replace CTP for most roles that CTP plays in the cell, most notably incorporation into DNA, causing strand termination after the next nucleotide being incorporated into the growing strand of DNA as such it is a very potent radiosensitizer and should not be

generally combined with radiotherapy (Brunton, et al., 2006). Gemcitabine is associated with myelosuppression, flu-like syndrome, asthenia, rarely interstitial pneumonitis and over many months of treatment can cause progressive hemolytic uremic syndrome (loss of red blood cells due to lysis and acute renal failure).

Doxorubicin is an anthracycline antibiotic isolated from the fungus *Steptococcus peucetius* var. *caesius* (Brunton, et al., 2006). It exerts anti-cancer activity though multiple ways, intercalating with DNA, forming a complex with topoisomerase II that prevents ligase activity of topoisomerase II, and stimulates the production of superoxide (Staquet, Rozencweig, Duarte-Karim, & Kenis, 1977). Doxorubicin causes an array of toxicities in patients such as myelosuppression, thrombocytopenia, stomatitis, alopecia, and GI disturbances, but by far the most serious long term side effect is cardiomyopathy.

Another semi-synthetic compound that was found to have activity against lung cancer in this period is irinotecan, structurally related to camptothecin, and as such causes an accumulation of single stranded breaks in DNA leading to cell death. Currently irinotecan is not approved for NSCLC treatment, but has been explored as part of platinum based combination treatment (Pass, Pogrebniak, Steinberg, Mulshine, & Minna, 1992). Pemetrexed is the newest of the antifolates. Folic acid is a critical co-factor for *de novo* purine and thymidylate synthesis, and the antifolates function at different steps in this pathway to disrupt *de novo* purine and thymidylate synthesis.

1.5.3 PLATINUM BASED DOUBLET CHEMOTHERAPY

A clinical strategy for improving the effectiveness of anti-neoplastic chemotherapy is to combine multiple cytotoxic agents with different mechanisms of action and non-overlapping toxicities (Pass et al., 2010). Platinum, the generic term for platinum containing drugs such as cisplatin or carboplatin, based doublet chemotherapies have been the mainstay for NSCLC treatment for the last three decades, and remains a standard of care for patients currently(Arriagada et al., 2004; Besse & Le Chevalier, 2008; Carbone & Minna, 1995; Cardenal et al., 1999; Clarke et al., 2002; Ettinger, 2002; Goffin, Lacchetti, Ellis, Ung, & Evans, 2010; Heinemann et al., 2006; Ihde et al., 1980; Manegold et al., 2000).

Platinum was chosen as the basis for combinations because it was initially thought to be the most active out of cisplatin, vinblastine, and nitrogen mustards. It remains because clinical trials have not been able to show that any other chemotherapy is better to use for combinations (Dienstmann, Martinez, & Felip, 2011; Pass, et al., 1992; Wu et al., 2011).

1.5.4 MOLECULARLY TARGETED AGENTS

Over the last two decades, a new approach to engineering treatments for cancer has emerged molecularly targeted agents. Molecularly targeted agents are attractive because in theory they should only act on tumor but not normal cells,

currently there are two types of MTAs, small molecule inhibitors, and antibody based therapy.

1.5.4.1 Tyrosine Kinase Inhibitors

With the discovery that a chromosomal fusion, the Philadelphia chromosome, found in 95% of CML patients, as well as in some cases of ALL and AML, resulted in the fusion of BCR and ABL genes and the product of this fusion was a constitutively active from of the Abl kinase leading to transformation (Buchdunger et al., 1996). Small molecule screens were conducted looking for an inhibitor for Abl, Novartis identified, characterized, and optimized a candidate drug which eventually became imatinib and in 2001 became the first FDA approved tyrosine kinase inhibitor (TKI) (Beran, et al., 1998; Buchdunger, et al., 1996; Kimura, et al., 2010).

Tyrosine kinases sit upstream of many key survival and proliferation pathways, and as such are attractive anti-cancer targets. EGFR is a tyrosine kinase that sits directly upstream of Ras, which is known to be mutated in many cancers, so controlling Ras activation in cancers is quite desirable. Targeting of EGFR by gefitinib or erlotinib results in dramatic regression of tumors in patients harboring EGFR mutations (Pao, et al., 2004). However, patients see recurrence of disease either from secondary EGFR mutations conferring resistance to TKIs or undefined acquired resistance (Benedettini et al., 2010; Pallis et al., 2011; Vikis et al., 2007). At present there are many TKIs in use in the clinic currently (Table

1.5) (Dienstmann, et al., 2011; Druker & Lydon, 2000; Gerber & Minna, 2010; Kimura, et al., 2010; Lowery & Han, 2011).

One of the newest targets of TKIs is the anaplastic lymphoma kinase (ALK), which is found as part of a fusion product in glioblastomas, NSCLC, and anaplastic large-cell lymphomas (Gerber & Minna, 2010; McDermott et al., 2008; Sabbatini et al., 2009; Settleman, 2009). Activation of ALK is regulated by protein tyrosine phosphatase ζ, phosphatase activity is inactivated by binding of pleiotrophin to PTPζ, and fusions of Alk with other genes abrogate the requirement for PTPζ regulation. Pfizer recently got FDA approval for crizotinib for the treatment of late stage NSCLC with EML4-ALK fusions (Dienstmann, et al., 2011; McDermott, et al., 2008; Sabbatini, et al., 2009).

One of the problems that TKIs present is that most if not all target the ATP binding pocket of tyrosine kinases, so target specificity of a given TKI is a relative term (Scheffler, Di Gion, Doroshyenko, Wolf, & Fuhr, 2011). Imatinib for example not only targets Abl, but also targets cKit and PDGFRb (Druker & Lydon, 2000). Additionally no TKIs, perhaps except imatinib, are curative as single agents (Scheffler, et al., 2011).

1.5.4.2 Monoclonal Antibodies

An alternative to targeting enzymatic activity is targeting of membrane bound proteins with monoclonal antibodies, trastuzumab and bevacizumab being two such agents that are used in the clinic. Trastuzumab is a humanized mouse

monoclonal antibody that targets Her2 which is often found to be over expressed in breast cancer, and when used to treat breast cancer causes a decrease in proliferation signals and also induces an immune response against tumor cells that it is bound to (Kostyal et al., 2011). Bevacizumab is also a humanized monoclonal antibody targeting angiogenesis by disrupting VEGF-A from binding VEGFR1 and VEGFR2 (Pietras & Hanahan, 2005). Similarly to TKIs, monoclonal antibody single agent treatment is not curative.

Cetuximab targets EFGR, as discussed earlier a target in NSCLC, but it also a target in colorectal cancer (Chung et al., 2005). Cetuximab is a monoclonal antibody that blocks signaling through EGFR homodimers, and is in use for colorectal cancer; however, it is not of much utility in NSCLCs because they also express HER2, and can signal efficiently with EGFR-HER heterodimers.

1.5.4.3 SMAC MIMETICS OR IAP INHIBITORS

With the advances in the understanding of the apoptotic process, targeted approaches to remove cancer cells resistance to apoptosis has moved into the mainstream of drug development. Removal of BCL-2 and IAP inhibition are the two major ways that this is being accomplished. BH3 only mimics such as ABT737 and ABT263 are being currently developed with ABT263 undergoing clinical trials currently (Fesik, 2005; Oltersdorf et al., 2005). IAPs are being targeted by deriving small molecule mimics of the four most N terminal amino acids of SMAC, AVPF (Bockbrader, Tan, & Sun, 2005; Flygare & Fairbrother,

2010; LaCasse et al., 2008; L. Li et al., 2004; Z. Liu et al., 2000; Schimmer et al., 2004; Haiying Sun et al., 2004; H. Sun, Z. Nikolovska-Coleska, C. Y. Yang, L. Xu, Y. Tomita, et al., 2004). Many labs and pharmaceutical companies are exploring this as a therapeutic strategy, but the initial work was done at UTSW by Xioadong Wang's lab (Table 1.6) (L. Li, et al., 2004). They showed that SMAC mimetic (compound 3) could bind to XIAP, induce activation of caspase-3 in cell free assays, and that the combination of SMAC mimetic with TNFα or TRAIL could induce caspase activation (L. Li, et al., 2004). In a large screen across 50 NSCLCs they also found that roughly 15% are sensitive to SMAC mimetic alone, which is due to an autocrine TNFα loop that is dependent on TNFα, TNFR1, caspase-8, and RIPK1 (Gaither et al., 2007; Petersen et al., 2007; Varfolomeev et al., 2007; Vince et al., 2007).

1.6 RNAi

The RNA interference pathway (or RNAi) involves gene silencing as a result of complementarity between small duplex RNA molecules and mRNA. Small duplex RNAs that are expressed endogenously within a cell with the function of silencing genes are called microRNAs (miRNAs also referred to as miRs), which usually contain a 3' seed sequence of ~8 nucleotides that are complementary to the mRNA with additional regions of complementarity. Degree of complementarity determines the mechanism by which the gene is silenced. In the cases where the miRNA is 100% complementary to the mRNA, the target

mRNA is cleaved and then fully degraded; however, when there is less than full complementarity, the miRNA remains bound to the mRNA and physically blocks translation of the target mRNA. Pri-miRNAs are transcribed by RNA polymerase II and then processed by Drosha in the nucleus and then Dicer in the cytoplasm, to yield mature miRs (Figure 1.10) (Davidson & McCray, 2011; Kuehbacher, Urbich, Zeiher, & Dimmeler, 2007). Mature miRs are then loaded into a RNA induced silencing complex (RISC)

Synthetic small interfering RNAs (siRNAs) are designed to be completely complementary to the target mRNA, and function through endogenous RNAi machinery, after introduction into a cell; siRNAs are loaded into a RISC and then cause cleavage of a target mRNA through cleavage of the mRNA.

Transcription of genes can be altered by introduction of so called anti-gene RNAs (agRNA) (Janowski et al., 2005; Janowski et al., 2006; Ting, Schuebel, Herman, & Baylin, 2005). While agRNAs are similar in chemistry to siRNAs; they differ in the intended target, siRNAs target mRNA, and agRNAs are designed to target the genomic DNA upstream of transcription start sites (TSS).

1.7 Hypothesis and Specific Aims

While both detection and resistance to treatment are key reasons for the lack of increases in long term survival of lung cancer patients, this work focuses on improving treatment. And not improving treatment by finding new and

exciting cancer-specific targets and targeting them by small molecules or antibodies, but improving treatment by rationally combining conventional chemotherapy with molecularly targeted techniques to further sensitize lung cancer cells to existing chemotherapies. I thus hypothesized that chemotherapy and molecularly targeted techniques can be combined in such a way that the result of the combination is greater than the sum of each agent alone that would be more effective than current combination regimens. Thus I set up three aims to assess this hypothesis.

Aim1: Systematically evaluate current combination chemotherapy regimens in preclinical models to find areas to exploit to make future combinations more effective.

Aim 2: Using molecular biology approaches, target cellular molecules implicated in drug resistance or cancer cell survival to sensitize NSCLC to conventional chemotherapies.

Aim 3: Evaluate, using small molecules, the ability of the re-engagement of the apoptotic pathway to sensitize NSCLCs to conventional and targeted chemotherapies.

1.7.1 Aim 1: Systematically evaluate current combination chemotherapy regimens in preclinical models to find areas to exploit to make future combinations more effective.

Platinum based chemotherapy combinations remain the mainstay of NSCLC treatment when chemotherapy is deemed necessary as part of the overall treatment plan. These combinations arose from combining two chemotherapies with different dose limiting toxicities at the highest tolerable dose of each drug. Using clinically relevant doses of gemcitabine + cisplatin, pemetrexed + cisplatin, and paclitaxel + carboplatin, equivalent molar ratios were calculated and used to create an in vitro dose response curve for each combination, which were used to screen a panel of 53 NSCLCs. From the dose response curves for each cell line, IC_{50}s were calculated and used with single agent IC_{50}s for each drug in the combination to compare the IC_{50}s by fold decrease, and were used to statistically analyze the effect of combining the two drugs by calculating CI values for each cell line tested. Finally using microarray data for these 53 cell lines signatures of synergy/antagonism were created and used to predict response using leave on out cross validation.

1.7.2 Aim 2: Using molecular biology approaches, target cellular molecules implicated in drug resistance or cancer cell survival to sensitize NSCLC to conventional chemotherapies.

Altered levels of miRs were linked to resistance to gemcitabine, paclitaxel, and vinorelbine by miRNA profiling being correlated with drug response. Using mimics and inhibitors of miR19a, miR129, and miR337 the ability of altering

endogenous miR levels to affect response to gemcitabine or paclitaxel was tested using MTS based micro titer plate assays. Based on a paclitaxel synthetic lethal screen, the specificity of six hits was tested against a small panel of anti-mitotic agents that are structurally similar or act similarly to paclitaxel. Mutations in p53 are the most common mutation in lung cancer, targeting of mutant p53 would be a major step forward with regards to targeted treatment that would be relevant for more than a small subpopulation as is the case with EGFR-TKIs. Reactivation of wild type p53 activity was achieved by targeting of the promoter region of *TP53* with agRNAs, specificity of the agRNAp53 were tested across a panel of tumor lines (NSCLC and others) with varying mutations in p53, homozygous deletions of p53, and wild type p53.

1.7.3 Aim 3: Evaluate, using small molecules, the ability of the re-engagement of the apoptotic pathway to sensitize NSCLCs to conventional and targeted chemotherapies.

Evasion of apoptosis is one of the hallmarks of cancer, and being able to re-engage the apoptotic pathway is an attractive method for sensitizing cancers to chemotherapy treatment. A small molecule SMAC mimetic (IAP antagonist) was used across a panel of NSCLCs with a panel of chemotherapeutics. Drug responses of JP1201 in combination with each chemotherapy was analyzed statistically using CI calculations to determine synergy, additively, or antagonism.

In vitro results of synergy were validated with two cell line xenograft models in NOD/SCID mice. Mechanisms of synergy were determined using siRNAs to perturb pathways suspected in synergy.

Risk factor	Risk estimate (95% CI)	Comments	Refs
Environmental ETS	1.19 (90% CI: 1.04–1.35)	Meta-analysis of 11 US studies of spousal exposure (females only)	48
	1.21 (1.13–1.30)	Meta-analysis of 44 case–control studies worldwide of spousal exposure	52
	1.22 (1.13–1.33)	Meta-analysis of 25 studies worldwide of workplace exposure	52
	1.24 (1.18–1.29)	Meta-analysis of 22 studies worldwide of workplace exposure	51
Residential radon	8.4% (3.0–15.8%) per 100 Bq m^3 increase in measured radon	Meta-analysis of 13 European studies	56
	11% (0–28%) per 100 Bq m^3	Meta-analysis of 7 North American studies	57
Cooking oil vapours	2.12 (1.81–2.47)	Meta-analysis of 7 studies from China and Taiwan (female never smokers)	71
Indoor coal and wood burning	2.66 (1.39–5.07)	Meta-analysis of 7 studies from China and Taiwan (both sexes)	71
	1.22 (1.04–1.44)	Large case–control study (2,861 cases and 3,118 controls) from Eastern and Central Europe (both sexes)	158
	2.5 (1.5–3.6)	Large case–control study (1,205 cases and 1541 controls) from Canada (significant for women only)	159
Genetic factors: family history, *CYP1A1* Ile462Val polymorphism, *XRCC1* variants	1.51 (1.11–2.06)	Meta-analysis of 28 case–control, 17 cohort and 7 twin studies	99
	2.99 (1.51–5.91)	Meta-analysis of 14 case–control studies of Caucasian never smokers	103
	2.04 (1.17–3.54)	Meta-analysis of 21 case–control studies of Caucasian and Asian never smokers (significant for Caucasians only)	104
	No association	Meta-analysis of 13 case–control studies	160
	No association overall; reduced risk 0.65 (0.46–0.83) with Arg194Trp polymorphism and 0.56 (0.36–0.86) with Arg280His for heavy smokers	Large case–control study from Europe (2,188 cases and 2,198 controls)	161
	Increased risk for never smokers 1.3 (1.0–1.8) and decreased risk for heavy smokers 0.5 (0.3–1.0) with Arg299Gln	Large case–control study from the US (1,091 cases and 1,240 controls)	105
Viral factors: HPV 16/18	10.12 (3.88–26.4) for never smoking women >60 years	Case–control (141 cases, 60 controls) study from Taiwan of never smoking women	107

Bq, becquerels; ETS, environmental tobacco smoke; EPA, Environment Protection Agency; HPV, human papillomavirus.

TABLE 1.1 Summary of selected studies of risk factors for lung cancer in never smokers.

Factors associated with lung cancer in never smokers that have been studied. Adapted from Sun et al., 2007.

T classifications	
TX	Primary tumor cannot be assessed, or tumor proven by the presence of malignant cells in sputum or bronchial washings but not visualized by imaging or bronchoscopy.
T0	No evidence of primary tumor.
Tis	Carcinoma *in situ*.
T1	Tumor ≤3 cm in greatest dimension, surrounded by lung or visceral pleura, without bronchoscopic evidence of invasion more proximal than the lobar bronchus (i.e., not in the main bronchus).
T1a	Tumor ≤2 cm in greatest dimension.
T1b	Tumor >2 cm but ≤3 in greatest dimension.
T2	Tumor >3 cm but ≤7 cm or tumor with any of the following features (T2 tumors with these features are classified T2a if ≤5 cm): Involves main bronchus. ≥2 cm distal to the carina. Invades visceral pleura (PL1 or PL2). Associated with atelectasis or obstructive pneumonitis that extends to the hilar region but does not involve the entire lung.
T2a	Tumor >3 cm but ≤5 cm in greatest dimension.
T2b	Tumor >5 cm but ≤7 cm in greatest dimension.
T3	Tumor >7 cm or one that directly invades any of the following: Parietal pleural (PL3) chest wall (including superior sulcus tumors), diaphragm, phrenic nerve, mediastinal pleura, or parietal pericardium. Tumor in the main bronchus (<2 cm distal to the carina but without involvement of the carina). Associated atelectasis or obstructive pneumonitis of the entire lung or separate tumor nodule(s) in the same lobe.
T4	Tumor of any size that invades any of the following: Mediastinum, heart, great vessels, trachea, recurrent laryngeal nerve, esophagus, vertebral body, carina, or separate tumor nodule(s) in a different ipsilateral lobe.

N classifications	
NX	Regional lymph nodes cannot be assessed.
N0	No regional lymph node metastases.

N1	Metastasis in ipsilateral peribronchial and/or ipsilateral hilar lymph nodes and intrapulmonary nodes, including involvement by direct extension.
N2	Metastasis in ipsilateral mediastinal and/or subcarinal lymph node(s).
N3	Metastasis in contralateral mediastinal, contralateral hilar, ipsilateral or contralateral scalene, or supraclavicular lymph node(s).

M Classifications	
M0	No distant metastasis.
M1	Distant metastasis.
M1a	Separate tumor nodule(s) in a contralateral lobe or tumor with pleural nodules or malignant pleural (or pericardial) effusion
M1b	Distant metastasis.

TNM descriptors influence Staging

	Nodal Involvment			
Primary Tumor	N0	N1	N2	N3
T1a	IA	IIA	IIIA	IIIB
T1b	IA	IIA	IIIA	IIIB
T2a	IB	IIA	IIIA	IIIB
T2b	IIA	IIB	IIIA	IIIB
T3	IIB	IIIA	IIIA	IIIB
T4	IIIA	IIIA	IIIB	IIIB
M1a	IV	IV	IV	IV
M1b	IV	IV	IV	IV

TABLE 1.2 TNM Staging Guidelines.

Adapted from ("Lung," 2010)

Gene Symbol	Transcriptional p53 effect	p53 RE	Gene Symbol	Transcriptional p53 effect	p53 RE
14.3.3sigma	Activated	Yes	MCM4	Repressed	
AP-1	Activated	Yes	MCM6	Repressed	Yes
APAF1	Activated	Yes	MCM7	Repressed	Yes
ASK	Repressed		MDM2	Activated	Yes
AURKB	Repressed		MSH2	Activated	Yes
BAI1	Activated	Yes	MSH2	Repressed	
BAX	Activated	Yes	MSH6	Repressed	
BTG2	Activated	Yes	MYC	Repressed	
BUB1	Repressed		NEK2	Repressed	
BUB1B	Repressed		NOXA	Activated	Yes
CCNA2	Repressed	Yes	p53AIP1	Activated	Yes
CCNE2	Repressed	Yes	P53DINP1	Activated	Yes
CD95-Fas	Activated	Yes	P53R2	Activated	Yes
CDC2	Repressed		P53RDL1/UNC5B	Activated	Yes
CDC20	Repressed	Yes	P53RFP	Activated	Yes
CDC25A	Repressed	Yes	PA26	Activated	Yes
CDC6	Repressed	Yes	PAI-1	Activated	Yes
CDC7	Repressed		PCNA	Activated	Yes
CDK4	Repressed	Yes	PG13	Activated	Yes
CDT1	Repressed		PIDD	Activated	Yes
CENPF	Repressed		PIG3	Activated	Yes
C-FOS	Activated	Yes	PIR121	Activated	Yes
CHEK1	Repressed	Yes	POLE2	Repressed	
CON-A	Activated	Yes	PRC1	Repressed	Yes
CON-B	Activated	Yes	PRIM1	Repressed	
CON-C	Activated	Yes	PSF2	Repressed	
CSPG6	Repressed		PTEN	Activated	Yes
CSR	Activated	Yes	PTGF-beta/GDF15	Activated	Yes
CyclinG	Activated	Yes	PUMA	Activated	Yes
DUT	Repressed		RAD54B	Repressed	
EGFR	Activated	Yes	RFC3	Repressed	
FEN1	Repressed		RGC	Activated	Yes
GADD45	Activated	Yes	RPS27L	Activated	Yes
GML	Activated	Yes	RRM2	Repressed	Yes
HCAP-G	Repressed		S100A2	Activated	Yes

HGFIN	Activated	Yes	SEMA3F	Activated	Yes
HUNTINGTIN	Activated	Yes	SMC2L1	Repressed	
IGF-BP3	Activated	Yes	SMC4L1	Repressed	
KAI1/CD82	Activated	Yes	STK6	Repressed	
KIF23	Repressed		TOP2A	Repressed	
KILLER/DR5	Activated	Yes	TOPK	Repressed	
KNTC2	Repressed		TPX2	Repressed	
MAD2L1	Repressed	Yes	TYPE IV COLLAGENASE	Activated	Yes
MASPIN/SERPINB5	Activated	Yes	UBE2C	Repressed	
MCM2	Repressed	Yes	WAF1	Activated	Yes
MCM3	Repressed	Yes	WTH3	Activated	Yes

TABLE 1.3 Transcriptional Targets of p53.

Sourced from (Olivier et al., 2002; Spurgers et al., 2006; Yu & Zhang, 2005)

Proteins found bound to promoter region of p53	
pol2	GATA
NFkB	IRF1
TFR	MAX
YY1	JUN
STAT3	GABP
CEBPB	PAX5
TAF1	SIX5
SP1	TCF4
TBP	p300
POU2F2	ELK4
HEY1	FOXA2
AP2 γ	FOXA1
OCT2	cFOS
RXRα	BCL3
Sin3a	BCLAF1
HMGn3	EGR1
cMYC	Erα
NF-YB	BRCA1
ETS1	

TABLE 1.4 Factors that have been found to regulate *TP53* Transcription.

Data from ("Identification and analysis of functional elements in 1% of the human genome by the ENCODE pilot project," 2007).

Name	Agent Class	Target(s)	Tumor Types	FDA Approval
Bevacizumab (Avastin)	Monoclonal Antibody	VEGF	Colorectal cancer	2004
			NSCLC	2006
			Breast cancer	2008
Cancertinib (CI-1033)	Small Molecule TKI	Pan-erbB	Phase II - SCC, ovarian, metastatic breast cancer	
Cetuximab (Erbitux)	Monoclonal Antibody	EGFR	Colorectal cancer	2004
			HNSCC	2006
			Phase III - pancreatic cancer, NSCLC	
			Phase II - HCC	
Crizotinib (Xalkori)	Small Molecule TKI	ALK	NSCLC	2011
dasatinib (Spryce)	Small Molecule TKI	BCR-Abl, Src	CML, ALL	2010
EKB-569	Small Molecule TKI	EGFR	Phase II - advanced colorectal cancer, NSCLC	
Erlotinib (Tarceva)	Small Molecule TKI	EGFR	NSCLC	2004
			Phase II - HCC	
			Pancreatic cancer	2005
Gefitinib (Iressa)	Small Molecule TKI	EGFR	NSCLC	2003
			Phase I HCC	
Imatinib (Gleevec)	Small Molecule TKI	KIT, PDGFR, BCR-ABL	CML, ALL, GIST	2002
Lapatinib (Tykerb)	Small Molecule TKI	EGFR, HER-2	Breast cancer	2007
Matuzumab (EMD 72000)	Monoclonal Antibody	EGFR	Phase I/II - NSCLC, ovarian, pancreatic cancer	
nilotinib (Tasigna)	Small Molecule TKI	BCR-Abl, KIT, LCK, EPHA,	CML	2010

Panitumumab (Vectibix)	Monoclonal Antibody	DDR, PDGFRb EGFR	Colorectal cancer Phase I - refractory solid tumors	2006
Ponatinib	Small Molecule TKI	pan-BCR-Abl, LYN, PDGFRa, FGFR1, Src, KIT, VEGFR2	Phase I CML, ALL	
Semaxanib (SU5416)	Small Molecule TKI	VEGFR, EGFR, KIT	Phase II - metastatic melanoma	
Sorafenib (Nexavar)	Small Molecule TKI	VEGFR, PDGFR, KIT, FLT-3, RAF	Renal Cancer HCC	2005 2008
Sunitinib (Sutent)	Small Molecule TKI	VEGFR, PDGFR, KIT, FLT-3, RET	Renal Cancer, GIST	2006
Temsirolimus	Small Molecule S/T kinase inhibitor	mTOR	Renal cancer	2007
Trastuzumab (Herceptin)	Monoclonal Antibody	HER-2	Breast cancer	1998
vandetanib (Caprelsa)	Small Molecule TKI	Pan-erbB, VEGFR, RET, TIE2, EphR, BRK, Src	medullary thyroid cancer	2011
Vatalanib	Small Molecule TKI	VEGFR, PDGFR	Phase III - colorectal cancer	
vemurafenib (Zelboraf)	Small Molecule TKI	BRAF	Phase II - GIST, prostate and kidney cancer Advanced or Metastatic Melanoma	2011

TABLE 1.5 TKIs.

Data sourced from (Lowery & Han, 2011; O'Hare et al., 2009)

SMAC Compound	Pharmaceutical Company	Clinical Trial	Clinical Trial #
AT-406	Ascenta	Phase I	NCT01265199
		Phase I	NCT01078649
GDC0917	Genentech	Phase I	NCT01226277
HGS1029	Human Genome Sciences	Phase I	NCT00708006
		Phase I	NCT01013818
LCL161	Novartis	Phase I	NCT01240655
TL32711	TetraLogic	Phase I/II	NCT01188499
		Phase I	NCT00993239
JP1201	Joyant	none	

TABLE 1.6 SMAC MIMETIC/IAP ANTAGONISTS IN DEVELOPMENT.

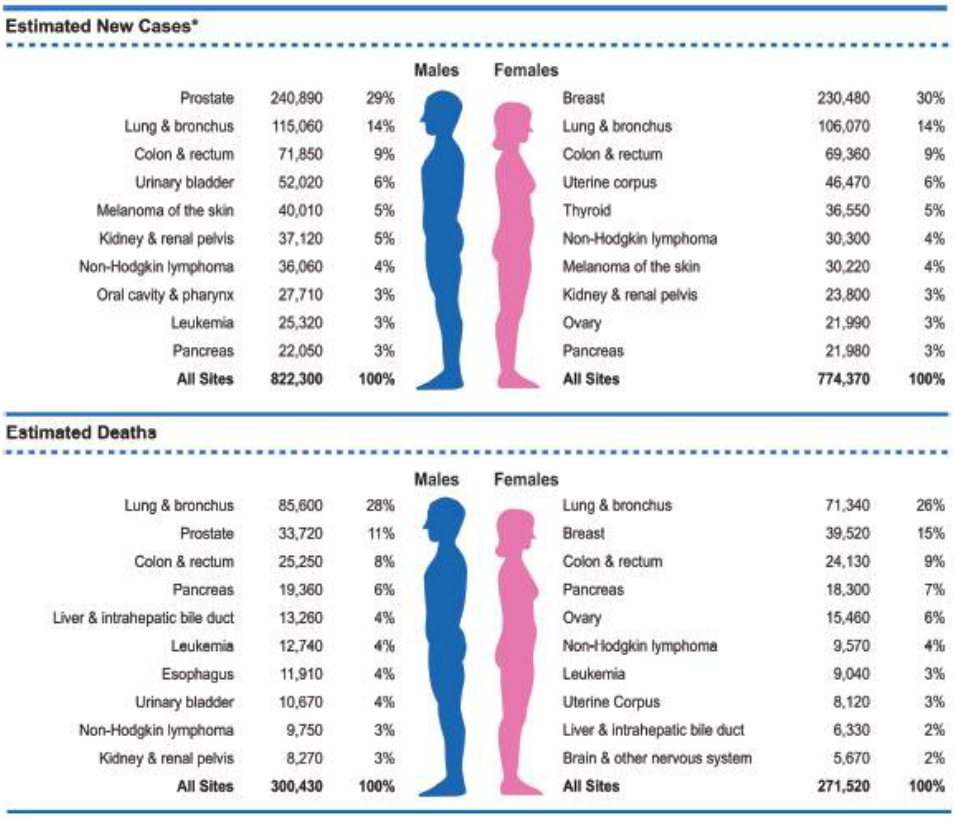

Estimated New Cases*

Males				Females		
Prostate	240,890	29%		Breast	230,480	30%
Lung & bronchus	115,060	14%		Lung & bronchus	106,070	14%
Colon & rectum	71,850	9%		Colon & rectum	69,360	9%
Urinary bladder	52,020	6%		Uterine corpus	46,470	6%
Melanoma of the skin	40,010	5%		Thyroid	36,550	5%
Kidney & renal pelvis	37,120	5%		Non-Hodgkin lymphoma	30,300	4%
Non-Hodgkin lymphoma	36,060	4%		Melanoma of the skin	30,220	4%
Oral cavity & pharynx	27,710	3%		Kidney & renal pelvis	23,800	3%
Leukemia	25,320	3%		Ovary	21,990	3%
Pancreas	22,050	3%		Pancreas	21,980	3%
All Sites	**822,300**	**100%**		**All Sites**	**774,370**	**100%**

Estimated Deaths

Males				Females		
Lung & bronchus	85,600	28%		Lung & bronchus	71,340	26%
Prostate	33,720	11%		Breast	39,520	15%
Colon & rectum	25,250	8%		Colon & rectum	24,130	9%
Pancreas	19,360	6%		Pancreas	18,300	7%
Liver & intrahepatic bile duct	13,260	4%		Ovary	15,460	6%
Leukemia	12,740	4%		Non-Hodgkin lymphoma	9,570	4%
Esophagus	11,910	4%		Leukemia	9,040	3%
Urinary bladder	10,670	4%		Uterine Corpus	8,120	3%
Non-Hodgkin lymphoma	9,750	3%		Liver & intrahepatic bile duct	6,330	2%
Kidney & renal pelvis	8,270	3%		Brain & other nervous system	5,670	2%
All Sites	**300,430**	**100%**		**All Sites**	**271,520**	**100%**

FIGURE 1.1 Ten Leading Cancer Types for the Estimated New Cancer Cases and Deaths by Sex, United States, 2011.

* Estimates are rounded to the nearest 10 and exclude basal and squamous cell skin cancers and in situ carcinoma except urinary bladder. Adapted from (Siegel, et al., 2011).

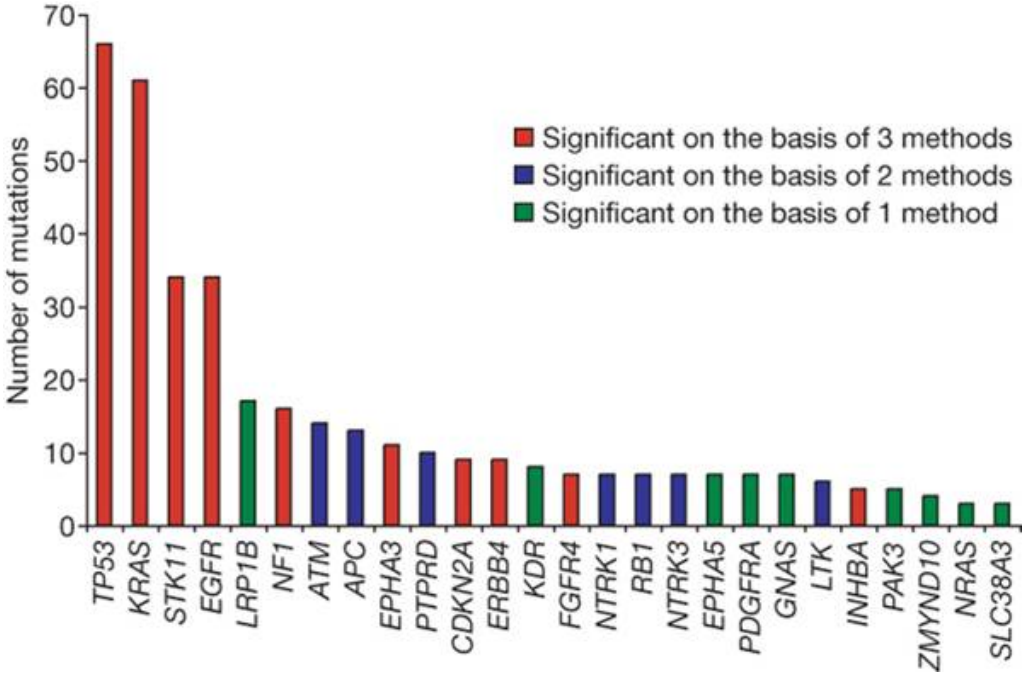

FIGURE 1.2 Common somatic mutations in lung cancer.

Hight of the bars indicates the number of mutations for each gene in 188 tumor/normal pairs. Standard, gene-specific and category-based tests were used for this analysis. *TP53*, Kras, STK11/LKB1, and EGFR are the most common mutations found. Adapted from (Ding, et al., 2008).

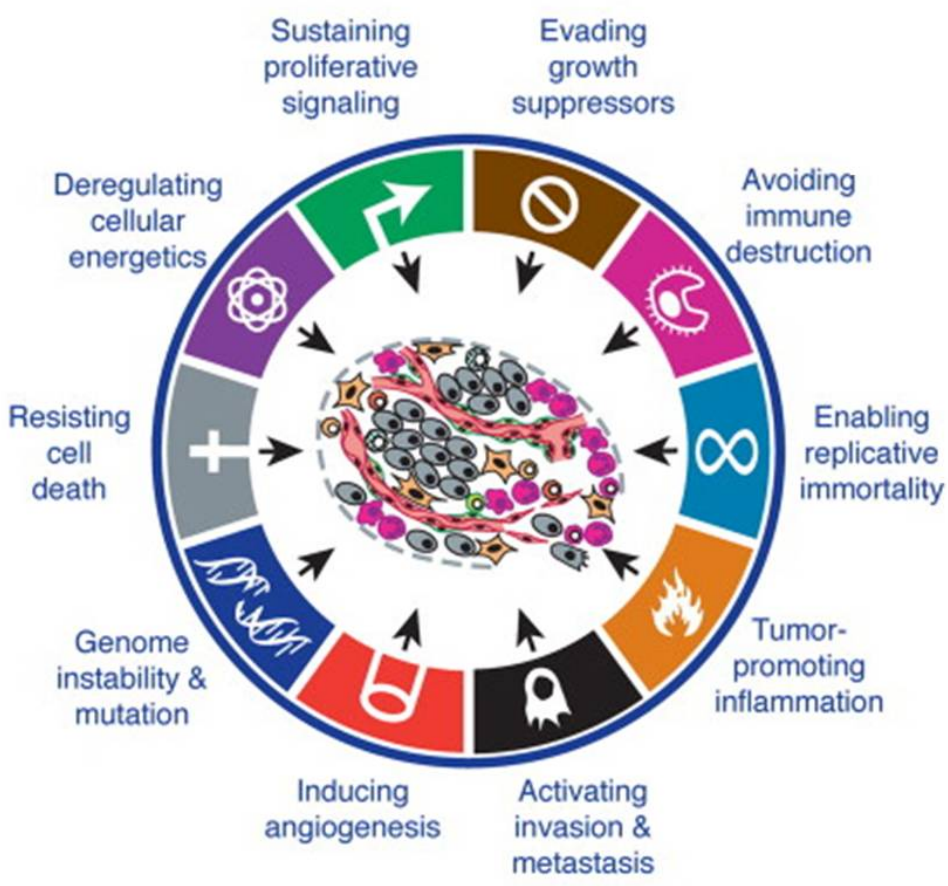

Figure 1.3 Hallmarks of Cancer.

The hallmarks of cancer include ten biological capabilities acquired during the multistep development of human tumors, giving a framework for rationalizing the complexity of cancer. They include sustaining proliferative signaling, evading growth suppressors, resisting cell death, being able to replicate indefinitely, inducing angiogenesis, activating invasion and metastisis, genetic instability, inflammation, evading immune destruction, and reprogramming of metabolic pathways. Modified from (Hanahan & Weinberg, 2011).

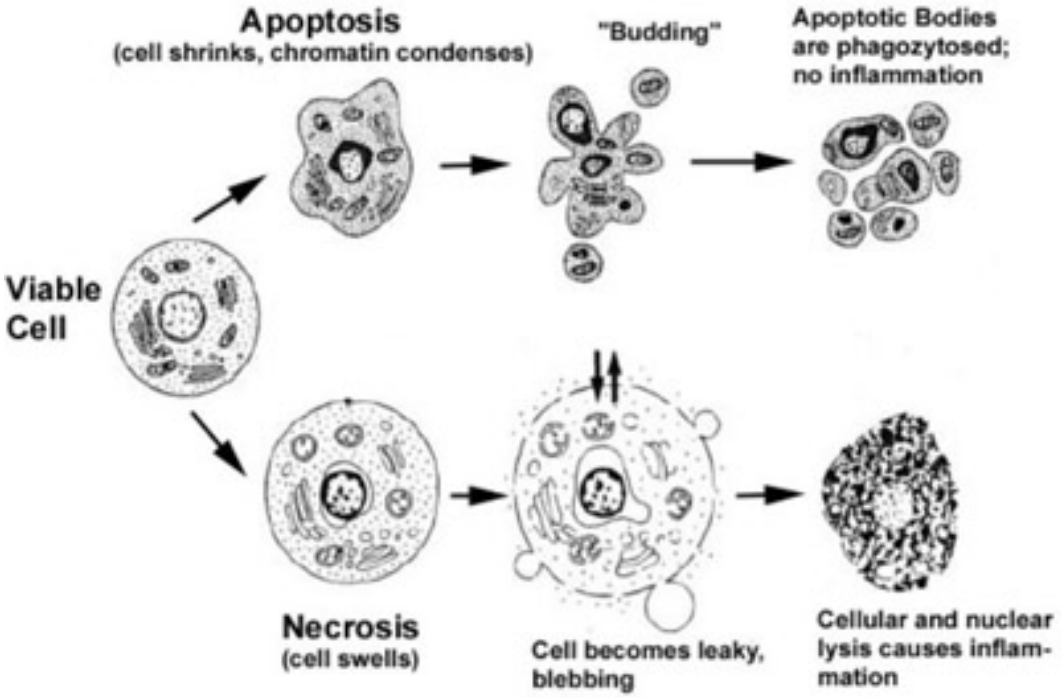

FIGURE 1.4 Characteristics of apoptosis and necrosis highlighting the differences between the two forms of cell death.

Apoptosis is characterized by cellular shrinkage, chromatin condensation and fragmentation, membrane blebbing, and clearance by macrophages in the absence of inflammation. Necrosis is characterized by cell swelling, leakage of cytoplasmic contents, some membrane blebbing, cellular and nuclear lysis, and clearance through induction of inflammation. Modified from (Van Cruchten & Van den Broeck, 2002).

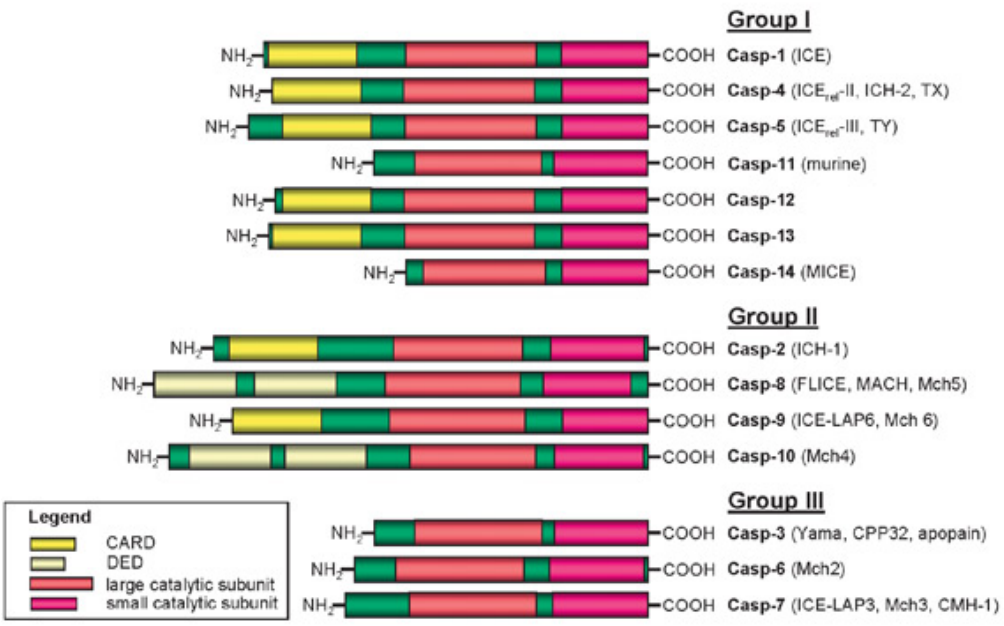

FIGURE 1.5 Human Caspase Family.

There are three functional groups within the caspases family, group I caspases are not believed to be involved in apoptosis, but are involved in the biogenesis of active IL-1b. Group II caspases are the initiator caspases, which are directly activated by cellular stresses, and activate downstream executioner caspases or other initiator caspases to amplify the apoptotic signal. Group III caspases are the executioner caspases which go on to cleave cellular substrates such as ICAD, PARP, as well as other targets and are responsible for the death of a cell. Adapted from (Lavrik & Krammer, 2009).

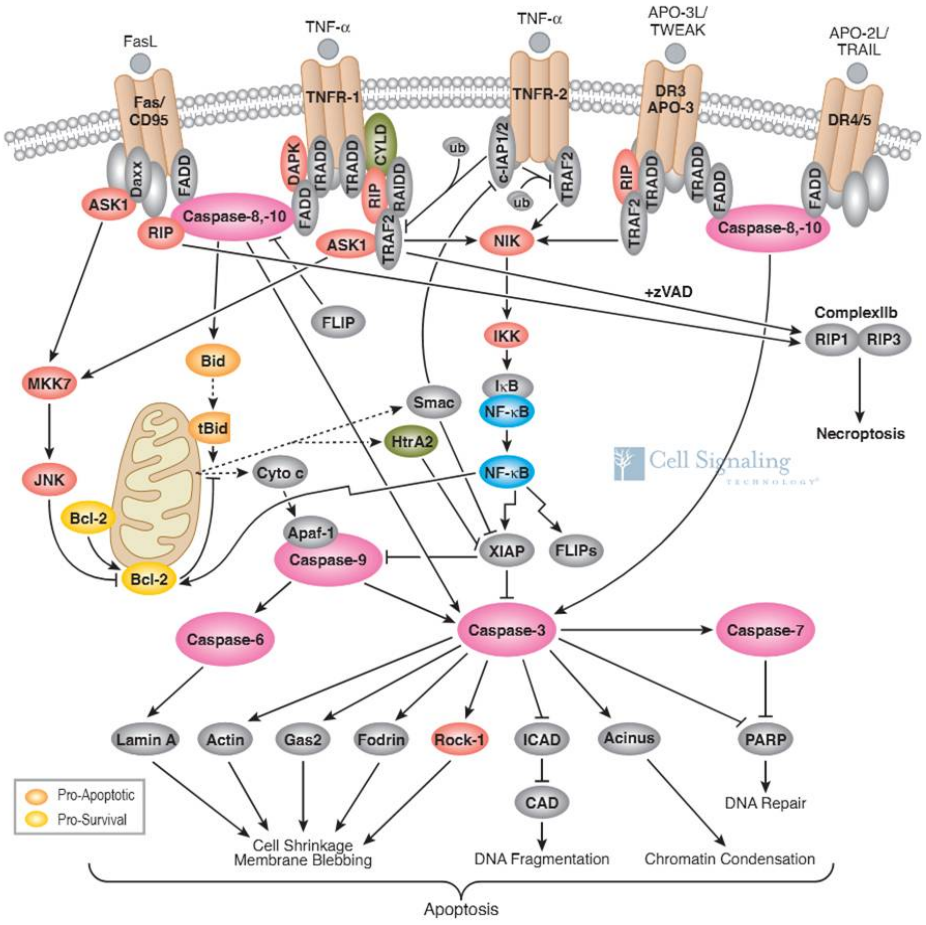

FIGURE 1.6 Extrinsic Apoptotic Pathway.

Activation of death receptors, TNFR1, DR4/DR5, FAS by binding of cognate ligands (TNFα, TRAIL, FasL) activates the death inducing complex (DISC) which includes FADD and caspase-8. In some cases activation of caspase-8 is not sufficient for induction of apoptosis, but caspase-8 can cleave Bid to form t-Bid which amplifies the pro-death signal through the mitochondria resulting in apoptosis. Adapted from Cell Signaling

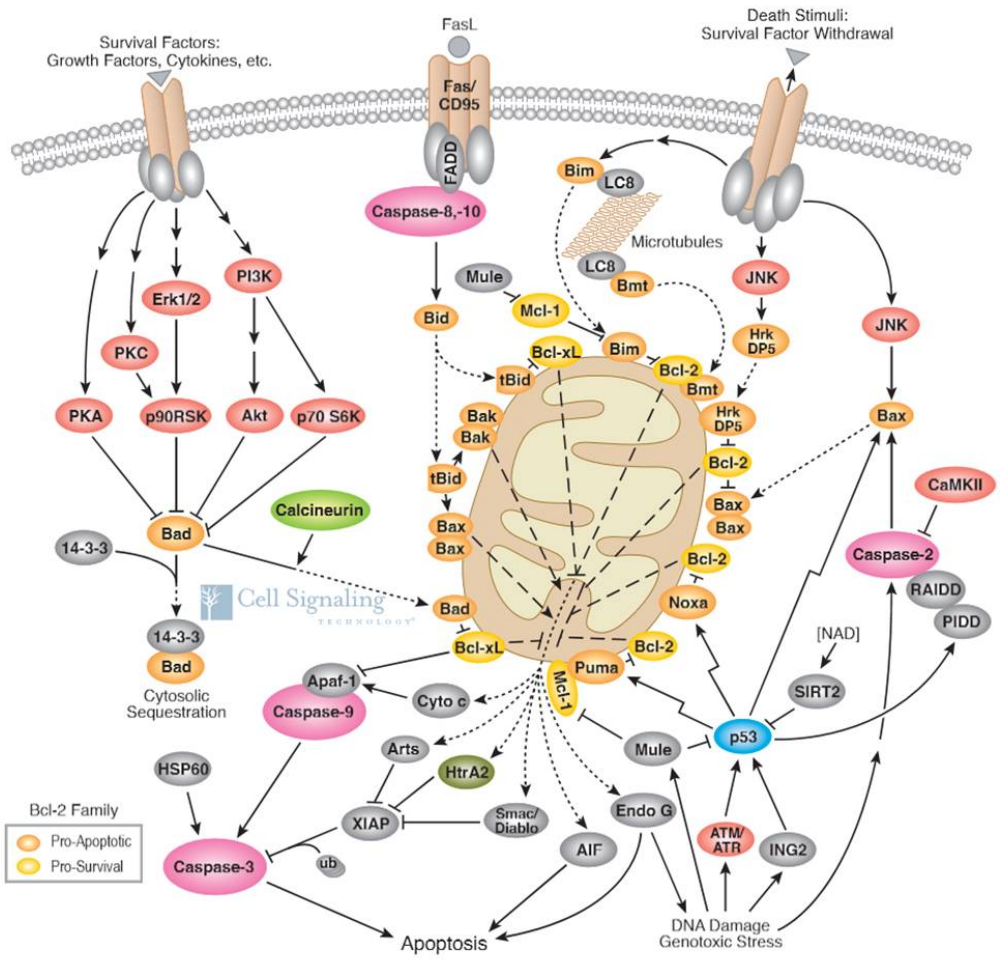

FIGURE 1.7 Intrinsic Apoptotic Pathway.

The balance between the pro-apoptotic (BAX, BAK, Bad, BCL_{xs}, Bid, Bim, PUMA, and NOXA) and anti-apoptotic BCL-2 (BCL-2, BCL_{xL}, MCL-1) family members determines if cytochrome c and other apoptogenic activators are released from the mitochondria. Release of cytochrome c leads to activation of caspase-9 through complex formation of APAF-1, cytochrome c, and caspase-9 (the apoptosome). Activation of caspase-9 is not dependent on caspase-9, and

results in activation of downstream caspase-3,-6,and -7 and ultimately cell death. Adapted from Cell Signaling.

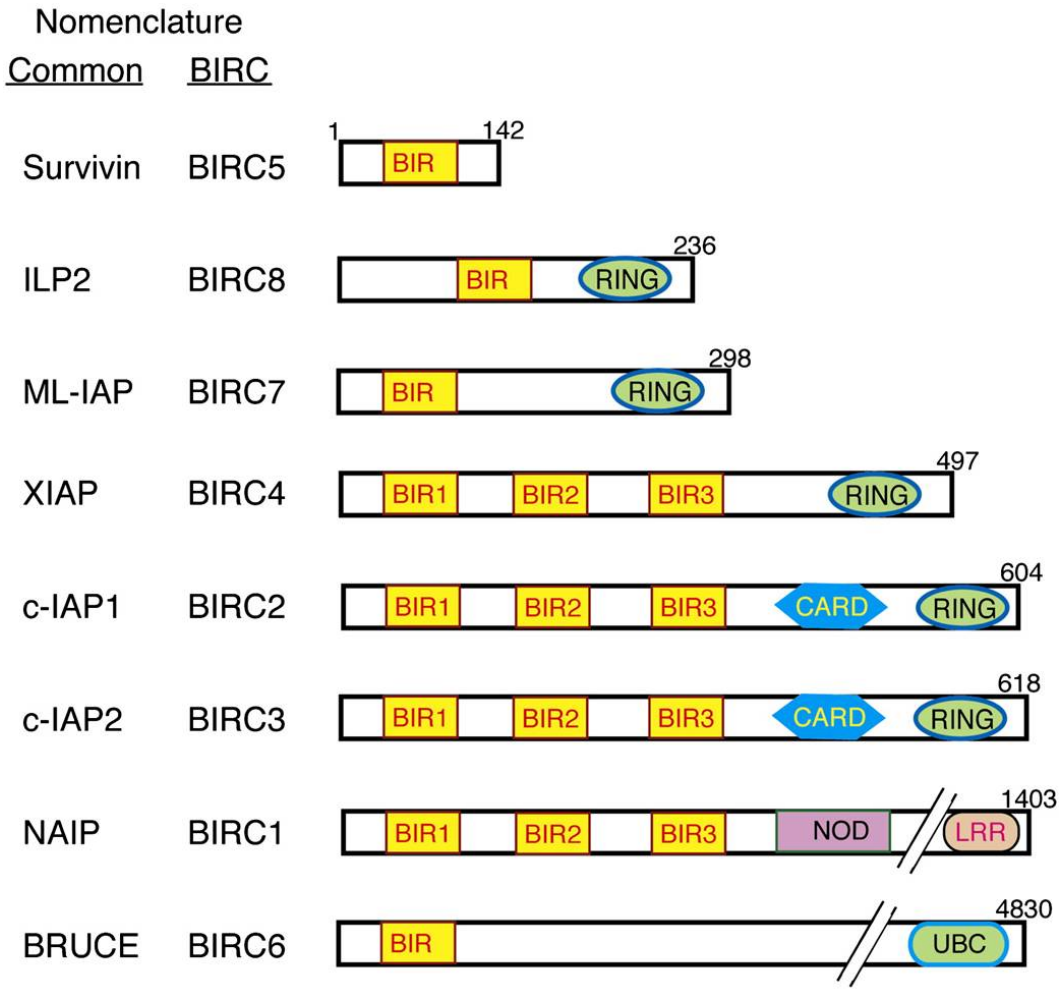

FIGURE 1.8 Human Inhibitors of Apoptosis Protein Family.

The human IAP family consists of 8 proteins, the best studied of this family are XIAP, cIAP1, and cIAP2. XIAP is the only IAP that can inhibit active caspases catalytic activity. cIAP1 and cIAP2 are recruited to the TNFR complex I by direct interactions with TRAF2, and regulate NF-κB and JNK activation by TNFR1, as well as inhibit activation of caspases-8 by inhibiting RIPK1 being incorporated

into complex II. Survivin regulates the cell cycle by direct tubulin interactions. Adapted from (Srinivasula & Ashwell, 2008).

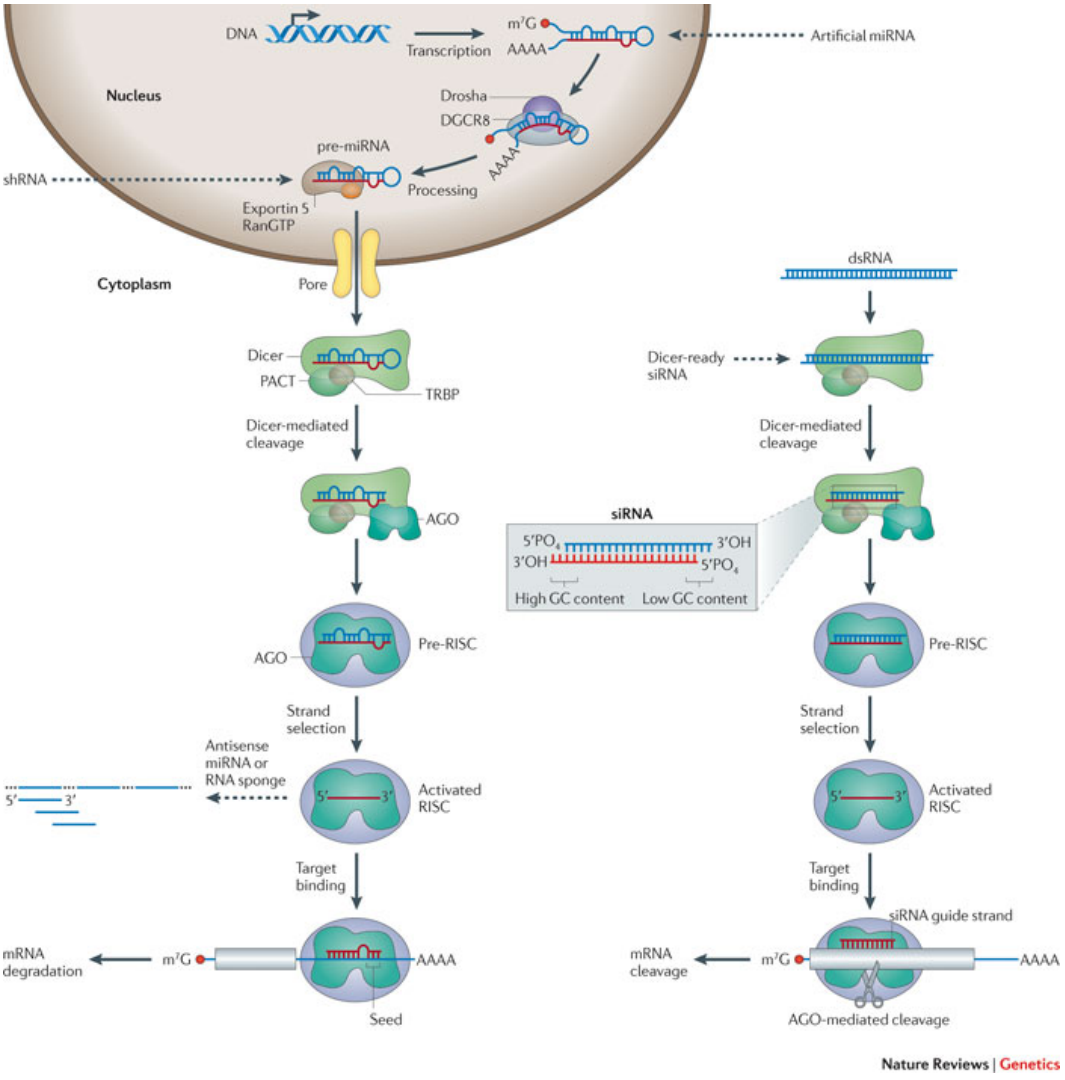

FIGURE 1.9 The miRNA and siRNA pathways of RNAi in mammals.

Primary microRNAs (pri-miRNAs) are transcribed by RNA polymerases and are trimmed by the microprocessor complex (comprising Drosha and microprocessor complex subunit DCGR8) into ~70 nucleotide precursors, called pre-miRNAs (left side of the figure). miRNAs can also be processed from spliced short introns

(known as mirtrons). pre-miRNAs contain a loop and usually have interspersed mismatches along the duplex. pre-miRNAs associate with exportin 5 and are exported to the cytoplasm, where a complex that contains Dicer, TAR RNA-binding protein (TRBP) and PACT processes the pre-miRNAs into miRNA–miRNA* duplexes. The duplex associates with an Argonaute (AGO) protein within the precursor RNAi-induced silencing complex (pre-RISC). One strand of the duplex (the passenger strand) is removed. The mature RISC contains the guide strand, which directs the complex to the target mRNA for post-transcriptional gene silencing. The 'seed' region of a miRNA is indicated; in RNAi trigger design, the off-target potential of this sequence needs to be considered. Long dsRNAs (right side of the figure) are processed by Dicer, TRBP and PACT into small interfering RNAs (siRNAs). siRNAs are 20–24-mer RNAs and harbor 3′OH and 5′ phosphate (PO_4) groups, with 3′ dinucleotide overhangs. Within the pre-RISC complex, an AGO protein cleaves the passenger siRNA strand. Then, the mature RISC, containing an AGO protein and the guide strand, associates with the target mRNA for cleavage. The inset shows the properties of siRNAs. The thermodynamic stability of the terminal sequences will direct strand loading. Like naturally occurring or artificially engineered miRNAs, the potential 'seed' region can be a source for miRNA-like off-target silencing. shRNA, short hairpin RNA. Adapted from (Davidson & McCray, 2011).

CHAPTER TWO

MATERIALS AND METHODS

2.1 MATERIALS

2.1.1 CELL LINES

With the exception of A549, Calu1, Calu3, Calu6, SOAS-2, T47D, MIA PaCa2, MDA-MB-231, Panc1, MCF7, DU145, and Hs766 which were purchased from the American Type Culture Collection (ATCC), all tumor cell lines were established by Drs Minna and Gazdar and are deposited at the ATCC, or are available upon request (A. F. Gazdar et al., 1998; Phelps et al., 1996; Ramirez et al., 2004; Sato, et al., 2006). Lung cancer cell lines that were established at the National Cancer Institute are denoted with the prefix H and lung cancer cell lines that were established at the UTSW Hamon Center for Therapeutic Oncology Research are annotated as HCC (Adi F. Gazdar, Girard, Lockwood, Lam, & Minna, 2010). Human bronchial epithelial cells were immortalized using ectopic expression of cdk4 and hTERT, denoted by –KT at the end of the name were established by our laboratories (Ramirez, et al., 2004). Defined oncogenic changes, Kras G12V and p53 shRNA, were introduced in HBEC3KT cells and tumorigenic clones (clone 1, clone 5) isolated by soft agar formation (Sato, et al., 2006).

2.1.2 SMALL MOLECULE DRUG LIBRARY

Cisplatin (1 mg/mL; Teva Parenteral, Irvine, CA), carboplatin (10 mg/mL; Bristol-Myers Squibb, New York City, New York), doxorubicin (2 mg/mL; Teva Parenteral, Irvine, CA), gemcitabine (Eli Lilly and Company, Indianapolis, IN), paclitaxel (Bristol-Myers Squibb, New York City, New York), pemetrexed (Eli Lilly and Company, Indianapolis, IN), vinorelbine (Pierre Fabre Company, Castres, France), and erlotinib (OSI Pharmaceuticals, Melville, NY) were purchased at the University of Texas Southwestern Medical Center Campus Pharmacy. Cisplatin, carboplatin, paclitaxel, and pemetrexed were stored as received at room temperature; pemetrexed was dissolved in 0.9% saline fresh each time before use; gemcitabine was dissolved in 0.9% saline at 38 mg/mL and stored at room temperature. Doxorubicin and vinorelbine were stored as received at 4°C; erlotinib was dissolved in DMSO at 10 μM and stored at 4°C. SMAC mimetic (JP1201), diazonamide A (JP1036), and JP1798 (a diazonamide derivative) were obtained from Joyant pharmaceuticals, dissolved in DMSO at 10 μM and stored at -20°C, with the exception of JP1798 which was stored at 4°C. Peloruside A was obtained from Reata Pharmaceuticals, dissolved in DMSO at 10 μM and stored at -20°C.

2.2 Methods

2.2.1 Cell Culture

All cancer cell lines and tumorigenic HBEC clones were grown in RPMI-1640 medium (Life Technologies Inc., Rockville, MD) supplemented with 5%

fetal bovine serum (FBS). HBECs were grown in Keratinocyte Serum-Free Medium (KSFM) supplemented with bovine pituitary extract and recombinant human epidermal growth factor (Gibco, Carlsbad, CA). All cell lines were grown in a humidified atmosphere with 5% CO2, at 37°C, and have been DNA fingerprinted for provenance using the PowerPlex 1.2 kit (Promega) and confirmed to be the same as the DNA fingerprint library maintained by ATCC and the Minna/Gazdar lab (the primary source of the lines), and confirmed to be free of mycoplasma by the e-Myco kit (Boca Scientific).

2.2.2 DRUG RESPONSE CURVES

Cells were plated on day zero, so that by day 5, maximal MTS signal will be observed in the untreated cells. Chemotherapies were given on day one as four-fold dilutions with a maximum dose of 1000 nM for JP1306, JP1798, paclitaxel, peloruside, and vinorelbine, 2000 nM for gemcitabine and doxorubicin, or 100 μM for carboplatin, cisplatin, erlotinib, pemetrexed, and JP1201 alone. 10 μM or 100 nM of JP1201 was used in combination assays as indicated. Cells were incubated for four days then relative cell number was determined with MTS (Promega, Madison, WI, final concentration 333 μg/ml), incubating for 1 to 3 hours at 37°C, and reading absorbance at 490 nm plate reader (Spectra Max 190, Molecular Devices, Downington, PA). Each experiment contained eight replicates per concentration and the entire assay was performed in multiple replicates ($n \geq$

4). Drug sensitivity curves and IC_{50}s were calculated using in-house software (DIVISA).

2.2.3 Liquid Colony Formation Assay

Cells were seeded at 500 cells per well in 6 well dishes. The appropriate concentrations of drug were prepared from stock solutions in RPMI-1640 medium with 5% fetal bovine serum, for 10-14 days depending on the cell line. At the end of the assay, medium was aspirated and cells were fixed and stained with 0.5% methylene blue in 50% ethanol for 30 minutes. After staining, wells were washed and black and white images of the plates were taken using a ChemiDoc XRS+ imager (Quantity One software v4.6.5, BioRad, Hercules, CA). Colony counts are averages of triplicate wells done in duplicate over a two week period.

2.2.4 Annexin V FACS Analysis

Induction of apoptosis was measured by flow cytometry using an Annexin V-FITC apoptosis kit (556547, BD Pharmingen) following the manufacturers guidelines. Cells were plated, allowed 24 hours to recover, and then given various doses of vinorelbine with or without 10 μM JP1201. Florescence activated cell sorting (FACS) analysis was preformed 48 hours after treatment, all florescence activated cell sorting was performed on a FACScan (Becton-Dickinson, Franklin Lakes, NJ) or four laser BD LSR II (BD Biosciences, San Jose, CA) flow cytometers. Flow cytometry data was analyzed using FlowJo (FlowJo version 8.02 Treestar, Ashland, OR).

2.2.5 96-WELL TRANSFECTIONS WITH DRUG RESPONSE

For reverse transfection, 0.5 µl of 20 µM stock of each agRNA or siRNA in a volume of 20 µl of serum free RPMI was delivered to each well of 96 well plate using a multichannel repeat pipetter. 0.25 µl of either Dharmafect 1 or 3 (Dharmacon) in 9.75 µl of RPMI was then delivered into each well again using multichannel repeat pipette. RNA-lipid complexes were allowed to form during a 20-30 minute incubation. Following the incubation 8,000 cells were added to each well in RPMI with 5% FBS, total volume per well 100 µl. For dose response to agRNA, complexes were prepared at highest concentration (either 100 nM or 25 nM) and then complexes were eight-fold serially diluted. Drugs were administered 24 hours after transfection as described in section 2.2.2.

2.2.6 WESTERN BLOT

siRNA mediated knockdowns were performed as reverse transfections with 25 nM final siRNA concentration, and a 1:2 lipid to oligo ratio. RNA-lipid complexes were formed in 6 well plates in a volume of 1 ml for a 20 minute incubation period, and then 5×10^5 cells were plated per well in RPMI with 5% FBS in a final volume of 3 ml. 48 hours later, cells were lysed in lysis buffer (40 µM HEPES-NaOH [pH 7.4], 150 µM NaCl, 0.5% Sodium deoxycholate, 1% Nonidet P-40, 0.1% SDS, and Complete mini protease inhibitor [Roche, Mannheim, Germany]), protein concentration determined by Bradford assay (Bio-Rad, Hercules, CA). Protein concentrations were normalized to total protein, and

SDS-PAGE, 10 -15% acrylamide, was performed followed by western blotting of primary antibody (cIAP1, 3180A-100, BioVision, Mountain View, CA; cIAP2, sc-7944, Santa Cruz Biotechnology, Santa Cruz, CA; XIAP, 2042, Cell Signaling, Danvers, MA; HSP90, sc-7947, Santa Cruz Biotechnology). The membranes were then developed with peroxidase-labeled antibodies (Thermo Fisher Scientific, Waltham, MA) by Super Signal chemiluminescence substrate (Thermo Fisher Scientific, Waltham, MA). HSP90 levels were used as a control for equal protein loading.

2.2.7 Enzyme-linked immunosorbant assay (ELISA)

Roughly 100,000 cells were plated per well in a 6 well plate and allowed to adhere overnight. Media was removed and replaced with serum free media containing 2000 nM gemcitabine, 1000 nM vinorelbine, 10 μM JP1201, or 1000 nM vinorelbine + 10 μM JP1201. 300 μL conditioned media was removed at 12, 24, 48, 72, and 96 hours after drug treatment. ELISAs were performed per manufacturer instructions (Abcam, Cambridge, MA). Samples were run in triplicate and data shown is the average of at least two separate experiments.

2.2.8 Mouse Xenograft Treatment Studies

Mouse work followed an IACUC approved protocol. NCI-H1395 and NCI-H157 cells were gently trypsinized, washed, and counted using trypan blue exclusion to assess viability. Cell suspensions with viability greater than 95% were used in animal studies. Subcutaneous tumors were established in

NOD/SCID mice as described (Dineen et al., 2010). Briefly, NCI-H1395 or NCI-H157 cells (1 x 10^6 in 100 μL) were injected subcutaneously on the left flank. Animals were monitored three times a week and tumors measured with digital calipers. Tumor volumes were calculated using the formula (D * 2d * 0.52), where D is the largest diameter and d is the shortest (Euhus, Hudd, LaRegina, & Johnson, 1986). At sacrifice, tumors were harvested and fixed in formalin. Treatment groups (8 mice per group) consisted of saline, 25 mg/kg gemcitabine, 2.4 mg/kg vinorelbine, 6 mg/kg JP1201, 6 mg/kg JP1201 + 25 mg/kg gemcitabine, 6 mg/kg JP1201 + 2.4 mg/kg vinorelbine, 12.5 mg/kg erlotinib, or 12.5 mg/kg erlotinib + 6 mg/kg JP1201; each injection given in a volume of 100 μL administered intraperitoneally (Bonfil, Russo, Binda, Delgado, & Vincenti, 2002; Dineen, et al., 2010). Saline, gemcitabine, and JP1201 were given three times a week, vinorelbine was given twice a week to minimize toxicity, and erlotinib was given by oral gavage every 12 hours (Bonfil, et al., 2002; Dineen, et al., 2010).

2.2.9 qPCR ANALYSIS OF siRNA KNOCKDOWN EFFICIENCY

Transfections were performed as described above with the exception of RNA-lipid complexes were formed in 6 well plates in a volume of 1 ml for a 20 minute incubation period, cells were plated at 70% confluency. 24 hours later, cells were harvested and total RNA prepared (RNeasy Plus Mini Kit, Qiagen, Hilden, Germany). cDNA was synthesized from 1 μg total RNA using the iScript

cDNA synthesis kit (BioRad, Hercules, CA). Gene specific TaqMan probes (Applied Biosystems, Foster City, CA) were used to quantitate GAPDH, cIAP1, cIAP2, XIAP, Caspase-3, -4, -8, and -9, RIPK1, TNFR1, and TNFα levels in biological duplicates as well as duplicate samples of siRNA transfected H1395 cells. The $2^{-\Delta\Delta CT}$ method was used to calculate relative expression levels (Livak & Schmittgen, 2001).

2.2.10 Microscopy

Formalin-fixed tissues were embedded in paraffin and cut in 10 μm sections and stained with hematoxylin & eosin. Immunofluorescent staining of xenograft tumor sections for rabbit anti- human TNFα (ab6671, Abcam, Cambridge, MA) was performed at 5μg/mL conjugated to rabbit-FITC secondary antibody (11-095-144, Jackson ImmunoResearch Laboratories Inc, West Grove, PA). Quantification of TNFα staining for each treatment group was performed by taking the average FITC signal across three fields each from three separate xenograft tumors. TUNEL staining was performed per manufacturer instructions (Promega, Madison, WI) on paraffin embedded tumor sections from three tumors per treatment group with data averaged from three images per slide, three slides per treatment group. Images of stained slides were taken using an Eclipse TE2000 epifluorescent microscope (Nikon). ImageJ (NIH) software was used to produce overlaid images of DAPI and antibody staining.

2.2.11 Luciferase Reporter Assay

Pathway analysis was performed using the Stress and Toxicity Cignal Finder 10 pathway reporter array (SA Biosciences, Fredrick, MD) following the manufacturer's instructions. Sixteen hours after cells were reverse transfected, they were treated with 1 μM vinorelbine with 10 μM JP1201 or 10 μM JP1201 as control, then incubated for an additional 24 hr. Luciferase activity was measured using the Dual Luciferase Assay system (Promega, Madison, WI) on a FLUOstar omega (BMG Biotech, Offenburg, Germany). Firefly luciferase was the experimental reporter and Renilla luciferase was the normalizing reporter, samples were further normalized to non-transfected control cells.

2.2.12 MICROARRAY

Transcript expression data for most lung cancer cell lines has been previously generated in the Minna Lab by both Affymetrix (U133 plus 2.0 and U133AB chips) and Illumina (WG6-V2 and V3 BeadChips) array platforms.

MATRIX (MicroArray Transformation in Microsoft Excel) software 1.482 is a Microsoft Visual Basic program with Microsoft Excel interface that was created by Dr. Luc Girard (luc.girard@utsouthwestern.edu) in the Minna Lab, was used to import and analyze microarray expression data. Three bioinformatics functions contained within MATRIX were used in these studies; gene correlation, subarray with a partial gene list, and class prediction. The gene correlation function calculates pearson correlations for sample properties (such as drug response to chemotherapy combinations) to gene expression. The subarray

with partial gene list function creates a new matrix (.mtx) file with a user defined gene list, which was used to create a subarray containing only genes that are involved in the NF-κB and apoptosis pathways. The results from both of these two functions can be further clustered using hierarchical clustering analysis. The class prediction function takes class data input (synergism [given a value of 1] or antagonism [given a value of 0]) for a "training" set of cell lines and creates a signature based on gene expression patterns from the cell lines indicated, and then applies that signature to predict synergism or antagonism in a "test" set of cell lines, to which the training set can be added to see how accurate the predictions are.

2.3 Statistics

2.3.1 Combination Index

Combination indicies (CI) for the drug sensitivity data were calculated using the Chou-Talay method (Chou & Rideout, 1991). Briefly, an effect level was chosen (40%) and doses were calculated for each drug alone (where DX1 is the chemotherapy and DX2 is JP1201), then doses were measured for each drug in combination with JP1201 that gave the chosen effect level (D1, D2). CI were then calculated using the following equation:

Where CI<1 Synergy, CI=1 Additivity, and CI>1 Antagonism. Standard deviations were calculated based on drug sensitivity data. Data from the xenograft studies were analyzed using GraphPad software (GraphPad Prism version 5.02, San Diego, CA, www.graphpad.com). Results are expressed as mean ± SEM. Data was analyzed by t-test or ANOVA and results are considered significant at $p < 0.05$.

2.3.2 Analysis of Variance (ANOVA)

ANOVA is a statistical test to determine if more than two groups are different by calculating if the variance within a group is different between the variance between groups.

2.3.3 Pearson Correlation

Pearson correlation (r) is a statistic test for linear dependence of two variables, values range from -1 to 1, is defined as the covariance of two variables divided by the product of their standard deviations, or for a given sample

CHAPTER THREE

PLATINUM BASED COMBINATION CHEMOTHERAPY

3.1 INTRODUCTION

Chemotherapy is a treatment option for tumors that are at least stage 2, which accounts for roughly 85% of NSCLC patients. The current mainstay of chemotherapy treatments for NSCLC consists of platinum based doublets, where either cisplatin or carboplatin are used in conjunction with a third generation chemotherapy agent, usually paclitaxel, gemcitabine, pemetrexed, vinorelbine, or docetaxel. These doublets arose from clinical trials where cisplatin was used in combination with new third generation chemotherapy and compared to best supportive care, or the third generation chemotherapy alone, or an older platinum based doublet (Non-small Cell Lung Cancer Collaborative, 1995; Pass, et al., 2010; Pass, et al., 1992). The most common rational for combining these agents was to pair chemotherapies that had different dose limiting toxicities. Since all these chemotherapies were already FDA approved, there was little to no preclinical testing to address these combinations.

Two major trends in therapeutic oncology research are developing new anti-cancer agents, or personalizing existing therapies. When references are made to personalized therapy what is meant is the ability to sample a patient's tumor and based on molecular profiling of that sample be able to determine which chemotherapeutic regimen that patient's tumor would respond best to.

In order to be able to personalize therapy, the range of responses for a particular cancer type need to be well defined in a large sample set, i.e. a large panel of cell lines. The responses then need to be correlated to other measurable parameters that also define the tumor state, such as mRNA gene expression profiles, protein expression and phosphorylation data, and other similar sets of data. The resulting correlations between expression profiles and response data (often called signatures of resistance or sensitivity) need then to be verified in a separate large sample set, to see how well the signatures predict response in a new set of samples. If the signatures predict response fairly accurately in the test set, then the signatures are then tested against different types of sets of data, response of cell line xenografts in mice, response of primary tumor samples grown solely as xenografts in mice, blinded retrospective analysis of patient data where expression profiles are available, etc.

In order to make combinations of chemotherapy more effective, it is important to know what effect current combinations have in the model system that will be used. To do this, three platinum based doublets were screened across a large panel of NSCLC cell lines, approximately 50 lines, initially using MTS based 96-well plate drug response assays to catalogue the responses to the combinations gemcitabine + cisplatin, paclitaxel + carboplatin, and pemetrexed + cisplatin.

3.2 METHODS

In order to best model the combinations, gemcitabine + cisplatin, paclitaxel + carboplatin, and pemetrexed + cisplatin, the ratio of non-platinum agent to platinum agent was calculated for each combination, for example, gemcitabine + cisplatin is usually dosed at 1250 mg/m^2 gemcitabine and 100 mg/m^2 cisplatin (Cardenal, et al., 1999).

molar ratio the corresponding amount of cisplatin was calculated at 140 nM. Using these values the molar ration was calculated to verify these amounts.

With these ratios set for each combination, the non-platinum drug was set as the limiting reagent in each case; the highest concentration of platinum agent was calculated based on the in vitro highest dose of each non platinum agent (Table 3.1).

3.3 RESULTS

A panel of 53 NSCLC cell lines was tested for drug response phenotypes to the combinations of gemcitabine with cisplatin, pemetrexed with cisplatin, and paclitaxel with carboplatin using an MTS based assay to determine cell viability relative to a control population of cells that had undergone the same handling as the drug treated cells. There was great heterogeneity in response to these combinations across the panel of cell lines (Table 3.2). When the data across the whole panel is shown as a dot plot where the IC_{50} for each cell line is a dot and the x-axis is the $\log_{10}$ of the concentration of chemotherapy, the overall spread of IC_{50}s of the panel of NSCLCs does not change; however, overall the spread shifts to the left with less cell lines being completely resistant to treatment (Figure 3.1). The combination of pemetrexed + cisplatin is the only combination in which no cell lines are resistant up to the highest dose of chemotherapy given.

Approximately 26% of the cell lines tested responded better to the combination of gemcitabine + cisplatin than the drugs as single agents, while 8% seemed to have a better response to either agent singularly.

15% of cell lines respond better to the combination of paclitaxel + carboplatin than to either drug as a single agent. While 26% of cell lines responded better to single agent paclitaxel or carboplatin treatment than to the combination, the majority of cell lines responded similarly to single agent paclitaxel as to the combination of paclitaxel + carboplatin.

Pemetrexed with cisplatin was the most "successful" combination regimen explored in this study in that over 50% (52%) of the cell lines tested responded better to the combination, than to either drug as a single agent. Conversely, this combination also has the highest rate of cell lines responding better to either agent as a single agent than the combination with 23% of cell lines responding better to single agent treatment. These data suggest that while pemetrexed given in combination with cisplatin can be a very successful treatment for some patients, it might also be detrimental to other patients, which encourages our goal of being able to predict which therapy is best suited for each patient.

6% of the cell lines responded better to all three combinations. 4% of the cell lines responded better to both the combination of paclitaxel with carboplatin and pemetrexed with cisplatin, but not with gemcitabine with cisplatin. 20% of the cell lines responded better to the combination of cisplatin with gemcitabine or pemetrexed, but not to the combination of paclitaxel and carboplatin. These data suggest that combining DNA damage agents or drugs that result in similar cell cycle checkpoint/apoptototic stimuli are more commonly successful in treating

lung cancer than combining drugs that target different steps in the cell cycle or initiate apoptosis in different manners. Only one cell line tested responded better to these chemotherapies as single agents than to any of the combinations tested.

3.3.2 Statistical Analysis for Synergy

These data, along with single agent drug response data within the lab, were used to calculate the combination index (CI) at the 40% cell death as the effect level (Chou & Rideout, 1991). 32% of cell lines tested showed synergism to the combination of paclitaxel and carboplatin, while 34% of the cell lines show antagonism to the combination, and the remaining 34% show additivity or no real effect between the combination of these two agents (Figure 3.2). Surprisingly most of the cell lines (60%) showed synergism to the combination of gemcitabine with cisplatin, while only 17% showed antagonism, and the remaining 23% showed additivity. The combination of pemetrexed with cisplatin showed synergism in 40% of the cell lines tested, and 38% of the cell lines showed antagonism, and only 22% showed additivity.

While it would be easy to assume that seemed to have a response as seen by IC_{50} directly or in fold change; however, that is just taking one variable into consideration while there are two drugs to consider for each combination. And while that assumption might work out decently well for the combinations of paclitaxel + carboplatin or gemcitabine + cisplatin because the platinum based

drug is given at a much lower level than single agent activity is seen on *in vitro*, the assumption does not work out well at all for the combination of pemetrexed + cisplatin because both agents are given on the micromolar (1×10^{-6} M) scale as single agents as well as in the combination. Another factor to consider is the experimental error involved in the drug dilution and comparing drug data collected over time, there can be up to a fourfold variation in the drug responses seen, so when evaluating these data by fold decrease in IC_{50} of one chemotherapy anything over a fourfold decrease in IC_{50} is considered a real effect; however this consideration is not able to be applied to the CI data, which is why more cell lines seem to be responding synergistically to the combination.

3.3.3 Confirmation of MTS data using colony formation

Upon repeating drug treatment using colony formation as the readout instead of MTS for a subset of cell lines, IC_{50} values were similar between the two assays, cell lines were always more sensitive to paclitaxel + carboplatin in colony formation (Table 3.3). This is likely due to the longer time frame that cells are exposed to paclitaxel in colony formation making the cells seem more sensitive, but cell death from paclitaxel is highly time sensitive. Another factor at play is the short time span of the MTS assay and that during the 96 hours that cells are exposed to drug, most cell lines only go through two population doublings, or one for the extremely slow growing cell lines, which makes these

slow growing cell lines seem artificially resistant to paclitaxel in an MTS assay especially when compared to drug response determined by colony formation.

3.3.4 Predictive Value of Signatures of Synergy

Using synergy and antagonism as fixed integers of 1 and 0 respectively, the ability of these data to create signatures has been explored using MATRIX. Unfortunately, using microarray data for this is not predictive by leave one out cross validation or in a test set where the results are already known. Many statistical approaches using MATRIX were tried; random forest, k nearest neighbor, support vector, and penalized linear regression (Figure 3.6-3.8).

One of the possible reasons for the lack of predictability from these data is that most prediction algorithms use two groups to make the predictions, however these data don't fit a two group model, there isn't just a sensitive and resistant group, instead there is more a general continuum of response to the combinations.

3.4 Discussion

Most patients that are seen for advanced NSCLC are treated with a platinum based chemotherapy combination regimen as part of their treatment course. And with the 15% 5-year survival rate, it is obvious that most of these patients either do not respond to treatment, or initially respond but progress and eventually the disease takes over. With the exception of the pemetrexed + cisplatin, these combinations are fairly toxic overall to the patient, with near MTD

doses of each chemotherapy given in the combination. Another drawback is that these large doses of chemotherapy often lead to chemotherapy induced leukemias. There is no basis on which a patient is given one of these platinum based regimens, it is purely at the doctor's discretion.

Single agent cisplatin and carboplatin tested across the 53 NSCLC panel yield one normal distribution of response, and when cisplatin is combined with gemcitabine at a fixed 7:100 molar ratio, the two distribution response to gemcitabine becomes one distribution in response to the combination. In fact response to gemcitabine across the panel of NSCLCs spans three orders of magnitude, while the combination of gemcitabine + cisplatin only spans ~2 orders of magnitude (Figure 3.1). Single agent paclitaxel and pemetrexed responses across the NSCLC panel results in two normal distributions, which are kept when combined with carboplatin and cisplatin respectively; however in all cases of the combination, the cell lines that were most sensitive to gemcitabine, paclitaxel, and pemetrexed as single agents are slightly less sensitive to that agent in the combination with platinum.

The majority of cell lines (68, and 60% respectively) showed additivity or antagonism to the combinations of paclitaxel + carboplatin and pemetrexed + cisplatin, suggesting that many patients are not receiving added tumor kill from getting combination chemotherapy, or that they are receiving the wrong combination of chemotherapeutic agents.

This study endeavored to use cell lines as surrogates for tumors and catalogue the response to gemcitabine + cisplatin, paclitaxel + carboplatin, and pemetrexed + cisplatin, and then using mRNA expression data on the cell lines to build signatures of response to each combination, and be able to use said signatures to predict response of other cell lines, and hopefully be able to use these signatures clinically as a method of personalizing therapy. The signatures created are not predictive using a test set of NSCLCs that were not used in the initial training set but that drug response to the combinations has been performed. One concern is that the signatures are made from mRNA profiling that was performed with untreated cells, it could be that mRNA profiling after treatment would also be needed and then subtracted from untreated cells, giving a profile of gene changes from treatment and then signatures of synergistic cell lines vs antagonistic cell lines could be more informative. Another concern is that mRNA profiling is a static measure, but response to drugs is a dynamic process and would require a different measure of a cell's properties, such as epigenetic profile (ie catalogue of current epigenetic marks and protein levels of HATs, HDACs, HMT's HDMs, DNMTs) especially since epigenetics have been implicated in drug resistance (S. V. Sharma et al., 2010).

This startling result of high amounts of antagonism to conventional chemotherapy combinations on NSCLC cell lines emphasizes the need for improved combination strategy.

	Gemcitabine/Cisplatin		Paclitaxel/Carboplatin		Pemetrexed/Cisplatin	
Plate Column #	Gemcitabine nM	Cisplatin nM	Paclitaxel nM	Carboplatin nM	Pemetrexed µM	Cisplatin µM
1	-	-	-	-	-	-
2	0	0	0	0	0	0
3	0	0	0	0	0	0
4	0.12	0.009	0.06	0.2	0.06	0.018
5	0.48	0.034	0.24	0.9	0.24	0.07
6	1.96	0.14	0.98	3.4	0.98	0.3
7	7.8	0.6	3.9	13.7	3.9	1.2
8	31.2	2.2	15.6	54.7	15.6	4.7
9	125	8.75	62.5	219	62.5	18.63
10	500	35	250	875	250	74.5
11	2000	140	1000	3501	1000	298
12	-	-	-	-	-	-

TABLE 3.1 Drug dosages for agents in platinum based chemotherapy combination regimens.

	Carboplatin		Cisplatin		Gemcitabine		Gemcitabine/ Cisplatin		Paclitaxel		Paclitaxel/C arboplatin		Pemetrexed		Pemetrexed/ Cisplatin	
Cell Line	IC50	SD	IC50	SD	IC50	SD	IC50	SD	IC50	SD	IC50	SD	IC50	SD	IC50	SD
A549	19.5	3.3	3	0.96	6.85	3.1	31	2	6.4	6.9	18	5.5	0.24	0.12	0.625	0.15
Calu-1	99	3.3	4.15	3.1	53.5	960	215	160	7.8	0.91	11	1.6	1000	0	40	4
Calu-3	42	17	1.9	0.45	13	26	6.3	0.52	1.49	0.94	1.87	1.2	1000	0	4.15	1.7
Calu-6	27.5	6.1	0.91	0.15	13.5	5.6	8.35	3.5	12.6	9.9	3.1	1.5	0.068	520	0.055	0.006
H1155	6.35	0.43	1.35	0.46	2.3	0.12	4.15	1.4	7.1	3.9	9.85	0.38	0.047	0.024	0.044	0.007
H1299	29.5	10	2.05	0.96	2.45	2.6	9.9	8.2	7	6.2	9.1	2.6	0.19	580	0.22	0.013
H1355	66.5	23	4.7	1.3	6	1.4	5.95	3.4	6.4	2.9	2.95	2.2	1000	0	7.85	1.3
H1395	24	2.9	3.85	2.1	1070	1000	9.15	3.6	140	510	25.5	1.7	1000	0	4.5	1.1
H157	28.5	10	2.5	1.2	5.6	3.4	6.5	0.68	2.05	1.5	3.35	1	0.215	0.13	0.535	0.36
H1648	49.5	12	4.9	2.1	27	990	11.5	5.7	5.25	14	4.25	2.4	1000	350	22.5	5.3
H1650	31.5	2.4	3.55	1.3	12.3	3.3	7.4	2.2	47.5	21	3.8	0.2	1000	0	6.5	0.82
H1693	57.5	7.9	4.7	1.2	1.03	0.74	1.9	0.29	4.4	1.1	2.55	2.5	0.048	410	0.041	0.003
H1770	19.5	2.9	1.9	4.4	13	3.8	8.35	4	7.65	410	3	0.44	0.54	1.3	2.65	2.5
H1819	110	21	9.3	2.9	43	870	9.45	2.1	11	6.5	8.6	2.3	1000	0	0.052	0.005
H1975	39	5.8	3.8	1.5	7.6	6	5.1	1.2	1.6	0.44	6.2	1	1000	520	5.1	0.93
H1993	160	55	8.2	3	6.1	2.3	4.8	2.2	2.9	1.7	5.65	1.3	0.04	0.018	0.056	0.002
H2009	32	16	5.05	11	4.3	21	5.45	2	1.8	1.5	3.3	1.4	0.038	460	17	20
H2073	26	8.3	1.8	0.96	6.55	2.3	5.4	1.7	150	98	135	84	0.109	0.034	0.15	0.01
H2077	32.5	13	2.85	0.38	37	24	23	9.1	3.85	1.8	0.895	0.23	0.024	0.008	0.043	0.015
H2085	57.5	12	10	2.3	1170	710	93.5	21	1000	410	2.9	0.19	0.165	0.067	30	2.6
H2086	50.5	14	4.2	0.79	74	6.2	135	950	1.2	0.06	2.15	0.5	1000	0	11.1	4.2
H2087	5.45	5	0.62	0.27	6.1	10	10.5	1.2	0.64	0.82	4.45	2.1	1000	0	1.3	0.32
H2106	58.5	9.8	4.25	1.1	39.5	13	41.5	6.5	0.5	0.23	0.615	0.51	0.35	13	0.51	0.23
H2126	78	23	4.05	2.5	2000	580	23.5	1.7	10.7	38	8.55	0.99	1000	0	2.45	0.26
H2170	14	0.58	1	0.21	7.3	0.49	6	1.6	2.8	3.6	3.9	0.18	0.14	550	0.18	0.083
H2228	25.5	11	2.65	0.47	11.4	6.3	6.4		0.865	0.81	0.895	0.36	0.048	0.029	0.057	
H2347	43	6.5	3.5	1.3	30.5	23	14	4.4	2.3	2.4	3.65	0.28	0.2	520	10.4	8.2
H2882	26	6.8	2	1.6	330	750	54	24	7.5	3.3	4.15	0.93	1000	170	13.5	2.9
H2887	61	1.7	11	2.4	1020	1100	31	3.3	44	330	63	9.8	1000		79.5	36
H322	129	66	18.5	2.4	2000	0	1010	1100	5.7	0.45	10	0.5	1000	460	22.5	12
H3255	30.5	1.7	2.15	0.96	20	5	6.25	0.35	5.3	1.8	4.6	0.57	0.055	0.045	18.5	1.7
H358	33.5	13	2.7	7	3.2	16	2.55	0.85	1.2	1.2	3.7	1.7	0.022	0.012	10.4	0.94
H441	29.5	3.9	5.85	4.1	40	57	3.7	0.22	2.15	13	5.75	1.3	1000	0	12.5	11
H460	22.5	37	4.7	5.3	3.2	1.4	2.4	0.64	4.6	2.1	6.5	0.7	1000	510	2.4	2.6
H820	13.5	2.1	1.35	0.33	29.5	10	15.6	18	2.75	0.61	7.35	1.1	0.11	0.052	1.66	0.97
HCC1171	83.5	3.6	8.8	12	9	870	1.8	0.17	1000	450	650	470	500	580	5.79	8.2
HCC1195	65	17	5.9	1.5	2000	1100	84.5	17	26	490	6.2	2.4	1000	170	31.1	33
HCC1359	70.5	26	7.3	2.5	42	19	49.5	8.1	54	500	15	3.7	1000	0	4.65	1.5
HCC15	48.5	5.4	6.1	1.8	17	7	7.15	0.24	1.6	0.92	5.3	0.75	0.023	0.008	9.4	1.6
HCC193	90.5	50	12	5	27	770	10.8	3	14	1.7	29.5	8.1	1000	0	0.049	0.012
HCC2279	67	13	8.6	1.7	2000	0	50	40	7.3	2.9	7.25	0.81	1000	0	59.5	3.7
HCC2935	260	18	43.5	7.3	2000	800	2000	0	1000	0	1000	480	1000	0	72.5	27
HCC366	22.5	1.7	4	1.9	11	970	5.05	0.75	16.7	510	1000	500	1000	0	2.95	1.2
HCC4006	72.5	5.7	14	4.9	110	8.2	12.5	2.4	1.95	0.41	3.8	0.15	1000	0	0.049	0.004
HCC4011	53	6.2	5.9	0.98	18	16	6.2	0.63	4.4	1.6	1.83	1.1	1000	0	0.103	8.5
HCC4017	23.5	3.6	3.8	0.89	12	6.9	32.5	1.3	6.1	510	6.1	0.5	0.037	500	0.048	0.002
HCC44	61	2.6	4.4	0.95	72.5	270	120	8.2	5.7	7.2	12	1.2	1000	0	0.16	0.047
HCC461	31.5	4	5.5	6.1	2000	1100	2.38	3.2	30.5	24	3.5	0.3	1000	0	3.55	1
HCC515	59.5	16	2.6	1.6	1010	1100	1.55	0.24	1000	420	13.5	3.2	1000	0	0.195	0.042
HCC78	20.5	3.6	0.65	0.84	16.5	2.1	2.75	0.36	2.4	1.5	3	0.15	0.028	0.002	0.023	0.006
HCC827	36	7.9	2.7	4	7	12	13.5	25	2.2	0.89	6.95	0.29	0.073	0.028	0.151	0.31
HCC95	18	3.4	2.2	1.4	2000	940	4.85	2.3	3.6	2.8	3.4	0.31	0.81	520	1.11	0.4

TABLE 3. 2 IC_{50}s of NSCLC cell line panel to platinum based chemotherapy combinations and each agent as a single agent.

	Gemcitabine/Cisplatin		Paclitaxel/Carboplatin		Pemetrexed/Cisplatin	
Cell Line	Gemcitabine IC_{50}	Cisplatin IC_{50}	Paclitaxel IC_{50}	Carboplatin IC_{50}	Pemetrexed IC_{50}	Cisplatin IC_{50}
HCC4017	6.91192771	0.96	3.010652	10.5	0.00372121	0.0011
H2228	51.2	7.2	0.48	1.68	0.71	0.21
H2087	183	25.6	0.68	2.38		
H1563	0.396	0.055	0.052	0.183		
H1355			0.0023	0.008		
HBEC30KT	0.69	0.097	0.606905	2.12	0.005	0.0014
HBEC34KT	1.04	0.145	0.651926	2.28	0.005	0.0014

TABLE 3.3 IC_{50}s of platinum based chemotherapy combinations in colony formation.

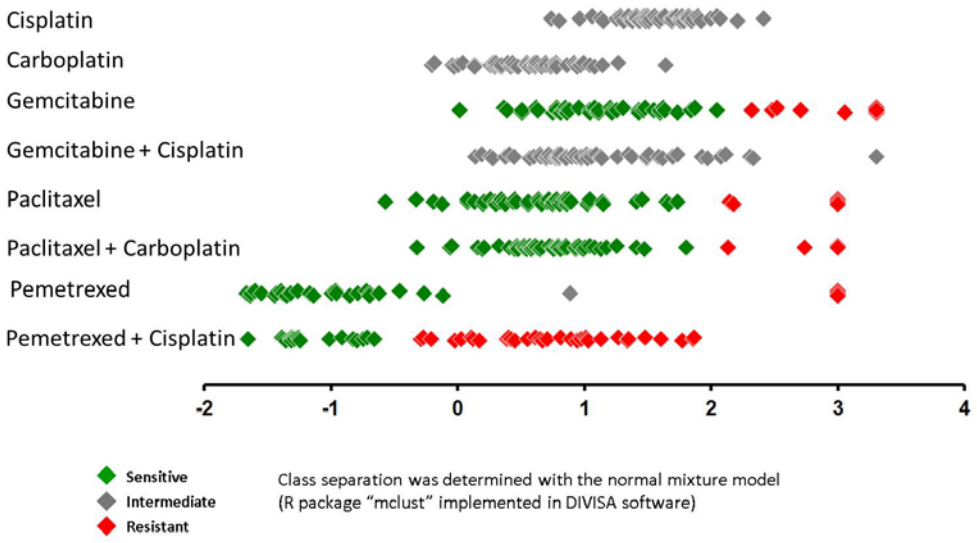

FIGURE 3.1 NSCLC Cell Line Drug Response Phenotypes to Gemcitabine + Cisplatin, Paclitaxel + Carboplatin, Pemetrexed + Cisplatin, and to Each Agent as a Single Agent.

Plot of IC_{50} data for a panel of 53 NSCLC cell lines for carboplatin, cisplatin, gemcitabine, paclitaxel, pemetrexed, gemcitabine + cisplatin, paclitaxel + carboplatin, and pemetrexed + cisplatin on a log scale of concentration of chemotherapy. Each symbol represents the average IC_{50} value for several MTS concentration curve assays ($n \geq 3$) to determine drug response phenotype. These phenotypes were stable ($r > 0.70$) on tests performed at different times.

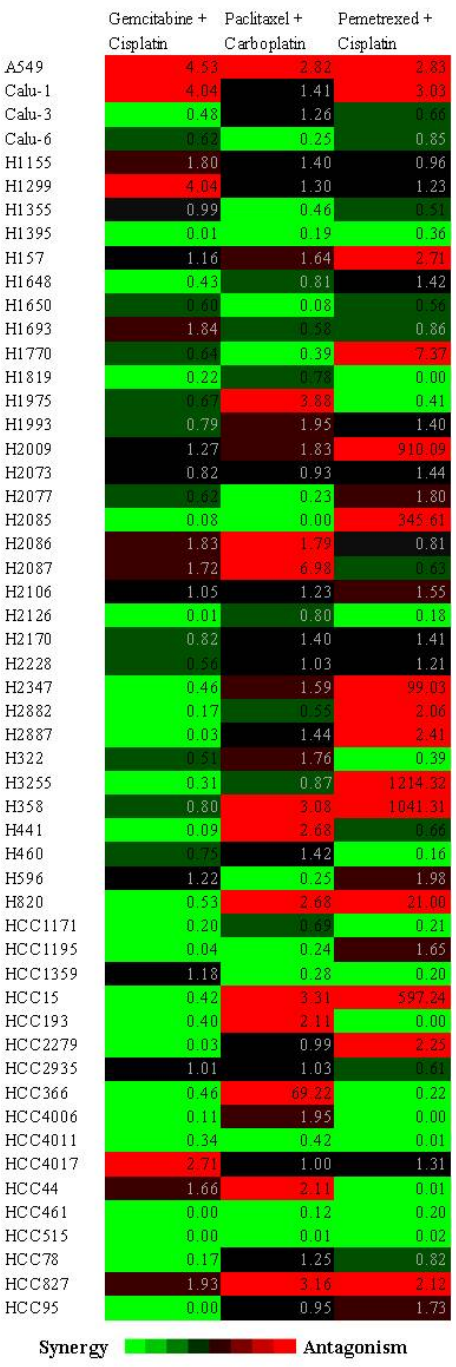

FIGURE 3.2 Combination Index Values for NSCLC Panel Treated with Gemcitabine + Cisplatin, Paclitaxel + Carboplatin, or Pemetrexed +

Cisplatin. Combination Index calculated for gemcitabine + cisplatin, paclitaxel + carboplatin, and pemetrexed + cisplatin.

Combination indices (CI) were calculated using the Chou-Talay method (Chou & Rideout, 1991). Briefly, an effect level was chosen and doses were calculated for each drug alone, then doses were measured for each drug in combination that gave the chosen effect level. These were then plugged into the CI equation and standard deviations were calculated based on the drug sensitivity data; CI<1 Synergy, CI=1 Additivity, CI>1 Antagonism. Green colored cells show synergy, red colored cells show antagonism, and black colored cells show additivity.

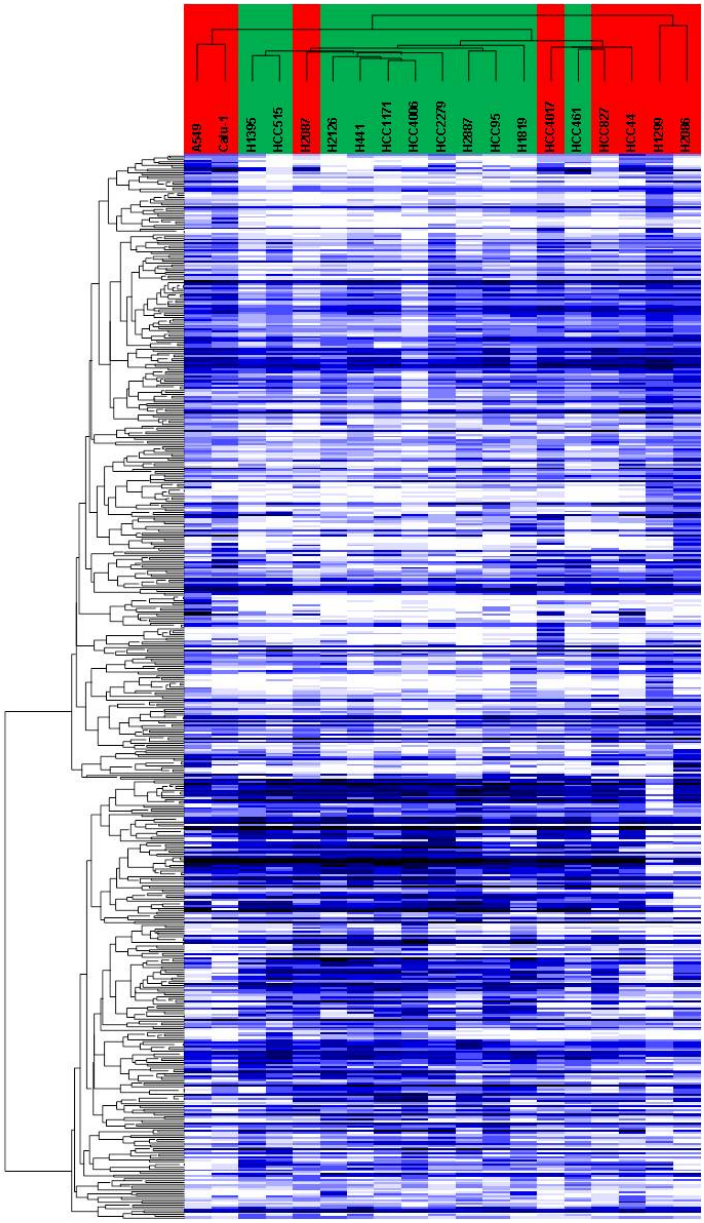

FIGURE 3.3 Hierarchical Clustering Analysis of mRNA Expression Data that Correlates with Synergism or Antagonism to the Gemcitabine + Cisplatin Combination.

Unsupervised clustering analysis is for both NSCLCs on the horizontal axis and genes on the vertical axis. Of approximately of 47,000 genes on the Illumina Human WG-6 v3, 567 genes correlate with synergy and antagonism ($p \leq 0.05$). Each column is a cell line and each row a gene. Gene expression levels are indicated by the coloring with blue being high expression and white being no expression.

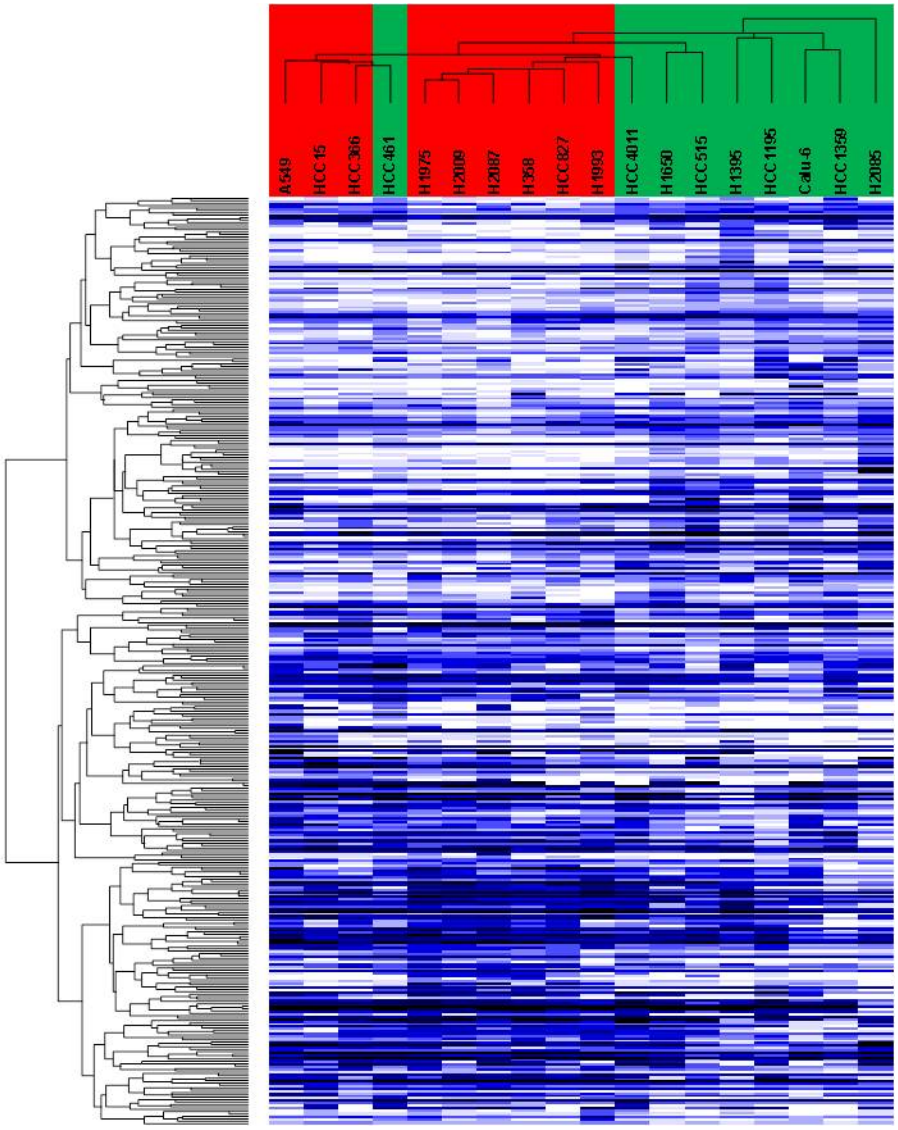

FIGURE 3.4 Hierarchical Clustering Analysis of mRNA Expression Data that Correlates with Synergism or Antagonism to the Paclitaxel + Carboplatin Combination.

Unsupervised clustering analysis is for both NSCLCs on the horizontal axis and genes on the vertical axis. Of approximately of 47,000 genes on the Illumina Human WG-6 v3, 387 genes correlate with synergy and antagonism ($p \leq 0.05$). Each column is a cell line and each row a gene. Gene expression levels are indicated by the coloring with blue being high expression and white being no expression.

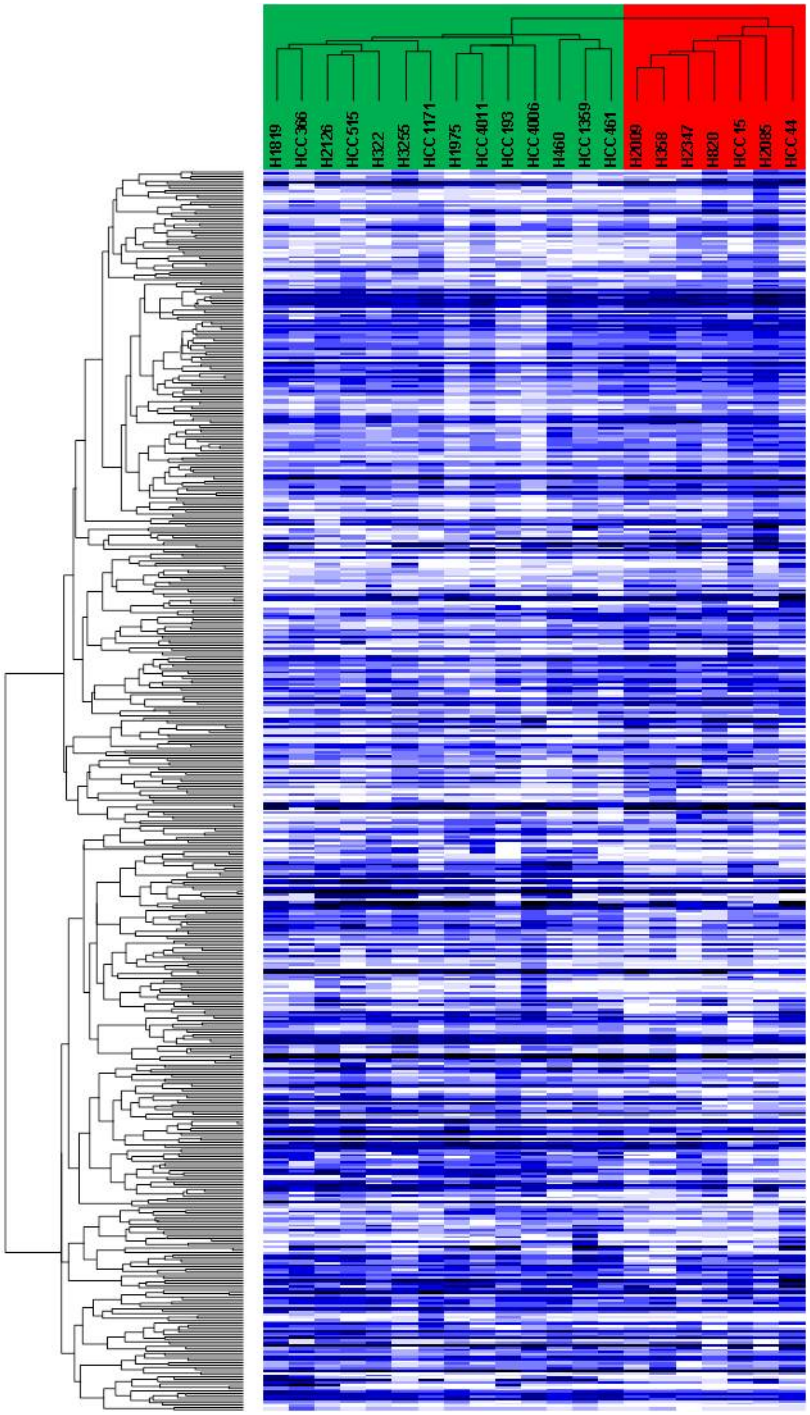
H1819
HCC366
H2126
HCC515
H322
H3255
HCC1171
H1975
HCC4011
HCC193
HCC4006
H460
HCC1359
HCC461
H2009
H358
H2347
H820
HCC15
H2085
HCC44

FIGURE 3.5 Hierarchical Clustering Analysis of mRNA Expression Data that Correlates with Sensitivity or Resistance to the Pemetrexed + Cisplatin Combination.

Unsupervised clustering analysis is for both NSCLCs on the horizontal axis and genes on the vertical axis. Of approximately of 47,000 genes on the Illumina Human WG-6 v3, 529 genes correlate with synergy and antagonism ($p \leq 0.05$). Each column is a cell line and each row a gene. Gene expression levels are indicated by the coloring with blue being high expression and white being no expression.

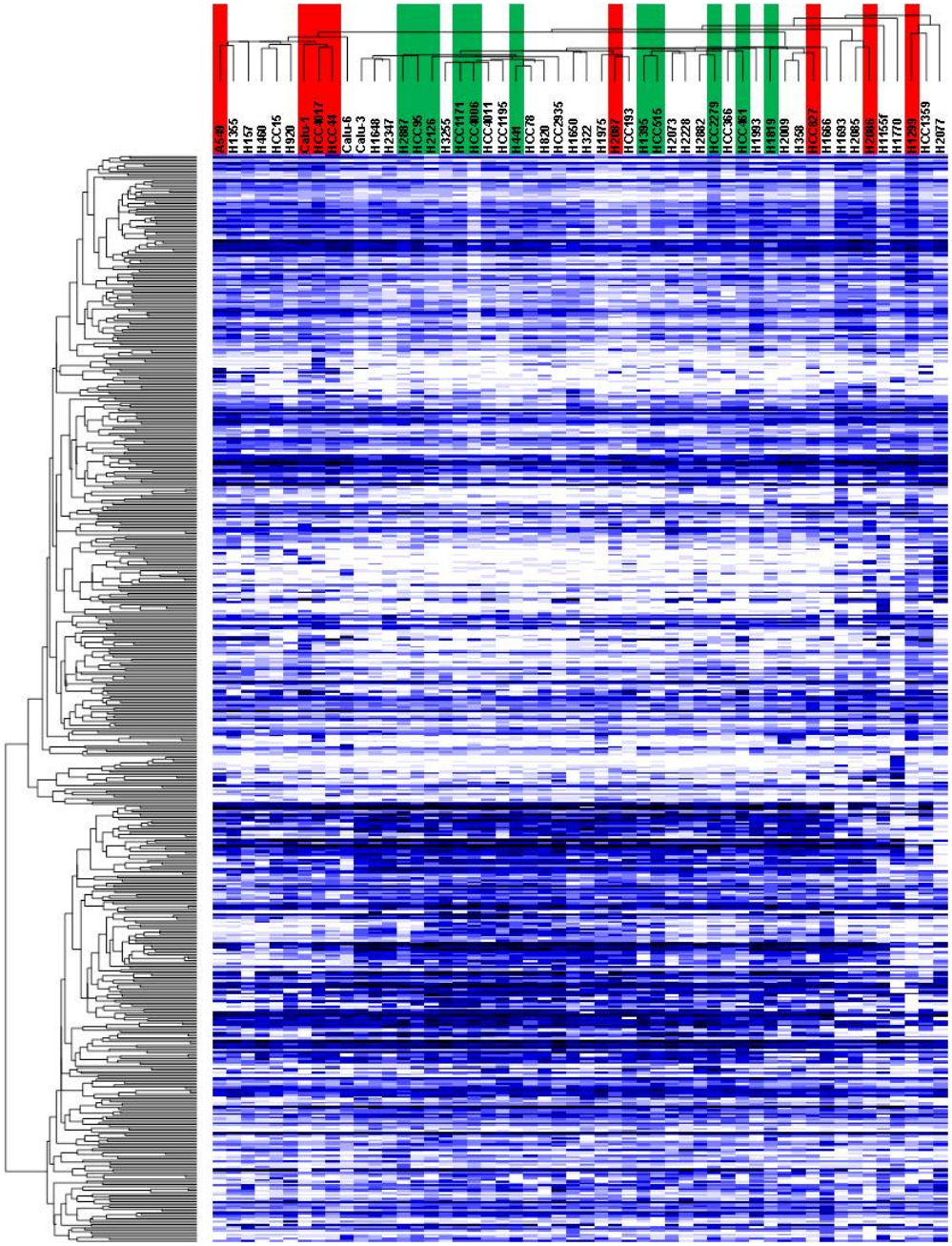

FIGURE 3.6 Hierarchical Clustering Analysis of mRNA Expression Data Correlating Combination Effect of Gemcitabine + Cisplatin in an Effort to Predict Response.

Unsupervised clustering analysis is for both 53 NSCLCs on the horizontal axis and 387 genes on the vertical axis. Each column is a cell line and each row a gene. Gene expression levels are indicated by the coloring with blue being high expression and white being no expression.

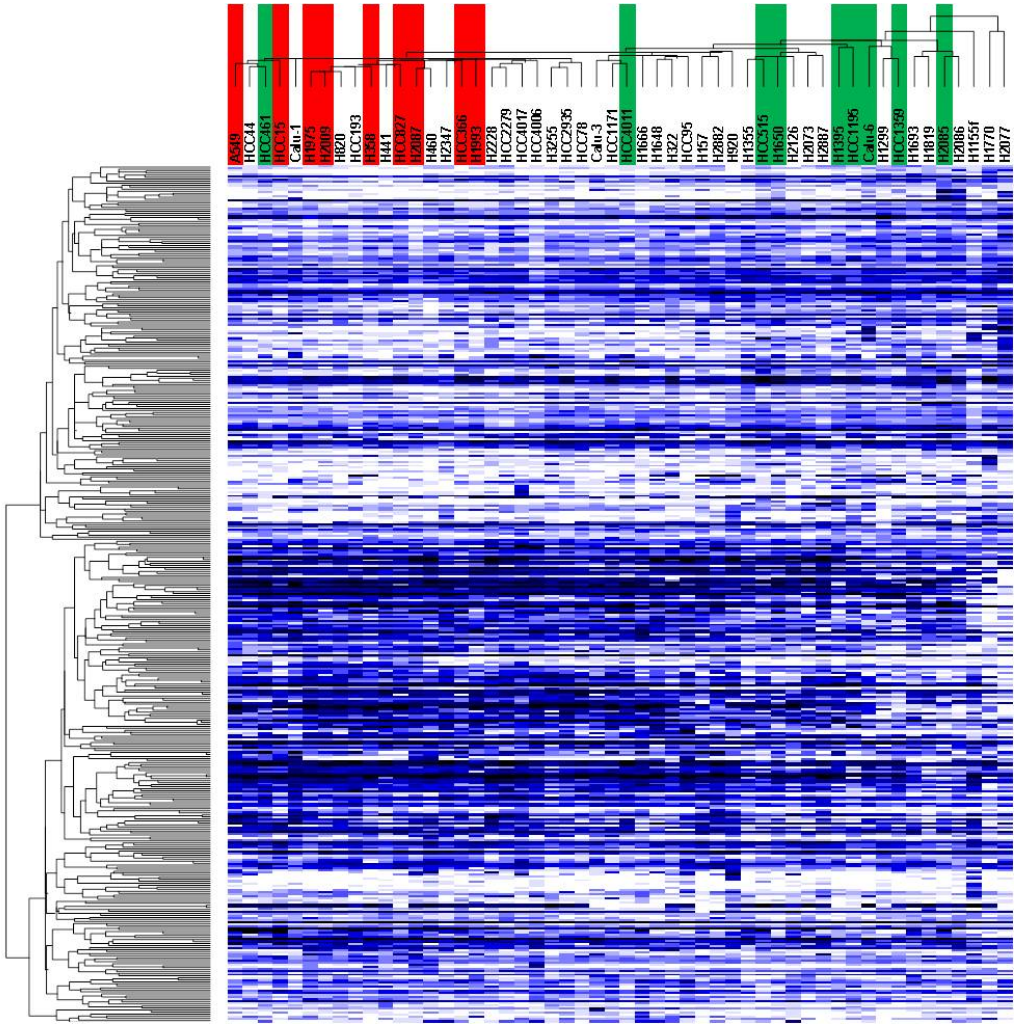

FIGURE 3.7 Hierarchical Clustering Analysis of mRNA Expression Data Correlating Combination Effect of Paclitaxel + Carboplatin in an Effort to Predict Response.

Unsupervised clustering analysis is for both 53 NSCLCs on the horizontal axis and 567 genes on the vertical axis. Each column is a cell line and each row a gene. Gene expression levels are indicated by the coloring with blue being high expression and white being no expression.

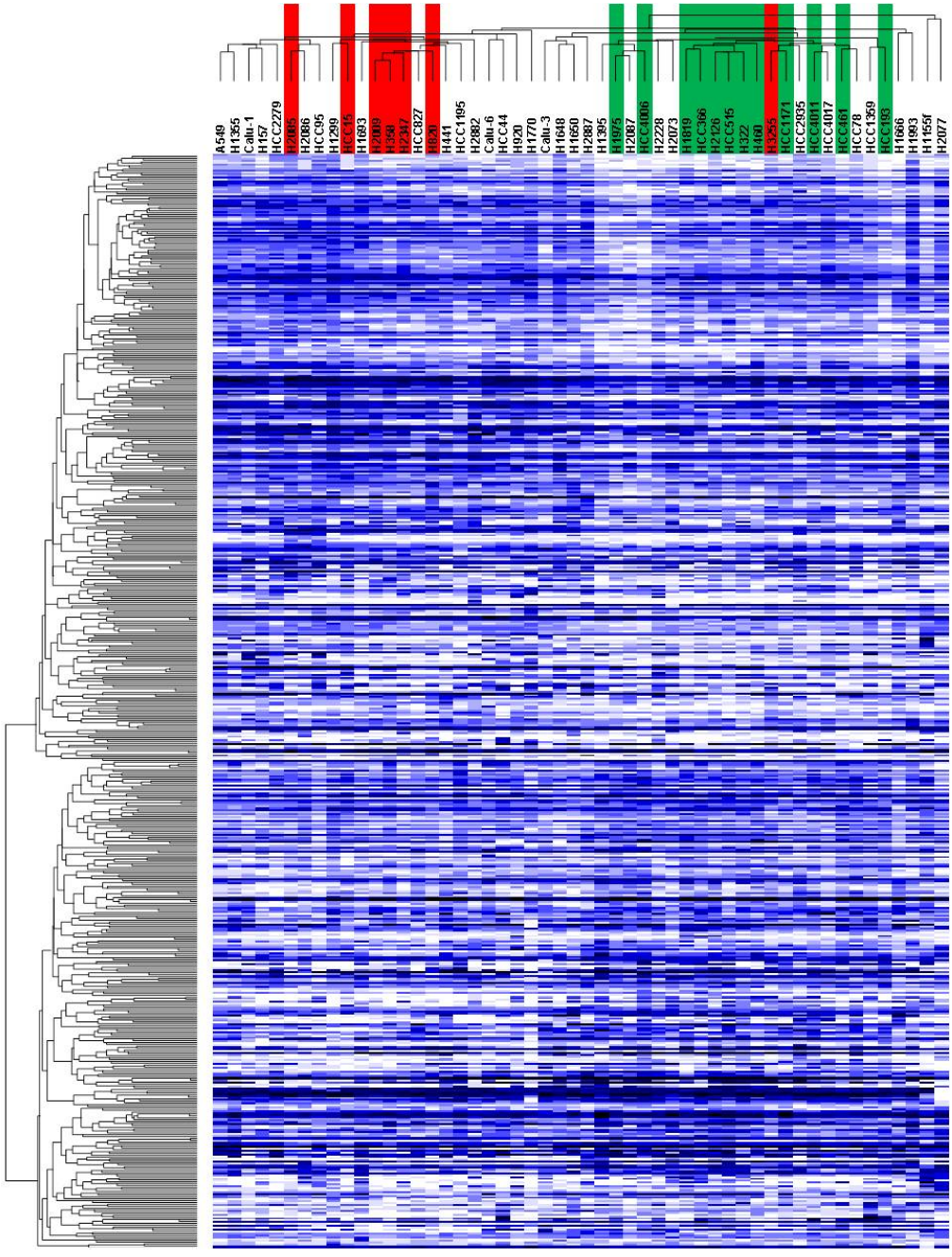
A549
H1355
Calu-1
H157
HCC2279
H2085
H2086
HCC95
H1299
HCC15
H1693
H2009
H358
H2347
HCC827
H820
H441
HCC1195
H2882
Calu-6
HCC44
H920
H1770
Calu-3
H1648
H1650
H2887
H1395
H1975
H2087
HCC4006
H2228
H2073
H1819
HCC366
H2126
HCC515
H322
H460
H1355
HCC1171
HCC2935
HCC4011
HCC4017
HCC461
HCC78
HCC1359
HCC193
H1666
H1963
H1155f
H2077

FIGURE 3.8 Hierarchical Clustering Analysis of mRNA Expression Data Correlating Combination Effect of Pemetrexed + Cisplatin in an Effort to Predict Response.

Unsupervised clustering analysis is for both 53 NSCLCs on the horizontal axis and 529 genes on the vertical axis. Each column is a cell line and each row a gene. Gene expression levels are indicated by the coloring with blue being high expression and white being no expression.

CHAPTER FOUR

TARGETED MOLECULAR BIOLOGY APPROACHES TO RATIONALLY DESIGNED COMBINATIONS

4.1 INTRODUCTION

Approximately only 10% of the human genome encodes for druggable target proteins half of which are relevant to disease, thus limiting the ability to selectively target cancer cells (Owens, 2007). However, advances in molecular techniques, including the discovery of the RNA interference (RNAi) pathway, have made it possible to modulate, at the expression level, any gene. In the RNAi pathway a double stranded RNA molecule, usually ~21-23 nt often called small interfering RNAs (siRNAs) that shares complementarity with a particular gene's mRNA, the degree of complementarity being the deciding factor to the type of inhibition of gene expression. If the siRNA shares 100% complementarity with the mRNA, it results in mRNA degradation; however if the siRNA does not share 100% complementarity with the mRNA, the mRNA is not degraded, but translation of the mRNA is blocked (Davidson & McCray, 2011; X. Liu et al., 2011). Micro-RNAs (miRNA) are endogenously expressed double stranded RNA molecules that are transcribed from the genome and form stem loop structures. These pri-miRNAs are transcribed by RNA polymerase II, and are then processed

by drosha/pasha which are de-branching enzymes resulting in pre-miRNAs. The pre-miRNAs are then exported into the nucleus where they are further processed by dicer into mature miRNAs which get loaded into RNA induced silencing complexes (RISC). Most mammalian miRNA tend to not be 100% complementary to the target mRNA; therefore, work by inhibiting translation, an additional benefit of not being completely complementary is that miRNAs are able to target multiple genes at once. Synthetic siRNAs are designed to have 100% complementarity to the target mRNA. Anti-gene RNAs (agRNA) are similar in chemistry to siRNAs; however, they differ in the intended target, siRNAs target mRNA, agRNAs are designed to target the genomic DNA upstream of transcription start sites (TSS) (Janowski, et al., 2005; Janowski, et al., 2006; Schwartz et al., 2008).

4.2 Altering miRNA levels can influence chemosensitivity in NSCLCs

Cancers not only have deregulation of mRNA and proteins, but also have a deregulation of miRNA expression which can act as oncogenes (oncomirs) or tumor suppressors (X. Liu, et al., 2011). Twenty three cell lines, 10 SCLC, 10 NSCLC, and 3 immortalized HBECs were profiled for miRNA expression on miRNA microarrays with probes for 136 nonredundant human and mouse miRNAs. A profile similarity search was used to identify miRNAs that might be involved in response to gemcitabine, paclitaxel and vinorelbine, three miRNAs were identified; miR19a, miR129, and miR337 (Figure 4.1). In cell lines that are

resistant to paclitaxel, gemcitabine, and vinorelbine express low levels of these miRNAs and conversely cell lines that are sensitive to paclitaxel and gemcitabine express higher levels of these miRNAs.

Could introduction of synthetic miRNA mimetics sensitize resistant cells to gemcitabine or paclitaxel? Conversely would introduction of antago-miRs (synthetic antagonists to miRNAs) into cells that are sensitive to paclitaxel or gemcitabine make these cells more resistant? Using H157, sensitive to paclitaxel and gemcitabine, H1819 and H2887, both of which are resistant to paclitaxel and gemcitabine the ability of altering miRNA levels to regulate response to gemcitabine and paclitaxel was tested. Since vinorelbine, gemcitabine, and paclitaxel were all inversely correlated with miR19a levels, H157 cells were transfected with mock control, a negative control miR, or a synthetic miR19a mimic, and then given a series of doses of gemcitabine, vinorelbine, and paclitaxel. In these cell lines, only treatment with paclitaxel after increase in miR19a levels selectively increased sensitivity to paclitaxel by a ten-fold leftwards shift in the drug response curve (Figure 4.2). To further explore the role of miR19a in response to paclitaxel treatment, and to investigate a potential role of miR337 in paclitaxel sensitivity, H157 cells were again transfected with a negative control miR, miR19a, or miR337, and again saw that increase of miR19a sensitized H157 cells to paclitaxel and saw a similar sensitization by miR337 to paclitaxel (Figure 4.3a). Additionally H157 cells were transfected with a negative

control antagomir, an inhibitor of miR19, or inhibitor of miR337, the inhibitor of both miR19a and miR337 desensitized H157 cells, meaning a right-ward shift in the drug response curve, to paclitaxel by ~6-fold (Figure 4.3b). In H1819 cells that were transfected with a negative control antagomir, an inhibitor of miR19, or inhibitor of miR337 the response to paclitaxel was not altered. However, H1819 cells that were transfected with either the miR19a or miR337 mimic were sensitized 20 fold to paclitaxel (a tenfold shift to the left) (Figure 4.4). Additionally, H2887 cells, which are also resistant to paclitaxel, were transfected with a negative control miR, miR19a, or miR337, treatment with miR19a and miR337 increased sensitivity to paclitaxel by 100 fold (a 100-fold shift to the left in the paclitaxel dose response curve, Figure 4.5). None of the cells IC_{50}s were altered with the miR129 mimic (Figure 4.6).

4.3 Evaluation of specificity of synthetic lethal siRNAs for paclitaxel

Synthetic siRNAs tend to be designed with 100% complementarity to the target mRNA, with a 19-21 nt seed sequence, and a double dT overhang. A paclitaxel synthetic lethal screen was done on H1155 cells with 1 nM dose of paclitaxel used (Whitehurst et al., 2007). Included in this study was confirmation that the candidate genes did not sensitize cells to any chemotherapeutic insult, by testing a few siRNAs and treated with gemcitabine or vinorelbine (Figure 4.7).

As was discussed in the introduction there are many antimitotics, including docetaxel, a structural relative of paclitaxel. Several new anti-mitotics were readily available to test against the paclitaxel synthetically lethal siRNAs, peloruside and diazonamide. Peloruside is a new tubulin binding drug that is water soluble, it binds to α-tubulin as opposed to β-tubulin like the taxanes. Across a panel of 50 NSCLCs peloruside is slightly less potent than the taxanes in vitro. Diazonamide phenotypically acts as an anti-mitotic in that it causes a large G_2/M block; however, it has yet to have been shown to directly bind to tubulin even though many groups have looked into it. The mechanism by which diazonamide works is still unknown; however, across a panel of NSCLCs diazonamide has a very large range of activity, and is more potent than the other anti-mitotics studied.

Ten of the top hits from the paclitaxel synthetic lethal screen were selected to test the hypothesis H1155 would be sensitized to docetaxel, but not peloruside, or diazonamide. For these experiments, H1155 cells were transfected with 20 nM siRNA, and eight wells per siRNA were treated with 1 nM paclitaxel, 1 nM peloruside, 1 nM docetaxel, and 0.1 nM diazonamide (Figure 4.8). Data was normalized to cells that were transfected with luciferase targeting siRNA treated with paclitaxel, peloruside, docetaxel, or diazonamide. Figure 4.9 shows that H1155 cells respond as reported to the indicated siRNAs (Whitehurst, et al., 2007). Not surprisingly, these cells also responded in the same manner to

docetaxel treatment as well as paclitaxel treatment. Additionally, these cells were not sensitized to peloruside at all by transfection of the indicated siRNAs (Figure 4.9). Most surprisingly however, is that two of the six siRNAs tested sensitized H1155 cells to diazonamide.

It was expected that these siRNAs would still be synthetically lethal to docetaxel because docetaxel is a structural analogue of paclitaxel, binds to the same site on tubulin and in theory should have the same activity within a cell. But diazonamide is not known to directly bind to tublin, even though it acts as an anti-mitotic (Williams et al., 2007). In fact, diazonamide' s mechanism of action still remains elusive, but it is clear that diazonamide acts as an anti-mitotic, and clusters with vinorelbine across our panel of NSCLCs by IC_{50} (Figure 4.10).

4.4 TARGETING MUTANT P53 IN NSCLC USING AGRNAS

While the definition of mutations in p53 is rather broad and encompasses p53 null cells, most mutations in p53 are within the DNA binding domain (mDBD-p53), and alter the ability of mDBD-p53 to bind to wild-type p53 response elements. This is not to say that mDBD-p53 is not able to regulate transcription as recent studies have shown that there is a specific subset of p53 target genes that are still regulated by mDBD-p53 (Strano, et al., 2007).

There are three documented TSS for *TP53*, one described in DBTSS, it is the most 3' TSS that is still upstream of the coding region of *TP53*, the TSS described by Lamb et al, and finally the most 5' one described by Bourdon et al

(Figure 4.11) (Bourdon et al., 2005; Lamb & Crawford, 1986). Three agRNAs were designed to target the Lamb and Lane TSS, the agRNAs were designed to be complementary to the -7 nt, -9 nt, or -11 nt from TSS, the oligos targeted to the Lamb TSS (L) were termed L7, L9, and L11, and the oligos targeted to the most 5' TSS were termed N7, N9, and N11. Transfection of H1355 (E285K) cells with L7, N7, or N9 decreases p53 levels, while control oligos do not affect p53 levels (Figure 4.12), but only transfection with N9 caused extensive cell death (data not shown). The induction of cell death was also found in other cell lines that transfection of N9 would cause cell death, so we chose to further pursue the cell death phenotype with N9. All control agRNAs were designed from the sequence of N9, a scrambled N9 (N9-scr), and a mismatch control with four mismatches (M4M), as well as siRNA that would target all potential isoforms of p53 (QsiR) (Table 4.1).

These new oligos were then tested again in H1355 cells, and similarly to the previous experiment, N7 and N9 transfection lowered p53 levels, and QsiR transfection lowered p53 levels so much that p53 could no longer be detected by western blot, while both scr and M4M transfection did not alter p53 levels and only N9 showed toxicity in H1355 (Figure 4.13). In quest of defining the p53 background necessary for N9-induced cytotoxicity, MIA PaCa2 (R248W), Panc1 (R273C, R273H), A549 (wt), and H1299 (null) were transfected with M4M, scr, QsiR, N7, andN9 (Figure 4.14). N7, N9, and QsiR decreased p53 levels in both

A549 and Panc1 cells; however, this was not seen in MIA PaCa2 cells. Most interestingly N9 caused toxicity in both Panc1 and MIA PaCa2 cells, but not in A549 nor H1299 cells. This suggests that knockdown of p53 is not required for cytotoxicity, but that mutant p53 is necessary for cytotoxicity. One possibility is that agRNA^{p53} was reactivating wild type p53 activity in these mutant cell lines.

To examine this possibility agRNA^{p53} was combined with doxorubicin, which normally causes activation of wild type p53, to see if a mutant-p53 containing cell line would be sensitized to doxorubicin. 100 pM N9 when combined with doxorubicin in H1355 results in a 10 fold shift in IC_{50} of doxorubicin in the presence of N9 in these cells compared to 100 nM N7, M4M, and scr (Figure 4.15). Similarly in MIA PaCa2 that were transfected with 100 pM N9, there is a 6 fold shift in IC_{50} compared to cells transfected with 100 nM N7, M4M, or scr, and most strikingly in Panc1 cells (containing mutations in both alleles of p53) there is a 130 fold shift in IC_{50} in cells transfected with 100 pM N9 and treated with doxorubicin compared to cells transfected with 100 nM N7, M4M, or scr and treated with doxorubicin (Figure 4.16).

In order to be able to properly analyze the combination of N9 and doxorubicin, the death induced by agRNA^{p53} needed to be defined and catalogued. To do this, transfections with N9 were done as a concentration curve, to determine the IC_{50} of transfection with N9, in essence treating N9 as a drug. H1355 was found to be sensitive to N9 down to the picomolar range (~10 pM)

(Figure 4.17). These experiments showed that sensitivity (pM) to N9 was dependent on the tumor line expressing mutant p53 as A549 (wt), H358 (null), nor H1299 (null) did not respond to N9 (Figure 4.18). In addition to testing cells by MTS for cytotoxicity by transfection of N9, H1355 (E285K), MIA PaCa2 (R248W), and H1155 (R273H) were transfected with 25 nM N9, M4M, or QsiR, and then plated for colony formation with either 100 cells/well or 1000 cells/well, which confirmed that N9 induces cell death to such an extent that these cell lines ability to form colonies was inhibited after cells were treated with N9 (Figure 4.19). To evaluate how many agRNAs could induce cytotoxicity, agRNAs were used to walk the promoter of *TP53* from -7 to -27 with respect to the Bourdan TSS skipping every other nucleotide. We found that N27 caused the greatest cytotoxicity in H2009 (Figure 4.20). From this point on, all experiments were done with N27 and scr and M4M versions of N27 were designed and synthesized (Table 4.1).

With these new N27 specific oligos, titration curves were done on H2009 (R273L), H358 (null), A549 (wt), H1355 (E285K), SAOS2 (null), MDA-MB-231 (R280K), and HBEC3-KT (wt) with N27 and (N27)M4M (Figure 4.21). H2009 has an IC50 ~600 pM, H1355 has an IC_{50} ~400 pM, and MDA-MB-231 has an IC50 ~100 pM. The only other cell line where an IC_{50} can actually be measured is SAOS2 (20 nM), which due to the high concentration is likely due to off target effects.

To better define the mutations in p53 that result in cytotoxic activity of N27, H157 was used because it has premature stop codon resulting in truncated p53 protein, and H1373 (P47L) was used because it has a mutation in the N-terminal transactivation domain. Using these cell lines, N27and M4M were titrated across these cell lines (Figure 4.22). Only H157 had a measurable IC_{50}, 22.7 nM, whereas H1373 did not respond to N27 up to 25 nM, indicating that the cytotoxicity induced by $agRNA^{p53}$ is dependent on mutant p53 when the mutations are contained within the DBD.

There has been a novel form of p53 reported in which alternative splicing occurs between exon 7 and 9, resulting in the removal of part of the DBD, including residues 257-322 (Rohaly et al., 2005). Potentially $agRNA^{p53}$ could be inducing alternative splicing resulting specifically in an induction of Δp53; however we failed to reliably detect an increase in this isoform (Figures 4.12-14).

Alternatively $agRNA^{p53}$ could be causing a change in the interactions between WRAP53 and p53 mRNA, because WRAP53 is known to regulate p53 response to DNA by agents such a camptothecin or mitomycin c (Mahmoudi, et al., 2009). However, after multiple transfections and q-RT-PCR runs for multiple cell lines, no clear response of WRAP53 was seen in response to N27 (Figure 4.23).

Regulation of pro-apoptosis genes that are thought to be p53 target genes have recently been described as being induced by a long non-coding RNA that is

a target of p53 (LincRNAp21) (Huarte et al., 2010). Using the q-RT-PCR primers previously described, I found that treatment with N27 causes a large induction in LincRNAp21 (Figure 4.24) (Huarte, et al., 2010).

4.5 DISCUSSION

4.5.1 ALTERING MIRNA LEVELS INFLUENCES CHEMOSENSITIVITY IN NSCLCS

During the course of these experiments, the data within the miRNA database (miRbase) has constantly been changing, and as a result the entire sequence of miR19a changed during the course of these studies. Although the data with miR19a was quite promising, it was dropped because there was no way to be sure what the actual sequence of it is.

Although miR129 expression correlated with response to chemotherapy (Figure 4.1), in our hands it does not appear to be functionally related with response to paclitaxel or gemcitabine. Only increasing miR129 levels was tested; however, it is still undetermined if inhibiting miR129 would affect chemotherapy response. This does seem unlikely, because even in the most sensitive line tested, H157, addition of miR19a or miR337 mimics further increased response to paclitaxel.

This study of miRNA induced sensitization to chemotherapy is completely void of any mechanistic data, and while mechanistic data is not per say necessary, it could be quite helpful in predicting possible side effects if increasing tumor

miR337 levels was to be pursued *in vivo*. However, that miR19a specifically sensitizes NSCLCs to paclitaxel, and that miR337 affects multiple NSCLC cell lines dose response curves to paclitaxel very similarly suggests that miR19a and miR337 act through a similar pathway that is dependent on microtubules. Using miRNA target prediction software, or alternatively there are websites (TargetScan www.targetscan.org) where miRNA target predictions are readily available, potential targets for miR337 need to be cross-referenced with proteins that are known to be involved in microtubule dynamics or paclitaxel sensitivity to narrow down the list of potential therapeutic targets of miR337. Alternatively, microarray run on samples from multiple cell lines whose miR337 levels have been altered, both my miR mimics and antagomiRs could shed light on the targets of miR337. One potential pitfall of the microarray experiment is there are likely to be confounding factors between antagomiRs and miR mimics so analysis of those samples would need to be run separately and the two lists compared looking for genes showing up on both lists. And once a potential target is found, it would need to be validated by a series of knockdown and over expression assays, looking to see if the knockdown of that gene would mimic miR337 mimic treatment in sensitizing NSCLCs to paclitaxel, and overexpression of the target gene would mimic miR337 inhibitor treatment in making NSCLCs more resistant to paclitaxel.

4.5.2 EVALUATION OF SPECIFICITY OF SYNTHETIC LETHAL SIRNAS FOR PACLITAXEL

That docetaxel and paclitaxel respond very similarly to the paclitaxel specific synthetic lethal siRNAs is a confirmation that these structurally related molecules act through the same pathway although docetaxel does so less effectively, but that diazonamide, an antimitotic with unknown mechanism of action, was sensitized to some, but not all of the 6 siRNAs is most remarkable. It implicates that the taxanes and diazonamide at some point are activating similar pathways that are not activated by vinorelbine. Testing more of the paclitaxel specific synthetic lethal siRNAs with diazonamide would be very interesting, and would give insight into the mechanism of diazonamide.

4.5.3 TARGETING MUTANT P53 IN NSCLC USING AGRNAS

The ability to reactive wild type p53 activity in cancers is something that researchers have been investigating since the discovery of p53 as such a major tumor suppressor. However, a way to therapeutically target p53 has remained elusive. In this work we used synthetic antigene-RNAs targeting 5' of the TSS of *TP53*, and found that two distinct sequences of agRNA targeting the 5' region of the *TP53* promoter induce cytotoxicity in a p53-DBD-mutant specific fashion, as cells harboring wild-type p53, have homozygous deletions of the *TP53* gene, truncation mutations of p53, or mutations outside of the DBD are not affected by agRNA treatment. While possible, it is not likely that this cytotoxicity is due to

simply decreasing mutant p53 levels as many cancers have homozygous deletions for p53, which effectively would be the same as removing mutant p53. The cytotoxicity specifically in the back ground of mutant-DBD-p53 suggests two things, the removal of mutant p53, and induction of wild-type p53 activity. This is because most mutants act in a dominant negative fashion by inhibiting wild-type p53 and also inhibiting p63 and p73, and that introduction of wild-type p53 into cancer cells causes cell death or differentiation (Baker, Markowitz, Fearon, Willson, & Vogelstein, 1990; Goyette et al., 1992).

We also showed that N9 treatment sensitizes NSCLCs and pancreatic cancers with mutant p53 to doxorubicin, which is known to activate p53 in wild type cells and that apoptosis induced by doxorubicin is dependent on p53. These data further suggest that agRNA^{p53} is causing a re-activation of wild type p53 activity.

There was no appreciable change in WRAP53 levels after agRNA^{p53} treatment to suggest that the agRNAs were acting in a WRAP53 dependent fashion; however, WRAP53 levels after agRNA^{p53} treatment and challenged with a DNA damaging agent was not tested in these studies.

There was a large induction of lincRNAp21 levels after agRNA treatment; however, the relevance of this observation has yet to be determined. The effect of over expression of lincRNAp21 needs to be evaluated as does the inhibition of lincRNAp21 expression, in cells with no other treatment, as well as in cells that

have been transfected with agRNA^{p53}s, to see if knockdown of lincRNAp21 would oblate the cytotoxic effect of agRNA^{p53} in p53-DBD-mutant containing cells. If this is the case, then these agRNAs act through induction of lincRNAp21 which has been shown to positively regulate pro-apoptotic p53 target genes.

Target sequences of duplex RNAs	
Name	**Target Sequence**
p53-N (-7)	**AATGCACCCTCCTCCCCAACT**
p53-N (-9)	**AATCTGCACCCTCCTCCCCAA**
p53-N (-11)	**AAACTCTGCACCCTCCTCCCC**
p53-N (-15)	**AACCTGACTCTGCACCCTCCT**
p53-N (-17)	**AAATCCTGACTCTGCACCCTC**
p53-N (-19)	**AAGAATCCTGACTCTGCACCC**
p53-N (-21)	**AAGAGAATCCTGACTCTGCAC**
p53-N (-23)	**AAGCGAGAATCCTGACTCTGC**
p53-N (-25)	**AACGGCGAGAATCCTGACTCT**
p53-N (-27)	**AAGTCGGCGAGAATCCTGACT**
p53-N (-29)	**AAAGGTCGGCGAGAATCCTGA**
p53-N (-31)	**AACCAGGTCGGCGAGAATCCT**
N9-Scr	**AAAGCTTCTCAAAAAGTTTTG**
N27-Scr	**AATGACTGTCGGCATCCAGAA**
N27-M4M	**AAGACGGAGAGACTCGTGACT**
N9-M4M	**AATGGACCCACCTGCCCATCT**
p53 si-554	**AACCTACCAGGGCAGCTACGG**
p53 QsiR	**AAGGAAATTTGCGTGTGGAGT**
p53 siR-788	**AATCTACTGGGACGGAACAGC**
p53 siR-807	**AAAACAGCTTTGAGGTGCGTG**

TABLE 4. 1 agRNAs and siRNAs to study p53 activity.

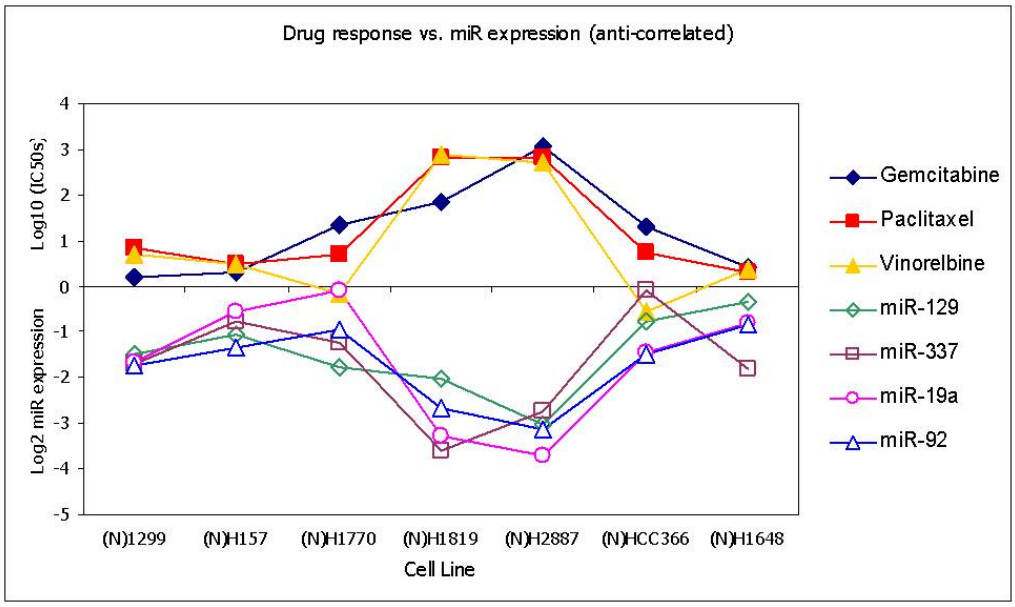

FIGURE 4.1 Correlation of miRNAs expression with drug response to gemcitabine, paclitaxel, and vinorelbine in NSCLC.

Expression of miR19a, miR129, and miR337 correlate in a negative fashion with response to paclitaxel, gemcitabine, and vinorelbine. Data for this figure is not from the author, Rachel Greer, instead it is unpublished from Alex Pertsemlidus.

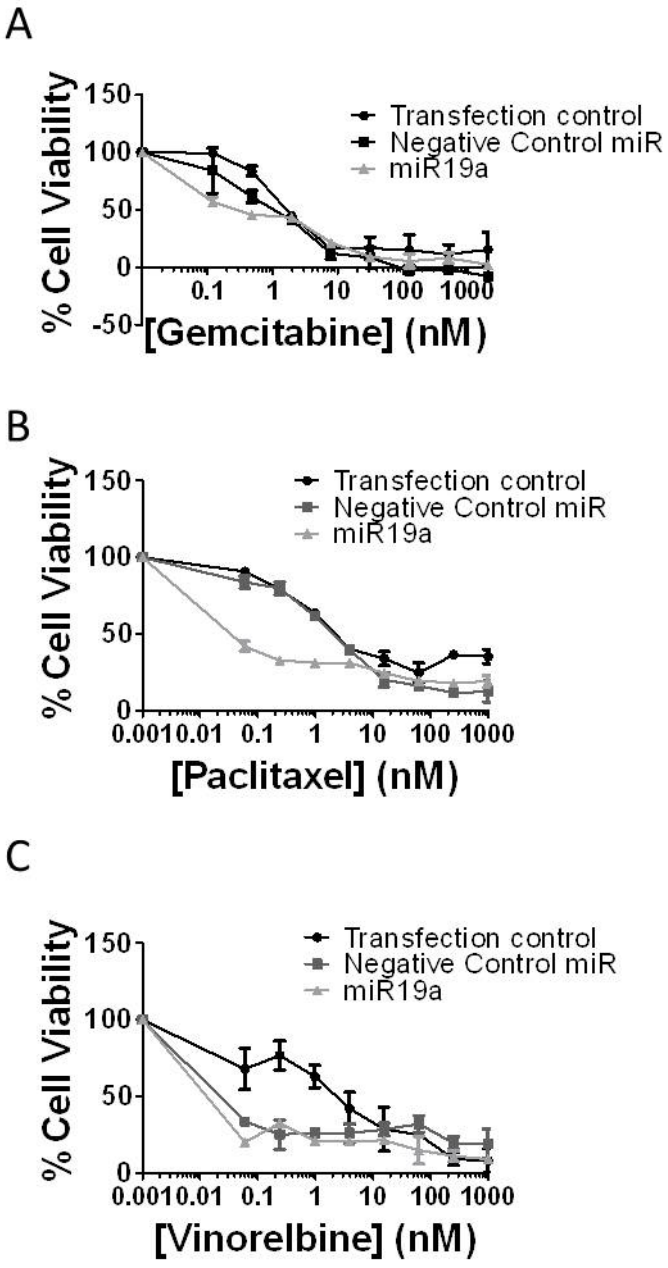

FIGURE 4.2 Alterations of miR19a levels can alter H157 response to chemotherapy.

H157 cells were transfected with mock reagents, negative control miR mimic (Dharmacon), or miR19a mimic. Twenty-four hours post transfection cells were treated with (A) gemcitabine, (B) paclitaxel, or (C) vinorelbine; after 96 hours post drug treatment, relative cell viability was determined using the MTS assay as described in methods.

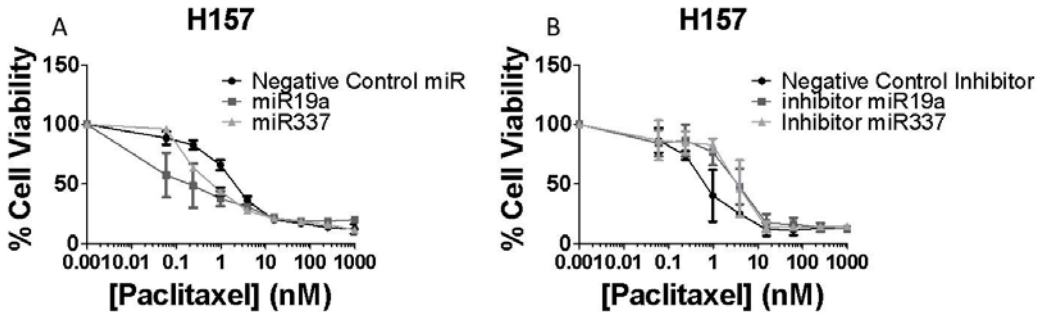

FIGURE 4.3 Figure 4.3 Alterations of miR19a and miR337 alter H157 response to Paclitaxel.

(A) H157 cells were transfected with 20 nM negative control miR (Dharmacon), miR19a mimic, or miR337 mimic and 24 hours later were treated with 4-fold increasing concentrations of paclitaxel and relative cell viability was determined 96 hours after treatment with paclitaxel using the MTS assay as described in methods. (B) H157 cells were transfected with 50 nM negative control antagomiR (Dharmacon), antagomiR19a, or antagomiR337. After 24 hours, cells were treated with 4-fold increasing concentrations of paclitaxel; relative cell viability was determined 96 hours later using the MTS assay as described in methods.

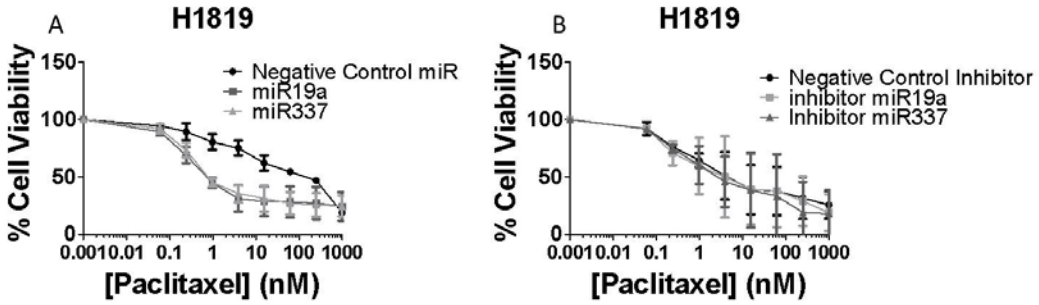

FIGURE 4.4 Alterations of miR19a and miR337 alter H1819 response to Paclitaxel.

(A) H1819 cells were transfected with 20 nM negative control miR (Dharmacon), miR19a mimic, or miR337 mimic. After 24 hours cells were treated with 4-fold increasing concentrations of paclitaxel; relative cell viability was determined 96 hours after treatment with paclitaxel using the MTS assay as described in methods. (B) H1819 cells were transfected with 50 nM negative control antagomiR (Dharmacon), antagomiR19a, or antagomiR337. After 24 hours, cells were treated with 4-fold increasing concentrations of paclitaxel; relative cell viability was determined 96 hours later using the MTS assay as described in methods.

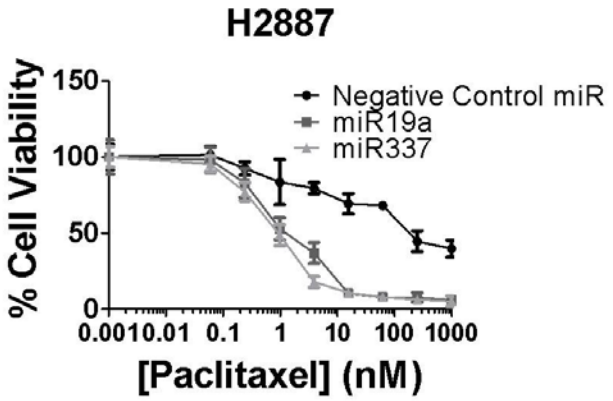

FIGURE 4.5 Figure 4.5 Alterations of miR19a and miR337 alter H2887 response to Paclitaxel.

H2887 cells were transfected with 20 nM negative control miR (Dharmacon), miR19a mimic, or miR337 mimic. After 24 hours cells were treated with 4-fold increasing concentrations of paclitaxel; relative cell viability was determined 96 hours after treatment with paclitaxel using the MTS assay as described in methods.

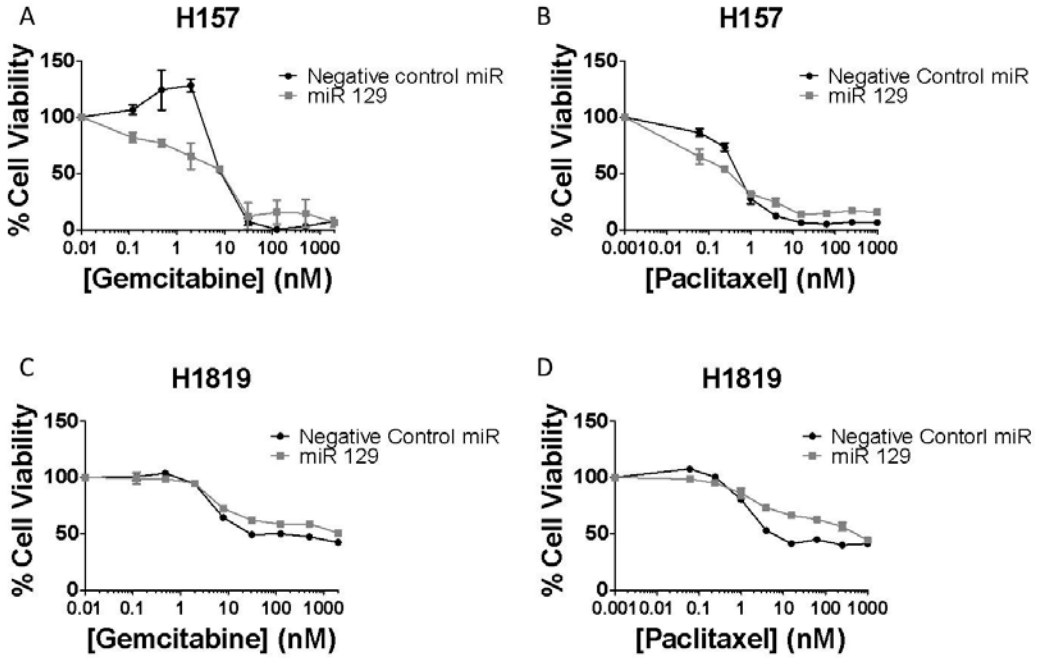

FIGURE 4.6 Increasing miR129 Levels Does Not Affect Drug Response to Gemcitabine or Paclitaxel.

(A-B) H157 and (C-D) H1819 were transfected with 20 nM negative control miR (Dharmacon) or miR129 mimic. Twenty-four hours post transfection cells were treated with 4-fold increasing concentrations of (A, C) gemcitabine or (B, D) paclitaxel; relative cell viability was determined 96 hours after drug treatment using the MTS assay as described in methods.

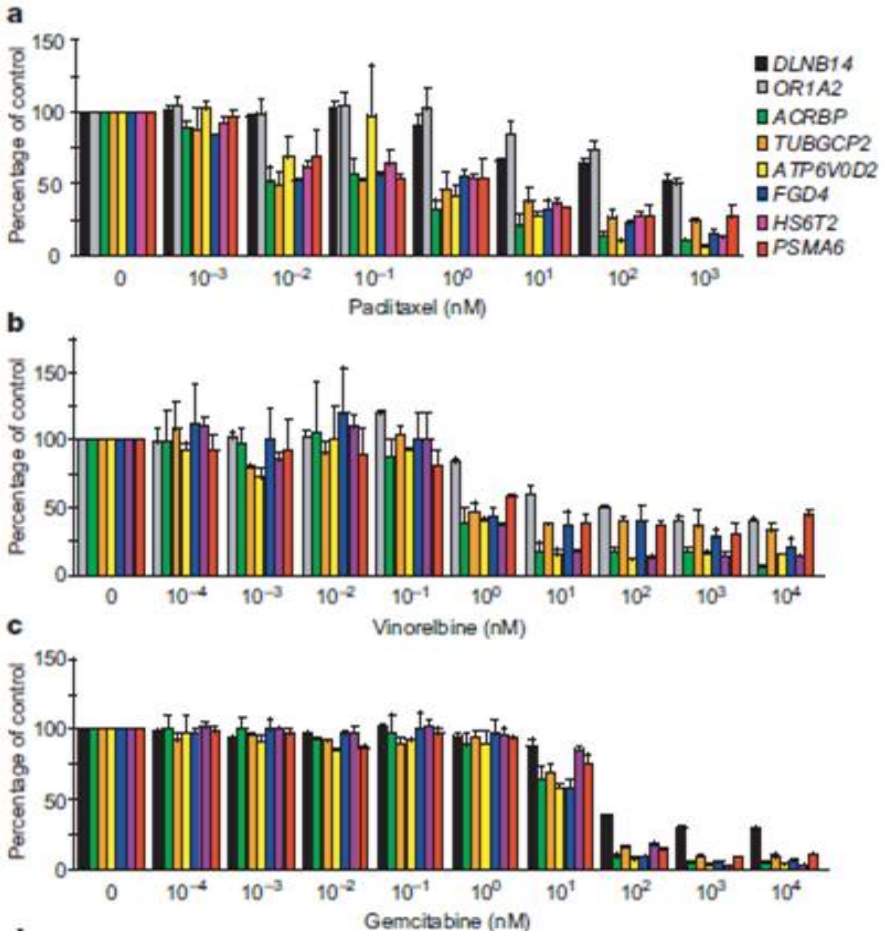

FIGURE 4.7 Drug sensitivity profiles of Paclitaxel Synthetic Lethal siRNAs.

(A-C) H1155 transfected with siRNAs targeting the indicated genes (DLNB1 and OR1A2 are control siRNAs) were exposed to (A) paclitaxel, (B) vinorelbine, or (C) gemcitabine 48 h after transfection at the indicated doses for 48 h. Results are viability normalized to siRNA-transfected samples in the absence of drug and are shown as means and s.e.m. Values are representative of three independent

experiments. Bars are cell viability obtained with Cell Titer Glo and are shown as means and s.e.m. Adapted from (Whitehurst, et al., 2007)

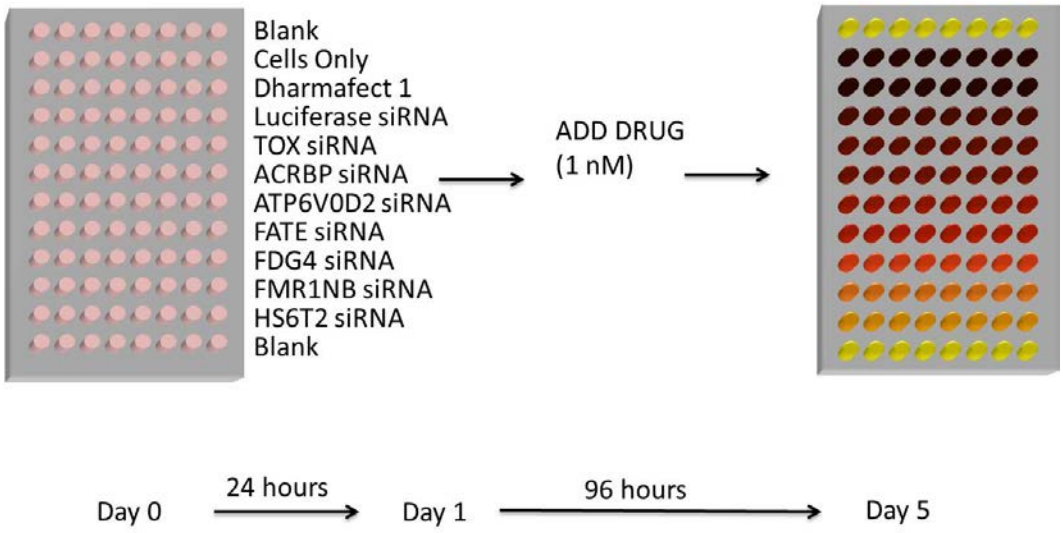

FIGURE 4.8 Overall Scheme for Testing Paclitaxel Synthetic Lethal siRNAs Against other Anti-Mitotics.

Transfect cells with 20 nM of the indicated siRNAs on day zero; 24 hours later, treat with 50 uL of 2 nM paclitaxel, peloruside, docetaxel, or 0.2 nM diazonamide. Use MTS assay (as described in methods) to quantitate relative cell kill.

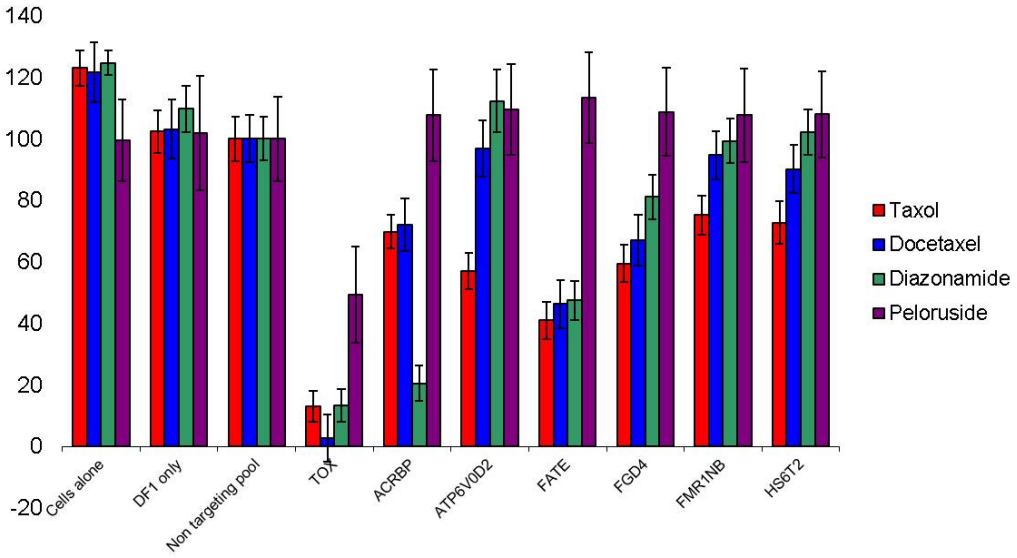

FIGURE 4.9 Figure 4.9 Paclitaxel-Specific Synthetic Lethals Are Not Completely Selective for Taxanes Only.

H1155 cells were transfected with 20 nM of the indicated siRNAs; 24 hours post transfection cells were treated with paclitaxel, docetaxel, peloruside (final concentration 1 nM), or diazonamide (final concentration 0.1 nM). Relative cell viability was determined 96 hours after drug treatment using the MTS assay; described in methods. Data was normalized to cells that were transfected with luciferase siRNA and treated with the test drug (paclitaxel, peloruside, docetaxel or diazonamide respectively). Data shown is the average of at least three separate experiments conducted on separate days.

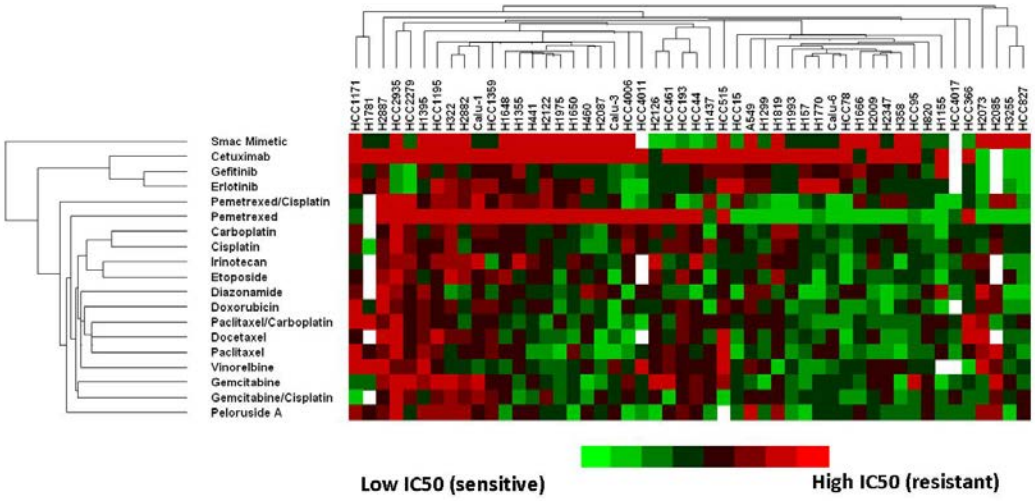

FIGURE 4.10 Clustering of Chemotherapies by IC_{50} across NSCLC Panel Roughly Clusters by Mechanism of Action.

Unsupervised clustering of chemotherapies based on response across a panel of 50 NSCLC (data collected by many members of the Minna lab). Diazonamide loosely clusters with vinorelbine and the taxanes for mechanism of action, strangely doxorubicin also clusters in the same group.

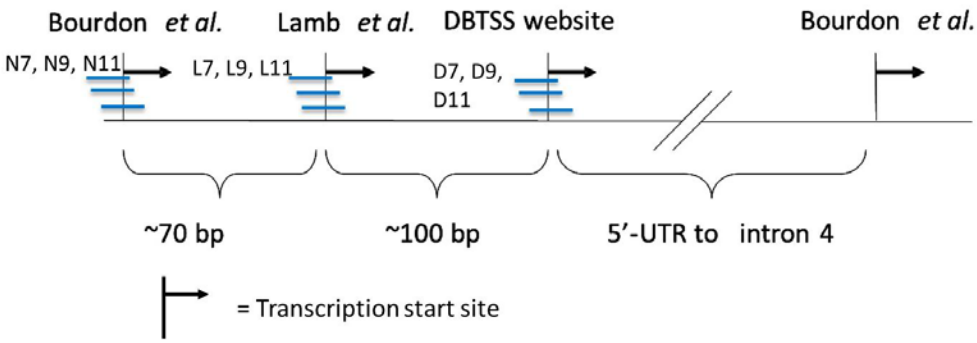

FIGURE 4.11 Design of agRNAs According to p53 Transcription Start Sites. While there are four TSS associated with the *TP53* gene, only the three upstream (5') promoters were targeted using agRNAs, they were designed to be complementary to the + strand to the indicated regions, specific sequence information of agRNAs is in Table 4.1.

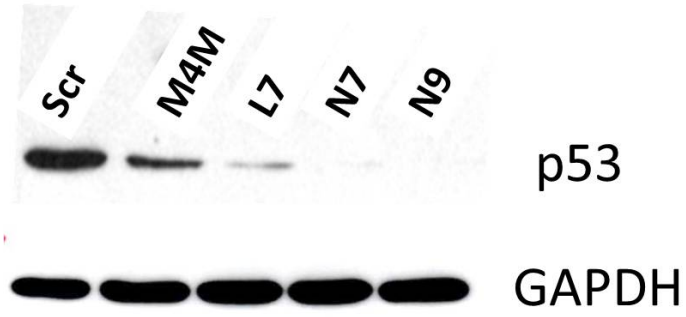

FIGURE 4.12 Targeting the 5' of the Transcription Start Site of p53 in H1355 Cells Results in Decreased p53 Expression.

Western blot analysis of lysates from H1355 cells transfected with mismatch (M4M-N9), scrambled N9 (N9-scr), L7, N7, and N9 collected 48 hours later.

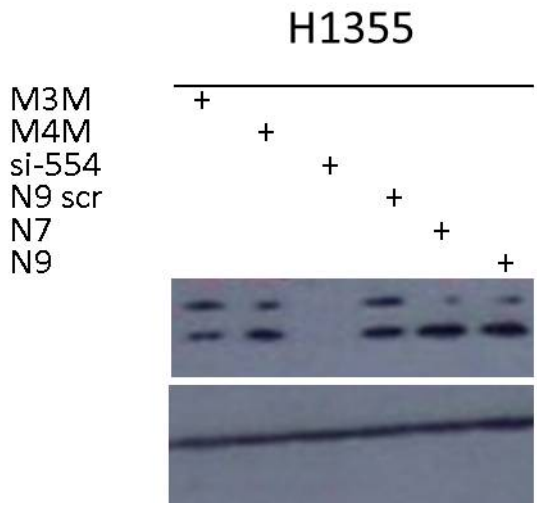

FIGURE 4.13 Induction of lower molecular weight p53 bands is induced by agRNA^{p53}.

H1355 cells were transfected with mismatch control agRNAs (M3M, M4M), N9-scr, QsiR, N7 or N9. Cells were harvested after 48 hours, cell lysates were analyzed using western blotting analysis for p53 (D01, Santa Cruz)and GAPDH (antibody specifics).

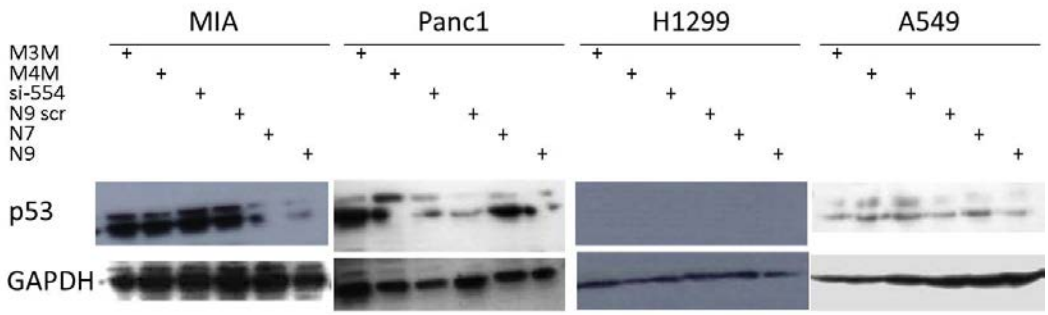

FIGURE 4.14 Figure 4.14 Western blot analysis of agRNA effects on p53 levels in p53 WT, mutant, and null cell lines.

A549, H1299, Mia PaCa2, and Panc1 cells were transfected with mismatch control agRNAs (M3M, M4M), N9-scr, QsiR, N7 or N9. Cells were harvested after 48 hours, cell lysates were analyzed using western blotting analysis for p53 (D01, Santa Cruz)and GAPDH (antibody specifics).

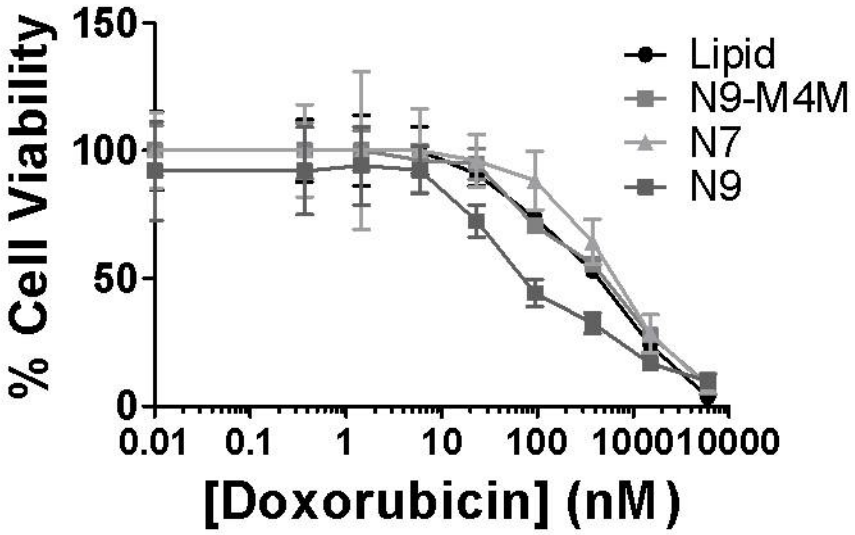

FIGURE 4.15H1355 Cells are Sensitized to a p53 Dependent Chemotherapy by Transfection with N9.

H1355 cells were reverse transfected with Dharmafect 1 lipid only, 100 nM N9-M4M, 100 nM N7, or 100 nM N9; 24 hours later cells were treated with four-fold decreasing dilutions of doxorubicin. Relative cell viability was determined 96 hours after doxorubicin treatment was given using the MTS assay as described in methods.

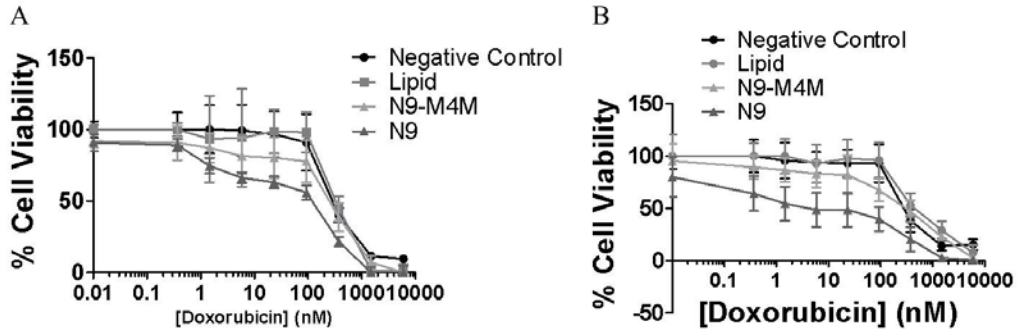

FIGURE 4.16 Mutant-p53 containing cell lines are sensitized by agRNA^{p53} to p53 inducing chemotherapy.

(A) Mia PaCa2 or (B) Panc1 cells were reverse transfected with Dharmafect 1 lipid only, 100 nM N9-M4M, 100 pM N9, as well as an untransfected control plate was plated in 96 well plate; 24 hours later cells were treated with four-fold decreasing dilutions of doxorubicin. Relative cell viability was determined 96 hours after doxorubicin treatment was given using the MTS assay as described in methods.

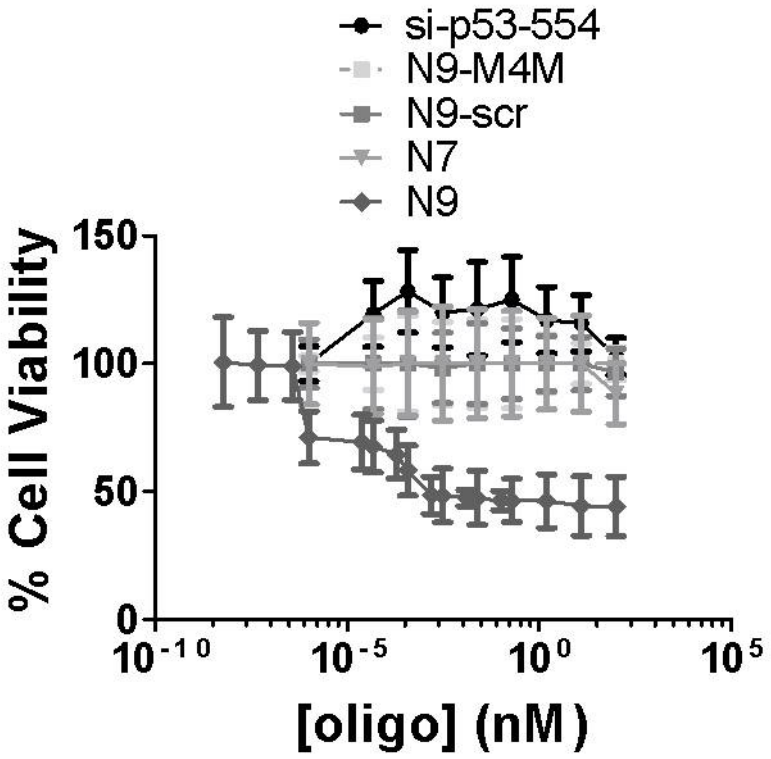

FIGURE 4.17 H1355 cells are killed selectively by N9.

H1355 cells were reverse transfected with 4-fold dilutions of siRNA:lipid or agRNA: lipid complexes with the indicated dsRNA oligo beginning at 100 nM on day zero, transfection complexes were handled in serum free RPMI, cells were plated in R5. Relative cell viability was determined 120 hours after transfection using the MTS assay as described in methods.

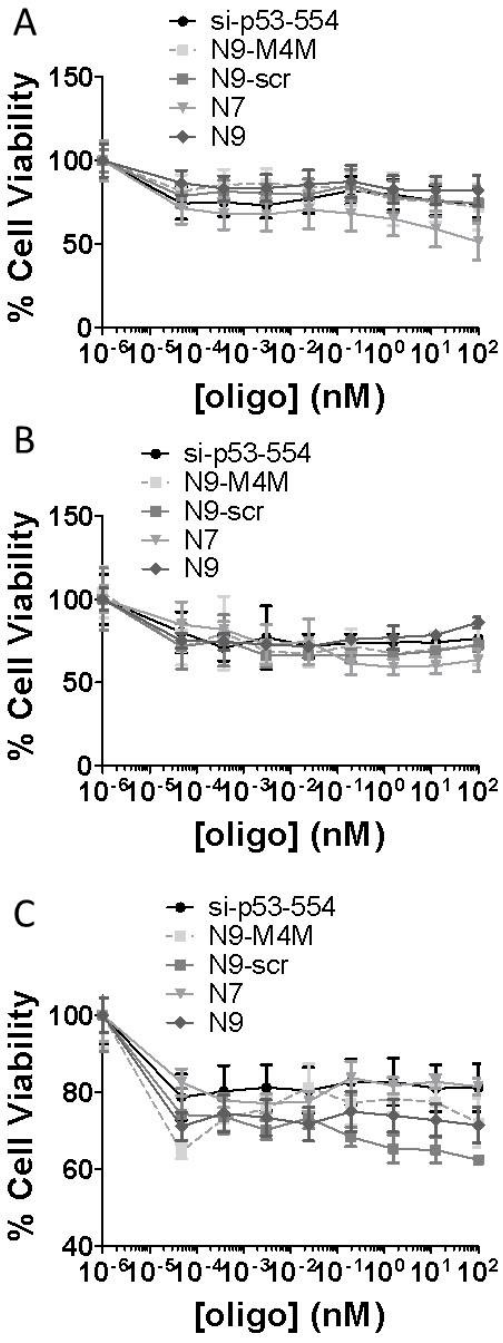

FIGURE 4.18 Figure 4.18 N9-induced cytotoxicity does not occur in wild-type p53 or p53 null cell lines.

(A) A549, (B) H358, and (C) H1299 cells were reverse transfected with 4-fold dilutions of siRNA:lipid or agRNA: lipid complexes with the indicated dsRNA oligo beginning at 100 nM on day zero, transfection complexes were handled in serum free RPMI, cells were plated in R5. Relative cell viability was determined 120 hours after transfection using the MTS assay as described in methods.

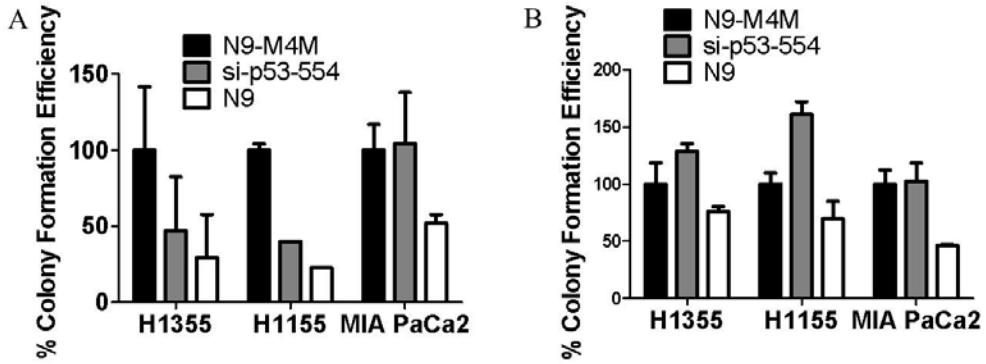

FIGURE 4.19 Colony Formation is inhibited in Cell Lines Harboring mutant-p53.

H1355, H1155, and MIA PaCa2 cells were transfected with 25 nM N9-M4M, si-p53-554, or N9. Twenty four hours after transfection the cells were split and plated for liquid colony formation assay with two wells per cell line per treatment plated at two different densities (A) 100 cells/well or (B) 1000 cells/well in a 6 well plate. Cells were allowed to grow undisturbed until colonies >50 cells/colony were visible, plates were then fixed and stained with 0.05% methylene blue and counted using ChemiDoc (BioRad, Hercules, CA).

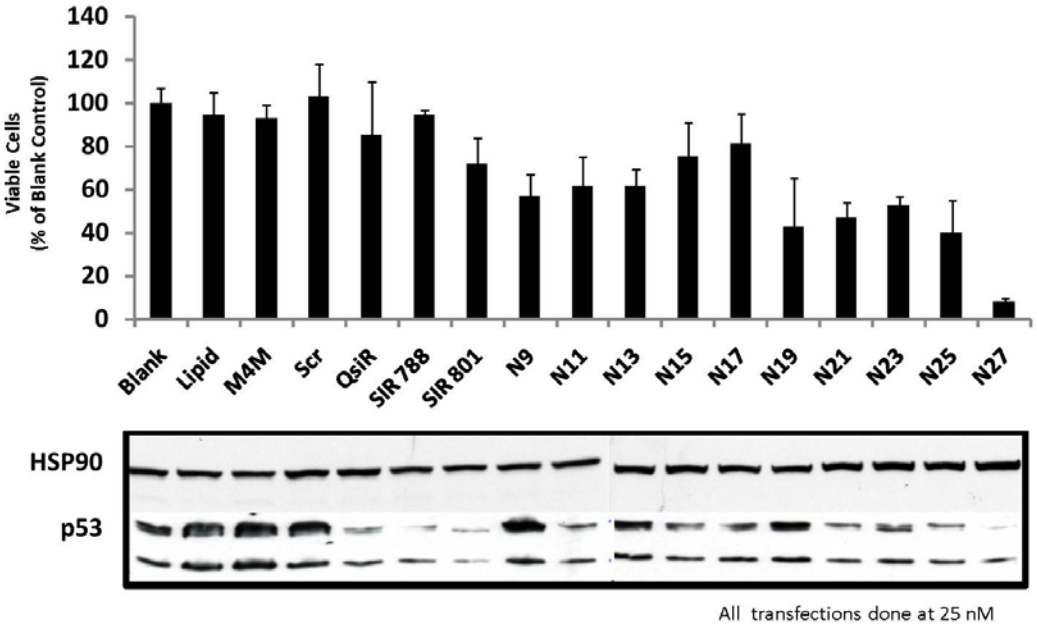

FIGURE 4.20 Targeting 5' of the coding region of *TP53* at multiple sites results in variable effects on p53 protein expression and cytotoxicity of cells. H2009 cells were transfected with 10 nM of the indicated dsRNA oligo, 96 hours post-transfection cells were harvested and viable cells were quantitated using the Trypan exclusion. Cell counts were normalized to control treated cells. H2009 cells were lysed and lysates analyzed by western blotting analysis. Changes in p53 protein expression were found after transfection with agRNAs^{p53}. Lipid is Dharmafect 1 alone. p53 has several lower molecular weight splice forms that are detectable by western blot. Data in this figure not produced by Rachel Greer.

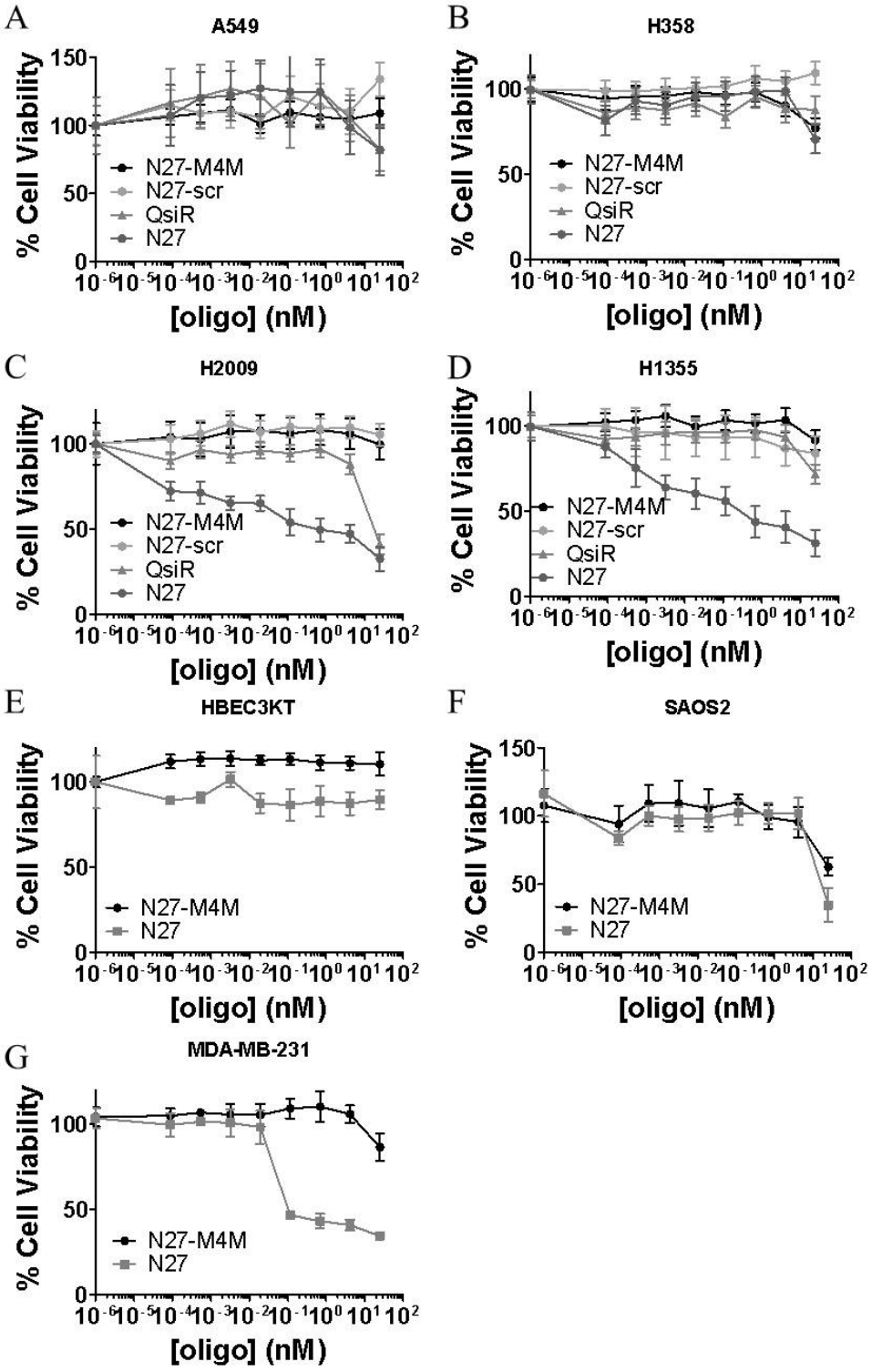
A
A549
% Cell Viability
150
100
50
0
N27-M4M
N27-scr
QsiR
N27
10-6 10-5 10-4 10-3 10-2 10-1 100 101 102
[oligo] (nM)
B
H358
% Cell Viability
100
50
0
N27-M4M
N27-scr
QsiR
N27
10-6 10-5 10-4 10-3 10-2 10-1 100 101 102
[oligo] (nM)
C
H2009
% Cell Viability
100
50
0
N27-M4M
N27-scr
QsiR
N27
10-6 10-5 10-4 10-3 10-2 10-1 100 101 102
[oligo] (nM)
D
H1355
% Cell Viability
100
50
0
N27-M4M
N27-scr
QsiR
N27
10-6 10-5 10-4 10-3 10-2 10-1 100 101 102
[oligo] (nM)
E
HBEC3KT
% Cell Viability
100
50
0
N27-M4M
N27
10-6 10-5 10-4 10-3 10-2 10-1 100 101 102
[oligo] (nM)
F
SAOS2
% Cell Viability
150
100
50
0
N27-M4M
N27
10-6 10-5 10-4 10-3 10-2 10-1 100 101 102
[oligo] (nM)
G
MDA-MB-231
% Cell Viability
100
50
0
N27-M4M
N27
10-6 10-5 10-4 10-3 10-2 10-1 100 101 102
[oligo] (nM)

FIGURE 4.21 Cells harboring mutant-p53 protein respond with cell death in response to agRNA^{p53}.

(A) A549, (B) H358, (C) H2009, (D) H1355, (E) HBEC3KT, (F) SAOS2, and (G) MDA-MB-231 cells were reverse transfected with N27-M4M, N27-scr, QsiR, and N27 as indicated as four-fold dilutions starting at 25 nM on day zero, transfection complexes were handled in serum free RPMI, cells were plated in R5. Relative cell viability was determined 120 hours after transfection using the MTS assay as described in methods.

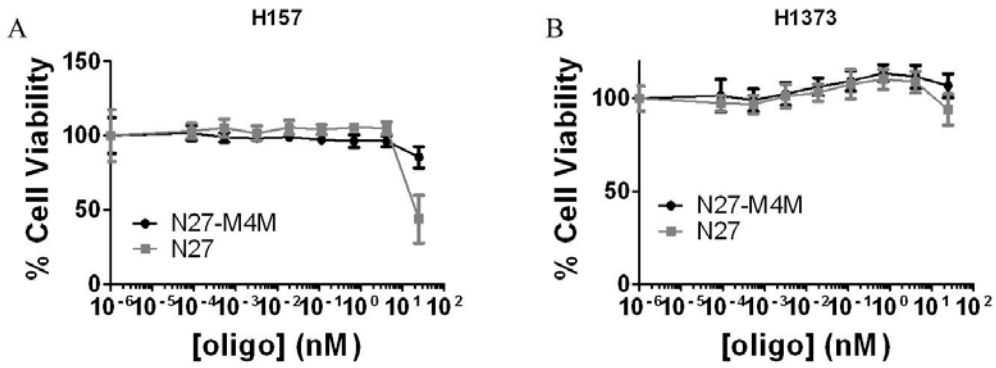

FIGURE 4.22 Cytotoxicity induced by agRNA^{p53} treatment is selective for cell lines with mutations within the DBD of p53.

(A) H157 and (B) H1373 cells were reverse transfected with N27-M4M or N27 as four-fold dilutions starting at 25 nM on day zero, transfection complexes were handled in serum free RPMI, cells were plated in R5. Relative cell viability was determined 120 hours after transfection using the MTS assay as described in methods.

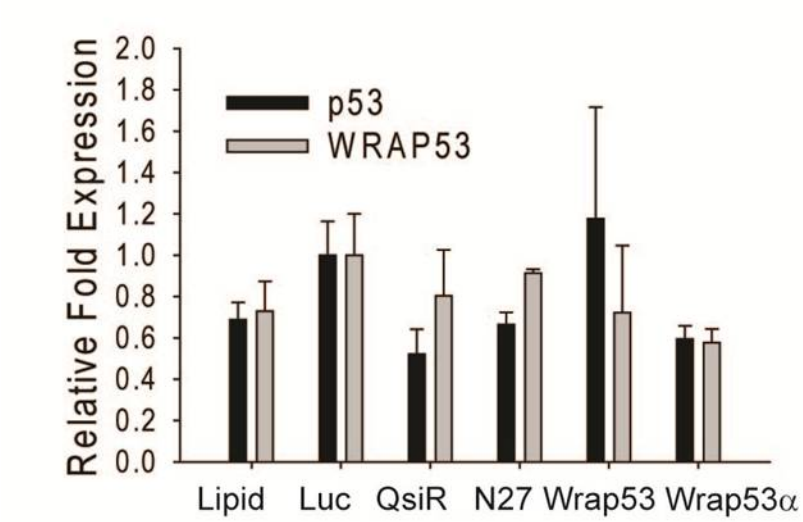

FIGURE 4.23 WRAP53 levels do not correlate with cytotoxicity from agRNAp53 treatment.

H2009 cells were transfected with 20 nM luciferase siRNA, QsiR, N27, WRAP53 siRNA, or WRAP53a siRNA. Cells were harvested after 24 hours, RNA was isolated using the RNeasy Plus kit (Qiagen), cDNA made using iScript kit, and expression levels quantitated using Taqman probes (ABI) targeting the indicated gene (p53 or WRAP53).

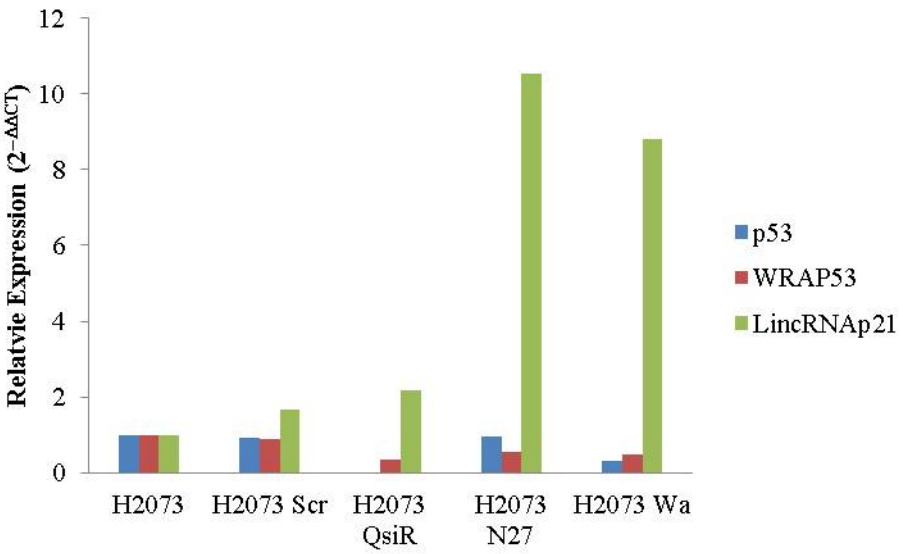

FIGURE 4.24 LincRNAp21 levels are dramatically induced by agRNAp53 treatment.

H2009 cells were transfected with 20 nM luciferase siRNA, QsiR, N27, WRAP53 siRNA, or WRAP53a siRNA. Cells were harvested after 24 hours, RNA was isolated using the RNeasy Plus kit (Qiagen), cDNA made using iScript kit, and expression levels quantitated using syber green based pPCR.

CHAPTER FIVE

SMAC MIMETICS AS AN ADJUVANT CHEMOTHERAPY COMBINATION

5.1 INTRODUCTION

Apoptosis is an evolutionarily conserved process that was originally described by a series of distinct morphological events (Kerr, et al., 1972). Characteristic features of apoptosis include cell shrinkage, nuclear fragmentation, loss of membrane architecture, membrane blebbing, as well as changes in plasma membrane lipid composition (Kerr, et al., 1972). Our understanding of the biochemical processes involved in apoptosis comes from genetic studies in C. elegans. During development of C. elegans, it is critical for excess cells to die, a mutation in a gene called ced3 casuses accumulation of these excess cells in the adult animal, they also saw that ced3 shared homology with human IL-1β converting enzyme (ICE) (Yuan, et al., 1993). These two proteins were the first to be discovered in a family of cysteine-dependent aspartate-directed proteases (caspases). The discovery of ced3 as a caspase was critical in bringing the field of apoptosis into mainstream science. There are twelve caspases in the human genome; however, not all are known to be involved in apoptosis (caspase-1[ICE], caspase-4, caspase-5, and caspase-11) (Yuan, 2006). There are two classes of apoptogenic caspases, initiator caspases and effector/executioner caspases.

Caspases are produced as inactive zymogens, and most require processing for maximal enzymatic activity. Initiator caspases (caspase-2, -8, -9, and -10) rely on upstream signals for activation, which requires being a part of a large protein complex and autoproteolysis. Effector caspases (caspase-3, -6, -7) require proteolytic cleavage by initiator caspases for maximal enzymatic activity, these caspases go on to cleave a number of proteins which facilitates the death of the cell such as PARP and ICAD (Yuan, 2006).

There are many pathways that can lead to apoptosis, one such pathway is the death receptor mediated (extrinsic) pathway. The death receptor mediated pathway is activated when a ligand (such as TNFα, TRAIL, FasL, etc…) binds to its cognate receptor, which sounds simple enough, but nothing is ever that simple. TNFα binding to the TNF receptor (TNFR) is not sufficient for signaling of apoptosis; there is a fine balance of both pro-survival and pro-apoptotic signaling that can occur through TNFR (Kieser, 2008). Upon ligand binding, TNFR trimerizes and recruits TRADD, TRAF2, TRAF1, cIAP1, cIAP2, and RIPK1 (termed complex I). Complex I signals for cell survival through the JNK and canonical NF-κB pathways, and involvement of both cIAP1 and cIAP2 prevents dissociation of TRADD, TRAF2, and RIPK1 from TNFR1. In the absence of cIAPs, TRADD, TRAF2, and RIPK1 associate in the cytosol with FADD and caspase-8 resulting in caspase-8 activation, cFLIP can also prevent caspase-8 activation. Regulation of cell death from the TRAIL receptors (DR4 and DR5) is

more straightforward, with trimerization of the receptor recruiting directly FADD, caspase 8 or caspase 10, and/or cFLIP. However, there are decoy receptors for TRAIL (DcR1, DcR2, and OPG) which can bind to TRAIL and prevent activation of DR4 and DR5. Fas is the last member of the TNFR super family (TNFRSF) of receptors that is known to signal for apoptosis. Like DR4 and DR5, activation of Fas induces receptor trimerization, and recruitment of FADD, caspase-8 or -10, and/or cFLIP.

Another pathway that activates apoptosis is the mitochondrial (or intrinsic) pathway. Activation of mitochondrial apoptosis is regulated by a family of both pro- anti-apoptotic proteins named for the founding member, BCL-2. There is a fine balance between the pro-apoptotic and anti-apoptotic BCL-2 family members, and that balance regulates how a cell will respond to an intrinsic apoptogenic stress (P. Li, et al., 2004). Classification as a BCL-2 super family member relies on homology of BCL-2 homology (BH) domains. There are four distinct BH domains, BH1, BH2, BH3, and BH4. Anti-apoptotic BCL-2 family members (BCL-2, BCLxL, BCL-W, A1, MCL-1) contain all four BH domains. The pro-apoptotic proteins BAX and BAK contain BH1-3, and the pro-apoptotic BH3 only family members (BAD, BID, BIM, NOXA, PUMA) only contain the BH3 domain. BAX and BAK are required to initiate mitochondrial-induced apoptosis, and BCL-2, BCLxL, as well as others antagonize the ability of BAX and BAK to lead to mitochondrial release of cytochrome c as well as other pro-

apoptotic proteins (P. Li, et al., 2004). The BH3 only proteins serve as upstream mediators of apoptosis, they sit and wait for a pro-apoptotic signal, whether it's by cleavage (BID), phosphorylation (BAD), or transcriptional activation (PUMA and NOXA), and then they antagonize the ability of the anti-apoptotic BCL-2 familiy members to bind BAX and BAK. Upstream signals for mitochondrial-induced apoptosis include genotoxic stress, removal of growth factors, metabolic crisis, oxidative stress, chemotherapy, and others.

A less well known pathway that activates apoptosis is ER stress-induced apoptosis. The ER is the primary site for protein synthesis and folding for secreted, membrane bound, and some organelle targeted proteins, it comprises roughly one third of the newly translated proteins in a cell. With such responsibility for the normal functioning of a cell, the ER is primed to respond quickly when stresses alter cellular energy levels; redox state; intra-ER concentration of Ca^{2+}; misfolded, unfolded, or excess protein in the ER lumen; lipid or glycolipid imbalances occur in the ER. So called ER stress can signal for three salvage pathways, the unfolded protein response (UPR), ER-associated degradation, and the control of protein translation (Figure 5.1) (Boyce & Yuan, 2006). However, if these salvage attempts fail, the ER can directly signal for apoptosis. In mice, ER stress causes the release of Ca^{2+} in a BAX-BAK dependent fashion from the ER, PUMA and NOXA expression is induced in a p53-dependent fashion, and directly activate mCaspase-12 (J. Li, Lee, & Lee, 2006;

Moenner, Pluquet, Bouchecareilh, & Chevet, 2007). The human gene encoding Caspase-12 contains a frame shift mutation which causes a premature stop codon preventing CASPASE-12 expression; however, further sequence analysis shows that even if CASPASE-12 were expressed that a protein coding mutation would obliterate enzymatic activity by mutation of the SGH box (mutated to SGS) (Fischer, Koenig, Eckhart, & Tschachler, 2002). In light of these findings, an alternative caspase was explored, and it was found by multiple groups that CASPASE-4 is activated by ER stress (Figure 5.2) (Fischer, et al., 2002; Hitomi et al., 2004; Pei-Chun Liao, 2008).

The second mitochondrial activator of caspases (SMAC) is the natural antagonist of IAP inhibition of caspases by binding to IAPs in a competitive fashion to caspases. SMAC is localized in mitochondria, within the inter membrane space, and is released along with cytochrome c when BAX and BAK signal for initiation of apoptosis to ensure that apoptosis occurs.

Evasion of apoptosis is one of the hallmarks of cancer; cancer cells have increased expression of BCL-2, BCL-xL, XIAP, surivivin, cFLIP, as well as other anti-apoptotic proteins. One targeted approach to overcome resistance to apoptosis has been target IAPs with a small molecule mimetic of SMAC. SMAC binds to IAPs using its 4 N-terminal residues, AVPI, so small molecules were designed to bind to bind BIR3 of XIAP in the same fashion as AVPI (L. Li, et al., 2004). In the initial paper from Xiaodong Wang's lab it was shown that SMAC

mimetic could bind to XIAP, could induce activation of caspase-3 in cell free assays, and that the combination of SMAC mimetic with TNFα or TRAIL could induce caspase activation (L. Li, et al., 2004). In a large screen across 50 NSCLCs it was found that roughly 15% are sensitive to SMAC mimetic alone, which is due to an autocrine TNFα loop that is dependent on TNFα, TNFR1, caspase-8, and RIPK1 (Petersen, et al., 2007). Two other studies that came out the same week as the Petersen paper from two other groups further showed that SMAC mimetics induce proteaosomal degradation of cIAP1 and cIAP2 but not XIAP, and that loss of cIAP1/2 from TNFR1 induces activation of both canonical and non-canonical NF-κB signaling that induces TNFα production (Varfolomeev, et al., 2007; Vince, et al., 2007).

While there is some single agent activity seen for SMAC mimetics, it is unlikely that any one molecule from this class of drugs would become FDA approved as a single agent, owing to the relatively low response rate in vitro. Therefore, the most likely route for SMAC mimetics to become used in the clinic is as part of a combination with one or more conventional chemotherapies; however the study of SMAC mimetics in combination with chemotherapy has been done on a limited basis. The first study published in 2005, explores compound 3 as a single agent as well as in combination with TRAIL or etoposide in a small panel of breast cancer cell lines (MDA-MB-231, MDA-MB-453, and T47D), and shows some single agent activity of compound 3 as well as synergy

between TRAIL or etoposide in combination (Bockbrader, et al., 2005). The next study was done on three colorectal carcinoma cell lines and found that co-treatment of NSAIDs with SMAC mimetics can sensitize colorectal carcinomas to NSAIDs by an increase in active caspase-3 (Bank, Wang, Du, Yu, & Zhang, 2008). Another study found that H460 cells can be sensitized to cisplatin by SMAC mimetics, by co-IPs of caspase-3 with XIAP, as well as propidium iodide staining, and caspase-3 activity assays (Checinska, Hoogeland, Rodriguez, Giaccone, & Kruyt, 2007). A group in China found that using luteolin to inhibit SMAC mimetic induced NF-κB activation could synergistically kill a lung and colon cancer cell line, while not harming normal immortalized human bronchial epithelial cell lines (Bai et al., 2009). An Italian group studied three hematological tumor lines, all from different malignancies, in combination with cytarabine, idarubicine, etoposide, and imatinib, and found that SMAC mimetics can sensitize hematological tumor lines to these drugs (Servida et al., 2010). Another study showed that four melanoma cell lines can be sensitized to TRAIL and bortezomib by SMAC mimetics as measured by PARP cleavage, and cell viability assays (Lecis et al., 2010). Sun et al found that four head and neck squamous cell carcinoma cell lines could be sensitized to cisplatin or etoposide by either SMAC overexpression or SMAC mimetic treatment characterized by caspase-3 cleavage and cytochrome c release from the mitochondria (Q. Sun, Zheng, Zhang, & Yu). Two similar studies from the same group found that

multiple pancreatic cancer cell lines (up to 8) can be sensitized to TRAIL, gemcitabine, and doxorubicin in vitro and in vivo (Awasthi et al., 2011; Dineen, et al., 2010). Probst et al find in a limited panel of cancer cell lines, consisting of 2 breast, 1 colon, 2 lung, 2 pancreatic, 1 prostate, and two melanoma cell lines, that JP1400 (a fourth generation compound 3 analogue) can sensitize to gemcitabine, paclitaxel, 5-FU, cisplatin and SN38, and claims that the sensitization is dependent on TNFα induction (Probst et al., 2010). Resistance to SMAC mimetics in this study was defined by induction of cell death by 100 nM JP1400. These ten cell lines were tested for IC_{50} to gemcitabine, paclitaxel, 5-FU, cisplatin, etoposide, and SN38 with or without addition of 100 nM SMAC mimetic. Most of the figures in this study are from experiments done on A2058 cells, which were the model cell line of the Varfolomeev et al study, one of the initial studies showing single agent SMAC mimetic activity was dependent on TNFα signaling (Probst, et al., 2010; Varfolomeev, et al., 2007). The study by Dean et al. was done using a different type of SMAC mimetic, XAC 1396-11, which binds on XIAP near the BIR2 domain instead of BIR3 like most other SMAC mimetics, which is why there is some single agent activity seen of the SMAC mimetic in this study on H460 and A549 (Dean et al., 2009). This study also claims that synergy is seen between SMAC mimetic and vinorelbine, cisplatin, or the combination of vinorelbine and cisplatin; however, only a table summarizing calculated CI values is given, no raw data or drug response curves

are ever shown, with the exception of one western blot showing that 2.5 nM vinorelbine with 5 μM SMAC mimetic causes an increase in PARP cleavage. These studies are very comprehensive in their experimental depth; however they are limited in by the small number of cell lines explored.

5.2 Results

5.2.1 SMAC mimetic synergizes with conventional chemotherapy in NSCLC cell lines by MTS assay.

While the ability to target patient populations that will respond to a targeted agent is an important strategy in designing clinical trials, for example (insert clinical trial where EGFR mutations was a selection criteria); the most likely route for a SMAC mimetic to get into the clinic is not by targeting patients that have circulating TNFα levels but instead as part of a combination chemotherapy regimen. Taking this into consideration, a sub-panel of the 50 NSCLCs studied in Petersen et al. were created by selecting NSCLCs that were resistant to SMAC mimetic (up to 100 μM), this panel included sixteen NSCLC cell lines resistant to JP1201 monotherapy, two immortalized human bronchial epithelial cells (HBECs), and two genetically modified malignant HBEC lines (Petersen, et al., 2007). These cell lines were used in combination studies where JP1201 (a second generation SMAC mimetic) was held at a constant concentration (10 μM) and conventional chemotherapies were given

simultaneously at varying concentrations. Cells were considered to respond to the combination of JP1201 + chemotherapy if the IC_{50} decreased at least by 20 fold (Table 5.1). In combinations of JP1201 with doxorubicin, erlotinib, gemcitabine, paclitaxel, vinorelbine, or the combination of carboplatin + paclitaxel in at least one cell line showed at least a 20-fold sensitization with co-treatment with JP1201, with some chemotherapies showing up to 31,000 fold decrease in IC_{50} in the presence of JP1201 (Table 5.1). There were three general phenotypes seen for the combination of JP1201 with doxorubicin, gemcitabine, erlotinib, paclitaxel, or vinorelbine, but only one phenotype seen for the combination of JP1201 with cisplatin (Figure 5.3). In the case of any single chemotherapy tested, there is substantial variability in the degree of response between cell lines to the combination with JP1201. Conversely, given any one cell line tested, there is heterogeneity of response between the combinations of JP1201 with the chemotherapies tested. All but one NSCLC line were sensitized to the combination of JP1201 + vinorelbine, while almost no cell lines were sensitized to the combination of JP1201 + cisplatin. Of importance, three NSCLCs with wild type EGFR were sensitized to the EGFR TKI, erlotinib.

One of the largest fold shifts in sensitivity identified by MTS assay was the combination of JP1201 with vinorelbine in H1819 cells (Figure 5.4). To confirm this shift in sensitivity, both colony formation and annexin V staining were used as alternative methods for measuring IC_{50}. The combination of JP1201

with vinorelbine on H1819 cells reduced colony formation greater than 50% at a dose of 500 pM vinorelbine and 10 μM JP1201 (Figure 5.4). Annexin V staining 48 hours after drug treatment showed approximately a 20% increase in apoptosis induction when treated with a combination of 10 μM JP1201 and 50 pM vinorelbine (compared to vehicle treated control cells), and 60% increase with a combination of 10 μM JP1201 and 500 nM vinorelbine (Figure 5.4). These data support the MTS assay showing at least a 10,000 fold decrease in IC_{50} when JP1201 is combined with vinorelbine and paclitaxel in H1819. Furthermore, we confirmed the range of sensitization seen in mass culture MTS assays with similar results for other cell lines in colony formation assays (Table 5.2).

5.2.2 Statistical analysis of drug combinations

Considering the possible outcomes when two drugs are combined, the ideal would be for the two drugs to yield synergy; synergy being where the effect of the drugs in combination is greater than the sum of the effect of each drug alone. The other possible outcomes would be additivity; which is where the effect of the drugs in combination is equal to the sum of the effect of each drug given alone, or antagonism; which is where the effect of the drugs in combination is less potent that the sum of each drug given alone. To quantitate the effects seen when JP1201 is combined with standard chemotherapy, combination indices (CI) were calculated for each cell line for each chemotherapy (Table 5.3) (Chou & Rideout,

1991). Both paclitaxel and vinorelbine show greater frequency of synergy in combination with 10 μM JP1201, while cisplatin shows no synergy in combination with 10 μM JP1201.

5.2.3 JP1201 EXHIBITS GREAT SELECTIVITY IN CHEMOTHERAPY SENSITIZATION IN ISOGENIC CELL LINE PAIRS

Included in this panel are several types of isogenic cell line pairs: a tumor /normal lung epithelial cell pair, HCC4017 and HBEC30KT established from the same patient; non-transformed HBEC transformed HBEC pair, HBEC3KT where defined oncogenic changes, Kras G12V and p53 shRNA, were introduced and tumorigenic clones (clone 1, clone 5) isolated by soft agar formation; and two sets of tumor lines that were each established from the same patient. These pairs were isolated before and after treatment of the same patients with cisplatin and etoposide: NCI-H1693 (before) and NCI-H1819 (after); NCI-H1993 (before) and NCI-H2073 (after) (Phelps, ramierez, sato). JP1201 sensitizes HCC4017 but not HBEC30KT to chemotherapy (Figure 5.5). HBEC3KT tumorigenic clones 1 and 5 are sensitized 10-20 fold to vinorelbine (20 fold) or paclitaxel (12-15 fold), while the parental HBEC3KT cells are not sensitized to chemotherapy (Figure 5.6). Surprisingly, H1819 and H2073; which were started from residual NSCLC cells harvested after neoadjuvant platinum and etoposide chemotherapy, were sensitized ~200 fold greater to chemotherapy than H1693 and H1993, which were

started from NSCLC samples from each respective patient prior to treatment (Table 5.1). Thus we found specificity of JP1201 sensitization for tumor compared to normal cells and even in tumor cells after neoadjuvant chemotherapy.

5.2.4 Combination of SMAC mimetic (JP1201) and chemotherapy control NSCLC xenograft growth

In vitro, NCI-H1395 cells demonstrated a 134- and 33-fold increase in sensitivity to gemcitabine and vinorelbine, respectively, when co-treated with JP1201. In order to determine if this effect is observed *in vivo*, NCI-H1395 subcutaneous xenografts were treated with the same drug combinations. One of the challenges in treating lung cancer is that patients are typically diagnosed with late stage disease. In order to most closely mimic human disease, tumors were allowed to grow before treatment began. NCI-H1395 cells were injected subcutaneously on the left flank of NOD/SCID mice and tumors were allowed to establish for 40 days (~150 mm^3). The mice were then randomized based on tumor volume, and treated for three weeks with saline; 25 mg/kg gemcitabine; 2.4 mg/kg vinorelbine; 6 mg/kg JP1201; 25 mg/kg gemcitabine and 6 mg/kg JP1201; or 2.4 mg/kg vinorelbine and 6 mg/kg JP1201 starting on day 43 post tumor injection. Saline, gemcitabine, and JP1201 were given i.p. three times a week, vinorelbine was given i.p. twice a week; the animals were sacrificed 24 hours

after the last treatment. Tumors in mice treated with saline, gemcitabine, or JP1201 alone continued to grow exponentially during the three week treatment period. Tumors in mice treated with vinorelbine continued to grow, albeit at a decreased rate through the treatment period. Tumors of animals treated with JP1201 + gemcitabine showed an inhibition of tumor growth, while the tumors of animals treated with JP1201 + vinorelbine showed tumor regression (Figure 5.7). These data agree with the average tumor weights per treatment group (Figure 5.8). Tumors from the JP1201 + vinorelbine group showed a 70% decrease in tumor burden as compared with the vinorelbine group. Similarly, tumors from the JP1201 + gemcitabine group showed a 60% decrease in tumor burden as compared with the tumors treated with gemcitabine.

The induction of apoptosis in the xenografts was explored using terminal deoxynucleotidyl transferase dUTP nick end labeling (TUNEL) immunofluorescence on paraffin embedded tumor sections from three tumors per treatment group, the data are the average of three images per slide, three slides per treatment group. There is a marked increase in TUNEL staining in the JP1201 + gemcitabine and JP1201 + vinorelbine groups, up to 90% increase compared to single agent and vehicle control treated tumors (Figure 5.9).

I then wanted to know if the reduction in tumor growth would translate to an increase in survival in NSCLCs with very aggressive xenograft growth, to study this NCI-H157 was used, which was one of the NSCLCs that showed a

large sensitization to erlotinib with JP1201. Mice received treatment; saline, 2.4 mg/kg vinorelbine, 12.5 mg/kg erlotinib, 6 mg/kg JP1201, 6 mg/kg JP1201 + 2.4 mg/kg vinorelbine, or 6 mg/kg JP1201 + 12.5 mg/kg erlotinib until tumor size reached the maximum allowable and mice were then sacrificed (Figure 5.10). The tumors of mice treated with saline continued to grow exponentially; median survival time was 19 days post tumor injection. Tumor growth was slowed by treatment with either vinorelbine or JP1201 and survival time was extended by 5 days compared to saline, however, the combination of JP1201 + vinorelbine further slowed tumor growth and extended median survival time by 15 days compared to control (Figure 5.11).

5.2.5 IAP SELECTIVE DEPENDENCE IN JP1201 AND CHEMOTHERAPY COMBINATIONS

JP1201 is a pan-IAP inhibitor, which is known to inhibit cIAP1, cIAP2, and XIAP, its activity against the other five members of the IAP family have not been looked at (L. Li, et al., 2004). I thus wanted to see which of these three IAPs contributes to chemotherapy resistance by using siRNAs directed at cIAP1, cIAP2, or XIAP and assaying for sensitization to gemcitabine, paclitaxel, and vinorelbine in the presence of IAP knockdown. Knockdown of cIAP1 or cIAP2 in the presence of gemcitabine does not sensitize H1395, H358, H1819, or H2887 to gemcitabine; while the knockdown of XIAP in the presence of gemcitabine in all

four cell lines does sensitize the cell lines to gemcitabine, in a similar fashion to combination of JP1201 and gemcitabine treatment in these cells (Figure 5.12). Knockdown of cIAP1, cIAP2, or XIAP gave increasing sensitization to paclitaxel which is best seen in H358 cells where the largest sensitization to paclitaxel is seen out of H1395, H358, H1819, and H2887 cells, additionally the triple knockdown of cIAP1, cIAP2, and XIAP yields the greatest amount of sensitization to paclitaxel in all cell lines (Figure 5.13). In the presence of vinorelbine knockdown of any one of these IAPs results in sensitization to vinorelbine, and the triple knockdown giving further sensitization (Figure 5.16). Knockdowns were validated in H1395 cells (Table 5.4).

5.2.6 TNFα SIGNALING DOES IS NOT THE MECHANISM FOR JP1201-INDUCED SENSITIZATION TO CHEMOTHERAPY

Autocrine TNFα secretion has been shown to be strongly predictive of sensitivity to JP1201 as a single agent in a subset of NSCLC (Petersen et al., 2007). Using a sandwich ELISA, TNFα secretion induced by treatment with JP1201, gemcitabine, or vinorelbine (with and without JP1201) was measured 12 hours post treatment in eight cell lines. H2126 (a JP1201 sensitive line) secreted TNFα under all conditions tested, with increased production when treated with 20 nM vinorelbine (Figure 5.17). The other seven cell lines tested (H157, H1819, H2073, H2882, H1395, H358, and A549); however, showed no TNFα secretion

even after treatment with 20 nM vinorelbine. Induction of TRAIL by chemotherapy could be another mechanism for JP1201-mediated sensitization to chemotherapy; however TRAIL was not secreted in the same eight cell lines after JP1201, vinorelbine, or gemcitabine treatment (Figure 5.18).

To see if TNFα is being turned on at later time points that would coincide with the length of the MTS assay conditioned media was collected at 12, 24, 48, 72, and 96 hours post treatment in the same eight NSCLC lines. No detectable TNFα secretion was found under any conditions tested (Figure 5.19).

I then tried the approach of using TNFα (10 pg/mL) in place of JP1201 in combinations with gemcitabine and vinorelbine, and found that no sensitization to gemcitabine or vinorelbine was seen. Finally; the combination of TNFα with gemcitabine or vinorelbine in the presence of XIAP knockdown showed no sensitization (Table 5.3).

5.2.7 Chronic JP1201 treatment induces TNFA secretion *in vitro* and *in vivo* in JP1201-resistant NSCLCs.

Previous studies using pancreatic cancer mouse models showed an induction of TNFα in xenografts after treatment with either JP1201 alone or JP1201 + gemcitabine (Dineen, et al., 2010). It could be that the treatment with JP1201 is having an effect on the microenvironment that is causing TNFα secretion or it could be a direct effect of chronic JP1201 treatment on the tumor

cells themselves. To test the second hypothesis, and to be able to compare these results with TNFα staining from the current xenograft experiment, H1395 cells were treated for three weeks with either 100 nM or 1000 nM JP1201. H1395 cells (untreated, 100 nM JP1201 pre-treated, and 1000 nM JP1201 pre-treated) were plated before an acute 12hr treatment with the following: no treatment, 100 nM JP1201, 1000 nM JP1201, 20 nM gemcitabine, 20 nM paclitaxel, or 20 nM vinorelbine (Figure 5.20). Conditioned media was collected after 12 hours to measure TNFα secretion. The parental (no long term JP1201 treatment) H1395 did not show any induction of TNFα with any acute treatment (Figure 5.21). H1395 cells pretreated for three weeks with 100 nM JP1201 showed induction of TNFα when treated with 20 nM gemcitabine, paclitaxel or vinorelbine. H1395 cells pretreated for three weeks with 1000 nM JP1201 showed induction of TNFα under all acute treatment conditions (including untreated control) except low dose (100nM) JP1201.

Immunofluorescent staining of H1395 xenograft tumor sections for an antibody selective for human TNFα shows a significant increase in TNFα staining in JP1201, JP1201 + gemcitabine, and JP1201 + vinorelbine treated tumors compared with saline, gemcitabine, or vinorelbine treated tumors (Figure 5.22). TNFα staining was measured using three slides per animal, three images per slide, average FITC signal per image was averaged for each treatment group. These

data show that the tumors receiving combination treatment have the largest induction of TNFα, with JP1201 + vinorelbine showing the most TNFα staining.

5.2.8 Inhibition of downstream TNFa signaling does not rescue NSCLCs from JP1201 + vinorelbine

NCI-H1395 cells were transfected with siRNAs against luciferase, RIPK1, caspase 8, TNFR1, and caspase 3, then treated with JP1201 + vinorelbine. The knockdown of caspase 8, RIPK1, or TNFR1 did not protect the cells from JP1201 + vinorelbine, while the knockdown of caspase 3 offered some protection against JP1201 + vinorelbine (Figure 5.23). Analysis of knockdown was done by q-PCR, which showed fairly good (greater than 50%) knockdown of each gene targeted (Table 5.4). These results suggest the effects of JP1201 + vinorelbine is dependent on an apoptotic pathway different from the TNFα-RIPK1 pathway, indicating JP1201 sensitization to standard chemotherapies occurs by a TNFα independent mechanism.

5.2.9 cIAP1 regulates activation of apoptosis at the ER membrane

The fact that both vinorelbine and paclitaxel are sensitized more often and to the greatest extent by JP1201 made me stop and consider what both agents share in common. Both agents are anti-mitotics, and while the general mechanism is quite clear, that they act by directly binding tubulin and thus alter tubulin dynamics. However, the complexity of the cellular response to such inhibition is

poorly understood, there are some reports in the literature where paclitaxel activates TNFα, and caspase-8, -10 dependent apoptosis and other reports where paclitaxel acts through caspase-9 dependent apoptosis (Park et al., 2004; Zhang, Qiu, Jin, Guo, & Guo, 2009). Scouring through the literature gave rise to the idea that anti-mitotics could potentially be interfering in ER to Golgi transport, on the assumption that binding of vinorelbine or paclitaxel would alter microtubule structure enough to disrupt dynein or kinesin progression down microtubules (Pei-Chun Liao, 2008). ER stress, such as inhibition of ER to Golgi transport, activates a multitude of signaling pathways, one such pathway is activation of CHOP by ATF4 and ATF6, treatment with paclitaxel and vinorelbine cause expression of CHOP in H2887 cells similar to treatment with tunicamycin, while treatment with gemcitabine does not cause expression of CHOP (Figure 5.24).

During times of ER stress, mammalian cells active IRE1 recruits TRAF2 and ASK1 which activates JNK (Boyce & Yuan, 2006; Marciniak & Ron, 2006). TRAF2 can activate JNK at the TNFR as well, and TRAF2 recruits cIAP1/2 to the TNFR, which left me wondering does TRAF2 recruit cIAP1/2 to the ER as well? I then looked for cIAP1 interactions with the IRE1 complex using monoclonal antibodies against ASK1 and TRAF2, as well as a polyclonal antibody against IRE1 and in all cases cIAP1 was pulled down from lysates from untreated H2887 cells (Figure 5.25).

5.2.10 ER STRESS INDUCED APOPTOSIS MEDIATED THROUGH CASPASE 4 AS MECHANISM FOR JP1201 + CHEMOTHERAPY SENSITIZATION

To better understand how NSCLCs are sensitized to the combination of JP1201 with vinorelbine, we used the Stress and Toxicity Cignal Finder 10-pathway reporter array. H1395 cells were reverse transfected with a set of pathway specific firefly luciferase reporter constructs and control renilla luciferase constructs. Twenty four hours after transfection, cells were treated with 1μM JP1201, 1 μM gemcitabine, 1 μM vinorelbine, or JP1201 + vinorelbine for an additional 24 hours. Gemcitabine treatment induced p53 activity compared to un-treated control (Table 5.5). No significant pathway activity was activated by JP1201 or vinorelbine alone; however, the combination of JP1201 + vinorelbine resulted in ER stress activation (as a function of CBF/NF-Y transcriptional activity) and JNK activity (as a function of AP-1 transcriptional activity).

HCC4017, HBEC30KT, H1395, and H157 were reverse transfected with a set of pathway specific firefly luciferase reporter constructs and control renilla luciferase constructs, and cells were treated with JP1201 or the combination of JP1201 + vinorelbine for 24 hours after transfection. Activity of the indicated pathway was determined by firefly luciferase activity relative to control renilla luciferase activity (Table 5.6). Only the ER stress pathway was activated by combination therapy in all three NSCLC lines but not the normal cells. Caspase-4 is the putative initiator caspase for the ER stress induced apoptotic pathway

(Hitomi, et al., 2004; Pei-Chun Liao, 2008). Knockdown of caspase-4 protects H1395 cells against the effect to a greater extent than knockdown of caspase-3 or -9 (Figure 5.26). Additionally, using an antibody that only recognizes pro-caspase-4 but not activated caspase-4, we found that vinorelbine treatment resulted in to activation of caspase-4 over time, similarly to agents that are known to activate the ER stress pathway, thapsigargan and tunicamycin (Figure 5.27).

5.3 DISCUSSION

Evaluation of the apoptotic machinery in tumors has led to the development of therapeutic agents targeting this machinery, including SMAC mimetics (L. Li, et al., 2004; Oost et al., 2004; S. Sharma, Straub, & Zawel, 2006; H. Sun et al., 2006; H. Sun, Z. Nikolovska-Coleska, C. Y. Yang, L. Xu, M. Liu, et al., 2004; H. Sun, Z. Nikolovska-Coleska, C. Y. Yang, L. Xu, Y. Tomita, et al., 2004; Zobel et al., 2006). This study addressed the utility of SMAC mimetic JP1201 in NSCLCs that do not express TNFα and are resistant to SMAC mimetic monotherapy. In a panel of NSCLC lines JP1201 frequently synergized with available chemotherapy agents, with considerable inter-tumor heterogeneity in NSCLC responses between drug combinations. In NSCLC xenografts, where JP1201 alone had little effect on tumor growth, the combination of vinorelbine or gemcitabine with JP1201 decreased tumor growth, which translated to an increase in survival of these mice. The frequent occurrence of synergy (particularly with paclitaxel and vinorelbine) suggests potential for JP1201 or similar drugs as a part

of combination chemotherapy for NSCLC. This agrees with the findings of Dean et al. (Dean, et al., 2009) who studied two NSCLC lines and found synergy with vinorelbine in combination with a different IAP antagonist that targeted XIAP.

JP1201 sensitized many NSCLC lines to concentrations of vinorelbine (10-15 nM) and paclitaxel (~100 nM) that are achievable in humans as steady state plasma (Leveque & Jehl, 1996; Rowinsky, Jiroutek, Bonomi, Johnson, & Baker, 1999). Also, three NSCLC lines, all wild-type for EGFR, were sensitized to the EGFR TKI, erlotinib at clinically achievable concentrations (Scheffler, et al., 2011). Studying a large panel of NSCLC lines, including the two studied by Dean et al., we found no synergy with JP1201 + cisplatin, while Dean using the BIR2 binding XIAP antagonist XAC 1296-11 saw synergy with cisplatin (Dean, et al., 2009). The reason for this discrepancy is not yet understood but suggests mechanistic specificity of the different SMAC mimetics. The lack of sensitization to cisplatin seen in this study correlates with p53 mutational status, indicating that p53 mutations may prevent cisplatin induced apoptotic signaling (Table 5.7).

Our panel includes three types of genetically paired cell lines, NSCLC lines started before (H1693 and H1993) and after etoposide/cisplatin treatment (H1819 and H2073), an isogenic HBEC3KT based system where oncogenic Kras and knockdown of p53 were introduced and tumorigenic clones were isolated from soft agar clones, and a tumor (HCC4017) and normal HBEC pair. Using these, we found sensitization by JP1201 to chemotherapy is specific for the

malignant phenotype, and NSCLC lines derived from samples after chemotherapy could be sensitized to chemotherapy more than NSCLCs that were chemo-naïve. Thus SMAC mimetic based combinations with chemotherapy may be effective in tumor cells resistant to chemotherapy alone.

XIAP is the only IAP with the ability to inhibit the enzymatic activity of an active caspase (Holcik, et al., 2001). Thus, it was reasonable to predict that stimulation of the intrinsic pathway of apoptosis would only require the inhibition of XIAP for apoptosis to occur (Yuan, 2006) such as was found in pancreatic cancer cell lines treated with JP1201 + gemcitabine (Dineen, et al., 2010). When we combine siRNA against cIAP1, cIAP2, or XIAP with gemcitabine, we see that the knockdown of XIAP mimics the combination of JP1201 + gemcitabine. By contrast we found knockdown of each cIAP1, cIAP2, or XIAP mimics to different degrees the effect seen when JP1201 is combined with paclitaxel or vinorelbine, suggesting unique roles for each IAP in sensitizing NSCLCs to anti-mitotics.

Inhibition of tubulin dynamics such as with vinorelbine can inhibit ER to Golgi transport, a trigger for ER stress-induced apoptosis (Boyce & Yuan, 2006; Pei-Chun Liao, 2008). Analysis of pathways activated by the combination of JP1201 + vinorelbine in multiple cells lines revealed that the ER stress pathway is activated. Furthermore, western blotting, and siRNA-mediated rescue experiments also showed that caspase-4, the putative ER stress induced caspase, is activated after vinorelbine treatment, and knockdown of capsase-4 protected

NSCLCs from treatment of JP1201 + vinorelbine better than knockdown of the executioner caspase, caspase-3. There are reports that suggest cIAP1 is involved in a complex at the ER membrane that is responsible for activating apoptosis; however, further studies are needed to characterize the role of the ER stress pathway in sensitizing NSCLCs to chemotherapy by SMAC mimetics (Cheung, Lynn Kelly, Liston, & Korneluk, 2006; Hitomi, et al., 2004; Szegezdi, Logue, Gorman, & Samali, 2006).

We found JP1201 resistant NSCLC lines do no induce or secret TNFα after chemotherapy indicating the synergy seen between doxorubicin, gemcitabine, paclitaxel, or vinorelbine with JP1201 is TNFα independent. Studies adding recombinant TNFα with gemcitabine or vinorelbine also suggest that TNFα is not involved in the JP1201 induced sensitization to chemotherapy. This is further strengthened by the lack of additional sensitization when the combination of TNFα and gemcitabine or vinorelbine is given to cells where XIAP expression has been knocked down. The lack of protection of combinations of JP1201 + vinorelbine by the knockdown of caspase 8, RIPK1, or TNFR1 further suggests JP1201 is promoting apoptosis in a TNFα independent fashion (Petersen, et al., 2007; Varfolomeev, et al., 2007; Vince, et al., 2007).

In conclusion, we find that: a SMAC mimetic significantly sensitizes NSCLC lines to chemotherapy and EGFR targeted therapy; the sensitization varies between NSCLCs and between chemotherapeutic agents; the sensitization

is tumor specific and is stronger in NSCLCs that have progressed after neoadjuvant therapy; the required IAP target to be inhibited varied between chemotherapeutic agents; and the sensitization appeared to be TNFα independent, but dependent on two complementary apoptotic pathways, mitochondrial and ER Stress. These data strongly suggest the need to explore SMAC mimetics in combination with standard doublet chemotherapy as a new treatment approach for NSCLC patients.

	Absolute fold decrease in IC_{50} of chemotherapy agents when combined with JP1201						
cell line	**Vinorelbine**	**Paclitaxel**	**Doxorubicin**	**Gemcitabine**	**Cisplatin**	**Erlotinib**	**Paclitaxel/Carboplatin**
H2073	31000	1	1	1	0.4	1	1
H1819	4400	5600	1	6	0.7	4	18
H2887	3600	22	7726	23	1	1	20
H1993	270	6	1	2	0.4	0.7	5
H358	397	17	13	4	1	6	12
H441	181	3	4	16	0.5	4	2.8
A549	100	4	5	2	0.7	18	4.6
H2882	73	11	1	21	0.6	0.7	10
H460	36	2	3	1	1.2	10	1.8
H1395	33	43	10	134	1	0.4	23
H1355	22	10	1	1	0.7	1	NT
H157	16	32	3	2	1	111	15
H1693	15	6	1	7	0.6	NT	NT
H2009	12	4	1	3	1	1	NT
H2087	1	4	4	1	1.4	1	3.6
HCC4017	25	10	6	15	0.7	1	NT
HBEC30KT	1	1	1	1	1	1	NT
HBEC3KT	1	1	1	1	1	1	NT
HBEC3KT clone1	20	12	3	7	NT	NT	NT
HBEC3KT clone5	20	15	2	9	NT	NT	NT

TABLE 5.1 JP1201 Sensitizes NSCLC to doxorubicin, erlotinib, gemcitabine, paclitaxel, and vinorelbine *in vitro*.

Fold change is determined by dividing the median IC_{50} for each chemotherapy as a single agent ($n \geq 4$) by the median IC_{50} for each chemotherapy in combination with 10 μM JP1201 ($n \geq 3$). NT represents instances where the combination was not tested.

	IC_{50} as determined by liquid colony formation							
cell line	Gemcitabine	JP1201 + Gemcitabine	Paclitaxel	JP1201 + Paclitaxel	Vinorelbine	JP1201 + Vinorelbine	Erlotinib	JP1201 + Erlotinib
H157	1.7	0.05	0.27	0.1	0.3	0.03	5.2	0.9
H1693	1.5	0.04	0.5	0.021	0.33	0.2	-	-
H1819	1.6	0.06	1.2	0.03	0.43	0.1	-	-
H1993	0.09	0.06	0.24	0.09	0.26	0.004	4.5	0.08
H2009	0.09	0.07	0.02	0.009	0.43	0.038	-	-
H2073	0.1	0.06	0.25	0.13	0.3	0.004	2.5	1.2
HBEC3KT	1.7	2.1	1.6	2.3	0.3	0.5	-	-
HBEC3KT RL53-S1	5.2	7.9	2.5	0.26	0.083	0.029	-	-
HBEC3KT RL53-S5	0.3	0.3	0.53	0.01	0.24	0.006	-	-
HBEC30KT	1.2	1.5	2.5	1.5	0.8	0.9	-	-
HCC4017	21.3	7.7	2.3	0.11	11.8	1.6	-	-

TABLE 5.2 Confirmation of NSCLC response to combination of 100 nM JP1201 with gemcitabine, paclitaxel, vinorelbine, or erlotinib.

Cells were seeded at 500 cells per well in 6 well dishes. The appropriate concentrations of drug were prepared from stock solutions in medium and given to cells for 10-28 days depending on the cell line. At the end of the assay, medium was aspirated and cells were fixed and stained with 0.5% methylene blue in 50% ethanol for 30 minutes. After staining, wells were washed and black and white images of the plates were taken using a ChemiDoc XRS imager and colonies counted (Quantity One software v4.6.5, BioRad, Hercules, CA). Colony counts are averages of triplicate wells done in triplicate over a two week period.

- indicates where no drug sensitivity data has been determined.

	Combination Indices of Chemotherapy with 10 μM JP1201					
cell line	Vinorelbine	Paclitaxel	Gemcitabine	Doxorubicin	Cisplatin	Erlotinib
H2073	0.10 ± 0.00	1.58 ± 0.54	1.43 ± 0.53	1.05 ± 0.59	3.09 ± 2.54	0.83 ± 0.01
H1819	0.10 ± 0.00	0.12 ± 0.00	0.27 ± 0.1	1.22 ± 0.2	1.74 ± 0.29	0.29 ± 0.011
H2887	0.17 ± 0.00	0.23 ± 0.002	0.23 ± 0.001	0.17 ± 0.03	1.46 ± 1.3	1.00 ± 0.24
H1993	0.27 ± 0.001	0.5 ± 0.01	0.87 ± 0.01	1.49 ± 0.67	1.55 ± 1.37	0.61 ± 0.1
H358	0.10 ± 0.001	0.16 ± 0.01	0.35 ± 0.04	0.18 ± 0.01	1.01 ± 1.23	0.25 ± 0.01
H441	0.11 ± 0.22	0.44 ± 0.17	0.17 ± 0.02	0.35 ± 0.08	2.32 ± 1.95	0.22 ± 0.02
A549	0.11 ± 0.01	0.41 ± 0.11	0.79 ± 0.48	0.33 ± 0.07	1.59 ± 0.7	0.16 ± 1.2
H2882	0.12 ± 0.01	0.20 ± 0.02	0.15 ± 0.003	1.20 ± 1.13	1.97 ± 1.05	1.37 ± 0.3
H460	0.13 ± 0.01	0.72 ± 0.08	1.44 ± 0.03	0.43 ± 0.02	0.99 ± 0.92	0.21 ± 0.05
H1395	0.13 ± 0.01	0.13 ± 0.04	0.10 ± 0.01	0.22 ± 0.06	0.99 ± 0.1	1.14 ± 1.2
H1355	0.15 ± 0.02	0.21 ± 0.03	0.63 ± 0.03	0.93 ± 0.03	1.12 ± 1.04	1.07 ± 1.1
H157	0.19 ± 0.02	0.16 ± 0.02	0.72 ± 0.02	0.45 ± 0.03	1.22 ± 1.9	0.13 ± 0.001
H1693	0.19 ± 0.01	0.3 ± 0.08	0.27 ± 0.03	1.23 ± 1.15	1.22 ± 1.01	NT
H2009	0.19 ± 0.01	0.34 ± 0.01	0.47 ± 0.01	0.93 ± 0.41	1.89 ± 1.17	1.12 ± 0.4
H2087	2.42 ± 1.37	0.36 ± 0.02	0.90 ± 0.36	0.36 ± 0.02	0.92 ± 0.87	0.99 ± 0.1
HCC4017	0.33 ± 0.01	0.23 ± 0.03	0.59 ± 0.02	1.05 ± 0.21	1.28 ± 0.97	1.13 ± 0.2
HBEC30KT	62.96 ± 5.37	15.65 ± 1.3	1.41 ± 0.3	0.80 ± 0.17	1.65 ± 0.1	2.35 ± 0.1
HBEC3KT	34.39 ± 2.39	2.54 ± 1.1	3.01 ± 0.71	1.3 ± 0.02	1.25 ± 0.61	5.19 ± 1.1
HBEC3KT RL53 s1	0.12 ± 0.01	0.21 ± 0.08	1.77 ± 0.7	1.20 ± 0.1	NT	NT
HBEC3KT RL53 s5	0.13 ± 0.01	0.24 ± 0.1	1.2 ± 0.31	1.18 ± 0.2	NT	NT

TABLE 5.3 JP1201 can synergize with chemotherapy.

Combination indices (CI) were calculated using the Chou-Talay method (Chou & Rideout, 1991). CI values that are less than 1 ± 0.2 indicate synergy, values that are equal to 1 ± 0.2 indicate additivity, and values that are greater than 1 ± 0.2 indicate antagonism. Error was calculated by propagating the error from the drug sensitivity phenotypes from MTS data. Data represents average of ≥3 determinants.

qRT-PCR mRNA levels relative to siLuc control (2-ΔΔCT values)

	H1395											
	siLuc	si-cIAP1	si-cIAP2	siXIAP	si-cIAP1, si-cIAP2, siXIAP	JP1201	siCasp3	siCasp4	siCasp9	siCasp8	siRIPK1	siTNFR1
cIAP1	1	0.132	1.23	0.79	0.139	1.28	-	-	-	-	-	-
cIAP2	1	1.85	0.44	1.55	1.99	5.68	-	-	-	-	-	-
XIAP	1	0.67	1.3	0.1	ND	7.9	-	-	-	-	-	-
Caspase 3	1	-*	-	-	-	-	0.014	0.94	1.105	0.91	-	-
Caspase 4	1	-	-	-	-	-	0.85	0.14	1.09	1.3	-	-
Caspase 9	1	-	-	-	-	-	0.776	0.864	0.007	0.947	-	-
Caspase 8	1	-	-	-	-	-	0.78	1.1	1.15	0.24	-	-
TNFR1	1	-	-	-	-	-	-	-	-	-	1.36	0.358
RIPK1	1	-	-	-	-	-	-	-	-	-	0.123	1.31
TNFα	ND**	ND	ND	ND	ND	ND	ND	ND	ND	ND	ND	ND

TABLE 5.4 Changes in mRNA expression after siRNA knockdown are validated by q-RTPCR. Studies of H1395 cells associated with Figures 5.21, 5.25.

H1395 cells were transfected with siRNAs against: firefly luciferase, cIAP1, cIAP2, XIAP, caspase-3, caspase-4, caspase-9, caspase 8, RIPK1, TNFR1, or pooled siRNAs of cIAP1, cIAP2, and XIAP, or treated with JP1201. 24 hours later, cells were harvested and total RNA prepared (RNeasy Plus Mini Kit, 74134, Qiagen, Hilden, Germany). cDNA was synthesized from 1 µg total RNA using the iScript cDNA synthesis kit (BioRad, Hercules, CA). Gene specific TaqMan probes (Applied Biosystems, Foster City, CA) were used to quantitate GAPDH, cIAP1, cIAP2, XIAP, Caspase-3, -4, -8, and -9, RIPK1, TNFR1, and TNFα levels in biological duplicates as well as duplicate samples of siRNA transfected H1395 cells. The $2^{-\Delta\Delta CT}$ method was used to calculate relative expression levels (Livak & Schmittgen, 2001). Expression of target genes were normalized to GAPDH

expression, and expression was normalized to H1395 cells transfected with luciferase siRNA.

* - indicates where no gene expression data has been determined.

** ND indicates where gene expression was not detected

	Fold change in relative luciferase activity of treated H1395 cells compared to untreated control			
Pathway	**JP1201**	**Gemcitabine**	**Vinorelbine**	**Vinorelbine + JP1201**
1	0.9	1.1	0.8	1.3
2	0.8	**2.6**	0.7	1.1
3	0.8	0.9	0.9	1.1
4	0.9	0.8	1.1	1.1
5	1.4	1.7	0.8	**3.5**
6	0.6	0.8	1.1	1.1
7	0.8	1.3	1	1
8	1.1	0.8	1.4	1.1
9	1.3	0.9	0.8	**2.5**
10	1.2	1.3	0.7	1.3

TABLE 5.5 Analysis of pathways activated by JP1201 + chemotherapy using Cignal finder assay system (SABiosciences).

The combination of JP1201 + vinorelbine selectively activates the ER stress pathway. H1395 cells were reverse transfected with firefly luciferase reporter constructs that contain response elements for the indicated pathways and control renilla luciferase constructs, then treated with 10 μM JP1201, 1 μM gemcitabine, 1 μM vinorelbine, or JP1201 + vinorelbine for 24 hours, luciferase activity was assayed, firefly luciferase activity was normalized to renilla luciferase activity for each sample, and normalized to un-transfected cells.

* Pathways are: 1) oxidative stress, 2) p53, 3) NF-κB, 4) hypoxia, 5) ER stress, 6) heavy metals, 7) heat shock, 8) the glucocorticoid receptor, 9) the JNK pathway, or 10) the xenobiotic receptor

** Bolded and underlined values have $p < 0.001$ by two-way ANOVA.

	Fold change in relative luciferase activity of cells treated with JP1201 + vinorelbine compared to JP1201 alone			
Pathway	**H1395**	**H157**	**HCC4017**	**HBEC30KT**
1	**3.4**	0.7	1.1	0.4
2	**1.7**	**2.6**	0.4	0.4
3	2.2	0.9	1.1	1.5
4	**2.5**	0.8	0.6	0.7
5	**4.4**	**2.1**	**3.8**	0.5
6	**1.7**	**2.8**	0.4	0.4
7	**1.7**	**3.5**	0.7	0.5
8	0.9	1.3	0.3	0.4
9	**4.7**	1.1	0.5	0.9
10	0.8	1.3	0.7	0.7

TABLE 5.6 Analysis of pathways activated by JP1201 + chemotherapy using Cignal finder assay system (SABiosciences).

ER stress pathway is activated by the combination of vinorelbine + JP1201. H1395, H157, HCC4017, and HBEC30KT cells were reverse transfected with the indicated firefly luciferase reporter construct, treated with JP1201 + vinorelbine. Firefly luciferase activity was normalized to renilla luciferase for each sample, and to JP1201 treated cells.

* Pathways are: 1) oxidative stress, 2) p53, 3) NF-κB, 4) hypoxia, 5) ER stress, 6) heavy metals, 7) heat shock, 8) the glucocorticoid receptor, 9) the JNK pathway, or 10) the xenobiotic receptor

** Bolded and underlined values have $p < 0.001$ by two-way ANOVA.

Analysis of Oncogenotype and Drug Response Phenotypes of Combination Therapy with JP1201							
	(Pearson r values)						
	Vinorelbine	Paclitaxel	Doxorubicin	Gemcitabine	Cisplatin	Erlotinib	Paclitaxel/Carboplatin
p53	0.17	-0.33	-0.2	-0.28	-0.51	0.16	-0.39
Braf	-0.1	-0.07	-0.08	**0.64***	**0.61**	-0.13	0.2
SMARCA4	-0.07	0.46	-0.11	-0.15	-0.15	**0.63**	0.19
STK11	0.27	-0.17	-0.17	0.19	-0.17	0.35	-0.13
PI3K	-0.07	-0.05	-0.05	-0.1	0.33	0	-0.35
Kras	-0.26	-0.25	0.21	-0.21	0.14	0.31	-0.12

TABLE 5.7 Pearson correlations of gene mutation and absolute fold decrease in drug IC_{50} when combined with JP1201.

There are significant negative and positive correlations with various oncogene and tumor suppression gene mutations.

* Bold figures identify significant Pearson correlations ($p<0.05$).

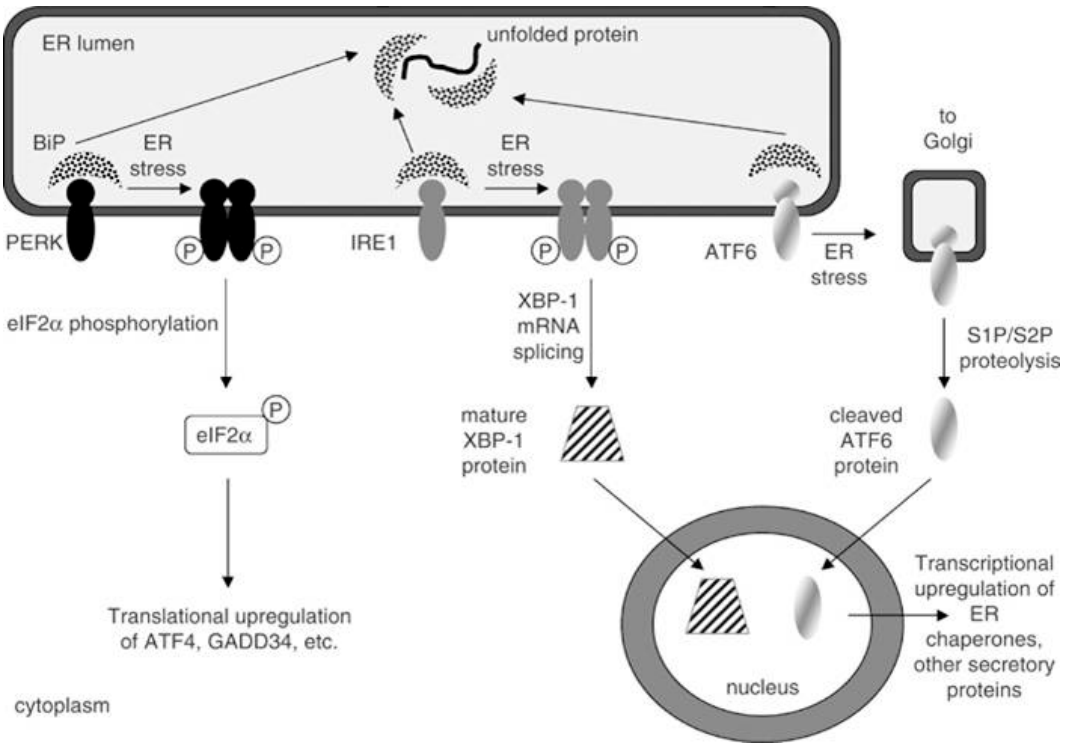

FIGURE 5.1 Mammalian ESR signaling.

Unfolded protein in the ER lumen titrates BiP away from three sentinels of ER stress: PERK, IRE1 and ATF6. Activated PERK phosphorylates the translation initiation factor eIF2 to slow global protein synthesis temporarily and upregulate certain stress-inducible messages, such as ATF4. Activated IRE1 splices the mRNA for XBP-1 to allow the translation of mature XBP-1 protein, a transcription factor that mediates the transcriptional upregulation of numerous genes involved in mammalian ER function and the secretory pathway in general. Similarly, during ER stress ATF6 traffics to the Golgi, where it is cleaved by

S1P/S2P proteases and thereby released from the membrane to activate a distinct but overlapping set of genes in the nucleus. Adapted from Boyce et al., 2006.

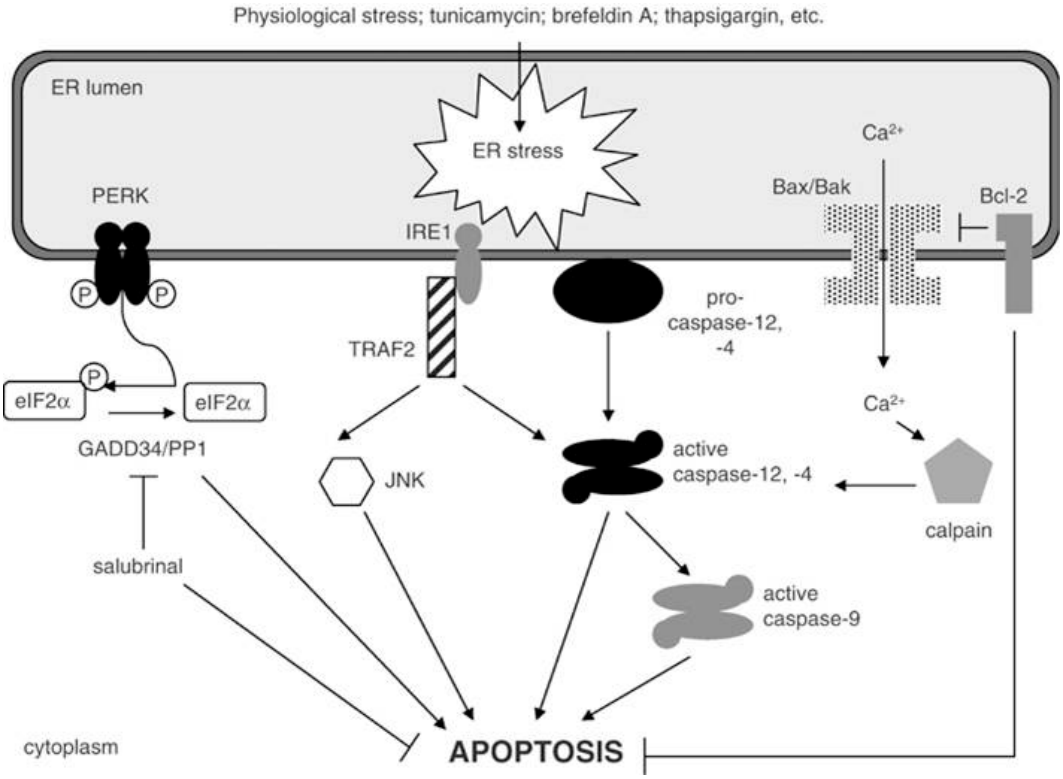

FIGURE 5. 2 Simplified depiction of selected apoptotic pathways induced by ER stress.

Physiological or experimentally induced ER stress leads to the activation of PERK and, eventually, the GADD34/PP1 phosphatase complex, which dephosphorylates eIF2alpha, promoting apoptosis. Genetic strategies or chemicals (e.g., salubrinal) that enforce eIF2alpha phosphorylation protect cells from ER stress-induced apoptosis. Caspase-12 (mice) or -4 (humans) is associated with the cytoplasmic face of the ER membrane and can be activated by ER stress in several ways, including via IRE1 and TRAF2, or by cleavage by calpain, itself activated by the release of calcium from ER stores. Bcl-2 family members also

reside in the ER membrane and influence apoptosis induced by ER stress, both through the regulation of calcium flux and amplification of the apoptotic signal via the mitochondrial pathway (not shown). Adapted from Boyce et al., 2006.

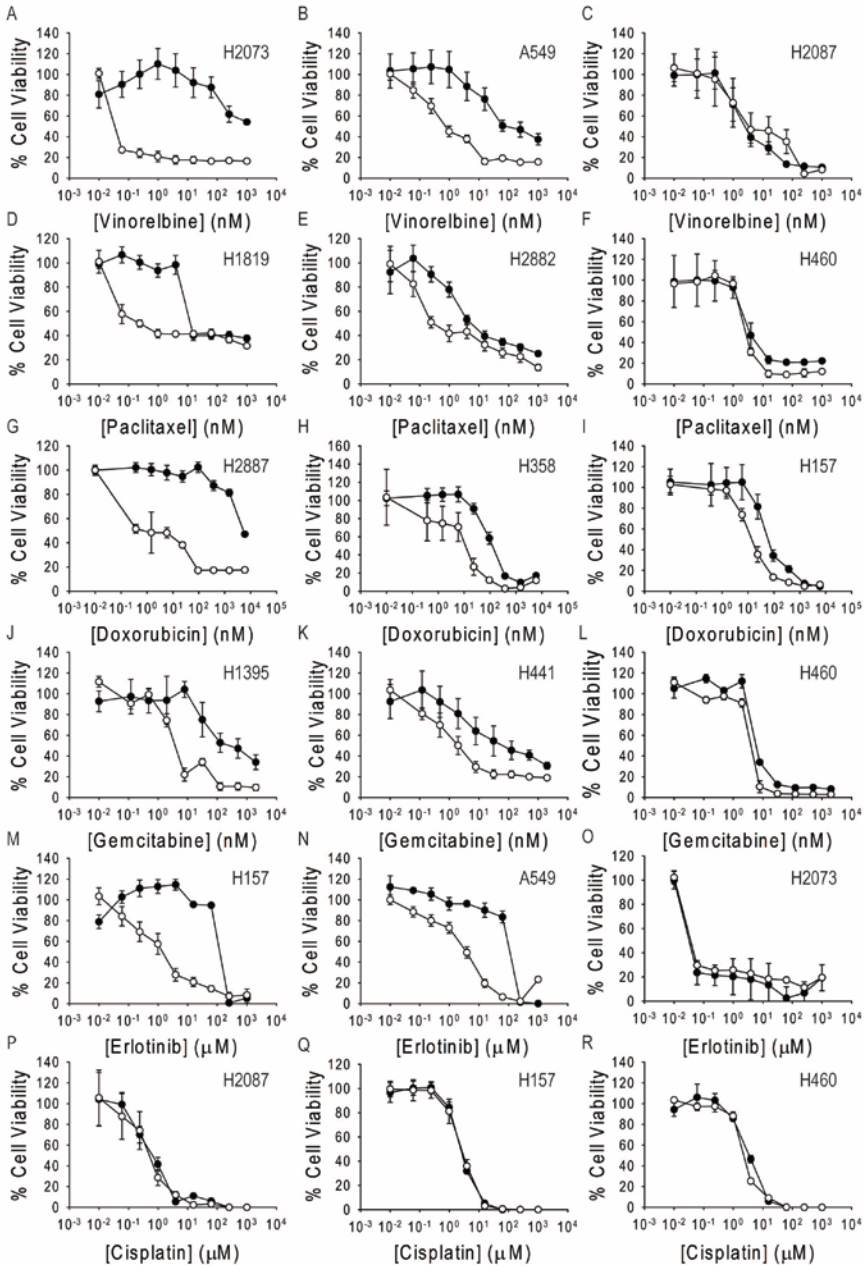

FIGURE 5.3 Drug sensitivity profiles of chemotherapy in combination with JP1201 have three distinct phenotypes.

(A) NCI-H2087 (B) NCI-H157 and (C) NCI-H460 were treated with cisplatin (black circles) or cisplatin in combination with 10 μM JP1201 (open circles). (D) NCI-H2887 (E) NCI-H358 and (F) NCI-H157 were treated with doxorubicin (black circles) or doxorubicin in combination with 10 μM JP1201 (open circles). (G) NCI-H1395 (H) NCI-H441 and (I) NCI-H460 were treated with gemcitabine (black circles) or gemcitabine in combination with 10 μM JP1201 (open circles). (J) NCI-H1819 (K) NCI-H2882 and (L) NCI-H460 were treated with paclitaxel (black circles) or paclitaxel in combination with 10 μM JP1201 (open circles). (M) NCI-H2073 (N) A549 and (O) NCI-H2087 were treated with vinorelbine (black circles) or vinorelbine in combination with 10 μM JP1201 (open circles). (P) NCI-H157 (Q) A549 and (R) NCI-H2073 (bottom) were treated with erlotinib (black circles) or erlotinib in combination with 10 μM JP1201 (open circles).

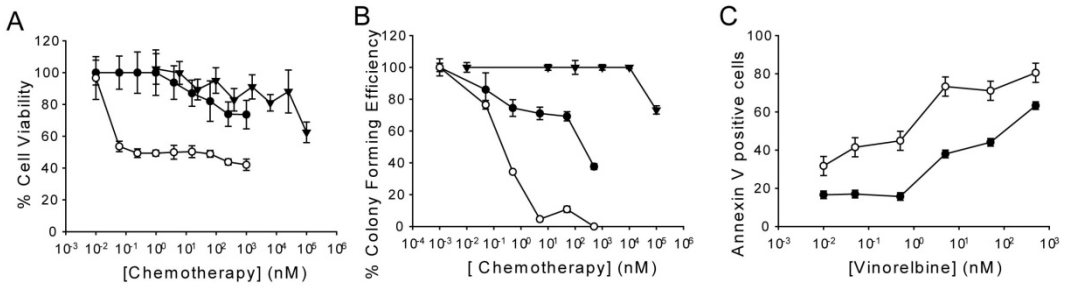

FIGURE 5.4 JP1201 Can Synergize with Chemotherapy *In Vitro*.

(A) Cell viability curves of NCI-H1819 treated with vinorelbine alone (black circles), in combination with 10 μM JP1201 (open circles), or JP1201 alone (black triangles), data is representative of at least three replicates of independently preformed 96 well plate assay. (B) Colony forming efficiency expressed as a percent of untreated NCI-H1819 in the presence of vinorelbine alone (black circles), in combination with 10 μM JP1201 (open circles), or JP1201 alone (black triangles) for two weeks, data is representative of two independent assays performed 3 weeks apart. (C) Number of Annexin V positive NCI-H1819 cells which were treated with vinorelbine alone (black circles), or vinorelbine with 10 μM JP1201 (open circles) 48 hours after drug treatment as determined by FACS analysis.

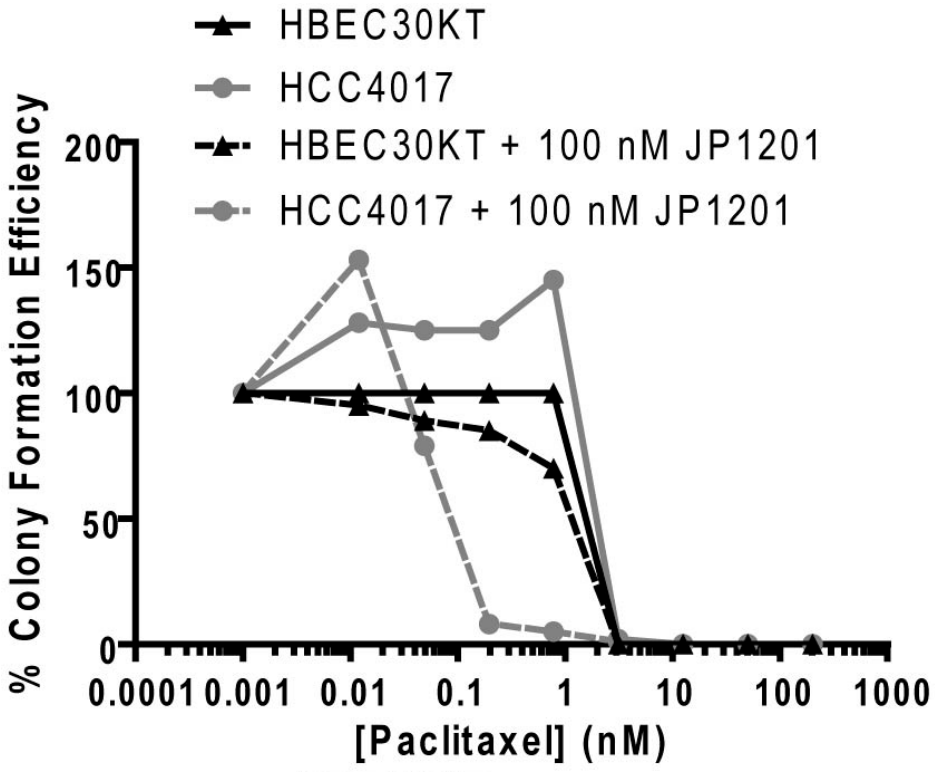

FIGURE 5.5 JP1201 Specifically Sensitizes Tumorgenic Cell Lines in a Tumor/Normal Isogenic System.

Colony forming efficiency expressed as a percent of untreated HCC4017 (circles) and HBEC30KT (triangles) in the presence of paclitaxel alone (solid line), or in combination with 100 nM JP1201 (dashed line), data is representative of two independent assays.

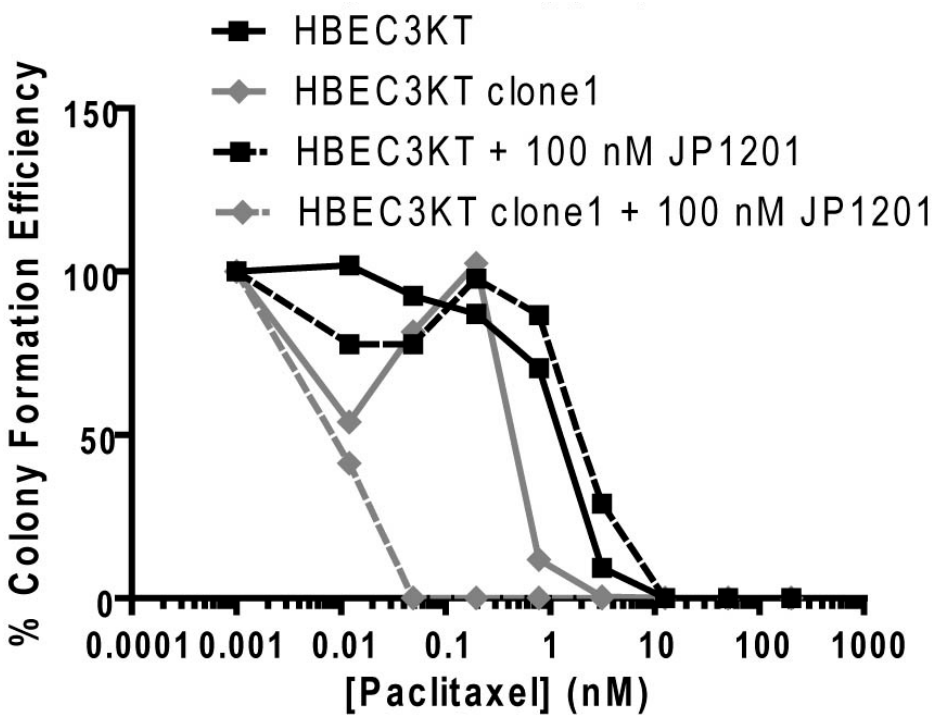

FIGURE 5.6 JP1201 Specifically Sensitizes Tumorgenic Cell lines in an Isogenic System.

Colony forming efficiency expressed as a percent of untreated HBEC3KT RL53 clone1 (diamonds) and HBEC3KT (squares) in the presence of paclitaxel alone (solid line), or in combination with 100 nM JP1201 (dashed line), data is representative of two independent assays.

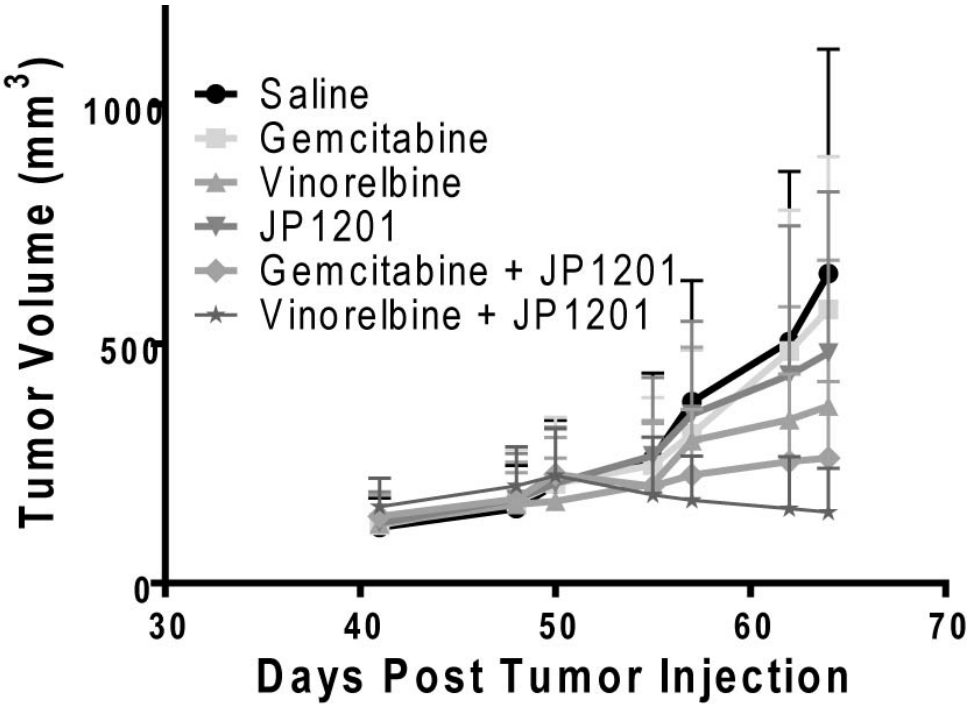

FIGURE 5.7 JP1201 in Combination with Gemcitabine or Vinorelbine Is Effective in Controlling NCI-H1395 Xenograft Growth.

Tumor growth curves during the course of treatment, treatment began on day 41, saline, 25 mg/kg gemcitabine and 6 mg/kg JP1201 were given thrice weekly, 2.4 mg/kg vinorelbine given twice weekly.

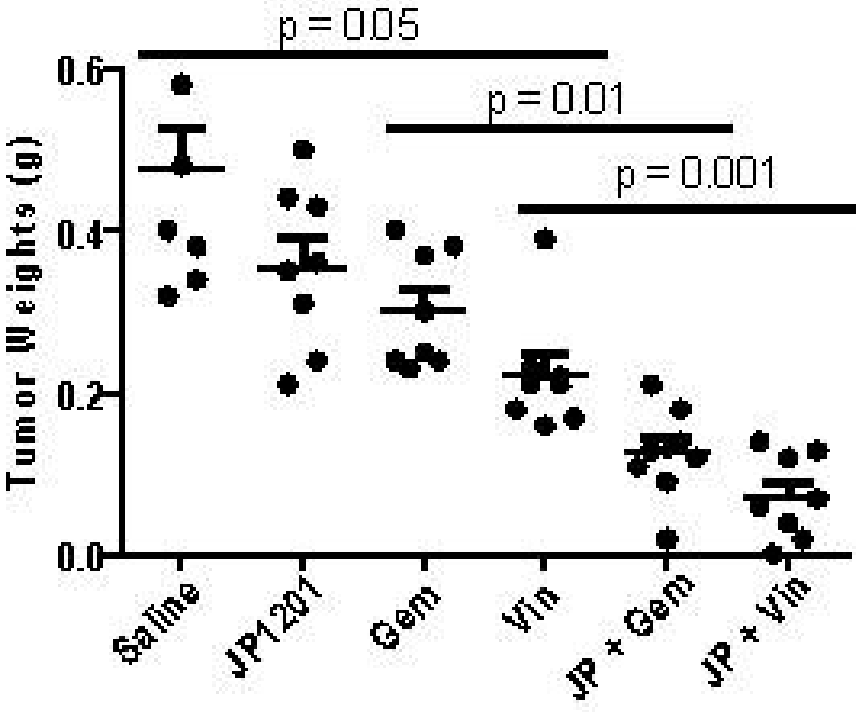

FIGURE 5.8 JP1201 in Combination with Gemcitabine or Vinorelbine Results in Smaller Overall NCI- H1395 Tumor Size.

Tumor weights of xenografts were harvested 24 hours after the final treatments, treatment began on day 41, saline, 25 mg/kg gemcitabine and 6 mg/kg JP1201 were given thrice weekly, 2.4 mg/kg vinorelbine given twice weekly. Treatment was given for three weeks.

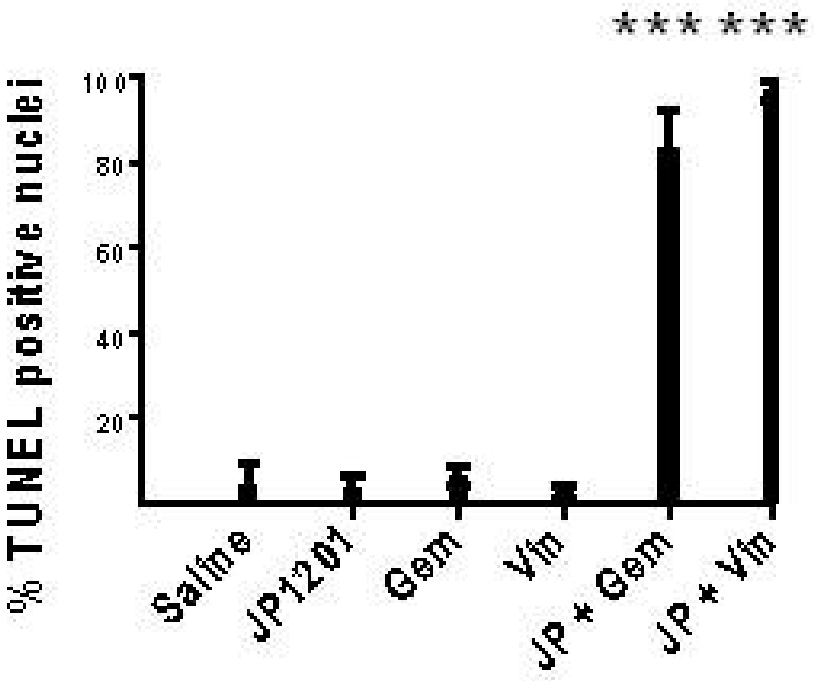

FIGURE 5.9 JP1201 in Combination with Gemcitabine or Vinorelbine Is Effective in Controlling NCI-H1395 Xenograft Growth by Inducing Apoptosis.

Induction of apoptosis was analyzed using TUNEL immunofluorescence. Data from a minimum of three tumors per treatment group were normalized to the saline group, and are representative of at least two independent assays, *** $p < 0.0001$.

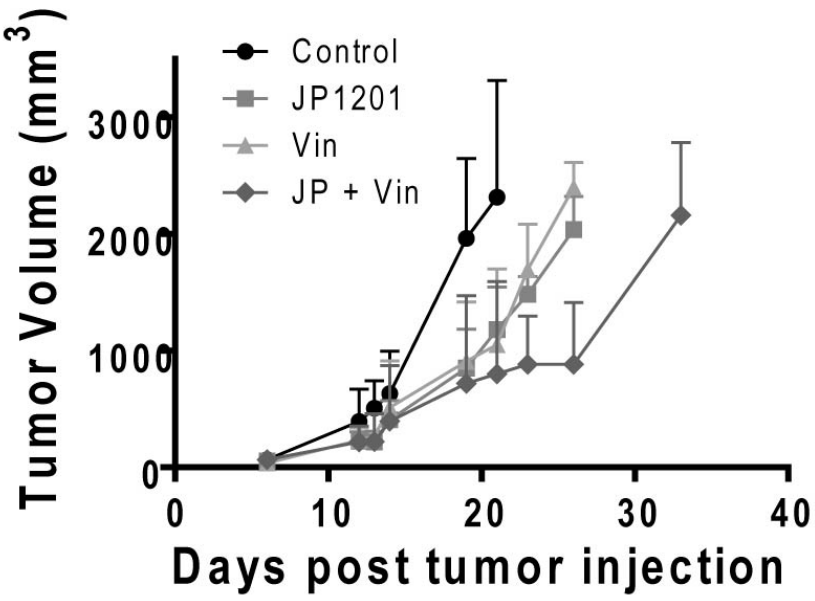

FIGURE 5.10 JP1201 in Combination with Vinorelbine Is Effective in Controlling NCI-H157 Xenograft Growth.

Tumor growth curves for xenografts, animals were sacrificed throughout the study due to tumor burden. Treatment began on day 14, saline and 6 mg/kg JP1201 were given thrice weekly, 2.4 mg/kg vinorelbine given twice weekly.

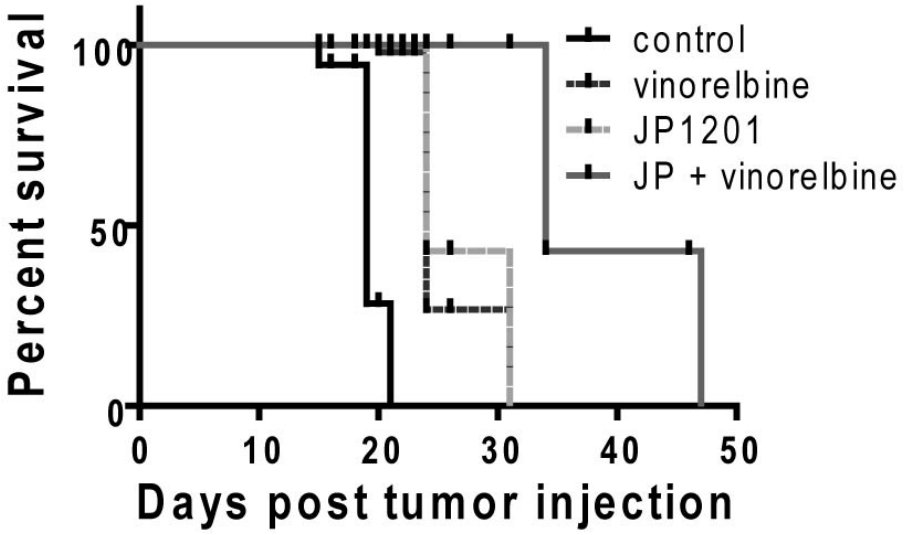

FIGURE 5.11 JP1201 in Combination with Vinorelbine Extends Survival Time of Mice Carrying NCI-H157 Xenografts.

Kaplen-Meyer survival curves. Animals had median survival times of 19, 24, 24, and 35 days respectively for saline, vinorelbine, JP1201, and JP1201 with vinorelbine.

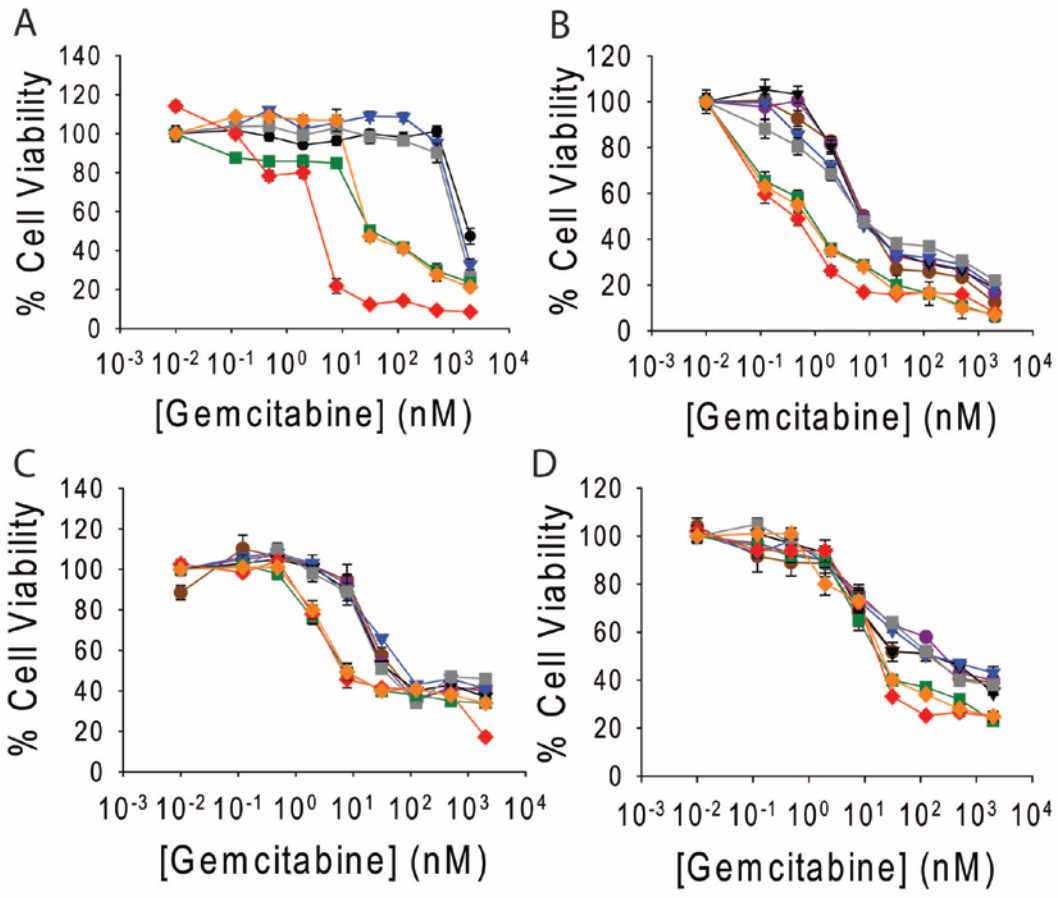

FIGURE 5.12 siRNA Mediated Knockdown of XIAP Can Mimic JP1201 When Co-Treated with Gemcitabine in NSCLCs.

Knockdown of XIAP is sufficient and necessary to mimic combination of JP1201 with gemcitabine On day zero (A) NCI-H1395, (B) NCI-H358, (C) NCI-H1819, and (D) NCI-H2887 cells were transfected in 96 well format with firefly luciferase siRNA, cIAP1 siRNA, cIAP2 siRNA, XIAP siRNA, or cIAP1, cIAP2, and XIAP siRNAs as indicated and on day one treated with increasing amounts of gemcitabine.

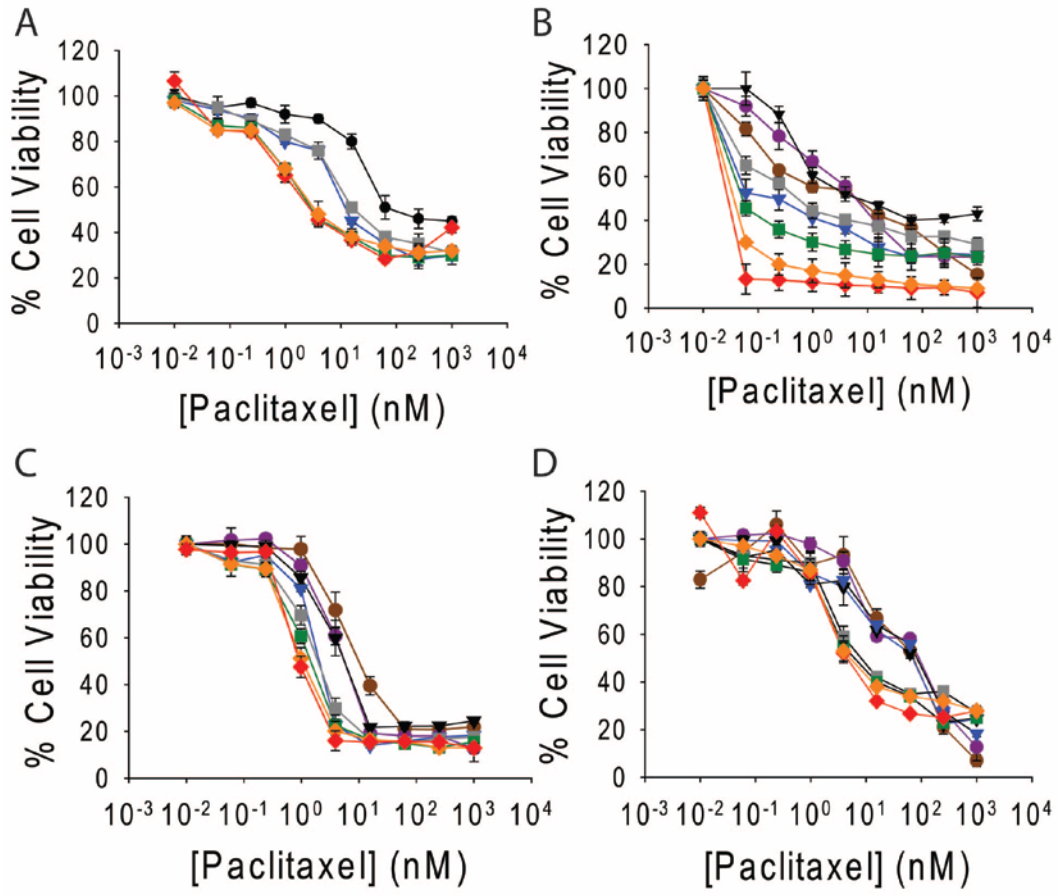

FIGURE 5.13 siRNA Mediated Knockdown of cIAP1, cIAP2, and XIAP Are All Required to Mimic JP1201 When Co-Treated with Paclitaxel in NSCLCs. Knockdown of cIAP1, cIAP2, and XIAP gives maximal sensitization to paclitaxel. On day zero (A) NCI-H1395, (B) NCI-H358, (C) NCI-H1819, and (D) NCI-H2887 cells were transfected in 96 well format with firefly luciferase siRNA, cIAP1 siRNA, cIAP2 siRNA, XIAP siRNA, or cIAP1, cIAP2, and XIAP siRNAs as indicated and on day one treated with increasing amounts of paclitaxel.

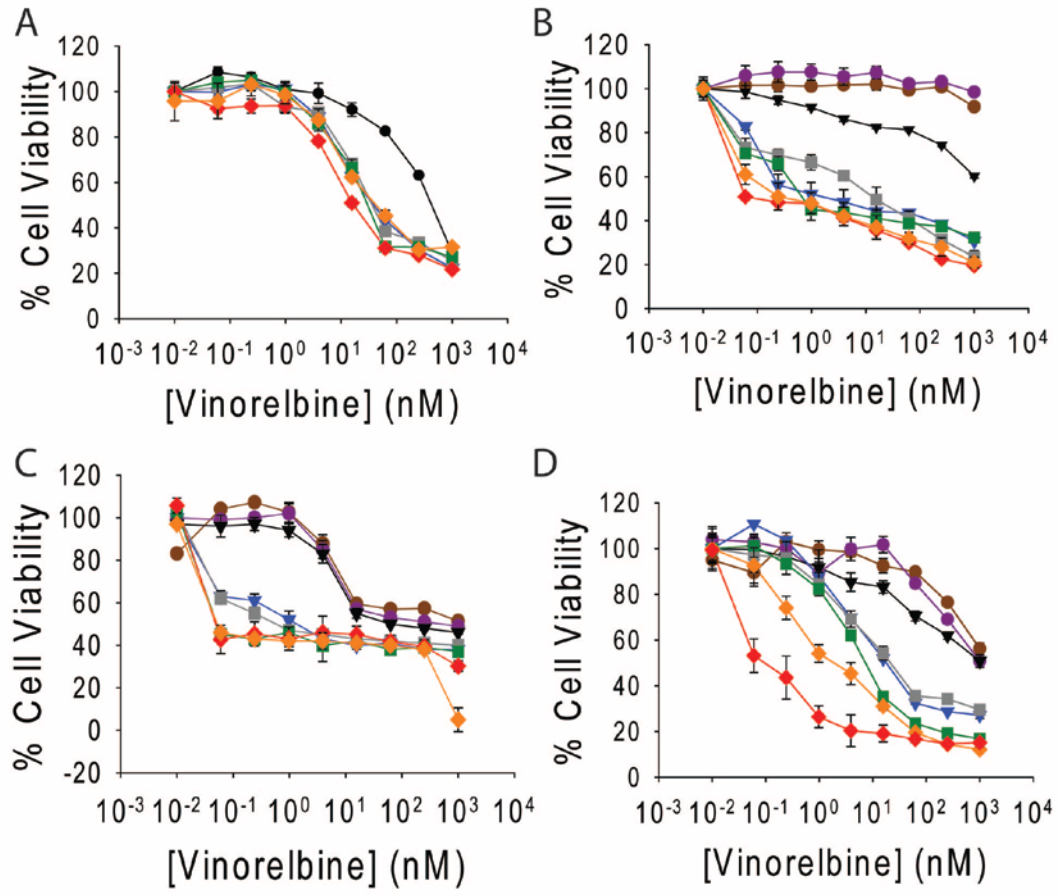

FIGURE 5.14 siRNA Mediated Knockdown of cIAP1, cIAP2, or XIAP Can Mimic JP1201 When Co-Treated with Vinorelbine in NSCLCs.

Knockdown of cIAP1, cIAP2, or XIAP mimics the sensitization to vinorelbine seen when treated with JP1201. On day zero (A) NCI-H1395, (B) NCI-H358, (C) NCI-H1819, and (D) NCI-H2887 cells were transfected in 96 well format with firefly luciferase siRNA, cIAP1 siRNA, cIAP2 siRNA, XIAP siRNA, or cIAP1,

cIAP2, and XIAP siRNAs as indicated and on day one treated with increasing amounts of vinorelbine.

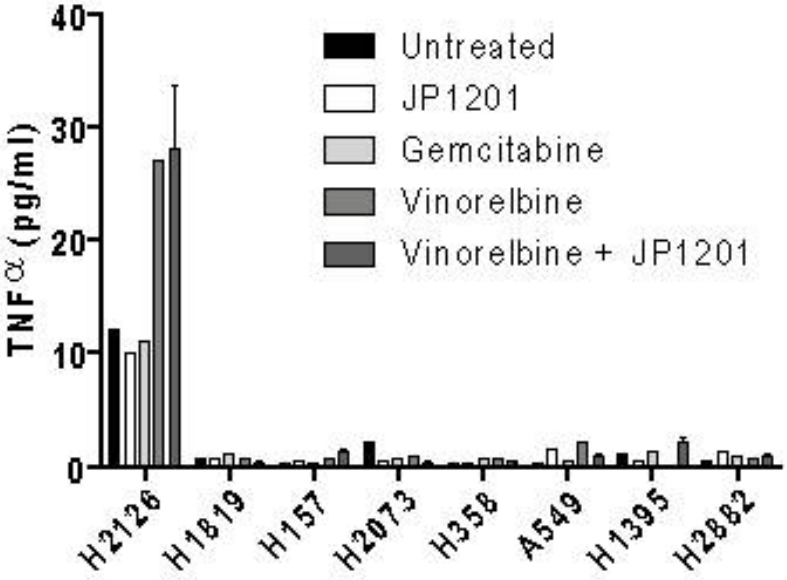

FIGURE 5.15 ELISA Analysis Shows that TNFα Is Not Induced in JP1201-Resistant Cell Lines by Vinorelbine Treatment.

Conditioned medium samples were taken from NCI-H2126 (a JP1201 sensitive NSCLC line), and seven other NSCLC cell lines (JP1201 resistant) 12 hrs after being placed in RPMI with the following treatments: untreated, 100 nM JP1201, 500 nM gemcitabine, 100 nM vinorelbine, and 100 nM vinorelbine with 100 nM JP1201, to test if treatment with chemotherapy can cause TNFα secretion.

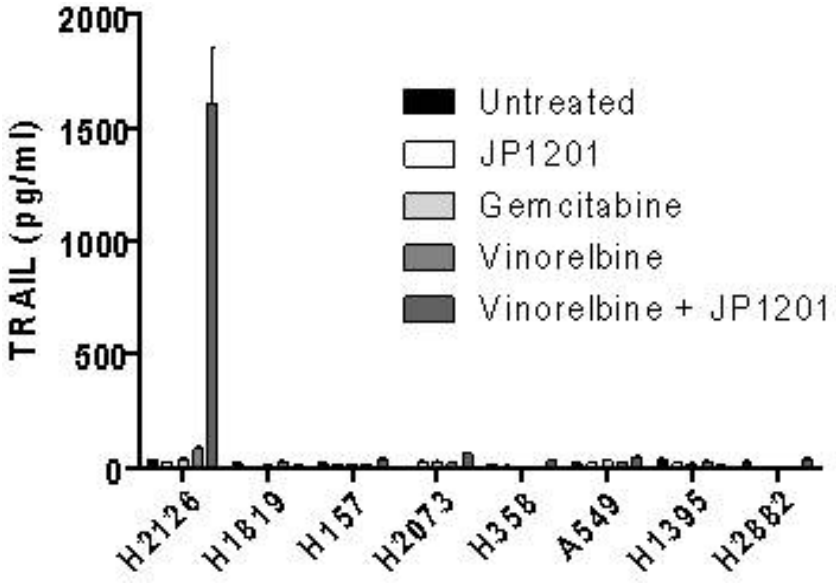

FIGURE 5.16 ELISA Analysis Shows that TRAIL Is Not Induced in JP1201-Resistant Cell Lines by Vinorelbine Treatment.

Conditioned medium samples were taken from NCI-H2126 (a JP1201 sensitive NSCLC line), and seven other NSCLC cell lines (JP1201 resistant) 12 hrs after being placed in RPMI with the following treatments: untreated, 100 nM JP1201, 500 nM gemcitabine, 100 nM vinorelbine, and 100 nM vinorelbine with 100 nM JP1201, to test if treatment with chemotherapy can cause TRAIL secretion.

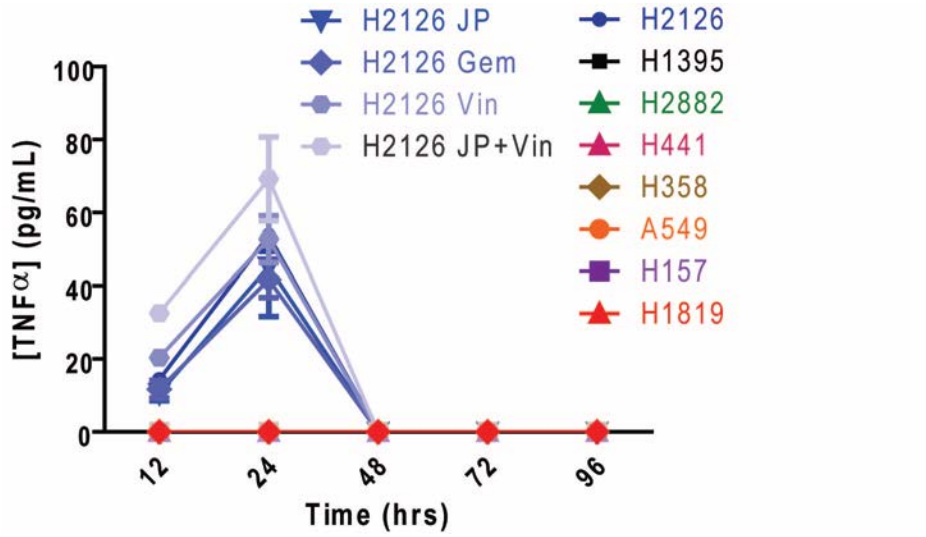

FIGURE 5.17 ELISA Analysis Shows that TNFα Is Not Induced in JP1201-Resistant Cell Lines by Vinorelbine Treatment.

Conditioned medium samples were taken from NCI-H2126 (a JP1201 sensitive NSCLC line), and eight other NSCLC cell lines (JP1201 resistant) 12, 24, 48, 72, and 96 hrs after being placed in RPMI with the following treatments: untreated, 10 µM JP1201, 2000 nM gemcitabine, 1000 nM vinorelbine, and 1000 nM vinorelbine with 10 µM JP1201, to test if treatment with chemotherapy can cause TNFα secretion.

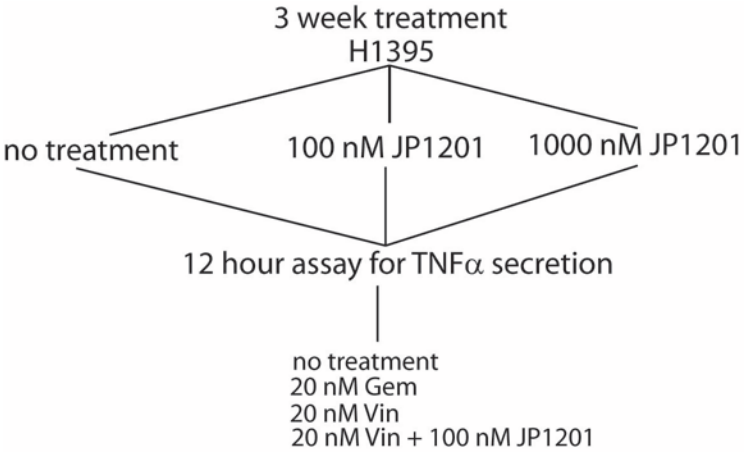

FIGURE 5.18 Scheme for Testing if Chronic JP1201 Treatment Induces TNF*α* Expression in NCI-H1395 Cells *In Vitro*.

NCI-H1395 cells were treated for three weeks with either 100 nM or 1000 nM JP1201, which was given to the cells three times a week in mass culture. Parental (untreated) NCI-H1395 cells as well as the pretreated 100 nM NCI-H1395, and 1000 nM NCI-H1395 cells were plated in six well plates at time zero and were treated for twelve hours with no treatment, 100 nM JP1201, 1000 nM JP1201, 20 nM gemcitabine, 20 nM paclitaxel, or 20 nM vinorelbine.

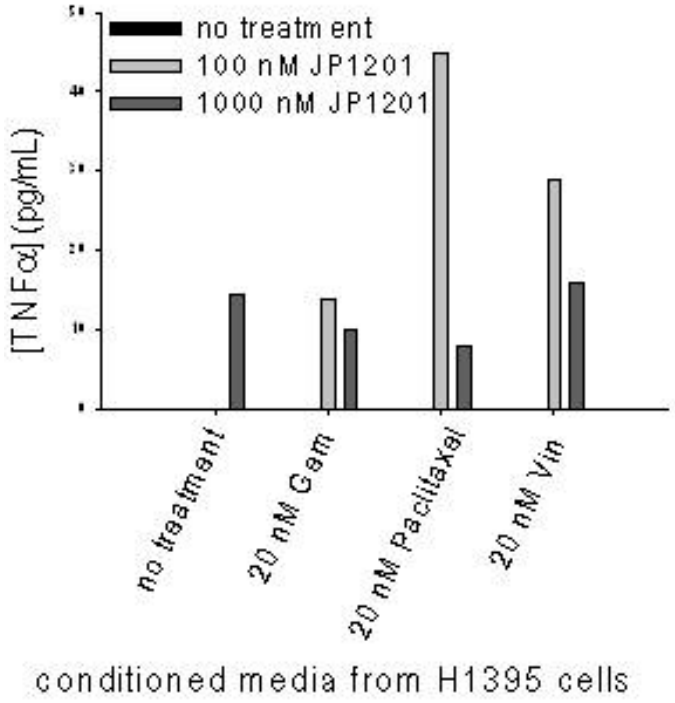

FIGURE 5.19 Chronic JP1201 Treatment Induces TNFα Expression in NCI-H1395 Cells *In Vitro*.

NCI-H1395 cells were treated for three weeks with either 100 nM or 1000 nM JP1201, which was given to the cells three times a week in mass culture. Parental (untreated) NCI-H1395 cells as well as the pretreated 100 nM NCI-H1395, and 1000 nM NCI-H1395 cells were plated in six well plates at time zero and were treated for twelve hours with no treatment, 100 nM JP1201, 1000 nM JP1201, 20 nM gemcitabine, 20 nM paclitaxel, or 20 nM vinorelbine. Conditioned media was collected and analyzed for TNFα secretion by competitive ELISA.

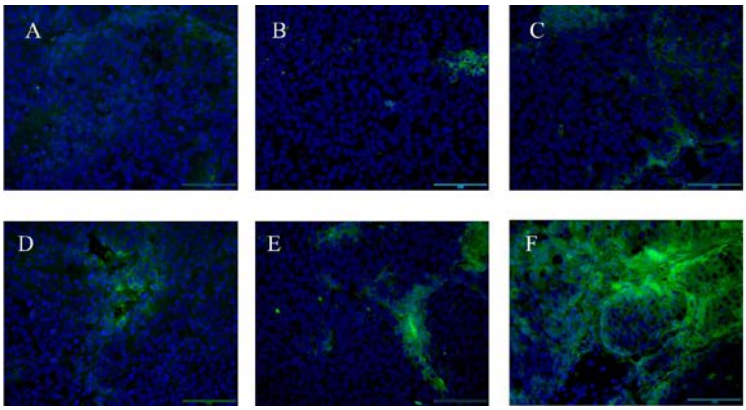

	% TNFα staining of saline group
saline	0
gemcitabine	0
vinorelbine	3
JP1201	25
JP + Gem	40
JP + Vin	80

FIGURE 5.20 Chronic JP1201 Treatment Induces TNFα Expression in NCI-H1395 Cells *In Vivo*.

Formalin fixed, paraffin embedded sections of NCI-H1395 xenograft tumors were stained with a human specific antibody against TNFα for three tumors within each treatment group. Average level of TNFα staining in NCI-H1395 xenografts by treatment group. Data from a minimum of three tumors per treatment group were normalized to saline group, and are representative of at least two independent assays, * $p < 0.01$, *** $p < 0.0001$. GEM, gemcitabine; VIN, vinorelbine; JP, JP1201; JPG, gemcitabine and JP1201; JPV, vinorelbine and JP1201.

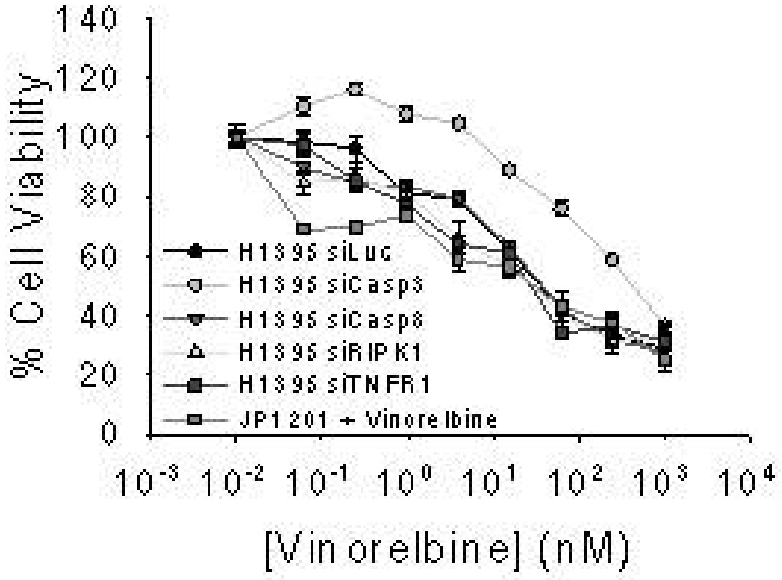

FIGURE 5.21 Synergy of Vinorelbine and JP1201 Does Not Act Through TNFα/RIPK1-Dependent Pathway.

Knockdown of caspase 3 protects H1395 cells from the effects of JP1201 + vinorelbine. H1395 cells were transfected with siRNAs that are specific for the indicated target in 96 well plates and treated with vinorelbine + 10 μM JP1201, the MTS assay was used to produce drug response curves for each transfection.

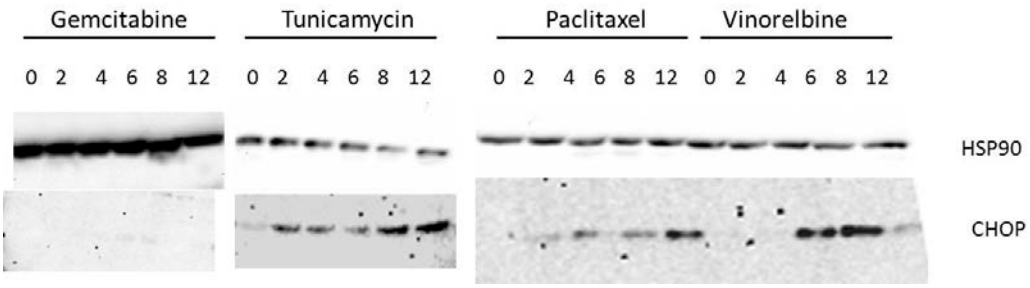

FIGURE 5.22 CHOP Expression is Induced by Vinorelbine and Paclitaxel Treatment Similarly to Known ER Antagonist Tunicamycin.

NCI-H1395 cells were treated with 1 μM tunicamycin, 100 nM paclitaxel, 100 nM vinorelbine, or 500 nM gemcitabine for the indicated hours, at which point cells were harvested and lysates made. Cell lysates were analyzed by western blotting for CHOP (612201, BioLegend) or HSP90 (sc-13119, Santa Cruz) as a loading control.

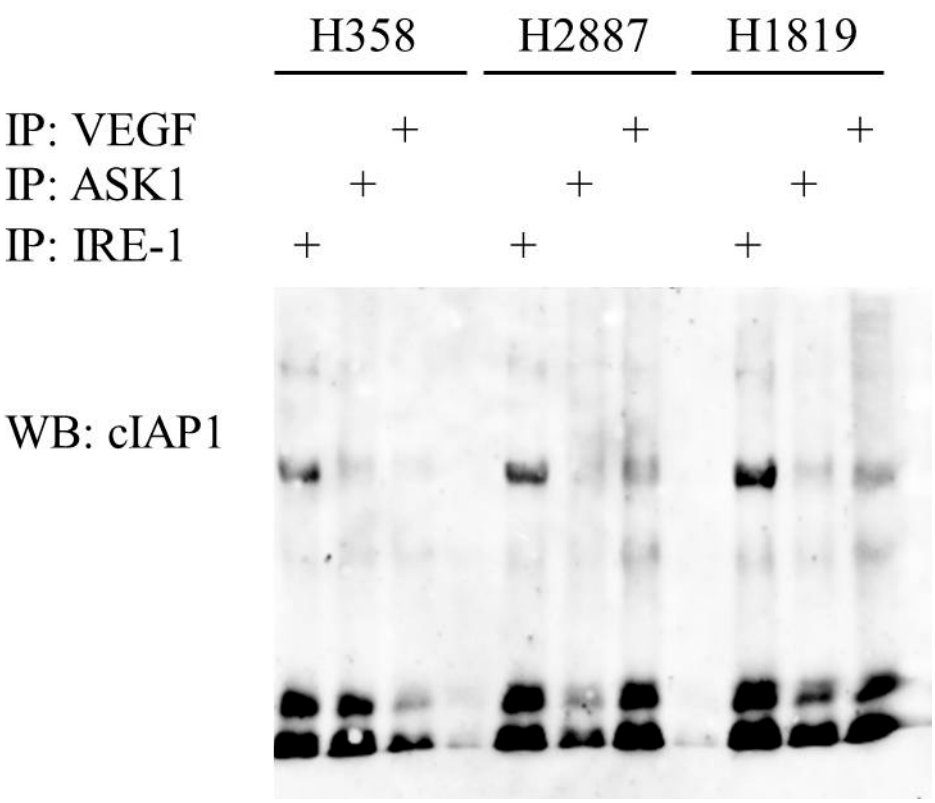

FIGURE 5.23 cIAP1 Co-immunoprecipitates with IRE1, ASK1, and TRAF2. NCI-H358, NCI-H2887, and NCI-H1819 cell pellets were lysed using IP lysis buffer, and pre-cleared using protein A/G-agarose and a control antibody (targeting VEGF, obtained from RAB) lysates were then incubated at 4C for 2 hours with an antibody against IRE1 (sc-20790, Santa Cruz), ASK1 (sc-5294 Santa Cruz), or TRAF2 (sc-7346, Santa Cruz), protein A/G-agarose was added and incubated overnight at 4C. Pellets were spun down and washed 5 times with 1000 fold excess lysis buffer. 1X SDS buffer was added to pellets which was then

boiled for 5 minutes at 94C, and then analyzed by western blot analysis for cIAP1/2 (sc-12410, Santa Cruz).

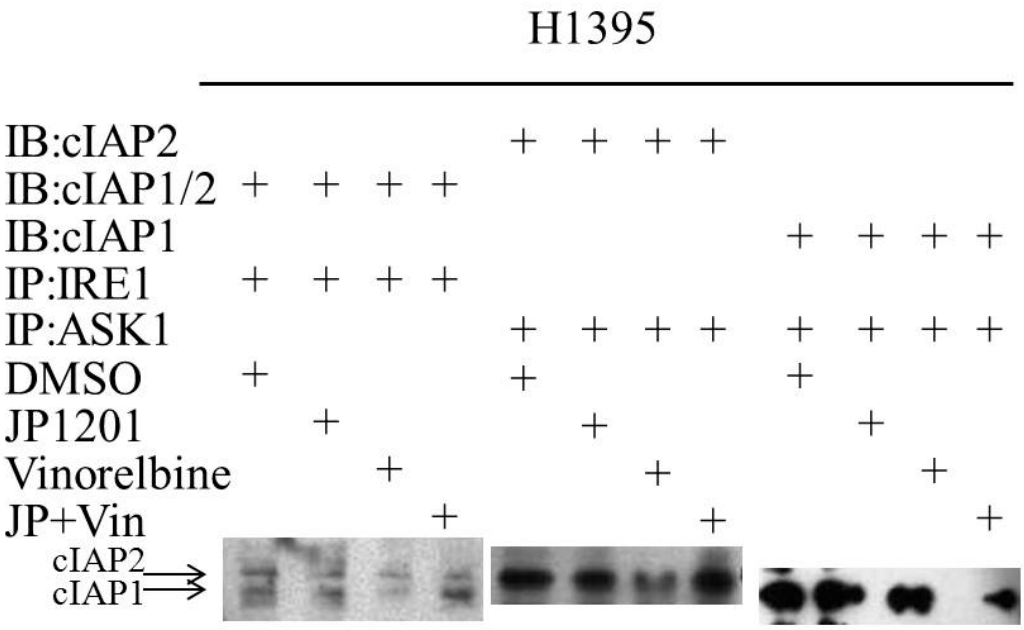

FIGURE 5.24 Treatment with Vinorelbine + JP1201 abolishes the ability of cIAP1 and cIAP2 to be Co-immunoprecipitated with IRE1 and ASK1.

NCI-H1395 cells were treated with DMSO, 1 μM JP1201, 1 μM vinorelbine, or 1 μM JP1201 + 1 μM vinorelbine. After 12 hours of treatment, cells were lysed using IP lysis buffer and pre-cleared using protein A/G-agarose and a control antibody (targeting VEGF, obtained from RAB) lysates were then incubated at 4°C for 2 hours with an antibody against IRE1 (sc-20790, Santa Cruz) or ASK1 (sc-5294 Santa Cruz), protein A/G-agarose was added and incubated overnight at 4°C. Pellets were spun down and washed 5 times with 1000 fold excess lysis buffer. 1X SDS buffer was added to pellets which was then boiled for 5 minutes at 94°C, and then analyzed by western blot analysis for cIAP1/2 (sc sc-12410, Santa Cruz), cIAP1 (3180A-100, BioVision) and cIAP2 (sc-7944, Santa Cruz).

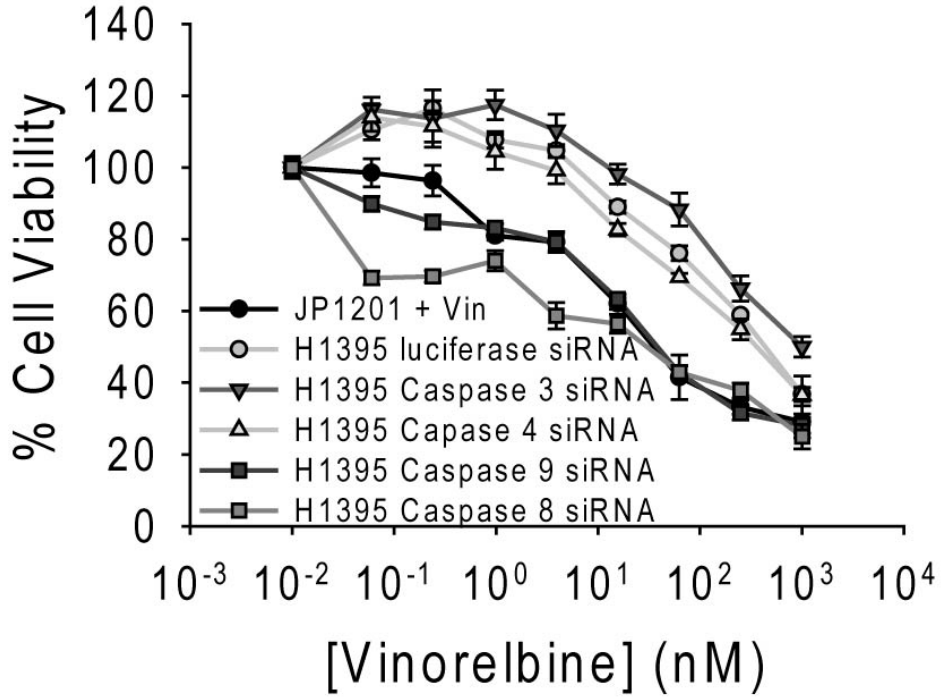

FIGURE 5.25 Caspase-4, -9, and -3 are Activated in Response to JP1201 + Vinorelbine Treatment in NCI-H1395 Cells.

Determination of which caspases are involved in cell kill induced by vinorelbine + JP1201. NCI-H1395 cells were transfected with siRNAs that are specific for the indicated target in a 96 well plate format and treated with vinorelbine + 10 μM JP1201, the MTS assay was used to produce drug response curves for each transfection. Validation of knockdowns are found in Table 5.5.

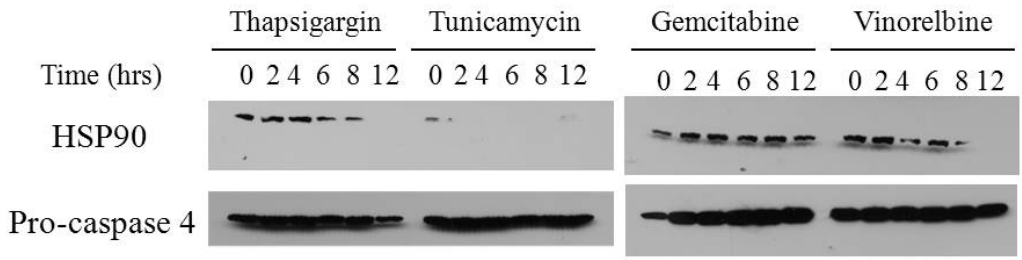

FIGURE 5.26 Pro-caspase-4 Protein Levels Decline After Vinorelbine Treatment, Similarly to Known ER Antagonists Tunicamycin and Thapsigargin.

NCI-H1395 cells were treated with 300 nM thapsigargin, 1 µM tunicamycin, 500 nM gemcitabine, or 100 nM vinorelbine for the indicated hours at which point cells were harvested and lysed. Cell lysates were then analyzed at 50 ug per well by western blot analysis probing for pro-caspase-4 (sc-56056, Santa Cruz) and HSP90 (sc-13119, Santa Cruz) as a loading control.

CHAPTER 6

CONCLUSIONS AND FUTURE WORKS

The work presented in this work shows that using targeted approaches that NSCLCs can be sensitized to conventional chemotherapies, whether it's by altering miRNA levels to modulate chemosensitivity, reactivating wild type p53 activity in mutant p53 background, or relieving negative inhibition on the apoptotic pathway. The broad range of approaches contained in this work leaves many avenues to pursue in the future, identification miR337 target genes that are responsible for increased sensitivity to paclitaxel, the mechanism by which $agRNA^{p53}$ induces lincRNAp21 expression, exploring the role of ER stress induced apoptosis in cancer, among others.

6.1 PLATINUM-BASED COMBINATION CHEMOTHERAPY

The initial study on platinum based chemotherapy combinations in a panel of NSCLCs highlights the inefficiency with which cancers are treated in the clinic (Figure 3.2). More often than not it would seem that patients are undergoing combination chemotherapy when a single agent would be just as effective at killing the actual tumor cells. However, as the lack of success in this study of defining signatures that would predict synergy or antagonism indicates, predicting response to treatment has not been successful as a method for personalizing therapy yet. There are several caveats to the experimental approaches used here that may contribute to the lack of predictability of the signatures derived herein

(Figure 3.3-5). One such caveat is that the signatures were created using genome-wide mRNA microarray expression profiling, and while this encompasses the expression levels of every gene at the mRNA level, these expression profiles were taken from cells with no treatment, so the ability of the cells to respond to stress is not really evaluated by this approach. Perhaps it would be more informative to profile the epigenetic profile of these cells by histone modifications or by protein array of epigenetic regulating enzymes (S. V. Sharma, et al., 2010).

Another caveat is that this analysis is based on the analysis of the two drugs as a combination compared to each drug as a single agent, instead of simply identifying responders and non-responders, and the MATRIX program used to analyze gene expression correlations with response is designed to make these correlations on a 1/0 scale. So the program is designed to analyze simply two groups and make correlations based on these two simple groups; however, response to chemotherapy is more of a continuum than two distinct populations of resonse (Figure 3.1), which is highlighted even more when you consider combination index, which loosely groups cell lines as antagonistic, additive, or synergistic. For these analyses, additive cell lines were simply ignored and signatures derived from antagonistic or synergistic cell lines across three platinum based combinations. And while analyses like this are often done, it completely ignores a real biological response to drug and as a result ignores some of the complexity within cancer cells that is regulating response to drugs, and thereby it

should be no surprise that the signatures made with such parameters is not predictive of a large panel of NSCLCs.

6.2 Targeted Molecular Biology Approaches to Rationally Designed Combinations

In this study where increasing endogenous miR337 levels by transfection of a synthetic mimic of miR337, NSCLCs were sensitized to paclitaxel, both in already fairly sensitive cell line H157 and in resistant cell lines H1819, H2887. Conversely it was shown that a sensitive cell line H157 could be made more resistant to paclitaxel by antagonizing miR337 activity using a miR337-specific antagomiR. While these data are encouraging,, there is a lot left unexamined before altering miR337 levels could become a potential therapeutic option for altering NSCLC response in mice, much less patients. The mRNA targets of miR337 are unknown, so the tumor selectivity of increasing miR337 levels sensitizing cells to paclitaxel has not been shown. If increasing miR337 levels sensitizes all cells, not just tumor cells to paclitaxel, it would not be useful as a cancer therapy, which is the goal of this entire body of work. Additionally, this work only showed that increasing miR337 levels was effective in vitro models, mouse studies need to be done showing that the synthetic miR337 mimic can also sensitize tumor cells in a living animal occurs. In addition to showing that the miR337 mimic could be effective in vivo, the in vivo properties; aka absorption, clearance, metabolism need to be evaluated to determine if use of the miR337

mimic would achieve such a standard state plasma level as to be effective at sensitizing tumor cells to paclitaxel, as well as to determine appropriate scheduling of dosing to keep a certain steady state plasma level.

Similar future works are also necessary for the taxane-specific synthetic lethal siRNAs, as considering to advance them as therapeutics to use in conjunction with paclitaxel or docetaxel, showing tumor specificity of sensitization, and in vivo efficacy of this sensitization. To further the analysis of diazonamide being sensitized by the "paclitaxel-specific" synthetic lethals, all 87 hits need to be tested with diazonamide initially in H1155 cells, the cell line used in the screen, and then take the best hits from that and screen them across multiple cell lines, maintaining diazonamide at an IC_{10} dose for each cell line.

The work on targeting the 5' from the TSS of *TP53*, shows that these agRNAs specifically cause cytotoxicity in cancer cell lines containing mutant p53 protein, specifically only mutants where the mutation lies within the DBD. Some of the experiments that need to be done to confirm this specificity is to take a cell line that has DBD-mutant-p53, and over express mutant p53 from an artificial promoter, and then test across a dilution range of agRNA looking for loss of cytotoxicity. The companion experiment to this, where mutant p53 is expressed from the endogenous *TP53* promoter is not possible in this system; however, using HBECs that are over expressing a mutant version of p53, while still expressing wild type p53 is underway. The mechanism by which these

agRNA^{p53}s induce cytotoxicity is still under investigation. Analyzing mRNA from both mutant p53 and wild type p53 containing cells where N27 has been transfected in for induction of pro-apoptotic p53 target genes is planned. As well as performing ChIP on lysates from cells transfected with N27 and N27-M4M using p53 as the immunoprecipitate target, looking for enrichment of p53 at pro-apoptotic target genes (PUMA, NOXA) as well as at the lincRNAp21 locus are planned experiments to better elucidate the mechanism by which these agRNA^{p53} induce cytotoxicity.

6.3 SMAC Mimetics as an Adjuvant Chemotherapy Combination

The work on using SMAC mimetic JP1201 is by far the furthest along of the projects within this body of work. However, as the most likely route of using SMAC mimetics in the clinic is as a part of chemotherapy combination therapy, and that most patients treated with chemotherapy for NSCLC are treated with a platinum based doublet, it is not likely that simply the combination of vinorelbine + JP1201 would likely be given to patients. Patients in Canada and Europe are routinely treated with the combination of cisplatin + vinorelbine, so further studies into using JP1201 in combination with cisplatin + vinorelbine in the *in vitro* system used here would be very necessary for planning a clinical trial.

That ER stress is inducing apoptosis in response to chemotherapy has never been described before, so the role of ER stress induced apoptosis is largely unexplored within cancer, and yields an as yet unexplored target for cancer

therapies. In addition to implicating ER stress as a dominant apoptogenic trigger, this work also shows that cIAP1/2 can negatively regulate apoptosis at an as yet un-described site within the cell.

6.4 Perspectives

It has long been known that each patient with cancer is different from every other patient with respect to presentation of disease, prognosis, response and tolerance to treatment, risk of recurrence, secondary malignancy, and long term complications from treatment; however, it has only been recently that clinicians and scientists have begun to explore the molecular heterogeneity of cancers. Identifying breast cancer patient subpopulations with overexpression of HER2 (ErbB2) and correlating that with increased chance of response to trastuzumab is one example of using knowledge of the heterogeneity of cancers to help personalize treatment, or cater treatment options to the molecular profile of an individual patient (Schilsky, 2010). And while trastuzumab is effective in HER2+ breast cancers, it is only in about 30% of this breast cancer subpopulation that it effectively controls disease, which points to a down fall of targeted therapies being the mainstay of cancer treatments based on molecularly defined subpopulations.

Another example that illustrates this is erlotinib used to treat NSCLC patients with activating mutations in EGFR. Erlotinib was showed to give a survival benefit in this selected population as a monotherapy, most if not all of

these patients have recurrence of disease due to resistance to erlotinib therapy. There have been numerous ways found that the tumors develop resistance to erlotinib, such as T790M mutations within EGFR that block binding of erlotinib into the ATP binding pocket of EGFR, upregulation of alternative growth factor receptors (MET, HER2 partnering with EGFR) to circumvent EGFR blockage, or downstream pathway activating mutations (Kobayashi 2005, engelman, 2007 2008, oreily 2006). These examples suggest that merely designing targeted agents to mutant proteins within a tumor are not sufficient for irradication of disease, with the exception of imatinib which controls CML for 90% of cases; however increasing evidence is coming to light showing that leukemia cells are developing resistance to imatinib (Kimura, et al., 2010).

Another approach to personalizing therapy is to use genome wide expression data, whether it's from microarray expression profiling, or protein arrays, to create signatures that are predictive of response to a given therapy. Usually these types of signatures are based off of cell line panels where multiple agents can be tested within the same cancer sample, which has its own set of caveats. Cell lines have shorter doubling times than tumor cells, and as a result have more opportunity to obtain genomic changes as a result of genomic instability (Adi F. Gazdar, Gao, & Minna, 2010). Additionally, cell lines are thought to only represent tumor cell subpopulations and not recapitulate the heterogeneity of the parent tumor, as well as lacking important interactions with

other cell types, such as stromal, inflammatory, immune, and vascularization (Adi F. Gazdar, Gao, et al., 2010). Although cell lines have the potential for loss of tumor heterogeneity, acquired mutations not relevant to the tumor in vivo, lack of tumor-associated immune and stromal cells; cell lines represent a basis for performing multiple assays on the same oncogenic background to be able to make comparisons between response to different therapies, whereas with a real patient, each sequential treatment alters the tumor, so comparisons between treatments in patients that receive multiple rounds of treatment cannot really be made. So while cell lines might not be ideal, they still provide a useful tool in creating signatures that can be later refined using xenograft data, and retrospective profiling of biopsy samples, such as from the BATTLE trial at MD Anderson (Printz, 2010).

The approach of introducing small duplex RNA molecules (miRNA, siRNA, or agRNA) into cancer cells to alter gene expression and thereby response to chemotherapy is quite ingenious; however, being able to treat a patient with such molecules is a bit more difficult. There are mechanisms in place throughout the human body to prevent foreign RNA or DNA molecules from entering cells and having an effect. One could imagine that foreign DNA/RNA being able to readily be taken up by cells could be detrimental to an organism, essentially viruses are clever ways of introducing DNA/RNA into a cell, and even injection of viral DNA/RNA directly into a cell can cause immune responses, such as the interferon response (Sledz, Holko, de Veer, Silverman, & Williams, 2003).

Additionally there are circulating DNases and RNases in blood to protect from systemic distribution of foreign DNAs/RNAs.

In tissue culture, lipids (usually cationic lipids to counteract the overall negative charge of the ribo-phosphate backbone of nucleic acids) are complexed with the nucleic acids to facilitate passive transport through the cell membrane; however these lipids often show toxicity even just in cell culture, and would likely be very toxic to a mouse, much less a human at the levels that would be needed to afford sufficient knockdown of the target gene in the desired location. There are many groups around the world working on the technical side of delivery; lipids, liposomes, cationic polymers, and direct conjugation of lipid moieties to the sugar-phosphate backbone are all currently being evaluated (Whitehead, Langer, & Anderson, 2009).

Another thing to be considered is the specificity of the target gene, which is even more important for the context of altering miRNA levels to achieve a clinical outcome. As far as we know miRNAs target multiple different mRNA targets, thus is goes to reason that altering the miRNA in a cancer might result in sensitization to chemotherapy (Figure 4.2-6), but will it have the same effect on normal cells, and not just normal cells in the same organ as the tumor but normal cells throughout the entire body? With miRNAs altering the expression of multiple genes, how does one determine which gene is important in the alteration of chemosensitivity, and will the changes in gene expression due to alterations in

miRNA level be the same throughout the body or will there be tissue specific changes that might or might not cause negative side effects just from the miRNA treatment? These are all things that need to be considered as RNAi mediated therapies make their ways into the clinics.

SMAC mimetics/IAP antagonists are much closer to being used in patients, in fact there are many clinical trials that have been completed or are underway evaluating the safety and determining dosing and safety of said molecules (Table 6.1). The studies understanding single agent SMAC mimetic induced apoptosis will no doubt be used to design clinical trials where one of the inclusion criteria is detectable serum TNFα; however, the levels of serum TNFα that coincide with SMAC mimetic tumor-lethality still need to be determined. The work presented here has shown that SMAC mimetics in combination with chemotherapy is a valid therapeutic strategy, and suggests that in clinical trials it would be best paired with an anti-mitotic, preferably vinorelbine, and that it is still effective when combined with an anti-mitotic as part of a platinum-based doublet.

Overall the studies presented herein show major advances in rationally designing combination chemotherapy strategies at different stages of preclinical development, with one such strategy being ready to begin being translated to the clinic as part of a clinical trial.

SMAC Mimetic	Trial Name	Pharmaceutical Company	Phase	NTC Number	Condition	Intervention
AT-406	Oral AT-406 in Combination With Daunorubicin and Cytarabine in Patients With Poor-risk AML	Ascenta	Phase I	NCT01265199	Acute Myelogenous Leukemia (AML)	AT-406 + daunorubicin/cytarabine
	Study of Safety and Tolerability of AT-406 in Patients With Advanced Solid Tumors and Lymphomas		Phase I	NCT01078649	Solid Tumors, Lymphomas	AT-406
GDC0917	GDC-0917 Administered to Patients With Refractory Solid Tumors or Lymphoma	Genentech	Phase I	NCT01226277	Solid Tumors	GDC0917
HGS1029	HGS1029 in Subjects With Advanced Solid Tumors	HGS	Phase I	NCT00708006	Advanced Solid Tumors	HGS1029
	HGS1029 in Subjects With Relapsed or Refractory Lymphoid Malignancies		Phase I	NCT01013818	Lymphoid Malignancies	HGS1029
LCL161	fety and Efficacy of LCL161 in Patients With Solid Tum	Novartis	Phase I	NCT01098838	Advanced Solid Tumors	LCL161
	LCL161 in Combination With Weekly Paclitaxel in Adult Patients With Advanced Solid Tumors		Phase I	NCT01240655	Solid Tumors	LCL161
TL32711	Docetaxel + carboplatin with TL32711, in Subjects With Advanced or Metastatic Solid Tumors	TetraLogic	Phase I/II	NCT01188499	Advanced Solid Tumors	(Paclitaxel/Carboplatin, Irinotecan, Docetaxel, Gemcitabine, Liposomal doxorubicin) + TL32711
	TL32711 in Adults With Refractory Solid Tumors or Lymphoma		Phase I	NCT00993239	Solid Tumors, Lymphomas	TL32711

TABLE 6.1 U.S.Clinical Trials involving SMAC mimetics.

APPENDIX A. 1188 GENES CORRELATING WITH SYNERGY TO GEMCITABINE + CISPLATIN

Gene ID	Symbol	Synergy Correlation	Correlation P value	Up or Down regulated
106	CARS	-0.37	0.042	D
118	GABARAPL2	-0.45	0.014	D
136	FUBP1	-0.39	0.034	D
198		-0.39	0.035	D
206	DARC	-0.39	0.032	D
243	ZBTB2	-0.42	0.019	D
280	HSD11B1	-0.38	0.040	D
283	GLIS1	-0.43	0.018	D
298	MAPKAP1	-0.51	0.004	D
322	KCNJ8	-0.50	0.005	D
405	SCML2	-0.43	0.018	D
415	BBS7	-0.45	0.014	D
467	HSPD1	-0.45	0.012	D
496	HSPE1	-0.58	0.001	D
516	C12orf29	-0.46	0.011	D
572	WHSC1	-0.37	0.043	D
621	SAA1	-0.52	0.003	D
778	DNTTIP2	-0.45	0.013	D
813	KDELC1	-0.39	0.034	D
815	ANAPC7	-0.37	0.047	D
855	DPH5	-0.44	0.015	D
869	GGH	-0.36	0.048	D
886	S1PR1	-0.52	0.003	D
953	ACCN1	-0.37	0.047	D
957	DHX36	-0.41	0.025	D
959	LAS1L	-0.37	0.046	D
977	CPSF6	-0.48	0.007	D
980	CCDC144NL	-0.36	0.049	D
989	UBE2N	-0.39	0.034	D
1035	RPRD1A	-0.40	0.030	D
1055	TMEFF2	-0.52	0.003	D
1062	AMZ2	-0.47	0.009	D

1066	OR4P4	-0.42	0.022	D
1067	HIPK1	-0.40	0.030	D
1075	ASCC3	-0.61	0.000	D
1076	RAD17	-0.45	0.012	D
1082	PRPSAP2	-0.41	0.024	D
1083	EBNA1BP2	-0.38	0.040	D
1115	MRPL44	-0.40	0.029	D
1165	ZNF182	-0.47	0.008	D
1242	TSPAN4	-0.51	0.004	D
1247	GPM6A	-0.38	0.038	D
1266	RPL23	-0.48	0.007	D
1284	RFXAP	-0.37	0.045	D
1286	SRSF1	-0.40	0.030	D
1359	CAPN7	-0.42	0.019	D
1380	C18orf21	-0.48	0.008	D
1399	SEPT7	-0.41	0.023	D
1489	XCL1	-0.42	0.020	D
1512	PTMA	-0.43	0.017	D
1514	IPO8	-0.40	0.030	D
1531	RABEPK	-0.53	0.003	D
1585	POSTN	-0.41	0.026	D
1618	RAD51C	-0.39	0.036	D
1642	ZNF331	-0.39	0.036	D
1661	SUMO2	-0.39	0.031	D
1708	SYN3	-0.39	0.032	D
1790	CXCL5	-0.37	0.044	D
1793	CEMP1	-0.41	0.024	D
1974	IQCB1	-0.57	0.001	D
1994	PRTG	-0.44	0.015	D
2065	FCRL3	-0.41	0.026	D
2249	SNRPF	-0.37	0.047	D
2254	RPS28	-0.40	0.030	D
2273	ZNF772	-0.44	0.016	D
2289	USP33	-0.43	0.017	D
2292	CLIP3	-0.53	0.003	D
2300	TBCB	-0.41	0.024	D
2316	PRDM10	-0.39	0.035	D
2416	MRPL48	-0.37	0.046	D

2435	NTRK1	-0.47	0.008	D
2442		-0.41	0.023	D
2443	MMP19	-0.40	0.027	D
2456	NRXN3	-0.38	0.038	D
2476	PRRG3	-0.42	0.022	D
2490	PAPPA	-0.39	0.032	D
2614	C12orf24	-0.42	0.020	D
2634	OR2M4	-0.39	0.034	D
2637	RTN4	-0.39	0.034	D
2714	TNNI3K	-0.49	0.006	D
2766	RPL5	-0.45	0.012	D
2783	NCF1C	-0.43	0.017	D
2807	CYBB	-0.38	0.037	D
2831	EXOSC10	-0.52	0.003	D
2836	NXPH2	-0.50	0.005	D
2846	RSPH9	-0.42	0.020	D
2890	PHYHIPL	-0.50	0.005	D
2907	MSH6	-0.37	0.046	D
2932	ZNF673	-0.43	0.018	D
2956		-0.38	0.036	D
3002	ASAP1	-0.42	0.020	D
3017	SNX16	-0.37	0.046	D
3024	TXNL1	-0.49	0.006	D
3025	EIF3M	-0.47	0.009	D
3063	SMCP	-0.40	0.029	D
3067	PCDHB6	-0.49	0.006	D
3085	SRGAP2	-0.38	0.039	D
3138	SPATS1	-0.44	0.016	D
3140	TAF9	-0.57	0.001	D
3145	SRSF11	-0.45	0.014	D
3152	ZNF280A	-0.43	0.018	D
3192	PSMG1	-0.42	0.021	D
3295	SULT1A4	-0.62	0.000	D
3300	FPR1	-0.55	0.002	D
3310	CDKN1B	-0.42	0.019	D
3338	COPS3	-0.41	0.024	D
3451	IGF2BP1	-0.49	0.006	D
3453	ZNF286A	-0.50	0.005	D

3542	AQR	-0.39	0.033	D
3582	FLCN	-0.41	0.024	D
3587	SPCS2	-0.40	0.028	D
3599	SF3B3	-0.39	0.033	D
3635	ARL6	-0.37	0.042	D
3658	FAM72D	-0.42	0.020	D
3672	SCRG1	-0.41	0.026	D
3683	HS2ST1	-0.43	0.019	D
3740	EBF1	-0.41	0.024	D
3795	FAM83G	-0.63	0.000	D
3798	ZNF804B	-0.51	0.004	D
3892	SGCB	-0.41	0.026	D
3977	FADS3	-0.38	0.040	D
4005	RPL26	-0.59	0.001	D
4019	FLJ16423	-0.39	0.034	D
4080	MOSPD2	-0.54	0.002	D
4090	RAB12	-0.44	0.016	D
4094	OR52D1	-0.37	0.046	D
4113	MRPL52	-0.39	0.031	D
4119	ANP32A	-0.56	0.001	D
4133	KDM3A	-0.42	0.020	D
4197	EYA4	-0.55	0.002	D
4261	UNC93A	-0.43	0.017	D
4309	C1S	-0.37	0.043	D
4358	MTHFD2	-0.40	0.027	D
4481	CRHR1	-0.39	0.031	D
4483	FXYD1	-0.37	0.042	D
4484	MATN1	-0.37	0.044	D
4514	TGIF1	-0.40	0.030	D
4536	GORAB	-0.37	0.045	D
4556	SF1	-0.62	0.000	D
4563	OR52A5	-0.36	0.047	D
4565	RPS6	-0.39	0.032	D
4566	R3HDM1	-0.49	0.006	D
4568	GSK3A	-0.40	0.027	D
4581	GOPC	-0.51	0.004	D
4603	GLI1	-0.37	0.043	D
4621		-0.39	0.031	D

4624	RPSA	-0.37	0.047	D
4802	EXOSC2	-0.36	0.048	D
4810	SSX2IP	-0.36	0.048	D
4823	ZKSCAN5	-0.38	0.039	D
4849	TRAPPC2L	-0.48	0.007	D
4858	EXOSC3	-0.46	0.011	D
4877	FSD1	-0.51	0.004	D
4893	RPL17	-0.45	0.014	D
4943	TRIM69	-0.37	0.043	D
4977	IL1F8	-0.41	0.026	D
5052	CWC22	-0.52	0.003	D
5059	PES1	-0.40	0.027	D
5083	HNRNPC	-0.44	0.014	D
5104	ATF7	-0.45	0.013	D
5220	DACT1	-0.40	0.027	D
5231	RNASEH1	-0.36	0.048	D
5278	C5orf34	-0.52	0.003	D
5364	MPHOSPH10	-0.37	0.047	D
5367	GPR62	-0.44	0.015	D
5467	SULT1E1	-0.36	0.050	D
5485	ID2	-0.37	0.046	D
5528	KIF21A	-0.40	0.028	D
5550	MCTS1	-0.38	0.036	D
5566	U2AF2	-0.41	0.023	D
5582	ATG3	-0.44	0.014	D
5621	C2orf57	-0.38	0.038	D
5708	NXF5	-0.38	0.040	D
5712	GPR19	-0.42	0.020	D
5734	PIGF	-0.38	0.036	D
5753	SLC38A2	-0.41	0.024	D
5754	USP10	-0.37	0.046	D
5781	ZNF711	-0.39	0.035	D
5783	RNASE13	-0.39	0.034	D
5797	MCRS1	-0.48	0.008	D
5806	RBM24	-0.55	0.002	D
5822	BOLA2	-0.40	0.031	D
5830	SYNE2	-0.45	0.012	D
5881		-0.37	0.043	D

5910	RAB21	-0.42	0.021	D
5931	MAPK7	-0.43	0.017	D
5974	PEMT	-0.45	0.012	D
5975	GRIA3	-0.38	0.038	D
5991	PSMB7	-0.62	0.000	D
6012	PTGES3	-0.39	0.035	D
6013	CCDC59	-0.37	0.046	D
6040	ZCCHC3	-0.44	0.014	D
6081	NME1	-0.51	0.004	D
6083	PAPSS1	-0.42	0.020	D
6127	WTAP	-0.37	0.045	D
6129	HLCS	-0.47	0.009	D
6132	SLC35F1	-0.38	0.038	D
6134	STARD6	-0.38	0.040	D
6159	EIF5A	-0.39	0.033	D
6177	HIAT1	-0.39	0.033	D
6189	MRGPRX1	-0.37	0.047	D
6254	ZNF831	-0.39	0.035	D
6260	NDUFAF4	-0.49	0.007	D
6294	RASSF2	-0.42	0.022	D
6323	CCNH	-0.51	0.004	D
6350	METTL6	-0.40	0.028	D
6351	FLCN	-0.37	0.042	D
6360	C10orf129	-0.46	0.011	D
6438	METTL1	-0.37	0.043	D
6474	ZCRB1	-0.41	0.024	D
6494	ZNF454	-0.37	0.042	D
6530	CCDC25	-0.40	0.030	D
6705	BAZ2A	-0.38	0.038	D
6717	EIF3A	-0.54	0.002	D
6859	CSRP2BP	-0.65	0.000	D
6912	RBBP7	-0.39	0.032	D
6917	ZFP1	-0.58	0.001	D
6951	QTRT1	-0.46	0.010	D
6977	NOL8	-0.41	0.024	D
7061	MC5R	-0.66	0.000	D
7076	BOLL	-0.39	0.035	D
7090	RNF212	-0.37	0.046	D

7163	RPL14	-0.49	0.006	D
7172	FBXO40	-0.37	0.042	D
7215	DNAJC18	-0.38	0.039	D
7329	SPRR2F	-0.41	0.025	D
7350	HAUS1	-0.41	0.026	D
7367	RAD51C	-0.44	0.014	D
7411	RAD1	-0.44	0.014	D
7431	KRTAP10-11	-0.65	0.000	D
7442	MPHOSPH6	-0.42	0.021	D
7517	RPSA	-0.54	0.002	D
7525		-0.39	0.032	D
7572	OR2J2	-0.40	0.026	D
7577	AGTPBP1	-0.37	0.041	D
7640	EYA4	-0.51	0.004	D
7643	CHD1	-0.39	0.032	D
7644	GNAS	-0.38	0.038	D
7653	TSNAXIP1	-0.38	0.038	D
7664	TBX18	-0.40	0.028	D
7676	RAN	-0.39	0.036	D
7698	GPR55	-0.48	0.007	D
7725	FADS1	-0.60	0.000	D
7736	H3F3A	-0.36	0.047	D
7749	KRT82	-0.38	0.036	D
7838	RPS15A	-0.36	0.050	D
7868	KCNH1	-0.39	0.034	D
7882	RORB	-0.42	0.022	D
7920	VCP	-0.40	0.029	D
7928	PSMG1	-0.48	0.007	D
7949		-0.55	0.002	D
8004	CCDC34	-0.41	0.026	D
8005	KIF18A	-0.42	0.020	D
8032	ZDHHC2	-0.38	0.040	D
8084	RTN3	-0.40	0.028	D
8093	ANKRD19	-0.41	0.025	D
8116	VHL	-0.38	0.040	D
8124	OR1D2	-0.57	0.001	D
8148	RANBP10	-0.41	0.025	D
8149	TCEAL5	-0.47	0.009	D

8173	C1D	-0.44	0.015	D
8208	TRMT61B	-0.44	0.015	D
8210	TRA2B	-0.39	0.034	D
8246	RFX5	-0.41	0.023	D
8324	GPR34	-0.41	0.025	D
8342	TMTC4	-0.37	0.044	D
8346	NACA2	-0.37	0.043	D
8348	FAM101A	-0.53	0.003	D
8397	AKT3	-0.59	0.001	D
8442	HNRPDL	-0.44	0.015	D
8444	PPHLN1	-0.57	0.001	D
8447	KIF5C	-0.40	0.029	D
8451	C4orf43	-0.36	0.049	D
8456	RTP3	-0.38	0.038	D
8496	PSMD14	-0.37	0.043	D
8545	AADACL4	-0.46	0.011	D
8608	CHST5	-0.45	0.012	D
8637	RNGTT	-0.38	0.041	D
8662	XAGE1D	-0.52	0.003	D
8678	RPF1	-0.45	0.012	D
8687	FAM49B	-0.40	0.029	D
8898	STC1	-0.39	0.034	D
8900	TMEM225	-0.40	0.027	D
8916	RPL7	-0.44	0.015	D
8926	CCDC129	-0.47	0.009	D
8944	R3HDM2	-0.39	0.031	D
8998	BEST3	-0.38	0.037	D
9005	MRPS23	-0.51	0.004	D
9088	MARS	-0.39	0.035	D
9182	SPECC1	-0.46	0.011	D
9250	CPEB3	-0.41	0.023	D
9253	RPL7A	-0.37	0.042	D
9272	C20orf27	-0.38	0.037	D
9275	SLITRK5	-0.57	0.001	D
9316	MTF2	-0.36	0.049	D
9363	C16orf73	-0.47	0.009	D
9368	TRIM35	-0.37	0.045	D
9402	SPECC1	-0.46	0.010	D

9440	NEGR1	-0.47	0.008	D
9506	CHAC2	-0.42	0.022	D
9551	KCTD12	-0.37	0.044	D
9560	CRX	-0.44	0.016	D
9566	PAGE5	-0.38	0.040	D
9603	NME7	-0.41	0.023	D
9635	VCAM1	-0.46	0.011	D
9659	PODNL1	-0.39	0.033	D
9696	HOXD9	-0.44	0.014	D
9705	LRRC4C	-0.44	0.014	D
9707	C18orf32	-0.56	0.001	D
9766	C9orf5	-0.42	0.022	D
9903	SLC39A6	-0.42	0.021	D
9913	MAK16	-0.38	0.038	D
9918	CIT	-0.36	0.048	D
9989	CNOT7	-0.40	0.028	D
10057	RPS13	-0.45	0.012	D
10078	NCRNA00152	-0.43	0.019	D
10089	SEMG2	-0.43	0.017	D
10122	STX8	-0.51	0.004	D
10136	FAM18B2	-0.36	0.050	D
10151	AKNAD1	-0.46	0.011	D
10156	UTP15	-0.36	0.049	D
10160	C11orf58	-0.49	0.006	D
10190	PPAP2C	-0.38	0.038	D
10197	DEFB108B	-0.44	0.014	D
10217	KCNT2	-0.48	0.007	D
10320	ZFPM2	-0.42	0.021	D
10375	IFT74	-0.41	0.025	D
10415	ZNF271	-0.44	0.014	D
10475	SYT4	-0.37	0.045	D
10476	MAP3K15	-0.43	0.017	D
10511	LYPD6B	-0.43	0.017	D
10536	MGA	-0.45	0.012	D
10546	ITPRIPL1	-0.40	0.027	D
10584	ATP5G2	-0.40	0.030	D
10595	DNAJC7	-0.40	0.028	D
10626	LAP3	-0.39	0.032	D

10676	SREK1	-0.45	0.013	D
10716	TDP2	-0.47	0.008	D
10736	TIMM10	-0.39	0.034	D
10785	FAM35A	-0.43	0.018	D
10847	MGC45800	-0.49	0.006	D
10874	SIGLEC12	-0.43	0.017	D
10962	HERPUD2	-0.45	0.013	D
10967	LILRA2	-0.41	0.025	D
10998	FREM2	-0.42	0.022	D
11012	PRKDC	-0.37	0.046	D
11016	RBMS1	-0.39	0.034	D
11037	NETO1	-0.44	0.014	D
11041	PDP2	-0.37	0.046	D
11059	RECK	-0.44	0.016	D
11069	MRRF	-0.38	0.036	D
11142	SRR	-0.38	0.041	D
11268	TRAPPC1	-0.36	0.049	D
11274	GTF2H1	-0.43	0.017	D
11312	FBN2	-0.53	0.003	D
11338	FECH	-0.44	0.015	D
11359	ELP3	-0.39	0.035	D
11363	HCCS	-0.37	0.044	D
11464	SCO1	-0.43	0.018	D
11484	RXRG	-0.45	0.012	D
11522	HEATR1	-0.37	0.047	D
11528	HDGFRP3	-0.43	0.019	D
11622	PTH2R	-0.39	0.032	D
11631	DACT1	-0.39	0.035	D
11656		-0.48	0.008	D
11713	FOXS1	-0.43	0.018	D
11722	CDKL3	-0.36	0.048	D
11755	C3orf26	-0.39	0.035	D
11767	TROVE2	-0.37	0.047	D
11768		-0.42	0.022	D
11772	OFD1	-0.38	0.039	D
11823	ROBO1	-0.71	0.000	D
11885	CDH4	-0.40	0.028	D
11886	OR4C45	-0.54	0.002	D

11905	AOX1	-0.37	0.046	D
11946	NOVA1	-0.42	0.020	D
12045	LDHAL6B	-0.44	0.015	D
12047	APOC2	-0.37	0.045	D
12066	DCP1B	-0.36	0.048	D
12092	SCN9A	-0.48	0.007	D
12159	PGA3	-0.45	0.012	D
12206	GPAM	-0.49	0.006	D
12209	C9orf50	-0.37	0.044	D
12217	PFAS	-0.49	0.006	D
12243	LARP4	-0.40	0.029	D
12255		-0.40	0.029	D
12347	CCDC77	-0.42	0.019	D
12387	HK1	-0.41	0.023	D
12431	TSEN15	-0.39	0.033	D
12492	C6orf58	-0.37	0.045	D
12503	OR52W1	-0.43	0.017	D
12560	HIST1H4C	-0.38	0.040	D
12588	NUP37	-0.41	0.026	D
12590	TOP3A	-0.36	0.049	D
12597	DNM1L	-0.44	0.016	D
12618	RPL14	-0.41	0.023	D
12625	COX10	-0.37	0.046	D
12652	EIF1AX	-0.50	0.005	D
12742	WNK3	-0.44	0.014	D
12750	KIF3A	-0.43	0.018	D
12762	TAF1B	-0.37	0.043	D
12770	YSK4	-0.44	0.014	D
12794	PPP1R1C	-0.43	0.017	D
12796	DOT1L	-0.38	0.036	D
12929	NAE1	-0.37	0.047	D
12941	ASTN2	-0.53	0.002	D
12961	SMC3	-0.49	0.006	D
12995		-0.42	0.020	D
13002	SGK196	-0.43	0.017	D
13018	CLEC18A	-0.43	0.019	D
13055	POLR1E	-0.42	0.022	D
13076	TMEM19	-0.38	0.037	D

13087	TEAD4	-0.37	0.043	D
13130	RAB6A	-0.39	0.032	D
13131	CDH7	-0.40	0.029	D
13168	PAICS	-0.45	0.012	D
13192	FLJ35409	-0.63	0.000	D
13226	TRMT6	-0.46	0.011	D
13259	DUSP11	-0.44	0.015	D
13306	PPAT	-0.47	0.009	D
13335	GFRA4	-0.38	0.039	D
13345	ATP6V1C2	-0.37	0.044	D
13367	SOX5	-0.37	0.047	D
13482	ZZZ3	-0.39	0.036	D
13560	AASDH	-0.48	0.008	D
13584	MUTED	-0.39	0.032	D
13590	TRPC1	-0.39	0.031	D
13622	TBX18	-0.40	0.030	D
13640	GPHA2	-0.40	0.029	D
13679	PDE1A	-0.42	0.019	D
13710	SNX24	-0.38	0.038	D
13764	LUZP4	-0.40	0.027	D
13802	C3orf75	-0.36	0.048	D
13839	FGF4	-0.38	0.038	D
13847	ANKRD17	-0.40	0.028	D
13909	DYNC2H1	-0.47	0.010	D
13942	LIN28B	-0.37	0.042	D
13993	TCP1	-0.37	0.043	D
14009	SET	-0.41	0.023	D
14054	ATP2B1	-0.48	0.008	D
14068	CALB2	-0.38	0.038	D
14123	STK4	-0.37	0.044	D
14134	DNAJC10	-0.38	0.040	D
14185	DHX37	-0.39	0.033	D
14196	ZNF23	-0.39	0.033	D
14223	PARD3B	-0.37	0.046	D
14238	GNAI1	-0.40	0.029	D
14241	AIFM3	-0.43	0.019	D
14305	PHF8	-0.39	0.032	D
14355	SLBP	-0.43	0.017	D

14356	PHF3	-0.43	0.016	D
14365	SEZ6L2	-0.43	0.018	D
14374	DPH5	-0.39	0.032	D
14464	UBA2	-0.40	0.031	D
14472	HNRNPH3	-0.52	0.003	D
14479	CCDC104	-0.44	0.015	D
14490	PRAMEF10	-0.40	0.028	D
14581	CRELD1	-0.37	0.046	D
14590	OR2V2	-0.46	0.012	D
14603	SEPT1	-0.46	0.011	D
14618	USP9X	-0.38	0.038	D
14651		-0.37	0.043	D
14750	KCNMB3	-0.37	0.042	D
14751	ACOX3	-0.44	0.016	D
14769	ROBO1	-0.45	0.012	D
14856	ATP5I	-0.48	0.007	D
14879	CNTROB	-0.41	0.025	D
14960	USP9X	-0.39	0.031	D
14971	RPS10	-0.44	0.015	D
15024	NME1	-0.43	0.018	D
15037	ACVR2A	-0.36	0.049	D
15088	ELOVL2	-0.38	0.040	D
15112	MLH1	-0.55	0.002	D
15114	ZNF804A	-0.42	0.021	D
15118	AGTRAP	-0.37	0.047	D
15165	PRR5L	-0.37	0.043	D
15192	RPL9	-0.48	0.007	D
15206	PLOD2	-0.39	0.032	D
15226	TRIM37	-0.51	0.004	D
15249	CDO1	-0.43	0.018	D
15250	UCHL1	-0.37	0.044	D
15335	TIPRL	-0.37	0.042	D
15382	EFHA2	-0.48	0.007	D
15427	C4orf46	-0.42	0.022	D
15442	IGFL2	-0.41	0.023	D
15474	UBE2D2	-0.45	0.014	D
15511	CDK7	-0.38	0.040	D
15543	RAB11FIP2	-0.44	0.016	D

15558	IL17A	-0.44	0.015	D
15559	LRRC40	-0.37	0.043	D
15576	CEP290	-0.37	0.043	D
15618	ANK2	-0.46	0.010	D
15683	STAT1	-0.45	0.013	D
15692	SPG7	-0.50	0.005	D
15823	NLGN2	-0.48	0.008	D
15844	SLC7A7	-0.37	0.047	D
15869	EMG1	-0.38	0.039	D
15881	C12orf68	-0.41	0.024	D
15892	HCFC1	-0.45	0.012	D
15909	ITSN1	-0.37	0.044	D
15943	EEF1E1	-0.38	0.038	D
15963	AKAP3	-0.50	0.005	D
15968	UTP18	-0.51	0.004	D
16013	GTDC1	-0.51	0.004	D
16019	C7orf69	-0.45	0.012	D
16074	ABL1	-0.40	0.026	D
16094	BDNF	-0.51	0.004	D
16109	SERTAD3	-0.38	0.036	D
16120	C19orf30	-0.36	0.049	D
16210	EXOSC10	-0.38	0.037	D
16216	SPATA22	-0.40	0.027	D
16299	SCG2	-0.48	0.007	D
16306	AMMECR1L	-0.38	0.037	D
16316	AGTRAP	-0.47	0.009	D
16337	RPL21	-0.41	0.025	D
16369	MAP3K12	-0.63	0.000	D
16478	ZEB2	-0.47	0.010	D
16479	RAD52	-0.44	0.016	D
16498	FGF5	-0.48	0.007	D
16515	LONRF1	-0.38	0.038	D
16591	DCAF6	-0.41	0.026	D
16596	IL16	-0.37	0.046	D
16615	OR8J1	-0.55	0.002	D
16703	CLCN5	-0.40	0.028	D
16743	MRPL47	-0.43	0.018	D
16765	TPRKB	-0.60	0.000	D

16853	CD3EAP	-0.40	0.028	D
16884	NARS	-0.43	0.018	D
16952	CHRNE	-0.39	0.031	D
16997	GPR149	-0.40	0.031	D
17027	SEMA4B	-0.38	0.040	D
17030	PA2G4	-0.37	0.046	D
17033	NXT2	-0.38	0.039	D
17034	MPDZ	-0.38	0.040	D
17056	COX8C	-0.37	0.047	D
17057	C12orf11	-0.38	0.039	D
17062	CCT7	-0.48	0.007	D
17089	HSDL1	-0.51	0.004	D
17257	OR8J3	-0.48	0.008	D
17270	SEC31B	-0.46	0.010	D
17322	KARS	-0.41	0.024	D
17335	TPTE	-0.39	0.035	D
17342	GDNF	-0.45	0.012	D
17377	ARHGAP12	-0.46	0.011	D
17413	MRFAP1L1	-0.46	0.010	D
17440	EPHA6	-0.40	0.030	D
17443	PROL1	-0.47	0.008	D
17481	OR14A16	-0.44	0.016	D
17487	RBM34	-0.37	0.046	D
17489	RASSF2	-0.45	0.014	D
17532	DICER1	-0.39	0.035	D
17545	LOC728643	-0.42	0.021	D
17559	GABRR2	-0.47	0.009	D
17567	SCARF2	-0.40	0.030	D
17610	ASAH1	-0.37	0.043	D
17687	MAP1LC3A	-0.41	0.026	D
17716	CCDC22	-0.37	0.041	D
17726	RABL5	-0.43	0.019	D
17753	FCAMR	-0.37	0.047	D
17770	LSM6	-0.49	0.006	D
17801	KCTD16	-0.38	0.039	D
17809	ADPRH	-0.36	0.048	D
17844	CCDC61	-0.42	0.021	D
17855	SYNE1	-0.40	0.030	D

17858	ATP6V1C1	-0.37	0.047	D
17877	RNMTL1	-0.38	0.036	D
17882	WDR11	-0.51	0.004	D
17897	SAMD14	-0.37	0.043	D
17940	GPR149	-0.39	0.034	D
18085	FBXO5	-0.56	0.001	D
18121	TOPORS	-0.39	0.036	D
18148	OSBPL11	-0.39	0.035	D
18162	TRUB2	-0.51	0.004	D
18178	CDK5RAP2	-0.40	0.028	D
18186	BAI3	-0.38	0.036	D
18187	HOXA7	-0.47	0.008	D
18218	PPM1D	-0.45	0.013	D
18222	ICOSLG	-0.41	0.026	D
18229	NETO1	-0.55	0.002	D
18237	CLEC4E	-0.47	0.009	D
18334	PIP5K1B	-0.47	0.009	D
18357	G3BP1	-0.49	0.006	D
18447	POLA1	-0.38	0.039	D
18672	UBE2CBP	-0.56	0.001	D
18710	GPR155	-0.38	0.036	D
18733	KIAA1632	-0.41	0.025	D
18745	ZNF620	-0.38	0.036	D
18829	TRIM58	-0.41	0.026	D
18838	RAP1B	-0.41	0.023	D
18871	L1CAM	-0.41	0.024	D
18896	DCAF16	-0.45	0.014	D
18898	SMURF2	-0.38	0.036	D
18915	LUC7L3	-0.44	0.014	D
18923	OR51T1	-0.40	0.027	D
18924	MRPL18	-0.43	0.017	D
18927	BATF3	-0.40	0.030	D
18962	HMGB2	-0.37	0.044	D
18964	PLXDC2	-0.37	0.046	D
19006	PCDH10	-0.44	0.015	D
19018	NOP56	-0.51	0.004	D
19025	RAD51C	-0.39	0.035	D
19045	LIAS	-0.40	0.028	D

19050	LRRC59	-0.55	0.002	D
19051	VSTM2A	-0.46	0.011	D
19058	PKIA	-0.46	0.011	D
19084	DRG2	-0.50	0.005	D
19111	ISCA1	-0.36	0.049	D
19121	ARL6IP1	-0.47	0.008	D
19122	SLC39A10	-0.37	0.046	D
19153	PMS1	-0.68	0.000	D
19302	CLDN17	-0.48	0.007	D
19324	ZBTB11	-0.50	0.004	D
19340	C18orf55	-0.37	0.043	D
19403	NFAM1	-0.41	0.026	D
19430	EIF1B	-0.38	0.039	D
19496	SNX12	-0.41	0.025	D
19586	IBSP	-0.43	0.018	D
19625	PIGL	-0.37	0.044	D
19670	NKAP	-0.42	0.023	D
19686	RPL7A	-0.45	0.013	D
19727	CPNE7	-0.44	0.016	D
19735	GPT	-0.37	0.047	D
19824	FBXO10	-0.38	0.041	D
19833	C1QTNF1	-0.42	0.020	D
19874	THBS4	-0.55	0.001	D
19885	FTCD	-0.40	0.029	D
19965		-0.41	0.024	D
19970	CLTA	-0.38	0.036	D
20025	SLC38A10	-0.43	0.018	D
20042	MYBBP1A	-0.37	0.045	D
20080	ARHGEF4	-0.40	0.028	D
20083	TSR2	-0.37	0.046	D
20113	KPNA2	-0.52	0.003	D
20151	ELMO2	-0.40	0.030	D
20155	CD47	-0.36	0.047	D
20178	SLC6A15	-0.40	0.031	D
20224	SMARCAD1	-0.39	0.033	D
20228	FTCD	-0.46	0.011	D
20310	PSMD7	-0.45	0.013	D
20318	RFC1	-0.37	0.046	D

20341	IL17RC	-0.42	0.021	D
20379	DYNC1LI1	-0.57	0.001	D
20454	SUV39H2	-0.38	0.040	D
20480	MCFD2	-0.41	0.026	D
20524	ZNF567	-0.45	0.012	D
20608	LEPROTL1	-0.48	0.008	D
20682	ROD1	-0.38	0.039	D
20712	FXYD7	-0.43	0.016	D
20717	TAF1C	-0.39	0.034	D
20781	ZNF385D	-0.40	0.029	D
20828	KIAA0368	-0.39	0.035	D
20896	EPN2	-0.36	0.049	D
20949	PAICS	-0.42	0.020	D
20964	ITSN1	-0.39	0.031	D
20983	RPL9	-0.46	0.011	D
21070	TPSAB1	-0.50	0.005	D
21097	IGDCC4	-0.39	0.033	D
21150	TXNDC3	-0.39	0.035	D
21197	NSMCE4A	-0.39	0.035	D
21273	NAE1	-0.51	0.004	D
21288	LIN7C	-0.52	0.004	D
21312	KSR2	-0.41	0.024	D
21352	ARL6	-0.58	0.001	D
21386	MSL2	-0.52	0.003	D
21462	MYO1A	-0.36	0.049	D
21488	PIK3C3	-0.48	0.007	D
21501	PHLPP2	-0.47	0.009	D
21538	INTS9	-0.44	0.015	D
21616	PNMAL1	-0.45	0.013	D
21648	GPR4	-0.44	0.015	D
21697	PITPNA	-0.46	0.010	D
21744	PAQR9	-0.37	0.044	D
21758	FAM26F	-0.39	0.031	D
21766	RAP1B	-0.40	0.027	D
21803	TRIM74	-0.39	0.032	D
21818	NAA50	-0.37	0.041	D
21828	DEFB114	-0.47	0.008	D
21853	ATMIN	-0.41	0.024	D

21861	NRXN3	-0.38	0.038	D
21894	LSM5	-0.37	0.046	D
21901	TRMT11	-0.42	0.021	D
21921	CLGN	-0.58	0.001	D
22014	DCUN1D4	-0.38	0.036	D
22108	BRAP	-0.36	0.049	D
22152	EYA4	-0.70	0.000	D
22159	OR52L1	-0.37	0.047	D
22195	C10orf85	-0.43	0.017	D
22207	UMOD	-0.42	0.021	D
22295	PPP2CB	-0.36	0.049	D
22300	RPL13P5	-0.41	0.024	D
22331	KPNB1	-0.48	0.007	D
22463	AMN1	-0.38	0.039	D
22470	PCNA	-0.53	0.002	D
22483	APBB1	-0.38	0.040	D
22552	HDAC2	-0.38	0.041	D
22564	PFN1	-0.40	0.029	D
22614	AKAP12	-0.36	0.048	D
22644	PAQR3	-0.38	0.040	D
22735	PDCL3	-0.46	0.010	D
22736	BMP6	-0.38	0.038	D
22740	PHF23	-0.38	0.040	D
22769	HUWE1	-0.52	0.003	D
22784	EFTUD2	-0.39	0.032	D
22910	MRPL52	-0.49	0.006	D
22917	C3orf31	-0.37	0.046	D
22939	OR8B12	-0.37	0.046	D
22951	NECAB1	-0.55	0.002	D
22995	TAF9	-0.44	0.016	D
23023	BNC2	-0.45	0.013	D
23036	ODZ3	-0.44	0.015	D
23125	ARID2	-0.36	0.049	D
23130	POLR2G	-0.45	0.012	D
23159	CCT2	-0.40	0.029	D
23189	ZNF607	-0.42	0.022	D
23190	DACT1	-0.41	0.024	D
23191	CEP57	-0.37	0.042	D

23203	NCRNA00188	-0.46	0.010	D
23246	CSTF1	-0.50	0.005	D
23404	UBQLN1	-0.37	0.044	D
23417	RBBP4	-0.40	0.029	D
23449	FECH	-0.41	0.023	D
23485	ATF1	-0.41	0.024	D
23497	LOXL3	-0.39	0.032	D
23510	MAPKAP1	-0.39	0.032	D
23553	BVES	-0.37	0.046	D
23579	BHLHB9	-0.41	0.023	D
23587	BTG3	-0.36	0.049	D
23612	FSD1	-0.46	0.011	D
23617	CERKL	-0.37	0.042	D
23645	NSFL1C	-0.39	0.036	D
23659	HNRNPA1	-0.37	0.044	D
23665	AMTN	-0.43	0.017	D
23671	LYNX1	-0.39	0.034	D
23688	UNC5D	-0.42	0.021	D
23710	GYPA	-0.43	0.017	D
23734	BDNF	-0.40	0.028	D
23738	ADNP2	-0.37	0.047	D
23740	WFDC8	-0.52	0.003	D
23803	CDK4	-0.51	0.004	D
23855	MBLAC2	-0.36	0.049	D
23887	UBE2C	-0.36	0.050	D
23924	CTU2	-0.50	0.005	D
23961	POU4F1	-0.38	0.037	D
23994	CETP	-0.41	0.023	D
24031	MSC	-0.41	0.025	D
24057	PLXNA2	-0.37	0.044	D
24058	NAA25	-0.50	0.005	D
24132	CYP26A1	-0.38	0.040	D
24135	ARHGAP8	-0.43	0.017	D
24186	NUDT11	-0.43	0.018	D
24202	NOC3L	-0.47	0.010	D
24204	RCN1	-0.52	0.003	D
24216	TMEM14B	-0.48	0.007	D
24259	NME1	-0.38	0.036	D

24264	ZNF625	-0.43	0.017	D
24276	DVL2	-0.43	0.019	D
24285	ZNF442	-0.45	0.013	D
24362	C10orf118	-0.41	0.024	D
24377	ITLN1	-0.38	0.039	D
24470	DCN	-0.57	0.001	D
24478	OR2M7	-0.42	0.020	D
24481	ERI1	-0.37	0.047	D
24483	METTL11A	-0.40	0.029	D
24503	BCAT1	-0.41	0.024	D
238	COPB2	0.44	0.016	U
318	GLIS2	0.37	0.046	U
484	FCRL3	0.36	0.048	U
508	TRAM1	0.38	0.037	U
539	GPR83	0.47	0.009	U
550	S100A16	0.55	0.002	U
591	MT1H	0.37	0.045	U
983	FAM134B	0.37	0.043	U
984	TMEM8A	0.41	0.026	U
998	RFNG	0.36	0.050	U
1018	TCL6	0.39	0.035	U
1030	SGSM3	0.46	0.010	U
1114	SHH	0.46	0.010	U
1124	EIF2C2	0.43	0.019	U
1270	ZFYVE21	0.37	0.042	U
1384	KRTAP17-1	0.39	0.035	U
1414	MID2	0.39	0.035	U
1461	CAPN13	0.38	0.038	U
1627	RNF208	0.41	0.024	U
1641	ESYT2	0.45	0.012	U
1668	HYOU1	0.38	0.036	U
1749	STEAP4	0.44	0.014	U
1756	KDELR3	0.45	0.012	U
1850	MOSPD3	0.39	0.033	U
1915	C1orf65	0.36	0.050	U
1935	IFNA1	0.51	0.004	U
2053	MALL	0.46	0.011	U
2066	ATG4A	0.36	0.049	U

2183	RAP1A	0.47	0.009	U
2233	LST1	0.37	0.044	U
2385	TMEM134	0.40	0.029	U
2388	TMEM61	0.49	0.005	U
2547	CA3	0.46	0.010	U
2590	SYTL2	0.37	0.043	U
2689	FOXA1	0.47	0.008	U
2691	LYPD5	0.39	0.035	U
2716	GMPPA	0.36	0.049	U
2743	TLR5	0.37	0.046	U
2794	GAD1	0.42	0.020	U
2886	CORO6	0.40	0.028	U
2936	TTC6	0.43	0.019	U
2945	PPARA	0.37	0.047	U
2981	PDIA2	0.39	0.033	U
2997	HRCT1	0.41	0.024	U
3040	FUT3	0.40	0.030	U
3087	PVRL1	0.38	0.037	U
3120	MCTP2	0.36	0.049	U
3249	MLL3	0.38	0.041	U
3326	C19orf10	0.44	0.014	U
3349	ARHGEF35	0.42	0.020	U
3360	LDLRAP1	0.36	0.049	U
3373	MAP4K4	0.49	0.007	U
3375	KIAA1147	0.38	0.039	U
3537	COPE	0.39	0.033	U
3695	RORA	0.37	0.042	U
3709	PXMP4	0.45	0.013	U
3806	SLC8A3	0.44	0.015	U
3820	GPRC5C	0.40	0.027	U
3835	TMPRSS15	0.39	0.031	U
3887	TXK	0.46	0.010	U
3894	NUDT16P1	0.37	0.047	U
3917	IER3	0.47	0.009	U
3973	NDRG1	0.53	0.003	U
3992	SYN1	0.40	0.029	U
3994	ICA1L	0.48	0.008	U
4025	AES	0.46	0.011	U

4031	SYNGR1	0.38	0.041	U
4074	PARM1	0.39	0.033	U
4097	BACE2	0.42	0.021	U
4166	SPINT2	0.46	0.010	U
4222	CYP7A1	0.37	0.044	U
4242	PPFIA1	0.40	0.027	U
4317	FAM83H	0.42	0.021	U
4328	LGMN	0.39	0.031	U
4346	ST3GAL1	0.43	0.019	U
4387	RALY	0.39	0.034	U
4528	MYO1D	0.51	0.004	U
4583	CCNDBP1	0.39	0.032	U
4598	RGR	0.40	0.031	U
4694	FGD4	0.37	0.045	U
4734	NET1	0.44	0.015	U
4765	LGALS9B	0.38	0.038	U
4800	HTRA4	0.38	0.040	U
4804	ALG1L	0.38	0.038	U
4805	GAD1	0.51	0.004	U
4927	HRCT1	0.38	0.039	U
4930	ANK3	0.49	0.006	U
4937	KIAA1217	0.45	0.012	U
5046	PTPN3	0.39	0.035	U
5057	LRRC45	0.42	0.019	U
5061	RPS6KA2	0.39	0.033	U
5065	KDELR2	0.38	0.039	U
5118	WNT7B	0.40	0.027	U
5146	CBX7	0.39	0.035	U
5152	MGST2	0.48	0.008	U
5327	LOC401296	0.36	0.050	U
5400	SLC35B2	0.41	0.026	U
5491	SERPINB10	0.37	0.042	U
5500	STAT6	0.37	0.047	U
5533	LGALS3	0.44	0.015	U
5556	CALML5	0.37	0.046	U
5568	ASL	0.54	0.002	U
5573	RNF19A	0.50	0.005	U
5606	CLDN16	0.37	0.043	U

5613	FAM53B	0.42	0.020	U
5697	ACHE	0.39	0.033	U
5714	C11orf63	0.53	0.003	U
5735	TMEM63A	0.36	0.048	U
5774	CHPF2	0.49	0.007	U
5803	LMF2	0.40	0.027	U
5994	TMUB1	0.43	0.019	U
6005	ADCK2	0.41	0.025	U
6055	INSIG1	0.36	0.048	U
6079	C2orf50	0.48	0.008	U
6142	APH1A	0.37	0.043	U
6145	ARTN	0.37	0.047	U
6179	NPDC1	0.41	0.025	U
6235	CNOT4	0.38	0.038	U
6266	LRRC14B	0.48	0.008	U
6271	PCDHGC3	0.43	0.017	U
6304	C16orf82	0.59	0.001	U
6307	MKRN1	0.41	0.026	U
6324	MYO5C	0.51	0.004	U
6325	RNF39	0.43	0.019	U
6418	CALML4	0.39	0.031	U
6488	CAMKK2	0.41	0.024	U
6543	FAM189A2	0.47	0.009	U
6649	ARID1A	0.39	0.031	U
6818	C20orf54	0.47	0.009	U
6828	RFNG	0.36	0.050	U
6862	AFTPH	0.49	0.006	U
6932	CDK2AP2	0.53	0.003	U
6964	VWA1	0.37	0.047	U
7074	PALMD	0.41	0.026	U
7128	GPR32	0.39	0.032	U
7355	BACE2	0.37	0.045	U
7375	GRIK1	0.47	0.009	U
7379	MS4A6A	0.47	0.009	U
7416	PTPN6	0.36	0.050	U
7490	KCNK17	0.40	0.028	U
7494	KCNC4	0.45	0.012	U
7718	ZNF645	0.42	0.022	U

7828	KCNK10	0.46	0.010	U
7834	TRIM26	0.39	0.033	U
7896	FAM133A	0.36	0.050	U
7929	RHEB	0.37	0.043	U
7933	XBP1	0.39	0.033	U
7963	FASTK	0.42	0.022	U
8038	ZSCAN16	0.40	0.029	U
8053	STAP2	0.46	0.011	U
8079	AKT1	0.47	0.008	U
8127	GPAA1	0.37	0.046	U
8177	ADCK5	0.37	0.043	U
8220	ADAM22	0.37	0.046	U
8495	MB	0.38	0.036	U
8513	HRH3	0.39	0.034	U
8569	WDR60	0.46	0.010	U
8587	WDR45L	0.36	0.049	U
8756	SUN2	0.45	0.012	U
8779	FAIM	0.43	0.019	U
8792	ARSJ	0.38	0.036	U
8794	BHLHE40	0.38	0.040	U
8805	NOMO1	0.40	0.028	U
8992	WDR24	0.40	0.030	U
9060	CSMD2	0.43	0.019	U
9178	MSRB2	0.37	0.042	U
9180	KIAA2013	0.37	0.046	U
9197	PKP3	0.36	0.048	U
9222	OR5H2	0.52	0.003	U
9248	ACTR3B	0.40	0.027	U
9258	SPHK1	0.50	0.005	U
9273	ARCN1	0.49	0.007	U
9312	GPM6B	0.41	0.023	U
9435	S100A6	0.49	0.006	U
9465	ZNF141	0.41	0.025	U
9619	SLC25A24	0.46	0.010	U
9645	PRAMEF7	0.41	0.025	U
9661	VEGFA	0.36	0.048	U
9684	BLVRA	0.46	0.011	U
9827	NET1	0.39	0.034	U

9849	TMF1	0.43	0.019	U
9924	ENPP4	0.38	0.041	U
9939	CARD14	0.40	0.029	U
10188	TRAK1	0.37	0.041	U
10291	APOBEC3B	0.43	0.018	U
10300	SMAD1	0.38	0.038	U
10325	MTSS1	0.50	0.005	U
10359	MAL2	0.39	0.033	U
10487	THNSL2	0.37	0.047	U
10498	ZNF688	0.39	0.032	U
10667	NCRNA00257	0.39	0.033	U
10703	S100A14	0.45	0.012	U
10718	C6orf89	0.47	0.008	U
10744	ACTG1	0.40	0.029	U
10793	KDELR3	0.44	0.014	U
10900	STK39	0.37	0.047	U
11217	PPP1R13B	0.42	0.020	U
11225	SLC37A3	0.39	0.032	U
11235	LRRC45	0.40	0.028	U
11295	PEX6	0.43	0.017	U
11296	SPO11	0.39	0.034	U
11475	TCF20	0.40	0.028	U
11542	RTN2	0.42	0.021	U
11553	TMPRSS13	0.41	0.024	U
11555	SH3PXD2A	0.43	0.019	U
11601	OR4D5	0.38	0.038	U
11613	TUBG2	0.39	0.031	U
11615	C9orf153	0.41	0.023	U
11682	AGPAT2	0.44	0.015	U
11700	DGAT1	0.43	0.017	U
11736	SLC26A5	0.48	0.007	U
11776	GUSB	0.37	0.045	U
11791	OR2A9P	0.39	0.035	U
11806	PDZD2	0.42	0.021	U
11808	SFN	0.48	0.007	U
11955	CORO1B	0.65	0.000	U
12055	FAM174B	0.41	0.024	U
12090	CDCA7L	0.37	0.045	U

12138	UNC13A	0.55	0.002	U
12204	B3GNT7	0.51	0.004	U
12212	OR5H1	0.37	0.045	U
12232	GAD1	0.37	0.044	U
12253	GMPR	0.42	0.022	U
12258	OR6C2	0.41	0.026	U
12361	AGPAT2	0.49	0.006	U
12428	KLHDC9	0.45	0.012	U
12495	MAPK3	0.38	0.037	U
12725	MAGEA5	0.41	0.025	U
12727	EDA	0.37	0.047	U
12756	TAPBP	0.37	0.047	U
12917	PPP2R2B	0.47	0.009	U
12940	XKRX	0.39	0.031	U
12990	ABCC9	0.41	0.026	U
13077	DNAJC5	0.44	0.014	U
13215	RREB1	0.38	0.038	U
13316	SPDYA	0.41	0.025	U
13324	ATP2B3	0.38	0.039	U
13347	TRIM41	0.44	0.016	U
13358	ZNF654	0.37	0.047	U
13528	ARHGEF5	0.39	0.032	U
13617	RHOD	0.45	0.014	U
13704	REM1	0.37	0.047	U
13707	RMND5B	0.40	0.028	U
13874	FMN2	0.37	0.041	U
13965	MT1F	0.44	0.016	U
14003	NAV2	0.38	0.037	U
14014	CD109	0.38	0.040	U
14095	EXOC5	0.38	0.039	U
14105	APOOL	0.41	0.025	U
14109	CHPF	0.41	0.024	U
14193	SRXN1	0.38	0.040	U
14211	TPH2	0.43	0.018	U
14335	CRYBA2	0.43	0.018	U
14367	SEC24C	0.42	0.020	U
14390	CD99	0.47	0.010	U
14407	TMC6	0.40	0.029	U

14416	OR5AN1	0.45	0.013	U
14429	PSG4	0.44	0.014	U
14546	RAB27A	0.42	0.021	U
14844	LGMN	0.36	0.048	U
14886	MAPK1	0.37	0.046	U
14896	LGR4	0.43	0.019	U
14913	FCAR	0.45	0.013	U
14984	ALS2CL	0.38	0.037	U
15068	LMBR1	0.37	0.043	U
15208	SNX31	0.45	0.012	U
15213	MAX	0.43	0.017	U
15246	SGMS2	0.44	0.015	U
15315	ZFP64	0.38	0.040	U
15357	ACP6	0.41	0.024	U
15424	SLC26A5	0.44	0.015	U
15461	LSR	0.47	0.009	U
15622	CAMK1D	0.47	0.009	U
15787	CHI3L2	0.50	0.005	U
15791	ITPKB	0.50	0.005	U
15868	GIPC1	0.40	0.031	U
16066	CLSTN1	0.42	0.022	U
16091	TRIOBP	0.44	0.015	U
16102	EHHADH	0.47	0.010	U
16123	GALNT12	0.45	0.013	U
16159	BRP44L	0.40	0.027	U
16209	GRAMD3	0.42	0.022	U
16238	RTN3	0.37	0.043	U
16244	DKK2	0.38	0.040	U
16246	C13orf39	0.37	0.044	U
16325	UBE2H	0.42	0.021	U
16326	C11orf75	0.51	0.004	U
16365	ERLEC1	0.39	0.035	U
16398	MB	0.36	0.050	U
16490	OPLAH	0.40	0.028	U
16512	TMEM62	0.40	0.027	U
16527	IL17RE	0.36	0.049	U
16639	AQP7	0.40	0.030	U
16851	RREB1	0.45	0.012	U

17014	PLEK2	0.41	0.023	U
17036	ALAS2	0.36	0.049	U
17148	MCEE	0.37	0.042	U
17206	STAP2	0.43	0.017	U
17211	CORO1B	0.69	0.000	U
17253	NRTN	0.37	0.042	U
17284	LRP5	0.43	0.019	U
17292	CRAMP1L	0.46	0.010	U
17362	AKAP8L	0.47	0.008	U
17437	MBIP	0.36	0.049	U
17439	RPS6KA2	0.45	0.012	U
17539	OR6N2	0.37	0.045	U
17649	PILRA	0.39	0.035	U
17684	PC	0.39	0.035	U
17720	PPP1R14C	0.37	0.046	U
17728	ATL1	0.38	0.041	U
17735	BDH1	0.48	0.008	U
17836	AKR1A1	0.44	0.015	U
17850	ALG11	0.38	0.041	U
17853	GH2	0.39	0.034	U
17892	STARD10	0.41	0.026	U
17933	CBR3	0.40	0.027	U
17974	TRIOBP	0.37	0.042	U
17975	GADD45G	0.36	0.048	U
18058	LOC399744	0.42	0.020	U
18067	KCNG2	0.37	0.046	U
18091	CASP14	0.44	0.015	U
18154	XBP1	0.46	0.011	U
18209	C11orf80	0.36	0.048	U
18220	SLC22A12	0.37	0.041	U
18231	TMEM134	0.37	0.044	U
18372	MPG	0.37	0.043	U
18751	KIAA0513	0.39	0.031	U
18775	SLC25A41	0.44	0.016	U
18856	FERMT1	0.39	0.036	U
18865	PC	0.41	0.025	U
18873	TPCN2	0.36	0.048	U
18982	PCDHA@	0.40	0.030	U

18990	ANXA11	0.42	0.021	U
19012	VAMP8	0.43	0.017	U
19057	SUMO1	0.36	0.047	U
19065		0.42	0.020	U
19081	STAP2	0.40	0.029	U
19110	AK5	0.42	0.020	U
19134	MASP1	0.39	0.032	U
19189	SUSD4	0.38	0.038	U
19257	TAS2R46	0.40	0.030	U
19389	SAMD10	0.39	0.034	U
19395	RBBP8	0.41	0.023	U
19604	TMEM198	0.37	0.044	U
19606	NET1	0.47	0.009	U
19765	ITPR3	0.37	0.044	U
19771	AES	0.48	0.007	U
19898	AKT1	0.45	0.014	U
19960	STX10	0.43	0.017	U
20007	MGAT4A	0.47	0.009	U
20087	GGA1	0.40	0.028	U
20088	NCRNA00086	0.57	0.001	U
20150	CD1B	0.40	0.030	U
20162	TRAK1	0.48	0.007	U
20193	LGALS8	0.45	0.013	U
20270	LONRF2	0.38	0.037	U
20328	UGT2B17	0.39	0.033	U
20429	GPC4	0.40	0.030	U
20450	PCDHA@	0.37	0.044	U
20475	PTK6	0.53	0.003	U
20510	PAX9	0.46	0.010	U
20514	FAM110C	0.40	0.030	U
20553	TSC22D3	0.38	0.040	U
20568	CCDC120	0.42	0.022	U
20569	TSC22D3	0.41	0.025	U
20577	ARHGAP26	0.36	0.048	U
20606	DRD1	0.37	0.041	U
20618	RSBN1	0.41	0.026	U
20705	TBC1D8B	0.38	0.036	U
20803	EPDR1	0.40	0.026	U

20877	NTN3	0.39	0.033	U
20945	OCIAD2	0.39	0.034	U
21035	APOL5	0.40	0.030	U
21043	DAB2IP	0.37	0.046	U
21108	ARHGAP1	0.37	0.042	U
21165	MGMT	0.39	0.032	U
21181	ATP9A	0.48	0.008	U
21199	COPG	0.39	0.033	U
21336	SLC24A2	0.40	0.030	U
21526	CRELD2	0.39	0.031	U
21630	CUL9	0.43	0.017	U
21695	CD6	0.40	0.029	U
21984	DCXR	0.38	0.039	U
22005	DYX1C1	0.37	0.046	U
22008	CSPG4P1Y	0.47	0.009	U
22113	RNF135	0.54	0.002	U
22290	EVPL	0.42	0.020	U
22310	FBXL16	0.55	0.002	U
22362	SLC16A5	0.36	0.050	U
22398	FAM46C	0.47	0.008	U
22430	FLJ43763	0.37	0.044	U
22646	STXBP2	0.37	0.046	U
22872	SLMO2	0.44	0.015	U
22902	DNAJC3	0.39	0.035	U
23008	DHRS3	0.43	0.017	U
23034	ZNF829	0.38	0.038	U
23077	ARL6IP6	0.39	0.034	U
23082	LILRB5	0.43	0.017	U
23112	LYST	0.39	0.034	U
23206	MST1R	0.47	0.008	U
23264	WDR91	0.38	0.037	U
23309	SLC45A4	0.39	0.033	U
23312	RNF19A	0.39	0.035	U
23339	C1orf146	0.48	0.007	U
23341	AGFG2	0.40	0.029	U
23371	KLHDC9	0.47	0.009	U
23438	GJB3	0.39	0.031	U
23448	ARID5A	0.38	0.037	U

23610	CHST15	0.48	0.008	U
23810	SERINC3	0.36	0.049	U
23943	HIST1H4D	0.40	0.028	U
23948	UPP1	0.41	0.024	U
23956	GSTT1	0.36	0.050	U
24028	GPR160	0.40	0.030	U
24040	GPR172B	0.41	0.025	U
24063	GPRC5C	0.49	0.006	U
24171	HDAC11	0.38	0.036	U
24175	TAPBP	0.40	0.027	U
24198	GCAT	0.42	0.020	U
24252	OSM	0.40	0.027	U
24345	UPP1	0.41	0.025	U
24445	EDARADD	0.41	0.026	U
24458		0.52	0.003	U
24466	GNA11	0.38	0.039	U

APPENDIX B. 1030 GENES CORRELATING WITH SYNERGISM TO PACLITAXEL + CARBOPLATIN

Gene ID	Symbol	Synergy Correlation	Correlation P value	Up or down regulated
980	CCDC144NL	-0.52	0.006	D
1585	POSTN	-0.56	0.003	D
3300	FPR1	-0.42	0.031	D
20341	IL17RC	-0.46	0.019	D
23246	CSTF1	-0.45	0.021	D
2053	MALL	-0.41	0.038	D
6324	MYO5C	-0.45	0.022	D
9197	PKP3	-0.41	0.036	D
11808	SFN	-0.48	0.013	D
12725	MAGEA5	-0.51	0.008	D
14003	NAV2	-0.44	0.025	D
19765	ITPR3	-0.47	0.017	D
20475	PTK6	-0.39	0.049	D
22005	DYX1C1	-0.45	0.022	D
23610	CHST15	-0.50	0.010	D
24466	GNA11	-0.40	0.041	D
83	ZNF365	-0.40	0.042	D
147	TRADD	-0.41	0.040	D
164	C2orf53	-0.43	0.027	D
253	SULT1A1	-0.42	0.032	D
293	NRN1L	-0.41	0.040	D
368	GLA	-0.40	0.042	D
414	C6orf201	-0.46	0.017	D
433	SYNPO2	-0.49	0.012	D
449	NOL3	-0.48	0.014	D
463	VCL	-0.45	0.023	D
479	GAS6	-0.41	0.036	D
507	PACRG	-0.39	0.048	D
511	GABRB2	-0.40	0.043	D
566	PTER	-0.59	0.001	D
573	SLC16A3	-0.46	0.019	D
594	ASB9	-0.44	0.026	D

599	GALNTL4	-0.44	0.026	D
602	LCK	-0.50	0.010	D
640	GPR107	-0.41	0.039	D
641	CTTN	-0.41	0.038	D
721	HS6ST1	-0.46	0.017	D
725	LCA10	-0.39	0.046	D
803	AK4	-0.44	0.025	D
806	PKM2	-0.42	0.034	D
818	C13orf15	-0.43	0.027	D
988	SLC7A5	-0.48	0.012	D
1014	SULT1A3	-0.41	0.035	D
1048	ABCC3	-0.50	0.010	D
1095	STARD13	-0.41	0.040	D
1138	SLC6A15	-0.39	0.046	D
1167	C9orf84	-0.43	0.027	D
1307	NLN	-0.39	0.046	D
1339	KRT81	-0.40	0.044	D
1342	G6PD	-0.57	0.003	D
1367	WDR53	-0.43	0.027	D
1370	CELA3A	-0.41	0.037	D
1464	TSPAN7	-0.42	0.034	D
1475		-0.42	0.033	D
1492	KLK3	-0.42	0.031	D
1507	C22orf40	-0.39	0.050	D
1574	SCRT1	-0.40	0.045	D
1606	CDC6	-0.40	0.045	D
1687	IKBKG	-0.43	0.029	D
1729	WISP3	-0.40	0.043	D
1838	INO80E	-0.41	0.040	D
1870	NOXO1	-0.42	0.033	D
1959	COBL	-0.50	0.010	D
2116		-0.44	0.023	D
2161	ZNF773	-0.42	0.031	D
2282	FAM125B	-0.40	0.043	D
2345	GPA33	-0.43	0.028	D
2351	RUSC1	-0.40	0.042	D
2391	HPD	-0.39	0.047	D
2401	LAMB3	-0.41	0.040	D

2432	TXNRD1	-0.40	0.041	D
2440	MSN	-0.40	0.044	D
2462	PCID2	-0.39	0.050	D
2572	TENC1	-0.39	0.047	D
2591	LAMP2	-0.39	0.049	D
2643	NQO1	-0.41	0.040	D
2645	SLC11A1	-0.44	0.024	D
2653	CKS2	-0.47	0.015	D
2669	XIRP1	-0.45	0.021	D
2677	SUPT16H	-0.46	0.017	D
2711	TSKU	-0.40	0.041	D
2722	OR56A4	-0.47	0.016	D
2747	PRKAR1B	-0.47	0.016	D
2753	GPR126	-0.52	0.006	D
2769	CNGA2	-0.44	0.025	D
2855	TRIM47	-0.40	0.042	D
2880	PRICKLE3	-0.40	0.041	D
2897	LMX1A	-0.43	0.028	D
3045	RABGGTA	-0.39	0.049	D
3234	C9orf140	-0.55	0.004	D
3308	CCL2	-0.44	0.023	D
3445	PLAC1	-0.47	0.015	D
3541	EFHD2	-0.48	0.013	D
3600	BCAN	-0.54	0.005	D
3754	CSNK1D	-0.41	0.039	D
3966	ACER3	-0.41	0.036	D
3967	TSPO	-0.41	0.039	D
3982	SLC5A2	-0.43	0.029	D
4013	ALAS2	-0.40	0.044	D
4112	RAB20	-0.46	0.018	D
4199	RAB11FIP5	-0.40	0.043	D
4295	DSCAM	-0.42	0.033	D
4304	MYLK	-0.43	0.030	D
4333	POLE3	-0.56	0.003	D
4351	FHOD3	-0.57	0.002	D
4354	FADD	-0.41	0.037	D
4370	STEAP3	-0.41	0.038	D
4404	DHRS4	-0.42	0.033	D

4477	OR14J1	-0.46	0.017	D
4529	IGSF11	-0.42	0.033	D
4542	AP2B1	-0.45	0.022	D
4679	PCDHGC3	-0.52	0.007	D
4700	MICAL2	-0.44	0.024	D
4773	SEPX1	-0.43	0.027	D
4897	SLC2A9	-0.39	0.048	D
4944	ZDHHC9	-0.45	0.020	D
5021	SEL1L3	-0.44	0.024	D
5098	MYH6	-0.50	0.009	D
5128	HSD3B7	-0.45	0.020	D
5213	MYH9	-0.51	0.008	D
5326	PRAMEF17	-0.42	0.032	D
5394		-0.46	0.018	D
5457	CRTAC1	-0.39	0.047	D
5466	CORO2B	-0.45	0.020	D
5490	FBXW2	-0.49	0.010	D
5524	DIRC1	-0.55	0.004	D
5579	GABPB1	-0.44	0.026	D
5608	OR2D3	-0.54	0.005	D
5614	CFI	-0.44	0.025	D
5629	UBE3C	-0.40	0.044	D
5658	HMCN2	-0.53	0.005	D
5715	LAMB4	-0.40	0.043	D
5717	SPRR2B	-0.41	0.037	D
5767	SNRPN	-0.48	0.013	D
5857	EPB41L4B	-0.43	0.030	D
5861	LOC400940	-0.45	0.023	D
5869	ZDHHC16	-0.45	0.023	D
5903	SIGLEC7	-0.45	0.020	D
5922	LIMCH1	-0.43	0.029	D
5934	CD99L2	-0.40	0.043	D
5990	SLC6A8	-0.52	0.007	D
6060	MAPK9	-0.49	0.011	D
6092	PCDHA@	-0.40	0.045	D
6112	SLC25A43	-0.57	0.003	D
6150	RPL39	-0.40	0.040	D
6220	CD151	-0.49	0.010	D

6223	FBXO32	-0.41	0.036	D
6255	PARVA	-0.49	0.011	D
6283	NCAPG2	-0.41	0.038	D
6316	C9orf95	-0.46	0.019	D
6361	ADAM15	-0.45	0.020	D
6434	ASTN1	-0.49	0.011	D
6464	IL25	-0.41	0.035	D
6517	OSBPL7	-0.51	0.008	D
6540	TMEM156	-0.41	0.036	D
6542	PITX1	-0.42	0.032	D
6562	AR	-0.53	0.006	D
6662	MORN1	-0.52	0.006	D
6673	KCND3	-0.42	0.031	D
6816	EMX2	-0.44	0.026	D
6855	TENC1	-0.66	0.000	D
6894	NEDD9	-0.39	0.049	D
6926		-0.41	0.037	D
6930	TNFAIP2	-0.41	0.036	D
6943	MYO1C	-0.49	0.011	D
7020	FBXL13	-0.41	0.035	D
7085	CYB5A	-0.45	0.023	D
7104	TMOD3	-0.49	0.012	D
7194	PRSS23	-0.51	0.007	D
7227	KLF10	-0.40	0.040	D
7286	C15orf52	-0.42	0.034	D
7312	TELO2	-0.42	0.031	D
7576	C6orf10	-0.46	0.018	D
7579	MAP4	-0.49	0.011	D
7619	ENPEP	-0.49	0.012	D
7776	C1orf49	-0.42	0.033	D
7893	PDK1	-0.43	0.028	D
7931	PARP4	-0.40	0.046	D
7989	KRT1	-0.45	0.022	D
8114	OR9G4	-0.54	0.004	D
8128	SNRPN	-0.49	0.011	D
8417	TNXB	-0.43	0.029	D
8446	CPN2	-0.41	0.035	D
8515	DPF3	-0.40	0.044	D

8548	INVS	-0.40	0.040	D
8641	TUBGCP2	-0.49	0.010	D
8657	CASP10	-0.56	0.003	D
8672	CAV2	-0.41	0.035	D
8690	NOVA1	-0.43	0.030	D
8757	KRTAP27-1	-0.45	0.021	D
8771	NPRL3	-0.45	0.022	D
8796	TAF1L	-0.40	0.042	D
8866	LRP12	-0.42	0.032	D
8911	CES1	-0.42	0.032	D
8928	TFAP4	-0.42	0.031	D
8979	MAP6D1	-0.39	0.046	D
9165	MAP1B	-0.46	0.019	D
9443	ABCB6	-0.42	0.033	D
9458	CCDC157	-0.49	0.011	D
9472	GRB10	-0.41	0.036	D
9494	FLJ41170	-0.43	0.029	D
9509	PLCB4	-0.40	0.045	D
9519	SCUBE1	-0.42	0.034	D
9558	TBC1D9B	-0.44	0.025	D
9570	UBA1	-0.43	0.026	D
9587	VCL	-0.45	0.022	D
9717	HPS6	-0.39	0.048	D
9762	CHRFAM7A	-0.41	0.037	D
9774	KCNK4	-0.46	0.018	D
9780	S100A2	-0.52	0.006	D
9832	SLC9A3R2	-0.41	0.036	D
9892	MRPL43	-0.52	0.007	D
9947	INF2	-0.45	0.021	D
9948	HILS1	-0.51	0.008	D
9957	RNASEH2C	-0.58	0.002	D
9985	TBC1D24	-0.42	0.032	D
10039	CFHR2	-0.51	0.008	D
10088	ARMCX5	-0.41	0.035	D
10130	ADK	-0.41	0.035	D
10175	GCNT2	-0.40	0.044	D
10268	EMD	-0.56	0.003	D
10349	TIAL1	-0.39	0.046	D

10393	FAM129B	-0.41	0.036	D
10486	NOL6	-0.45	0.023	D
10516	DDIT4	-0.42	0.034	D
10551	LRSAM1	-0.40	0.043	D
10611		-0.42	0.033	D
10613	PILRB	-0.52	0.006	D
10677	PPP1R2P9	-0.52	0.006	D
10790	TNKS1BP1	-0.39	0.047	D
10850	COL8A1	-0.41	0.038	D
10923	SGPL1	-0.44	0.025	D
10925	MPP6	-0.39	0.050	D
10942	ERCC6L	-0.51	0.008	D
10974	SMU1	-0.61	0.001	D
11033	ME1	-0.61	0.001	D
11176	RNPS1	-0.41	0.037	D
11271	GIMAP7	-0.50	0.009	D
11353	ADAM15	-0.47	0.015	D
11468	PARD3B	-0.53	0.005	D
11486	MYEOV2	-0.49	0.011	D
11491	CNDP1	-0.52	0.006	D
11495	TRIM54	-0.50	0.009	D
11676	CDH22	-0.43	0.028	D
11723	IDS	-0.40	0.042	D
11779	FAM151A	-0.42	0.035	D
11801	AR	-0.41	0.038	D
11878	AIMP1	-0.58	0.002	D
11899	PALLD	-0.57	0.002	D
11981	COL8A1	-0.40	0.045	D
12011	KRT7	-0.42	0.034	D
12025	ME3	-0.43	0.028	D
12128	LASS1	-0.55	0.004	D
12149	IL7R	-0.41	0.038	D
12190	KRT6A	-0.48	0.012	D
12201	TMEM119	-0.40	0.045	D
12221	PRDM1	-0.54	0.005	D
12254		-0.45	0.021	D
12271	GCLC	-0.46	0.019	D
12313	FAM46D	-0.58	0.002	D

12359	SLC25A33	-0.46	0.018	D
12379	C9orf25	-0.45	0.022	D
12487	SLC7A3	-0.53	0.005	D
12561	CNTN1	-0.40	0.041	D
12583	C9orf78	-0.43	0.030	D
12585	TRIM6	-0.41	0.037	D
12591	LAMP2	-0.52	0.006	D
12709	CHST3	-0.49	0.010	D
12757	SLAMF9	-0.48	0.014	D
13044	HSD17B6	-0.41	0.039	D
13063	IRAK1	-0.46	0.017	D
13095	TUBB3	-0.43	0.029	D
13129	CNTN4	-0.42	0.033	D
13141	IP6K3	-0.46	0.017	D
13154	ELFN2	-0.41	0.039	D
13177	RAB44	-0.49	0.011	D
13220	BTNL8	-0.50	0.009	D
13225	TRAF3IP2	-0.47	0.015	D
13317	PSMD10	-0.40	0.042	D
13322	RGS12	-0.45	0.022	D
13372	FAM129B	-0.42	0.034	D
13379	PLSCR4	-0.48	0.013	D
13438	TMEM100	-0.39	0.049	D
13448	PATZ1	-0.39	0.046	D
13461	MAZ	-0.45	0.021	D
13541	LRRFIP2	-0.40	0.045	D
13717	DEFB118	-0.40	0.043	D
13738	G6PD	-0.48	0.012	D
13741	DRGX	-0.44	0.023	D
13742	FLJ39061	-0.42	0.032	D
13752	FAM113B	-0.41	0.036	D
13915	CTSZ	-0.40	0.041	D
13980	NOXO1	-0.48	0.013	D
14012	BRCC3	-0.47	0.015	D
14040	SPINLW1	-0.39	0.046	D
14146	CYP4B1	-0.43	0.030	D
14315	RCOR1	-0.46	0.019	D
14330	RAPH1	-0.47	0.015	D

14358	GAS6	-0.39	0.047	D
14363	KRT86	-0.43	0.029	D
14447	TXN	-0.42	0.034	D
14535	GEMIN7	-0.48	0.012	D
14582	ASB9	-0.47	0.016	D
14595	FGFRL1	-0.43	0.027	D
14602	THADA	-0.39	0.047	D
14636	CCNY	-0.46	0.019	D
14644	MBL2	-0.42	0.031	D
14757	LIMS3	-0.43	0.027	D
14857	RNF216	-0.49	0.010	D
14869	CDH24	-0.59	0.002	D
14978	OPN1LW	-0.46	0.019	D
15006	TPSG1	-0.40	0.045	D
15034	IFNA21	-0.46	0.019	D
15041	MCCD1	-0.43	0.030	D
15072	C8orf34	-0.46	0.018	D
15161	MOCOS	-0.44	0.026	D
15346	HTATIP2	-0.39	0.047	D
15440	PILRB	-0.39	0.048	D
15455	CHRNB3	-0.46	0.017	D
15615	LRP8	-0.42	0.032	D
15627	PRPS1	-0.44	0.023	D
15662	IMPDH1	-0.52	0.007	D
15752	ZNF484	-0.44	0.025	D
15762	RGP1	-0.40	0.042	D
15865	WDR5	-0.50	0.009	D
15901	EYA1	-0.40	0.041	D
15989	RAPH1	-0.43	0.030	D
16032	C10orf93	-0.46	0.017	D
16061	CDH7	-0.46	0.017	D
16075	C1orf124	-0.42	0.031	D
16222	PRR4	-0.43	0.027	D
16224	C1orf61	-0.44	0.026	D
16226	SH3BP4	-0.41	0.037	D
16247	KIAA1715	-0.41	0.039	D
16250	HAPLN3	-0.60	0.001	D
16354	FLYWCH2	-0.45	0.020	D

16390	INF2	-0.48	0.013	D
16391	TCEAL4	-0.41	0.037	D
16445	ERCC6L	-0.41	0.040	D
16468	OR2K2	-0.39	0.049	D
16536	PRSS3	-0.45	0.020	D
16565	FARSB	-0.39	0.048	D
16593	ACTL6A	-0.39	0.048	D
16633	C9orf89	-0.44	0.024	D
16674	ANKZF1	-0.44	0.023	D
16709	MECP2	-0.46	0.018	D
16718	PHLDB1	-0.46	0.019	D
16732	NAAA	-0.45	0.021	D
16764	GABRE	-0.44	0.024	D
16897	FLNB	-0.40	0.044	D
16905	TMEM187	-0.40	0.040	D
16910	RNF41	-0.45	0.020	D
16989	TSC22D1	-0.49	0.010	D
17018	DIAPH2	-0.43	0.027	D
17043	PPP1R8	-0.42	0.034	D
17064	ALPK2	-0.39	0.047	D
17098	PDE5A	-0.41	0.040	D
17110	COL18A1	-0.45	0.022	D
17210	DEFB112	-0.43	0.030	D
17261	MPP1	-0.41	0.039	D
17267	AKR1B10	-0.42	0.035	D
17410	DUX4	-0.53	0.006	D
17427	NQO1	-0.43	0.027	D
17615	CD99L2	-0.40	0.043	D
17664	GPX3	-0.42	0.033	D
17820	AGTR2	-0.46	0.019	D
17870	MFGE8	-0.42	0.034	D
18006	SH3RF2	-0.44	0.024	D
18072	PRKACB	-0.55	0.004	D
18157	MAP1B	-0.42	0.032	D
18431	HSD11B1	-0.41	0.038	D
18463	CYB5A	-0.45	0.020	D
18466	HNRNPAB	-0.39	0.049	D
18530	C5orf44	-0.39	0.047	D

18538	TYRO3	-0.45	0.022	D
18578	C1orf35	-0.47	0.016	D
18673	GLDN	-0.41	0.037	D
18678	C17orf54	-0.40	0.041	D
18680	MARCH10	-0.49	0.010	D
18837	RBM18	-0.46	0.019	D
18864	C20orf71	-0.39	0.048	D
18911	RGR	-0.41	0.037	D
18917	SLC11A1	-0.39	0.049	D
18981	MAML1	-0.53	0.005	D
19085	SYCP3	-0.58	0.002	D
19138	BCL9L	-0.44	0.025	D
19171	GRB10	-0.47	0.017	D
19359	TRIM6	-0.43	0.028	D
19409	CMTM4	-0.42	0.031	D
19429	C3orf70	-0.43	0.030	D
19431	RPS6KA4	-0.51	0.008	D
19475	GCGR	-0.43	0.028	D
19520	PRPF4	-0.54	0.004	D
19584	TRERF1	-0.41	0.036	D
19682		-0.39	0.049	D
19740	KCNAB1	-0.40	0.045	D
19750	STBD1	-0.49	0.012	D
19781	CDC42EP2	-0.42	0.033	D
19783	DYNLT3	-0.46	0.017	D
19841	POLR2L	-0.40	0.045	D
19846	IGSF1	-0.43	0.029	D
19924	OR6C74	-0.41	0.038	D
19929	ITIH3	-0.41	0.039	D
20021	PLCE1	-0.39	0.048	D
20068	PPIE	-0.43	0.027	D
20095		-0.44	0.023	D
20101	KLHL14	-0.40	0.044	D
20108	EFEMP1	-0.44	0.023	D
20238	PDZD7	-0.43	0.028	D
20312	PSRC1	-0.41	0.038	D
20320	SDPR	-0.40	0.042	D
20324	SLC16A9	-0.45	0.022	D

20380	SUN5	-0.56	0.003	D
20386	SERPINB5	-0.48	0.014	D
20398	PDLIM3	-0.40	0.045	D
20403	ANXA7	-0.39	0.050	D
20458	CD151	-0.50	0.009	D
20516	NCRNA00152	-0.40	0.043	D
20645	CSRP1	-0.40	0.041	D
20706	NAA20	-0.39	0.048	D
20736	STOML3	-0.41	0.037	D
20744	F8	-0.42	0.033	D
20799	GJB5	-0.44	0.025	D
20804	CASP1	-0.43	0.029	D
20818		-0.41	0.038	D
20836	SULT1A2	-0.44	0.025	D
20855	RGS20	-0.41	0.039	D
20895	ANO1	-0.41	0.037	D
21007	FAM69C	-0.45	0.021	D
21033	LEFTY2	-0.39	0.048	D
21053	PTGR1	-0.43	0.028	D
21115	ADAM15	-0.45	0.021	D
21154	COL4A6	-0.41	0.037	D
21167	PHACTR4	-0.46	0.019	D
21216	PORCN	-0.44	0.024	D
21239	LPA	-0.49	0.011	D
21251	ANKS3	-0.47	0.015	D
21259	IL17D	-0.44	0.025	D
21285	COMMD10	-0.40	0.041	D
21423	CD151	-0.42	0.034	D
21447	LOC440944	-0.46	0.019	D
21461	MAP4	-0.46	0.019	D
21481	JAG2	-0.41	0.036	D
21617	CTSW	-0.39	0.048	D
21763	APTX	-0.43	0.030	D
21890	CDON	-0.40	0.041	D
22043	DHDPSL	-0.41	0.036	D
22231	SYT8	-0.42	0.031	D
22267	BICD2	-0.45	0.021	D
22367	CRYBA4	-0.45	0.022	D

22427	FOXK1	-0.45	0.023	D
22452	TSPO	-0.46	0.019	D
22510	NEIL3	-0.39	0.047	D
22515	EFEMP1	-0.46	0.017	D
22532	EPHX1	-0.48	0.012	D
22540	RPL39L	-0.41	0.036	D
22602	MID1	-0.47	0.015	D
22604	PHOX2B	-0.44	0.023	D
22679	FOSL1	-0.41	0.036	D
22692	UBE2A	-0.44	0.024	D
22694		-0.46	0.017	D
22768	DKC1	-0.58	0.002	D
22861	C9orf24	-0.39	0.048	D
22915	TMEM31	-0.39	0.047	D
22933	PLEKHG5	-0.54	0.005	D
22973	MGC44328	-0.42	0.031	D
23143	HES2	-0.39	0.048	D
23169	CCDC136	-0.46	0.017	D
23329	STX17	-0.45	0.020	D
23331	NCS1	-0.44	0.023	D
23360	MYLK	-0.40	0.040	D
23373	UBN1	-0.48	0.013	D
23385	GPC1	-0.40	0.044	D
23399	C12orf50	-0.42	0.034	D
23445	TPP2	-0.42	0.032	D
23522	PGM2L1	-0.50	0.010	D
23545	EIF6	-0.42	0.035	D
23564	RFC4	-0.41	0.038	D
23639	CDH24	-0.39	0.047	D
23827	ARAP3	-0.40	0.043	D
23879	NINJ1	-0.43	0.028	D
23974	C1S	-0.40	0.045	D
24088	KCTD5	-0.40	0.042	D
24127	HYDIN	-0.45	0.021	D
24149	DENND2C	-0.52	0.007	D
24169	CAPN9	-0.40	0.046	D
24236	DAOA	-0.45	0.022	D
24274	HMGB3	-0.43	0.029	D

24344	UNKL	-0.40	0.043	D
24370		-0.48	0.013	D
24425	SLC6A10P	-0.52	0.007	D
24429	GCK	-0.45	0.021	D
24497	STUB1	-0.45	0.022	D
1284	RFXAP	0.43	0.027	U
4133	KDM3A	0.42	0.033	U
4536	GORAB	0.59	0.001	U
5220	DACT1	0.47	0.016	U
7329	SPRR2F	0.45	0.022	U
7572	OR2J2	0.45	0.021	U
7882	RORB	0.41	0.040	U
8608	CHST5	0.41	0.038	U
8900	TMEM225	0.43	0.030	U
9316	MTF2	0.40	0.043	U
13259	DUSP11	0.46	0.017	U
14618	USP9X	0.39	0.049	U
16369	MAP3K12	0.58	0.002	U
17770	LSM6	0.39	0.047	U
19430	EIF1B	0.45	0.020	U
20224	SMARCAD1	0.46	0.017	U
21488	PIK3C3	0.41	0.039	U
23189	ZNF607	0.41	0.039	U
4025	AES	0.41	0.038	U
4583	CCNDBP1	0.48	0.013	U
9312	GPM6B	0.47	0.014	U
12204	B3GNT7	0.39	0.046	U
24445	EDARADD	0.40	0.045	U
3	PHF7	0.39	0.049	U
18	GNG5	0.41	0.036	U
55	TM2D1	0.46	0.019	U
116	NDUFAF3	0.43	0.030	U
218	LAIR2	0.42	0.035	U
277	NDRG4	0.43	0.028	U
320	ZNF74	0.39	0.048	U
397	ACBD4	0.44	0.024	U
416	COL8A2	0.46	0.019	U
514	CHST11	0.45	0.021	U

544	TERF1	0.39	0.048	U
554	OR2T35	0.46	0.017	U
601	PDE1B	0.45	0.021	U
648	STAT2	0.45	0.022	U
687	SMARCB1	0.42	0.034	U
738	B3GALT5	0.45	0.021	U
761	ARSB	0.41	0.036	U
797		0.48	0.013	U
817	TRIM39	0.44	0.023	U
888	TBC1D15	0.47	0.014	U
902	ZNF627	0.40	0.043	U
922	PPM1F	0.42	0.034	U
968	ZACN	0.48	0.013	U
1096	HMGB3L1	0.48	0.014	U
1203	ADNP	0.49	0.011	U
1217	B3GNT2	0.40	0.043	U
1257	LACRT	0.51	0.007	U
1300	SCMH1	0.43	0.030	U
1324	OR2W3	0.42	0.032	U
1350	HIST1H2BG	0.46	0.018	U
1364	NLRP12	0.67	0.000	U
1418	CNTN4	0.56	0.003	U
1462	HIST1H2BC	0.39	0.047	U
1481	TRIM9	0.48	0.013	U
1493	PLIN2	0.41	0.039	U
1649	AKIRIN1	0.40	0.044	U
1670	GNL2	0.47	0.015	U
1750	WFIKKN1	0.39	0.048	U
1797	UTY	0.45	0.021	U
1804	KIF19	0.46	0.018	U
1833	NDNL2	0.45	0.021	U
1865	TTC21A	0.43	0.026	U
1890	PRRX1	0.43	0.030	U
1948	ZSCAN29	0.49	0.012	U
1982	WAC	0.46	0.017	U
1985	PGS1	0.43	0.030	U
2041	LANCL3	0.58	0.002	U
2141	KRT23	0.42	0.033	U

2164	NMS	0.43	0.027	U
2202	TOE1	0.49	0.012	U
2369		0.43	0.030	U
2418	ZNF16	0.41	0.037	U
2602	SGK2	0.39	0.047	U
2661	SLC22A6	0.58	0.002	U
2868	USP6	0.56	0.003	U
2878	MS4A14	0.56	0.003	U
2908	C11orf57	0.47	0.015	U
2914		0.43	0.027	U
2920	MAP2K7	0.44	0.024	U
2927	C14orf101	0.44	0.026	U
2928	ECSIT	0.41	0.039	U
2946	ASB8	0.46	0.017	U
2991	PHTF2	0.45	0.020	U
3042	CLDN14	0.44	0.023	U
3047	PRTFDC1	0.46	0.017	U
3048	C13orf26	0.39	0.049	U
3070	NFATC1	0.52	0.006	U
3080	BCL7A	0.47	0.016	U
3107	SF3B4	0.43	0.030	U
3336	PHF2	0.45	0.021	U
3424	HAMP	0.41	0.038	U
3432	TTLL1	0.47	0.015	U
3742	BEX4	0.40	0.043	U
3773		0.54	0.005	U
3882	VPS28	0.56	0.003	U
3891	FAM92B	0.39	0.046	U
3922	KRTAP4-4	0.39	0.046	U
3933	PPFIA2	0.42	0.031	U
3939	PLAGL1	0.43	0.030	U
3981	LRRC48	0.46	0.018	U
4009	RERE	0.49	0.010	U
4021	CHD3	0.51	0.007	U
4033	COMMD3	0.41	0.036	U
4043	ABAT	0.54	0.004	U
4064	PTCH2	0.42	0.035	U
4092	C10orf53	0.48	0.013	U

4117	GPR137B	0.43	0.027	U
4134	PIK3CA	0.39	0.046	U
4234	TTLL3	0.46	0.019	U
4239	ARHGAP21	0.41	0.037	U
4321	TRMT2A	0.42	0.034	U
4344	DNMT3A	0.46	0.018	U
4472	PTOV1	0.45	0.022	U
4523	FDXR	0.43	0.028	U
4564	ZFAT	0.44	0.024	U
4649	SOCS7	0.40	0.041	U
4735	CYS1	0.46	0.018	U
4754	SDC1	0.41	0.039	U
4757	DRAM2	0.39	0.047	U
4760	CCR10	0.44	0.023	U
4768	OR2B2	0.39	0.049	U
4794	LTK	0.55	0.003	U
4880	DLX1	0.39	0.048	U
4882	ERCC1	0.49	0.010	U
4890	BLOC1S1	0.44	0.025	U
4911	HIST1H2BE	0.41	0.038	U
4942	GTPBP1	0.46	0.018	U
4968	C18orf8	0.40	0.045	U
4981	TMEM35	0.42	0.031	U
4994	C19orf43	0.58	0.002	U
5006	PDE9A	0.43	0.028	U
5076	ACP1	0.42	0.034	U
5078	PCBP1	0.61	0.001	U
5090	RANBP2	0.40	0.044	U
5121	GDF7	0.45	0.020	U
5131	SYF2	0.39	0.049	U
5147	VARS2	0.41	0.040	U
5163	CDNF	0.55	0.004	U
5262	GGA3	0.39	0.050	U
5317	USP44	0.44	0.025	U
5320	C1orf86	0.39	0.050	U
5356	HCST	0.39	0.046	U
5392		0.44	0.026	U
5477	ATP6V0A1	0.50	0.009	U

5785	HSPC159	0.45	0.022	U
5851	KRTAP19-2	0.43	0.030	U
5860	SCGBL	0.43	0.028	U
5862	CTSE	0.42	0.031	U
5905	TNKS2	0.39	0.046	U
5947	TAAR2	0.42	0.033	U
5948	LOC374491	0.45	0.021	U
5959	HIF3A	0.41	0.040	U
6086	ZNF428	0.41	0.039	U
6090	HIST2H2AA3	0.53	0.006	U
6321	DEDD	0.45	0.022	U
6468	WFDC8	0.39	0.049	U
6596	SCYL3	0.59	0.002	U
6623	SERPING1	0.39	0.050	U
6650	NBAS	0.58	0.002	U
6659	CCK	0.49	0.011	U
6660	CUL7	0.52	0.007	U
6667	HSD17B7	0.50	0.010	U
6678	SEPHS2	0.41	0.038	U
6745	UBE2E1	0.43	0.028	U
6804	MTMR14	0.50	0.009	U
6827	SLC12A5	0.42	0.035	U
6911	ALS2CR8	0.41	0.035	U
6933	FBXO11	0.42	0.034	U
6935	B3GNT3	0.42	0.033	U
6939	ALLC	0.47	0.016	U
6978	COL3A1	0.40	0.041	U
6980	TNFRSF8	0.45	0.022	U
6991	ATP5S	0.42	0.033	U
7019	PRDM16	0.52	0.007	U
7068	SH2D4B	0.42	0.033	U
7071	PRKAG1	0.42	0.034	U
7129	HIST1H3D	0.41	0.040	U
7173	ARNT	0.48	0.014	U
7199	EIF3L	0.54	0.004	U
7226	ADCY6	0.41	0.036	U
7267	RGPD1	0.49	0.011	U
7284	HSD17B14	0.58	0.002	U

7376	HCST	0.51	0.008	U
7380	PLCG1	0.42	0.032	U
7410	CACNB4	0.42	0.031	U
7455	SAP30L	0.42	0.032	U
7556	TCEAL6	0.56	0.003	U
7601		0.50	0.010	U
7625	ESCO1	0.66	0.000	U
7646	ARL6IP4	0.39	0.046	U
7689	FLRT3	0.63	0.001	U
7731	NIPBL	0.54	0.004	U
7769	SLC22A17	0.44	0.024	U
7782	DPM1	0.55	0.004	U
7788	DDT	0.43	0.030	U
7802	TOM1	0.61	0.001	U
7803	MTRR	0.46	0.017	U
7967	NKG7	0.41	0.040	U
8066	FRG1	0.45	0.021	U
8103	NPAS4	0.39	0.050	U
8207	CLEC2B	0.43	0.028	U
8235	ZNF644	0.40	0.042	U
8327	GOLGA6A	0.48	0.013	U
8431	SH3YL1	0.41	0.037	U
8437	GSTTP2	0.41	0.036	U
8493	CEP76	0.41	0.037	U
8561	ARID4A	0.47	0.017	U
8680	FTMT	0.40	0.044	U
8733	HBA1	0.41	0.040	U
8832	EEF1B2	0.41	0.037	U
8834	C8orf30A	0.41	0.038	U
8843	ZNF749	0.43	0.029	U
8891	ITSN1	0.43	0.026	U
8919	YPEL5	0.39	0.049	U
8972	RPL41	0.40	0.045	U
9063	MYL4	0.60	0.001	U
9090	ZNF320	0.40	0.041	U
9110	OR5M9	0.49	0.012	U
9114	ATXN7L2	0.41	0.036	U
9123	QARS	0.48	0.012	U

9138	ENOSF1	0.43	0.027	U
9249	RGAG4	0.39	0.048	U
9366	FAM175A	0.40	0.042	U
9383	FARP1	0.44	0.023	U
9476	PHF20L1	0.53	0.005	U
9599	TDRKH	0.51	0.008	U
9649	MED9	0.62	0.001	U
9710	POMGNT1	0.42	0.030	U
9716	QPRT	0.40	0.041	U
9742	CCDC8	0.39	0.049	U
9791	CAND2	0.41	0.038	U
9942	PTPN13	0.46	0.018	U
10103	AP1G2	0.43	0.030	U
10119	ADAM10	0.40	0.045	U
10147	RRP36	0.40	0.044	U
10157	POLR2B	0.44	0.026	U
10229	PTPN12	0.40	0.042	U
10233	SCAP	0.41	0.039	U
10263	OR51B5	0.42	0.034	U
10355	FLJ33360	0.47	0.016	U
10424	ELMO2	0.44	0.024	U
10437	SCYL3	0.52	0.006	U
10468	PIGU	0.44	0.023	U
10490	ARHGEF1	0.48	0.014	U
10500	IMMT	0.41	0.037	U
10541	TGFBR3	0.42	0.033	U
10612	PCMTD1	0.41	0.036	U
10642	C12orf23	0.44	0.025	U
10660	NFYC	0.46	0.018	U
10682	C14orf166	0.43	0.030	U
10728	ALKBH7	0.57	0.002	U
10773	TBKBP1	0.51	0.008	U
10804	RBMXL3	0.41	0.038	U
10846	PPIL2	0.39	0.048	U
11011	SDHD	0.42	0.033	U
11021	ACBD5	0.43	0.028	U
11068	SEMA5A	0.39	0.047	U
11072	MDH1	0.39	0.046	U

11115	NIPSNAP3A	0.50	0.009	U
11180	WAC	0.45	0.022	U
11190	CIB2	0.41	0.037	U
11315	KCND3	0.52	0.007	U
11418	SPATA6	0.40	0.043	U
11425	MSMP	0.43	0.027	U
11472	PPM1B	0.46	0.018	U
11511	SRGAP2	0.40	0.041	U
11513	C19orf53	0.39	0.049	U
11608	RAD23A	0.43	0.027	U
11669	TSHR	0.47	0.015	U
11683	RS1	0.50	0.009	U
11826	PQLC2	0.48	0.012	U
11860	PRSS48	0.47	0.016	U
11888	MRPL45	0.51	0.008	U
11895	SIRPB1	0.40	0.044	U
11904	LILRA1	0.46	0.019	U
11944	HTR7	0.56	0.003	U
11961	SIK2	0.40	0.041	U
11966	SF3B14	0.40	0.045	U
11997	RCOR3	0.39	0.050	U
12002	C19orf56	0.46	0.017	U
12039	FAM110B	0.40	0.043	U
12086	NCRNA00115	0.41	0.037	U
12129	ZNF791	0.58	0.002	U
12132	CSAG1	0.40	0.041	U
12188	MRPS21	0.41	0.038	U
12210	ERCC1	0.45	0.020	U
12225	SLC26A6	0.43	0.029	U
12288	FAM81B	0.56	0.003	U
12297	SNRNP35	0.44	0.025	U
12344	PEBP1	0.46	0.019	U
12380	MS4A5	0.43	0.026	U
12398	OR11H12	0.46	0.019	U
12509	TNFRSF6B	0.39	0.046	U
12606	NLRP10	0.39	0.047	U
12666	C2orf76	0.39	0.048	U
12714	DOK1	0.52	0.006	U

12748	FBXW8	0.47	0.016	U
12833	TMEM91	0.43	0.028	U
12863	OR2L8	0.39	0.047	U
12870	TADA3	0.47	0.017	U
12886	ACSL4	0.41	0.037	U
12921	DERL2	0.44	0.023	U
12966	CBY1	0.42	0.030	U
12971	B4GALT6	0.53	0.005	U
13021	APOL2	0.44	0.023	U
13104	KIR2DS4	0.39	0.047	U
13117	RNF170	0.43	0.027	U
13126	MASP1	0.45	0.020	U
13155	LIG4	0.43	0.027	U
13231	ATP5F1	0.41	0.039	U
13310	DCAF6	0.41	0.037	U
13354	ATP5L	0.47	0.015	U
13390	KISS1R	0.43	0.027	U
13536	HELQ	0.42	0.031	U
13557	CCDC121	0.41	0.037	U
13639	SFSWAP	0.46	0.018	U
13652	THRB	0.40	0.043	U
13745	BRWD1	0.63	0.001	U
13828	TMED5	0.42	0.035	U
13929	SPN	0.41	0.035	U
13941	C6orf81	0.42	0.033	U
13956	CEACAM20	0.50	0.009	U
13960	PFDN5	0.42	0.035	U
13988	ABCC6	0.43	0.030	U
14031	PDK2	0.41	0.038	U
14084	NUPL1	0.40	0.042	U
14099	CYP7B1	0.39	0.049	U
14119	KLHDC3	0.43	0.027	U
14167	COIL	0.44	0.025	U
14253	NAA38	0.54	0.004	U
14257	PAK7	0.54	0.005	U
14262	F8A1	0.40	0.046	U
14272	GP1BA	0.51	0.008	U
14277	CBY1	0.40	0.044	U

14395	FAM69B	0.43	0.028	U
14414	COLQ	0.42	0.031	U
14482	C1orf129	0.56	0.003	U
14501	UBE2V1	0.46	0.019	U
14593	CDC42SE1	0.56	0.003	U
14634	PLA2G5	0.47	0.015	U
14683	RGS1	0.41	0.039	U
14684	BEX4	0.39	0.047	U
14733	PI15	0.56	0.003	U
14773	RSRC2	0.43	0.027	U
14787	CDC42SE1	0.57	0.002	U
14799	NLRP3	0.46	0.019	U
14807	PCSK6	0.48	0.014	U
14928	SIRT4	0.41	0.037	U
15020	SHOC2	0.43	0.029	U
15110	C1orf103	0.44	0.024	U
15171	OSTC	0.43	0.028	U
15419	BTG1	0.40	0.046	U
15423	GREB1	0.39	0.050	U
15451	AMIGO1	0.48	0.014	U
15498		0.44	0.023	U
15566	FBXO7	0.47	0.017	U
15599	NID1	0.47	0.014	U
15666	TMEM151A	0.52	0.006	U
15769		0.49	0.012	U
15795	DPP4	0.45	0.020	U
15878	RNMT	0.53	0.006	U
15941	CTRB1	0.56	0.003	U
16016	ARL1	0.42	0.032	U
16079	RERG	0.46	0.018	U
16086	ABHD8	0.43	0.028	U
16105	ZBTB17	0.50	0.009	U
16113	MZF1	0.43	0.027	U
16125	MFSD9	0.40	0.043	U
16180	RFT1	0.39	0.046	U
16330	KCNJ12	0.43	0.028	U
16343	NCRNA00052	0.42	0.031	U
16350	IGDCC3	0.41	0.039	U

16364	PI4KA	0.43	0.029	U
16389	KIAA1143	0.53	0.006	U
16413		0.64	0.000	U
16448	CLPS	0.47	0.015	U
16509	TSPAN11	0.50	0.009	U
16647	SALL3	0.39	0.048	U
16660	PSD3	0.41	0.039	U
16667	RPS27	0.40	0.044	U
16687	MFAP2	0.43	0.029	U
16811	HAVCR2	0.40	0.044	U
16830	NEK5	0.41	0.039	U
16834	ALOX15	0.50	0.010	U
16838	AKT3	0.40	0.044	U
16870	HPCAL4	0.42	0.033	U
17047	LSP1	0.44	0.025	U
17126	SERHL2	0.61	0.001	U
17135	PDZD9	0.52	0.007	U
17173	C14orf4	0.48	0.012	U
17244	H2AFJ	0.57	0.003	U
17319	EGFL8	0.39	0.050	U
17374	SMCR8	0.42	0.032	U
17379	CEACAM1	0.52	0.006	U
17421	C16orf78	0.57	0.002	U
17546	C6orf162	0.42	0.033	U
17575	MINA	0.67	0.000	U
17641	BACH1	0.41	0.040	U
17652	C2orf42	0.46	0.019	U
17713	ZNF580	0.44	0.025	U
17761	GPRC5D	0.44	0.023	U
17816	MLLT10	0.40	0.043	U
17823	KCNMA1	0.44	0.023	U
17913	PPP1R1C	0.49	0.012	U
17994	HIST1H1C	0.44	0.025	U
18004	IQUB	0.47	0.016	U
18012	B3GALT5	0.43	0.030	U
18227	SHOX	0.40	0.041	U
18276	VPS28	0.59	0.002	U
18288	SERHL2	0.41	0.037	U

18316	KIAA1409	0.39	0.048	U
18394	CPSF3	0.52	0.006	U
18484	TRIM24	0.39	0.050	U
18488	FBXO25	0.50	0.010	U
18492	C22orf28	0.55	0.003	U
18503	LTB4R2	0.41	0.037	U
18565	CPB2	0.51	0.008	U
18608	HIST1H2AJ	0.49	0.012	U
18625	CAMP	0.39	0.047	U
18663	ZNF643	0.44	0.023	U
18703	IZUMO1	0.50	0.010	U
18708	PAIP2	0.48	0.012	U
18823	MED13	0.51	0.008	U
18906	FGF11	0.49	0.012	U
18922	NBR2	0.58	0.002	U
18932	OR11H4	0.46	0.017	U
18948	FUZ	0.54	0.004	U
19061	SYT11	0.51	0.007	U
19078	METTL14	0.43	0.030	U
19108	MOGAT1	0.39	0.047	U
19136	SLC35C2	0.42	0.031	U
19154	TMEM130	0.41	0.040	U
19212	EGR2	0.40	0.044	U
19220	GABRG2	0.52	0.007	U
19296	HORMAD2	0.41	0.035	U
19463	HIST2H2AC	0.48	0.012	U
19489	ZNF653	0.42	0.033	U
19561	INPP5F	0.43	0.029	U
19688	STAG3L1	0.42	0.033	U
19745	PCM1	0.44	0.024	U
19766	MRPL10	0.47	0.015	U
19788	ADAMTS5	0.40	0.042	U
19836	LAIR2	0.45	0.022	U
19902	CFDP1	0.40	0.040	U
20043	DHTKD1	0.50	0.010	U
20045	DTX3	0.40	0.041	U
20058	LZTFL1	0.45	0.020	U
20071	INGX	0.44	0.025	U

20137	PKIG	0.43	0.027	U
20201	TMEM120A	0.41	0.037	U
20313	AUP1	0.41	0.035	U
20343	CRH	0.43	0.029	U
20465	ZSCAN2	0.48	0.014	U
20499	H2AFB2	0.45	0.021	U
20520	OR5H6	0.39	0.050	U
20525	SON	0.40	0.043	U
20526	FAM84A	0.43	0.028	U
20539	IMPA1	0.39	0.048	U
20708	CAV3	0.42	0.031	U
20761	SRSF5	0.40	0.044	U
20765	NEUROD4	0.50	0.009	U
20770	WBP1	0.43	0.027	U
20795	OR2F1	0.47	0.016	U
20908	HSPBAP1	0.46	0.018	U
20915	DENND4A	0.47	0.017	U
20937	CHGB	0.45	0.021	U
20950	LRRC17	0.40	0.045	U
20968	TIFA	0.43	0.029	U
20982	CAPN3	0.39	0.050	U
21018	ADAM32	0.39	0.047	U
21055	DHPS	0.58	0.002	U
21120	ZNF335	0.48	0.012	U
21147	SLC17A1	0.48	0.013	U
21163	SH3BGRL	0.44	0.023	U
21194	FAM195B	0.40	0.043	U
21224	PPAN	0.49	0.011	U
21265	ARID3A	0.56	0.003	U
21296	SNF8	0.39	0.048	U
21355	ROCK1	0.39	0.050	U
21366	SLC2A10	0.44	0.024	U
21418	C1orf114	0.41	0.038	U
21441	CAMKK2	0.46	0.017	U
21472	WSB2	0.46	0.018	U
21479	FLJ41649	0.52	0.006	U
21544	CNTFR	0.44	0.026	U
21774	MAGEB3	0.40	0.042	U

21785	ATG13	0.51	0.008	U
21908	C9orf24	0.42	0.033	U
21940	MC4R	0.49	0.010	U
22058	WAC	0.58	0.002	U
22095	CHP	0.42	0.031	U
22166	IGFBPL1	0.47	0.015	U
22355	UMODL1	0.40	0.044	U
22421	NCALD	0.51	0.008	U
22546	ATP5S	0.50	0.010	U
22603	RRAGB	0.40	0.044	U
22631	PDGFRA	0.43	0.029	U
22639	C4orf38	0.59	0.002	U
22713	OR5K2	0.49	0.010	U
22716	EFTUD1	0.52	0.007	U
22748	DOCK3	0.47	0.016	U
22771	IRF4	0.44	0.026	U
22789	FGF1	0.39	0.046	U
22907	AGL	0.42	0.032	U
22914	MLC1	0.43	0.030	U
22946	NEURL2	0.51	0.007	U
23053	CDC20B	0.41	0.036	U
23069	DDA1	0.42	0.034	U
23090	FOXD4L3	0.45	0.022	U
23138	RBMXL2	0.39	0.046	U
23183	C7orf62	0.42	0.032	U
23221	ANKHD1	0.58	0.002	U
23232	CDKL5	0.45	0.020	U
23236	PMS2CL	0.45	0.022	U
23267	TGM6	0.45	0.020	U
23513	C1QL2	0.39	0.049	U
23558	USF2	0.49	0.011	U
23570	ZNF546	0.39	0.050	U
23630	GTSF1L	0.50	0.009	U
23634	HEMGN	0.41	0.037	U
23732	SVOPL	0.39	0.046	U
23751	MLANA	0.47	0.015	U
23775	WDR88	0.47	0.015	U
23781		0.40	0.041	U

23830	PAPOLG	0.40	0.044	U
23874	YIPF3	0.49	0.011	U
23936	SNAPC3	0.46	0.017	U
23940	FAM19A2	0.50	0.010	U
23986	DQX1	0.57	0.002	U
24006	SCAMP5	0.46	0.019	U
24152	S100A7A	0.54	0.004	U
24283	C22orf15	0.46	0.018	U
24382	GAL3ST3	0.47	0.016	U
24518	ENOX1	0.41	0.039	U

APPENDIX C. 1403 GENES CORRELATE WITH SYNERGY TO PEMETREXED + CISPLATIN

Gene ID	Symbol	Synergy Correlation	Correlation P value	Up or Down regulated
602	LCK	-0.52	0.004	D
1492	KLK3	-0.41	0.032	D
5490	FBXW2	-0.43	0.021	D
8928	TFAP4	-0.38	0.047	D
10039	CFHR2	-0.46	0.014	D
14869	CDH24	-0.38	0.046	D
15865	WDR5	-0.48	0.010	D
16674	ANKZF1	-0.42	0.026	D
17110	COL18A1	-0.41	0.031	D
19520	PRPF4	-0.38	0.043	D
22267	BICD2	-0.41	0.031	D
9316	MTF2	-0.60	0.001	D
13259	DUSP11	-0.42	0.025	D
416	COL8A2	-0.43	0.023	D
6991	ATP5S	-0.50	0.007	D
7455	SAP30L	-0.38	0.047	D
8066	FRG1	-0.40	0.034	D
10103	AP1G2	-0.39	0.041	D
11966	SF3B14	-0.39	0.038	D
17546	C6orf162	-0.48	0.010	D
106	CARS	-0.39	0.038	D
243	ZBTB2	-0.55	0.002	D
415	BBS7	-0.44	0.019	D
496	HSPE1	-0.51	0.005	D
1266	RPL23	-0.54	0.003	D
1399	SEPT7	-0.59	0.001	D
1512	PTMA	-0.62	0.000	D
1661	SUMO2	-0.62	0.000	D
2254	RPS28	-0.42	0.025	D
2273	ZNF772	-0.41	0.029	D
2300	TBCB	-0.42	0.028	D
2416	MRPL48	-0.55	0.002	D

2476	PRRG3	-0.40	0.033	D
2766	RPL5	-0.52	0.005	D
2831	EXOSC10	-0.48	0.010	D
2956		-0.46	0.013	D
3024	TXNL1	-0.54	0.003	D
3140	TAF9	-0.46	0.014	D
3145	SRSF11	-0.49	0.009	D
3310	CDKN1B	-0.47	0.012	D
3683	HS2ST1	-0.52	0.005	D
4005	RPL26	-0.39	0.043	D
4481	CRHR1	-0.41	0.030	D
4563	OR52A5	-0.49	0.008	D
4566	R3HDM1	-0.51	0.005	D
4603	GLI1	-0.51	0.005	D
4858	EXOSC3	-0.39	0.041	D
5083	HNRNPC	-0.49	0.008	D
5278	C5orf34	-0.44	0.019	D
5550	MCTS1	-0.43	0.022	D
5712	GPR19	-0.68	0.000	D
5806	RBM24	-0.47	0.011	D
5881		-0.42	0.026	D
5991	PSMB7	-0.41	0.030	D
6012	PTGES3	-0.54	0.003	D
6083	PAPSS1	-0.53	0.004	D
6177	HIAT1	-0.69	0.000	D
6260	NDUFAF4	-0.47	0.012	D
6323	CCNH	-0.55	0.003	D
6530	CCDC25	-0.44	0.019	D
6912	RBBP7	-0.50	0.006	D
6917	ZFP1	-0.39	0.042	D
6977	NOL8	-0.50	0.007	D
7163	RPL14	-0.40	0.036	D
7172	FBXO40	-0.50	0.007	D
7411	RAD1	-0.46	0.014	D
7431	KRTAP10-11	-0.46	0.014	D
7643	CHD1	-0.48	0.010	D
7698	GPR55	-0.39	0.041	D
7736	H3F3A	-0.38	0.048	D

7838	RPS15A	-0.39	0.039	D
8451	C4orf43	-0.38	0.045	D
8637	RNGTT	-0.41	0.032	D
8687	FAM49B	-0.63	0.000	D
8916	RPL7	-0.68	0.000	D
9253	RPL7A	-0.44	0.018	D
9272	C20orf27	-0.46	0.015	D
10078	NCRNA00152	-0.42	0.026	D
10160	C11orf58	-0.43	0.023	D
10197	DEFB108B	-0.40	0.037	D
10595	DNAJC7	-0.38	0.044	D
10676	SREK1	-0.64	0.000	D
10736	TIMM10	-0.38	0.048	D
10962	HERPUD2	-0.42	0.024	D
11012	PRKDC	-0.41	0.030	D
11363	HCCS	-0.49	0.008	D
11656		-0.44	0.019	D
12045	LDHAL6B	-0.38	0.045	D
12750	KIF3A	-0.38	0.044	D
13055	POLR1E	-0.45	0.017	D
13130	RAB6A	-0.41	0.032	D
14068	CALB2	-0.39	0.039	D
14223	PARD3B	-0.38	0.044	D
14355	SLBP	-0.42	0.027	D
14356	PHF3	-0.58	0.001	D
14490	PRAMEF10	-0.38	0.046	D
15335	TIPRL	-0.63	0.000	D
15474	UBE2D2	-0.41	0.030	D
15559	LRRC40	-0.59	0.001	D
16216	SPATA22	-0.45	0.015	D
16591	DCAF6	-0.50	0.007	D
16743	MRPL47	-0.56	0.002	D
17057	C12orf11	-0.55	0.002	D
17062	CCT7	-0.49	0.008	D
17443	PROL1	-0.55	0.003	D
17487	RBM34	-0.40	0.037	D
18162	TRUB2	-0.59	0.001	D
18178	CDK5RAP2	-0.39	0.039	D

18334	PIP5K1B	-0.39	0.042	D
18357	G3BP1	-0.54	0.003	D
18672	UBE2CBP	-0.50	0.007	D
18962	HMGB2	-0.41	0.029	D
19111	ISCA1	-0.41	0.033	D
19153	PMS1	-0.52	0.004	D
20113	KPNA2	-0.42	0.026	D
20682	ROD1	-0.57	0.002	D
20828	KIAA0368	-0.41	0.032	D
20983	RPL9	-0.66	0.000	D
21288	LIN7C	-0.39	0.041	D
21616	PNMAL1	-0.40	0.036	D
21766	RAP1B	-0.42	0.024	D
21894	LSM5	-0.71	0.000	D
21901	TRMT11	-0.39	0.039	D
22295	PPP2CB	-0.59	0.001	D
22300	RPL13P5	-0.42	0.026	D
22470	PCNA	-0.43	0.022	D
22552	HDAC2	-0.43	0.022	D
22784	EFTUD2	-0.38	0.047	D
22910	MRPL52	-0.41	0.029	D
23417	RBBP4	-0.59	0.001	D
23659	HNRNPA1	-0.38	0.049	D
23803	CDK4	-0.55	0.002	D
23994	CETP	-0.43	0.024	D
24031	MSC	-0.45	0.017	D
24216	TMEM14B	-0.39	0.040	D
18067	KCNG2	-0.44	0.018	D
15	CD164	-0.45	0.018	D
36	UBLCP1	-0.38	0.043	D
88	RASSF4	-0.38	0.044	D
126	ARPC5	-0.43	0.023	D
150	RNF157	-0.46	0.014	D
194	TEKT5	-0.52	0.005	D
268	DDHD2	-0.43	0.022	D
269	PDE9A	-0.55	0.002	D
276	LCE1B	-0.50	0.007	D
338	URM1	-0.39	0.039	D

360	C11orf76	-0.45	0.016	D
384	ACAP2	-0.40	0.036	D
393	UPF3A	-0.43	0.021	D
419	SLC22A24	-0.38	0.048	D
426	TMEM8A	-0.49	0.008	D
503	EML4	-0.40	0.036	D
533	SYMPK	-0.50	0.007	D
555	FBXL5	-0.39	0.041	D
632	OLFML1	-0.38	0.043	D
671	MED21	-0.43	0.021	D
772	KLHL7	-0.57	0.001	D
810	POTEE	-0.46	0.014	D
893	OR11A1	-0.38	0.049	D
907	CAND1	-0.42	0.026	D
944	TCF7	-0.38	0.048	D
964	PAIP2	-0.39	0.039	D
974	MRPL3	-0.42	0.028	D
982	MYO18A	-0.43	0.022	D
993	ZNF230	-0.43	0.024	D
1006	GADL1	-0.63	0.000	D
1052	C15orf21	-0.60	0.001	D
1063	SLC25A16	-0.38	0.048	D
1157	LHFPL2	-0.40	0.033	D
1243	C9orf82	-0.46	0.013	D
1277	TSC22D1	-0.38	0.048	D
1297	HSPA4	-0.40	0.036	D
1375	GPR25	-0.40	0.033	D
1393	RAB5C	-0.38	0.045	D
1402	PBLD	-0.39	0.038	D
1429	CXCR7	-0.38	0.048	D
1476	PAK4	-0.47	0.011	D
1478	DOC2A	-0.50	0.007	D
1505	SPAST	-0.48	0.009	D
1570	CCNB1IP1	-0.50	0.007	D
1629	CNTFR	-0.40	0.034	D
1643	ANKHD1	-0.51	0.005	D
1663	CLCN3	-0.38	0.047	D
1696	PJA2	-0.39	0.038	D

1709	CDH6	-0.40	0.034	D
1714	LOC151121	-0.39	0.038	D
1840	TFEC	-0.41	0.032	D
1891	DENND1A	-0.40	0.033	D
1972	SEPT6	-0.38	0.046	D
1976	CHRAC1	-0.38	0.044	D
1986	HECA	-0.46	0.015	D
2016	USP25	-0.39	0.040	D
2043	BNIP3L	-0.42	0.024	D
2088	ARHGAP6	-0.44	0.020	D
2133	STK33	-0.47	0.011	D
2211	TBX19	-0.39	0.042	D
2237	COMMD8	-0.51	0.005	D
2256	PSMD8	-0.45	0.015	D
2303	CORO1C	-0.39	0.039	D
2314	ORM1	-0.38	0.044	D
2319	FAM47B	-0.49	0.009	D
2321	TMEM169	-0.40	0.033	D
2323	ACTN2	-0.39	0.040	D
2339	KRTAP19-6	-0.46	0.013	D
2357	PPP6C	-0.43	0.021	D
2373	C2	-0.41	0.031	D
2426	VDAC3	-0.39	0.038	D
2450	TBC1D13	-0.53	0.004	D
2560	TSPAN32	-0.43	0.022	D
2568	CCBL2	-0.38	0.049	D
2597	INPP5F	-0.38	0.048	D
2695	SEZ6L	-0.39	0.039	D
2723	FAM104A	-0.44	0.018	D
2752	IL5RA	-0.52	0.005	D
2789	CLU	-0.39	0.043	D
2835	ADAMTS10	-0.38	0.045	D
2865	SPDYE3	-0.46	0.013	D
2912	PDS5B	-0.38	0.048	D
2913	CYP2S1	-0.55	0.002	D
3076	TMEM183A	-0.38	0.045	D
3099	PRKD2	-0.51	0.006	D
3112	RPL37A	-0.45	0.017	D

3168	CYTH2	-0.46	0.015	D
3182	SLC5A7	-0.45	0.017	D
3257	C20orf112	-0.50	0.007	D
3297	GRIK2	-0.39	0.039	D
3315	PLCG1	-0.41	0.028	D
3348	RRM2B	-0.39	0.042	D
3465	FBXO17	-0.38	0.045	D
3491	MED1	-0.54	0.003	D
3497	SLC12A3	-0.40	0.037	D
3656	GPBP1	-0.62	0.000	D
3660	METTL2B	-0.46	0.013	D
3670	CEP68	-0.38	0.048	D
3678	TIAL1	-0.42	0.028	D
3694	TATDN1	-0.55	0.003	D
3745	ITM2C	-0.42	0.027	D
3751	BRIX1	-0.53	0.004	D
3889	EMILIN2	-0.45	0.017	D
3900	REXO4	-0.39	0.038	D
3923	HTR1E	-0.41	0.031	D
4012	LIPK	-0.40	0.034	D
4017	SLC26A1	-0.48	0.009	D
4047	CCL13	-0.39	0.039	D
4075	TMEM30A	-0.46	0.014	D
4081	OR1G1	-0.46	0.014	D
4327	SOX30	-0.40	0.036	D
4339	TEX11	-0.39	0.042	D
4373	RGAG4	-0.41	0.032	D
4374	TGIF2	-0.42	0.028	D
4388	HSDL2	-0.54	0.003	D
4397	KCNAB2	-0.39	0.041	D
4438	UBR5	-0.56	0.002	D
4448	CCL21	-0.42	0.028	D
4456	FGFR1OP2	-0.48	0.009	D
4459	LUC7L2	-0.41	0.029	D
4515	TAAR9	-0.56	0.002	D
4522	ZNF396	-0.39	0.038	D
4539	LRRC32	-0.42	0.028	D
4548	EFHA1	-0.41	0.030	D

4555	CSF3R	-0.42	0.024	D
4558	PDLIM1	-0.43	0.024	D
4571	CDC26	-0.52	0.005	D
4611	KAT5	-0.40	0.033	D
4623	POP4	-0.63	0.000	D
4666	RASSF3	-0.40	0.034	D
4748	BID	-0.39	0.040	D
4777	XAGE2B	-0.39	0.040	D
4824	AGL	-0.44	0.018	D
4839	IL16	-0.39	0.040	D
5031	SPRR2G	-0.48	0.010	D
5043	CFHR1	-0.38	0.045	D
5074	KCNK7	-0.43	0.022	D
5153	LRCH4	-0.40	0.035	D
5158	DYRK1B	-0.45	0.017	D
5200	TMEM67	-0.52	0.004	D
5307	ZDHHC11	-0.46	0.013	D
5358	PAIP1	-0.57	0.002	D
5359	MAP3K10	-0.43	0.024	D
5396	EPB41	-0.39	0.042	D
5402	CD3D	-0.40	0.033	D
5409	AMICA1	-0.55	0.003	D
5456	AP2A1	-0.42	0.027	D
5596	TMEM128	-0.39	0.040	D
5617	NAGS	-0.40	0.034	D
5620	TREML4	-0.39	0.042	D
5671	SKP2	-0.38	0.048	D
5741	C9orf21	-0.38	0.048	D
5794	TOMM40	-0.51	0.006	D
5808	KCNA10	-0.42	0.027	D
5843	C3orf67	-0.47	0.013	D
5879	YWHAG	-0.54	0.003	D
5883	GALR1	-0.50	0.007	D
5887	SLC17A5	-0.47	0.013	D
5920	TMEM160	-0.56	0.002	D
5942	SAMD4B	-0.42	0.027	D
5957	C14orf73	-0.48	0.010	D
5967	ALKBH4	-0.39	0.041	D

5976	PCGF6	-0.43	0.021	D
6010	HNRNPUL1	-0.50	0.007	D
6011	DDX17	-0.41	0.031	D
6017	METTL7A	-0.38	0.044	D
6024	SLC43A2	-0.46	0.015	D
6128	C4orf33	-0.41	0.030	D
6137	SLC6A5	-0.41	0.031	D
6154	MRPS12	-0.52	0.004	D
6190	KAZ	-0.42	0.027	D
6311	SERPINB9	-0.46	0.013	D
6326	XKRY	-0.46	0.013	D
6343	LIMK1	-0.41	0.029	D
6362	HOMEZ	-0.39	0.041	D
6407	TRIM10	-0.41	0.031	D
6458	XRN1	-0.44	0.020	D
6467	PAK1IP1	-0.49	0.008	D
6520	MTA2	-0.38	0.047	D
6665	TTTY14	-0.38	0.043	D
6801	ZNF451	-0.44	0.018	D
6844	TM7SF3	-0.42	0.026	D
6879	RBX1	-0.45	0.016	D
6910	TGS1	-0.41	0.028	D
7003	TAOK2	-0.44	0.018	D
7059	SRPK2	-0.71	0.000	D
7062	MLC1	-0.38	0.045	D
7079	BASP1	-0.38	0.048	D
7093	ERMN	-0.55	0.002	D
7106	HSPD1	-0.42	0.027	D
7176	TMEM199	-0.44	0.019	D
7242	BRD9	-0.43	0.023	D
7245	EDDM3B	-0.39	0.040	D
7318	TTC35	-0.58	0.001	D
7334	OVOS2	-0.43	0.023	D
7335	USP32	-0.40	0.036	D
7396	GPATCH8	-0.47	0.012	D
7425	RAD21	-0.49	0.008	D
7448	MAGI2	-0.44	0.019	D
7449	CPNE5	-0.47	0.012	D

7469	ASB16	-0.48	0.010	D
7497	VASP	-0.46	0.013	D
7582	PCDHGC3	-0.49	0.008	D
7637	GJA9	-0.44	0.020	D
7818	ISM2	-0.38	0.048	D
7840	AKAP7	-0.39	0.039	D
7865	EGR3	-0.48	0.009	D
7897	PBLD	-0.40	0.036	D
7898	NAA38	-0.47	0.012	D
7918	TSC22D2	-0.44	0.020	D
7925	FLOT2	-0.39	0.041	D
7942	DGKB	-0.38	0.048	D
7947	PSORS1C1	-0.46	0.013	D
7969	TRIM33	-0.41	0.030	D
8013	CLEC18B	-0.43	0.023	D
8034	DUS4L	-0.38	0.044	D
8042	TBPL1	-0.42	0.026	D
8075	KATNAL1	-0.40	0.035	D
8126	SORD	-0.64	0.000	D
8134	DBI	-0.48	0.010	D
8146		-0.50	0.007	D
8153	STX6	-0.42	0.025	D
8223	SSX5	-0.38	0.048	D
8224	ARRB1	-0.57	0.002	D
8243	SLC25A17	-0.38	0.044	D
8244	C14orf104	-0.61	0.001	D
8285	CAPN10	-0.56	0.002	D
8287	EIF3E	-0.45	0.016	D
8301	SIRPG	-0.49	0.009	D
8304	MRPL55	-0.57	0.002	D
8326	NUP62	-0.55	0.003	D
8384	CLASRP	-0.40	0.033	D
8389	C9orf102	-0.42	0.028	D
8497	NCL	-0.40	0.036	D
8499	C19orf2	-0.51	0.005	D
8505	POLR2K	-0.39	0.040	D
8531	SACM1L	-0.44	0.018	D
8532	SURF2	-0.38	0.045	D

8576	GNPTAB	-0.40	0.033	D
8583	NCBP1	-0.38	0.048	D
8612	SUMO1	-0.48	0.010	D
8623	ARL5A	-0.42	0.027	D
8653	SSX3	-0.43	0.024	D
8664	KSR1	-0.42	0.028	D
8718	PRMT2	-0.40	0.033	D
8722	ZNF80	-0.51	0.006	D
8741	FKBP5	-0.43	0.023	D
8750	XPA	-0.51	0.005	D
8765	RUFY4	-0.42	0.027	D
8809	SMARCE1	-0.38	0.048	D
8880	GPBP1L1	-0.47	0.012	D
8903	ITM2C	-0.42	0.024	D
8983	SPAG1	-0.40	0.036	D
8997		-0.50	0.007	D
8999	HIF1A	-0.46	0.014	D
9073	UBE2U	-0.40	0.035	D
9105	FCGR2C	-0.39	0.040	D
9116	TARS	-0.52	0.005	D
9117	UTP6	-0.47	0.011	D
9172	TTBK1	-0.43	0.023	D
9218	CALM3	-0.43	0.022	D
9247	C6orf225	-0.53	0.003	D
9269	SPPL3	-0.53	0.004	D
9271	POLR2J2	-0.40	0.036	D
9330	PSMB1	-0.38	0.044	D
9335	DCAF13	-0.52	0.004	D
9351	PHF2	-0.39	0.040	D
9367	PDE6G	-0.45	0.016	D
9370	STK38L	-0.61	0.001	D
9424	EXOSC5	-0.43	0.021	D
9473	PTK2B	-0.40	0.037	D
9582	C7orf11	-0.40	0.035	D
9654	DDHD1	-0.43	0.022	D
9677	SRPK2	-0.38	0.048	D
9694	ENY2	-0.46	0.013	D
9697	AGL	-0.46	0.013	D

9763	UNC119	-0.41	0.029	D
9779	FGFR2	-0.41	0.028	D
9788	SHMT1	-0.41	0.032	D
9805	SCRIB	-0.42	0.025	D
9836	KCNQ2	-0.40	0.035	D
9838	GLUD2	-0.40	0.034	D
9847	CELSR1	-0.45	0.016	D
9868	PABPC1	-0.54	0.003	D
9872	TAF1A	-0.43	0.021	D
9910	MFAP4	-0.39	0.041	D
9916	MYO7B	-0.38	0.046	D
9940	SIAH3	-0.43	0.021	D
9999	ABHD12B	-0.39	0.043	D
10003	FAM117B	-0.40	0.036	D
10072	RFC2	-0.38	0.048	D
10090	C15orf40	-0.40	0.034	D
10092	BRPF1	-0.37	0.049	D
10123	HYAL1	-0.42	0.028	D
10206	ZNF146	-0.42	0.026	D
10240	ZNF92	-0.45	0.016	D
10246	ARHGAP18	-0.41	0.030	D
10396	NAIP	-0.40	0.033	D
10409	CASP4	-0.41	0.031	D
10514	MRPS27	-0.48	0.010	D
10523	GRK5	-0.42	0.028	D
10670	AKAP9	-0.38	0.046	D
10681	DPYSL2	-0.41	0.030	D
10782	OR5M8	-0.38	0.049	D
10812	TIMM8A	-0.39	0.039	D
10820	RPS20	-0.43	0.023	D
10830	PAX2	-0.51	0.005	D
10841	SMC2	-0.39	0.042	D
10891	CBWD1	-0.39	0.041	D
10908	RASL11B	-0.42	0.026	D
10920	WDR3	-0.44	0.018	D
10933	KRT85	-0.38	0.047	D
11019	C2orf69	-0.45	0.016	D
11065	C13orf33	-0.46	0.015	D

11075	TLR8	-0.38	0.046	D
11125	LCE1D	-0.37	0.050	D
11160	ICK	-0.39	0.041	D
11161	SMARCD1	-0.38	0.046	D
11197	HAT1	-0.41	0.029	D
11294	ANXA4	-0.38	0.046	D
11399	NSUN2	-0.40	0.036	D
11437	CSF2RB	-0.45	0.015	D
11439	NUDT15	-0.43	0.021	D
11441	CREB3L3	-0.43	0.024	D
11446	CCDC34	-0.51	0.005	D
11480	N6AMT2	-0.42	0.026	D
11516	H2AFV	-0.39	0.042	D
11592		-0.46	0.014	D
11594	TDGF3	-0.42	0.028	D
11623	NUMBL	-0.49	0.009	D
11626	LIG4	-0.39	0.040	D
11629	TSPAN11	-0.51	0.006	D
11663	EPHA10	-0.68	0.000	D
11757	SH2B2	-0.43	0.021	D
11774	C10orf120	-0.41	0.030	D
11830	DISC1	-0.43	0.023	D
11853	AHNAK	-0.51	0.006	D
11859	C6orf211	-0.43	0.022	D
11884	ARFGEF1	-0.59	0.001	D
11897	TIAF1	-0.38	0.049	D
11921	GRM6	-0.46	0.014	D
11922	RPL18	-0.51	0.005	D
11973	ST6GALNAC6	-0.44	0.020	D
12050	OVOS2	-0.51	0.006	D
12064	NCK1	-0.38	0.046	D
12083	XPO4	-0.54	0.003	D
12094	C11orf73	-0.58	0.001	D
12160	GPR151	-0.44	0.019	D
12279	KIR2DL5A	-0.39	0.038	D
12330	MTDH	-0.41	0.032	D
12338	TMEM167A	-0.62	0.000	D
12489	EHMT2	-0.48	0.010	D

12582	DEDD2	-0.38	0.047	D
12607	SMAD7	-0.60	0.001	D
12626	E2F3	-0.47	0.012	D
12645	U2AF1	-0.48	0.010	D
12707	FAM103A1	-0.45	0.017	D
12712	PRR3	-0.48	0.010	D
12717	HEBP2	-0.38	0.045	D
12751	CTR9	-0.44	0.019	D
12765	OSBPL8	-0.51	0.006	D
12768	SGK3	-0.42	0.025	D
12802	PUS7	-0.47	0.011	D
12830	CTCFL	-0.40	0.037	D
12864	PLEKHO2	-0.48	0.009	D
12947	PGBD1	-0.40	0.034	D
12989	CD86	-0.52	0.004	D
13149	C4orf41	-0.43	0.022	D
13222	ZNRD1	-0.40	0.035	D
13294	ICK	-0.42	0.028	D
13318	DDX4	-0.38	0.049	D
13389	PCDH8	-0.53	0.004	D
13418	ITGAE	-0.41	0.030	D
13473	REG3A	-0.48	0.009	D
13506	LAIR1	-0.50	0.007	D
13599	ABL1	-0.43	0.024	D
13609	C22orf9	-0.46	0.015	D
13628	LGALS12	-0.56	0.002	D
13642	PI4K2B	-0.45	0.016	D
13674	LOC84856	-0.47	0.012	D
13695	NUP62	-0.41	0.030	D
13750	LRRC37B	-0.44	0.018	D
13779	BPI	-0.41	0.030	D
13795	CHRNA2	-0.38	0.045	D
13803	CMTM2	-0.43	0.023	D
13804	MTPN	-0.42	0.024	D
13805	ELOVL5	-0.40	0.033	D
13820	MRPL13	-0.39	0.039	D
13851	IFT122	-0.42	0.025	D
13911	TOP1MT	-0.54	0.003	D

13926	C19orf2	-0.44	0.020	D
13970	PMPCB	-0.37	0.050	D
14033	BDH2	-0.49	0.008	D
14046	SREBF1	-0.44	0.020	D
14157	SSRP1	-0.39	0.040	D
14183	EFS	-0.39	0.039	D
14326	RNF166	-0.43	0.022	D
14383	STRN4	-0.39	0.042	D
14476	ELK4	-0.38	0.045	D
14583	KCNJ10	-0.38	0.046	D
14591	DEK	-0.42	0.026	D
14611	MRPL32	-0.41	0.032	D
14667	KIF21B	-0.39	0.040	D
14674	GFRA2	-0.46	0.015	D
14744	ECE2	-0.47	0.012	D
14794	LSM2	-0.53	0.004	D
14795	UFM1	-0.39	0.042	D
14800	GSR	-0.43	0.022	D
14843	HOXD12	-0.38	0.044	D
14863	FSCN1	-0.38	0.043	D
14867	NDUFA8	-0.43	0.022	D
14871	PTTG2	-0.50	0.007	D
14877	GDA	-0.45	0.017	D
14907	EEF1G	-0.44	0.019	D
15016	WRB	-0.47	0.012	D
15070	PNMA2	-0.44	0.020	D
15091	AAMP	-0.41	0.032	D
15096	OR10G4	-0.42	0.025	D
15169	CTNNA2	-0.42	0.026	D
15204	DYRK1B	-0.39	0.041	D
15234	ZFYVE27	-0.41	0.031	D
15242	HIATL1	-0.51	0.005	D
15298	CAPZB	-0.43	0.021	D
15309	CTRC	-0.41	0.030	D
15333	SEPT4	-0.40	0.037	D
15383	NOX1	-0.44	0.020	D
15389	SARS2	-0.55	0.002	D
15403	LMX1A	-0.56	0.002	D

15436	CLTC	-0.47	0.012	D
15493	ACSM2B	-0.41	0.031	D
15517	EIF3K	-0.51	0.006	D
15575	DIS3L2	-0.51	0.005	D
15658	FAM8A1	-0.39	0.042	D
15668	ACTL6B	-0.44	0.018	D
15809	GMNN	-0.41	0.031	D
15815	MYLIP	-0.42	0.027	D
15846	PLXDC1	-0.38	0.044	D
15877	CAMK2A	-0.39	0.042	D
15910	FLJ42102	-0.49	0.008	D
15918	PAOX	-0.41	0.032	D
15948	DCD	-0.44	0.020	D
16000	FAM172A	-0.38	0.044	D
16084	LDHAL6A	-0.45	0.018	D
16088	CTBP2	-0.41	0.031	D
16095	FBL	-0.62	0.000	D
16101	MAFF	-0.38	0.043	D
16112	NKX6-2	-0.39	0.040	D
16117	SYNCRIP	-0.39	0.042	D
16155	SIRT2	-0.42	0.026	D
16202	CCHCR1	-0.43	0.022	D
16280	TCF3	-0.42	0.024	D
16293	MED23	-0.39	0.039	D
16356	HTATSF1	-0.38	0.043	D
16538	ATXN1	-0.57	0.002	D
16578	SMR3A	-0.52	0.005	D
16630	DSG4	-0.44	0.018	D
16654	HSPA4	-0.40	0.037	D
16665	PLAA	-0.42	0.026	D
16673	PPP2R3A	-0.40	0.037	D
16698	ELOVL7	-0.39	0.038	D
16713	OR6B3	-0.42	0.027	D
16757	PIPOX	-0.45	0.015	D
16785	SERF1B	-0.39	0.042	D
16803	KRT73	-0.39	0.040	D
16832	RAD1	-0.47	0.012	D
16888	PIGX	-0.39	0.040	D

16892	NR1I3	-0.44	0.020	D
17003	MYBPC2	-0.38	0.047	D
17029	COL9A1	-0.44	0.018	D
17100	HIST1H2BB	-0.45	0.015	D
17102	C22orf42	-0.46	0.014	D
17130	PRR18	-0.45	0.016	D
17134	FBXO30	-0.58	0.001	D
17203	TDRD7	-0.42	0.026	D
17262	PHF20L1	-0.39	0.039	D
17278	FAM162A	-0.41	0.029	D
17281	PSIP1	-0.42	0.025	D
17290	NAA35	-0.41	0.031	D
17296	FOXN3	-0.38	0.049	D
17310	RALGAPA2	-0.46	0.013	D
17344	ABHD15	-0.41	0.029	D
17345	ANKRD55	-0.38	0.044	D
17347	MOG	-0.42	0.026	D
17371	STRBP	-0.39	0.038	D
17376	GHRHR	-0.46	0.013	D
17383	PPP2R3B	-0.38	0.045	D
17388	CCL23	-0.39	0.042	D
17389	GALNT9	-0.42	0.028	D
17390	GNLY	-0.41	0.031	D
17422	C2orf65	-0.52	0.005	D
17431	RAB2A	-0.43	0.023	D
17499	COX7A1	-0.43	0.021	D
17527	MOV10L1	-0.51	0.005	D
17597	OR1L6	-0.46	0.014	D
17600	CMTM1	-0.41	0.029	D
17689	EED	-0.38	0.045	D
17732	HLA-C	-0.39	0.040	D
17733	CCDC132	-0.40	0.033	D
17740	GJA3	-0.40	0.036	D
17776	AATK	-0.42	0.027	D
17808	LTF	-0.38	0.049	D
17834	OTUD6B	-0.50	0.006	D
17843	CIC	-0.38	0.044	D
17846	IKZF4	-0.58	0.001	D

17854	CASP6	-0.48	0.010	D
17905	RPS11	-0.38	0.047	D
17923	RAMP2	-0.40	0.034	D
17952	C6orf120	-0.44	0.020	D
17987	ING3	-0.49	0.008	D
18059	ING1	-0.44	0.018	D
18060	ECHS1	-0.37	0.049	D
18064	ANKRD27	-0.59	0.001	D
18107	TNFRSF9	-0.45	0.016	D
18111	PRR3	-0.42	0.026	D
18143	AZU1	-0.49	0.009	D
18204	SNTA1	-0.43	0.021	D
18206	MDGA1	-0.38	0.046	D
18323	EED	-0.46	0.013	D
18350	SF1	-0.38	0.044	D
18360	CPSF4	-0.38	0.048	D
18364	TMEM183B	-0.40	0.035	D
18398	GPX1	-0.41	0.030	D
18585	GGN	-0.41	0.031	D
18592	HNRNPK	-0.55	0.002	D
18619	CDK12	-0.40	0.037	D
18641	SNRPD2	-0.51	0.005	D
18668	ABCG1	-0.41	0.032	D
18690	EFCAB2	-0.54	0.003	D
18702	FAM163B	-0.43	0.022	D
18706	C9orf9	-0.38	0.048	D
18730	IKBKAP	-0.48	0.010	D
18758	TOP1MT	-0.44	0.020	D
18768	SULT1C3	-0.40	0.033	D
18787	FBXO24	-0.63	0.000	D
18807	CYP21A2	-0.41	0.032	D
18809	NKX6-1	-0.47	0.011	D
18876	BTNL8	-0.45	0.016	D
18879	BEND4	-0.43	0.024	D
18897		-0.41	0.029	D
18907	LOH12CR1	-0.40	0.033	D
18969	SEPT4	-0.48	0.009	D
19024	PIH1D1	-0.39	0.042	D

19030	ANKRD13B	-0.45	0.015	D
19090	PDGFRB	-0.39	0.040	D
19130	KCNQ3	-0.39	0.040	D
19151	DBR1	-0.43	0.023	D
19160	IGSF10	-0.43	0.024	D
19176	PPP4R2	-0.39	0.038	D
19192	SARS	-0.40	0.034	D
19242	PPP1R14A	-0.43	0.023	D
19244	ZNF3	-0.39	0.040	D
19256	NNT	-0.48	0.010	D
19294	PPP2R4	-0.45	0.015	D
19375	TALDO1	-0.39	0.038	D
19398	CNGA3	-0.40	0.034	D
19406	ZFR	-0.53	0.004	D
19425	ABCG1	-0.38	0.047	D
19452	RPL13	-0.41	0.032	D
19513	OR1S2	-0.54	0.003	D
19521	RHOJ	-0.51	0.005	D
19550	DNAH7	-0.42	0.026	D
19695	ABLIM1	-0.58	0.001	D
19705	TOP1MT	-0.47	0.013	D
19709	PTER	-0.39	0.041	D
19725	EGLN3	-0.49	0.008	D
19741	SPRR4	-0.44	0.019	D
19751	NEDD9	-0.50	0.006	D
19805	SLC2A6	-0.38	0.049	D
19806	FAM108B1	-0.53	0.004	D
19813	GDI2	-0.46	0.014	D
19849	CUL3	-0.40	0.033	D
19869	TBX5	-0.39	0.038	D
19872	NLK	-0.48	0.010	D
19903	ZBTB3	-0.41	0.030	D
19993	PCMT1	-0.51	0.006	D
20011	PSMD11	-0.38	0.047	D
20054	RAB14	-0.38	0.046	D
20057	OR4F15	-0.40	0.035	D
20103	ITGB1BP3	-0.56	0.002	D
20148	ARL5A	-0.50	0.007	D

20197	RPL23AP64	-0.55	0.003	D
20202	PPP2R5C	-0.41	0.032	D
20230	SEMA4D	-0.42	0.026	D
20335	C17orf50	-0.45	0.017	D
20349	ARL4A	-0.41	0.030	D
20371	HRSP12	-0.52	0.005	D
20461	SULF2	-0.38	0.044	D
20504	ITPA	-0.39	0.042	D
20554	MDK	-0.45	0.015	D
20581	CWC27	-0.61	0.001	D
20785	C19orf12	-0.50	0.007	D
20805	CST11	-0.43	0.024	D
20814	PRMT1	-0.47	0.012	D
21046	CCNB1IP1	-0.49	0.009	D
21064	FKBP3	-0.50	0.007	D
21082	MRPS28	-0.38	0.046	D
21179	FAM122A	-0.42	0.025	D
21204	CHEK2	-0.38	0.043	D
21238	KLHL25	-0.41	0.032	D
21252	PRKD2	-0.47	0.011	D
21310	KLF8	-0.43	0.021	D
21349	TLR1	-0.48	0.010	D
21353	SPACA4	-0.41	0.031	D
21368	SMNDC1	-0.41	0.032	D
21372	IQGAP1	-0.40	0.036	D
21426	RBPJL	-0.42	0.027	D
21473	ARMC8	-0.52	0.004	D
21506	EPB41L1	-0.38	0.044	D
21536	HNRPLL	-0.41	0.029	D
21546	BCAT2	-0.42	0.027	D
21554	RAET1G	-0.41	0.029	D
21586	C14orf19	-0.41	0.030	D
21597	ENTPD2	-0.43	0.023	D
21611	SNX16	-0.45	0.016	D
21622	SLCO2B1	-0.40	0.035	D
21637	OR8D4	-0.43	0.022	D
21669	LPHN1	-0.39	0.038	D
21724	TCF7	-0.43	0.021	D

21734	GRXCR2	-0.42	0.027	D
21737	NAP1L1	-0.40	0.033	D
21761	RAB24	-0.38	0.044	D
21769	RAD23B	-0.40	0.037	D
21800	OR4C13	-0.41	0.029	D
21815	ARPP19	-0.56	0.002	D
21819	LPHN3	-0.45	0.016	D
21863	WDR75	-0.40	0.036	D
21898	GNA13	-0.38	0.049	D
21903	PEX5	-0.42	0.024	D
21906	CCDC97	-0.38	0.044	D
21907	PITX2	-0.48	0.010	D
21918	NRAP	-0.48	0.010	D
21920	TRIM36	-0.40	0.035	D
21930	OR51M1	-0.52	0.004	D
21949	ZNHIT3	-0.44	0.018	D
21953	UEVLD	-0.70	0.000	D
21997	DGKZ	-0.51	0.006	D
22004	INTS8	-0.48	0.011	D
22075	YY1	-0.41	0.031	D
22099	LMOD1	-0.41	0.032	D
22169	TOX4	-0.50	0.007	D
22226	CYP2S1	-0.41	0.031	D
22241	USP8	-0.42	0.025	D
22243	TLK1	-0.50	0.007	D
22265	MYL6B	-0.42	0.024	D
22314	TSSK4	-0.39	0.041	D
22379	RPL12	-0.39	0.043	D
22511	CHCHD5	-0.40	0.037	D
22574	ACTR3	-0.44	0.018	D
22697	NOP2	-0.38	0.045	D
22700	TERF1	-0.45	0.016	D
22717	ADIPOR2	-0.38	0.043	D
22727	SPIC	-0.42	0.026	D
22786	MRPS12	-0.46	0.014	D
22793	SLMO1	-0.52	0.005	D
22795	ATP11A	-0.41	0.031	D
22814	SSX3	-0.46	0.015	D

22842	FAM153C	-0.55	0.003	D
22905	SNCG	-0.44	0.018	D
22919	AMY2B	-0.43	0.023	D
22931	C9orf41	-0.39	0.040	D
22978	C1orf212	-0.50	0.007	D
22984	ZNF226	-0.38	0.048	D
23088	SPINT4	-0.41	0.029	D
23092	TUBB2B	-0.40	0.036	D
23131	PFKM	-0.48	0.010	D
23154	RTCD1	-0.38	0.048	D
23187	PMFBP1	-0.37	0.049	D
23224	CASQ1	-0.41	0.029	D
23253	C7orf49	-0.38	0.048	D
23285	LCOR	-0.40	0.036	D
23298	FOLR4	-0.47	0.011	D
23421	CUL4A	-0.42	0.025	D
23429	ABCD4	-0.49	0.009	D
23530	DDX59	-0.45	0.017	D
23547	KBTBD7	-0.47	0.011	D
23618	C6orf106	-0.41	0.032	D
23649	CLEC1A	-0.37	0.050	D
23709	SNX4	-0.47	0.011	D
23724	SGK2	-0.42	0.028	D
23729	REEP2	-0.41	0.032	D
23767	PYHIN1	-0.47	0.012	D
23776	OR2W5	-0.42	0.026	D
23796	CNBP	-0.45	0.017	D
23880	ZFAND1	-0.49	0.008	D
23902	BTN1A1	-0.42	0.025	D
23907	P2RY10	-0.44	0.019	D
23908	ZNF707	-0.39	0.039	D
23938	RABL2A	-0.53	0.004	D
24007	CLDN18	-0.38	0.049	D
24017	LOC401589	-0.38	0.047	D
24157	NKAIN4	-0.45	0.017	D
24230	KRTAP20-2	-0.40	0.036	D
24244	ITCH	-0.40	0.036	D
24248	ELMO1	-0.41	0.030	D

24270	DHFRL1	-0.42	0.024	D
24286	LOC441956	-0.57	0.001	D
24386	HTR3D	-0.44	0.019	D
24389	PABPN1	-0.50	0.007	D
24393	HIST1H2BL	-0.37	0.050	D
24394	SLC22A2	-0.40	0.036	D
24433	SLCO1A2	-0.49	0.008	D
24457	MOBKL2C	-0.40	0.034	D
566	PTER	0.38	0.047	U
5326	PRAMEF17	0.41	0.033	U
13225	TRAF3IP2	0.38	0.044	U
19409	CMTM4	0.38	0.045	U
24236	DAOA	0.41	0.030	U
1324	OR2W3	0.40	0.035	U
11418	SPATA6	0.60	0.001	U
16667	RPS27	0.38	0.049	U
19463	HIST2H2AC	0.37	0.049	U
19489	ZNF653	0.44	0.020	U
21055	DHPS	0.44	0.018	U
22748	DOCK3	0.50	0.007	U
23090	FOXD4L3	0.38	0.045	U
23183	C7orf62	0.42	0.027	U
23236	PMS2CL	0.54	0.003	U
4261	UNC93A	0.38	0.045	U
9250	CPEB3	0.45	0.016	U
13076	TMEM19	0.43	0.021	U
16703	CLCN5	0.41	0.030	U
539	GPR83	0.47	0.012	U
983	FAM134B	0.40	0.037	U
1756	KDELR3	0.40	0.034	U
2385	TMEM134	0.48	0.009	U
2590	SYTL2	0.42	0.025	U
2716	GMPPA	0.51	0.005	U
3326	C19orf10	0.53	0.004	U
3537	COPE	0.39	0.039	U
4346	ST3GAL1	0.43	0.021	U
5568	ASL	0.40	0.037	U
5714	C11orf63	0.58	0.001	U

6179	NPDC1	0.49	0.008	U
7933	XBP1	0.50	0.007	U
8805	NOMO1	0.42	0.027	U
9465	ZNF141	0.46	0.014	U
9849	TMF1	0.40	0.035	U
10487	THNSL2	0.54	0.003	U
11955	CORO1B	0.47	0.012	U
12138	UNC13A	0.48	0.010	U
12727	EDA	0.49	0.008	U
13316	SPDYA	0.42	0.027	U
14896	LGR4	0.46	0.014	U
14984	ALS2CL	0.38	0.043	U
17211	CORO1B	0.38	0.044	U
18154	XBP1	0.48	0.011	U
18231	TMEM134	0.49	0.009	U
18751	KIAA0513	0.46	0.013	U
18865	PC	0.40	0.035	U
20007	MGAT4A	0.41	0.028	U
20270	LONRF2	0.39	0.042	U
20514	FAM110C	0.51	0.005	U
22872	SLMO2	0.49	0.009	U
23810	SERINC3	0.41	0.031	U
17	OR1J2	0.49	0.009	U
63	PDIA6	0.56	0.002	U
91	OR8H2	0.39	0.040	U
112	HIST2H2BF	0.53	0.003	U
115	OGDH	0.46	0.013	U
292	LPGAT1	0.38	0.045	U
305	BOLA2	0.44	0.020	U
430	CLCNKB	0.38	0.045	U
440	CD8B	0.39	0.039	U
441	OR4C11	0.38	0.043	U
488	RABEP2	0.48	0.010	U
683	AIM2	0.43	0.021	U
700	NBPF1	0.42	0.026	U
716	ACBD5	0.41	0.032	U
724	MAN2C1	0.39	0.040	U
752	SLITRK2	0.43	0.024	U

780	ANKRD36B	0.39	0.039	U
802	GPR89B	0.44	0.018	U
854	TCEAL8	0.38	0.047	U
934	SETD3	0.38	0.044	U
1069	MUTYH	0.39	0.041	U
1183	AMPH	0.47	0.011	U
1241	KCNRG	0.38	0.048	U
1261	PDLIM5	0.63	0.000	U
1279	MTX1	0.38	0.048	U
1301	TMCO4	0.42	0.026	U
1401	ALG9	0.47	0.012	U
1451	MT2A	0.42	0.026	U
1474	PARD6A	0.46	0.014	U
1500	ROPN1B	0.45	0.017	U
1520	PRSS50	0.46	0.013	U
1564	WDR45	0.42	0.027	U
1635	RRM2	0.44	0.019	U
1669	TMEM79	0.38	0.045	U
1683	TAOK2	0.38	0.048	U
1733	PRDX5	0.39	0.038	U
1758	SOS2	0.39	0.043	U
1836	MAPK10	0.40	0.037	U
1911	ETFDH	0.45	0.016	U
1942	ACADVL	0.52	0.004	U
1991	RBPMS	0.47	0.011	U
2007	SLC10A7	0.41	0.032	U
2087	ZNF2	0.38	0.045	U
2262	MRGPRX2	0.39	0.038	U
2305	OR6C1	0.40	0.033	U
2497	FBXO15	0.42	0.025	U
2663	HGF	0.46	0.015	U
2826	USP1	0.47	0.012	U
2898	PTPRC	0.42	0.028	U
2931	DEDD	0.39	0.038	U
2994	NR1I2	0.39	0.040	U
3006	PPM1G	0.39	0.042	U
3171	DRP2	0.41	0.031	U
3177	FAM21C	0.39	0.040	U

3185	TCTN3	0.41	0.032	U
3203	IFI6	0.38	0.045	U
3291	CCL1	0.41	0.029	U
3311	COG7	0.38	0.047	U
3329	SEC61A1	0.42	0.027	U
3352	STT3B	0.50	0.006	U
3399	POLD4	0.38	0.046	U
3459	HM13	0.46	0.013	U
3486	VPS13C	0.38	0.046	U
3571	ZNF354C	0.40	0.035	U
3617	UBFD1	0.43	0.021	U
3721	C15orf48	0.40	0.034	U
3733	GPHN	0.39	0.042	U
3799	MT1G	0.39	0.040	U
3808	ADAM3A	0.46	0.014	U
3844	ACADVL	0.38	0.044	U
3879	ZCCHC13	0.52	0.005	U
3901	LCLAT1	0.40	0.037	U
3949	WDR83	0.41	0.029	U
3955	AMBN	0.37	0.050	U
4042	GNAT2	0.50	0.006	U
4071	PHKB	0.43	0.023	U
4105	PATZ1	0.39	0.040	U
4141	ACADVL	0.44	0.019	U
4150	TBC1D29	0.43	0.023	U
4320	SOBP	0.44	0.019	U
4334	SPCS1	0.40	0.037	U
4349	ANKRD23	0.39	0.041	U
4375	PMVK	0.47	0.011	U
4395	REEP1	0.40	0.034	U
4458	RPN1	0.43	0.023	U
4526	YME1L1	0.41	0.030	U
4547	AMFR	0.44	0.018	U
4557		0.38	0.043	U
4647	THSD1	0.42	0.026	U
4651	USF1	0.38	0.045	U
4720	C1orf228	0.44	0.020	U
4846	PIGF	0.52	0.005	U

4857	CSTF1	0.51	0.006	U
4870	BEX5	0.48	0.010	U
4904	ERBB2IP	0.38	0.048	U
4974	CALCA	0.43	0.021	U
5164	LARP1B	0.42	0.025	U
5181	RMI1	0.44	0.018	U
5190	UHRF1	0.41	0.030	U
5234	NBPF1	0.42	0.024	U
5248	GLYATL1	0.39	0.042	U
5325	RAG1AP1	0.58	0.001	U
5391	WDFY3	0.51	0.005	U
5453	DHPS	0.39	0.040	U
5507	MTPAP	0.39	0.042	U
5518	CKLF	0.38	0.045	U
5543	ATP6V1D	0.37	0.050	U
5611	ARPP21	0.44	0.020	U
5699	FAM98B	0.44	0.021	U
5731	ARL5B	0.46	0.013	U
5737	C18orf25	0.48	0.010	U
5752	HAO1	0.39	0.042	U
5766	KCNAB3	0.40	0.036	U
5770	TMSB15A	0.41	0.030	U
5773	LGALS13	0.44	0.020	U
5838	SMARCA2	0.40	0.036	U
5846	C15orf24	0.38	0.043	U
5928	GYS2	0.43	0.023	U
5978	POGZ	0.40	0.033	U
5984	CES3	0.40	0.035	U
6200	MS4A1	0.43	0.021	U
6215	PSMA1	0.41	0.029	U
6258	CSTL1	0.45	0.017	U
6264	AGER	0.38	0.043	U
6272	UBASH3B	0.42	0.027	U
6313	DHX32	0.40	0.033	U
6373	UNC5A	0.43	0.023	U
6461	WIPI2	0.43	0.024	U
6491	SPEF1	0.44	0.019	U
6516	MMP17	0.53	0.003	U

6546	OR4E2	0.39	0.042	U
6632	ZBTB25	0.50	0.007	U
6668	CHRM5	0.47	0.012	U
6725	KRTAP5-4	0.38	0.046	U
6753	LPAL2	0.39	0.043	U
6764	ACVR1B	0.39	0.040	U
6836	TRPC4	0.42	0.025	U
6885	IGHMBP2	0.47	0.013	U
6889	ZNF568	0.52	0.004	U
7052	PCDHA@	0.49	0.008	U
7153	SLPI	0.46	0.013	U
7387	SRFBP1	0.38	0.045	U
7399	SPINK1	0.47	0.011	U
7418	EFCAB6	0.39	0.039	U
7444	GSTO2	0.52	0.005	U
7513	PATZ1	0.43	0.023	U
7514	SLC22A8	0.38	0.048	U
7530	ECHDC2	0.40	0.036	U
7551	CASP9	0.49	0.008	U
7616	UHMK1	0.44	0.020	U
7634	KCNK10	0.42	0.024	U
7691	TYMP	0.38	0.045	U
7813	ZNF274	0.45	0.016	U
7827	TEX11	0.39	0.040	U
7899	CHORDC1	0.40	0.034	U
8003	LILRB3	0.44	0.018	U
8029	SRGAP1	0.39	0.038	U
8070	C9orf116	0.39	0.042	U
8082	SPHK1	0.39	0.041	U
8098	XDH	0.45	0.017	U
8140	ELMOD2	0.38	0.048	U
8171	SUV420H1	0.38	0.045	U
8197	PLEKHH1	0.42	0.027	U
8312	OLIG3	0.39	0.041	U
8385	OGFOD1	0.42	0.026	U
8443	C21orf58	0.40	0.037	U
8480	ATF7IP	0.38	0.044	U
8482	STT3A	0.58	0.001	U

8502	CYFIP1	0.46	0.015	U
8568	SH3GL2	0.46	0.014	U
8591	TTC8	0.45	0.017	U
8606	PRDX5	0.41	0.032	U
8617	MAPT	0.39	0.039	U
8639	CYB5D2	0.47	0.012	U
8660	PSMD4	0.39	0.040	U
8674	ANK3	0.46	0.013	U
8735	SLC35F4	0.44	0.019	U
8742	MYPN	0.44	0.021	U
8785	CD300E	0.42	0.025	U
8789	NR1D2	0.41	0.029	U
8852	LIF	0.42	0.026	U
8868	LRPAP1	0.39	0.041	U
8933	DPAGT1	0.62	0.000	U
8953	CHP2	0.43	0.021	U
9031	C1orf77	0.45	0.017	U
9058	TBC1D23	0.41	0.030	U
9099	MPDU1	0.38	0.044	U
9100	TM2D3	0.48	0.010	U
9129	MFAP3	0.39	0.042	U
9205	TRMT2B	0.42	0.026	U
9261	MTX1	0.40	0.037	U
9304	TRIP11	0.40	0.033	U
9401	FBF1	0.40	0.036	U
9499	PHYH	0.42	0.028	U
9557	DPM3	0.51	0.006	U
9567	PCBP4	0.38	0.049	U
9581	H2AFY2	0.42	0.028	U
9673	CYP27B1	0.51	0.006	U
9674	SHANK1	0.46	0.014	U
9808	ABHD2	0.38	0.043	U
9893	GINS3	0.39	0.043	U
9943	HK3	0.40	0.037	U
9956	HIPK3	0.50	0.006	U
10043	PPOX	0.41	0.028	U
10058	OPRM1	0.40	0.037	U
10105	SIL1	0.47	0.011	U

10145	ATP5J	0.38	0.043	U
10248	AGR2	0.46	0.014	U
10311	FOXJ1	0.50	0.006	U
10318	MYOF	0.47	0.012	U
10344	CDC42BPA	0.49	0.009	U
10383	BTBD7	0.41	0.031	U
10411	SYNJ2BP	0.41	0.032	U
10432	PDXDC1	0.47	0.012	U
10446	STEAP2	0.49	0.009	U
10477	FAM134B	0.40	0.035	U
10503		0.41	0.031	U
10534	FAM115C	0.45	0.018	U
10643	PPP2R5B	0.39	0.038	U
10748	PIGO	0.40	0.033	U
10766	PRDX5	0.40	0.033	U
10776	RAPH1	0.40	0.037	U
10779	DOCK5	0.44	0.018	U
10849	BANP	0.39	0.041	U
10859	GALC	0.43	0.022	U
10929	LDHD	0.38	0.048	U
11020	EIF4E3	0.42	0.027	U
11053	C9orf86	0.39	0.038	U
11102	CASC4	0.40	0.034	U
11143	CHKB	0.48	0.009	U
11172	FRAT1	0.39	0.039	U
11173	SMCR7	0.45	0.017	U
11179	TPM3	0.49	0.008	U
11187	SLC38A7	0.45	0.017	U
11240	TSPAN13	0.38	0.049	U
11245	AKD1	0.52	0.005	U
11290	ZGPAT	0.40	0.036	U
11301	C21orf119	0.43	0.023	U
11358	GALC	0.39	0.039	U
11366	CLCC1	0.38	0.048	U
11383	HBB	0.44	0.018	U
11412	RIMS2	0.39	0.040	U
11633	SLC16A7	0.41	0.030	U
11690	MPV17	0.55	0.002	U

11728	LOC441268	0.37	0.049	U
11754	PEG3	0.38	0.048	U
11777	ARFGEF2	0.40	0.033	U
11896	AKAP2	0.37	0.050	U
11906	OSBP2	0.46	0.014	U
12026	ZXDA	0.39	0.041	U
12059	VPS45	0.46	0.015	U
12063	PLEKHB2	0.42	0.025	U
12116	LRRC36	0.45	0.017	U
12183	FAM91A2	0.50	0.007	U
12184	XAGE2B	0.39	0.038	U
12241	CTBP1	0.39	0.041	U
12353	ARHGEF4	0.40	0.034	U
12391	GSC2	0.44	0.018	U
12457	RIOK1	0.43	0.022	U
12491	MFSD10	0.40	0.033	U
12543	PIGO	0.47	0.011	U
12558	NCRNA00175	0.37	0.050	U
12581	DRD2	0.46	0.013	U
12598		0.45	0.016	U
12642	ARMCX2	0.49	0.007	U
12697	NCKAP1	0.44	0.020	U
12708	DHRS7	0.39	0.042	U
12713	PDLIM5	0.55	0.002	U
12729	TNPO1	0.47	0.012	U
12734	FAM46A	0.40	0.036	U
12747	RPS27	0.50	0.007	U
12760	DEFB110	0.40	0.035	U
12965	PIP	0.47	0.011	U
13062	DNASE1L1	0.44	0.020	U
13261	PHYH	0.39	0.042	U
13295	TMED10	0.39	0.043	U
13314	FGF12	0.39	0.041	U
13349	C16orf93	0.44	0.019	U
13373	C15orf48	0.45	0.017	U
13397	C9orf23	0.41	0.032	U
13449	FGF12	0.40	0.033	U
13478	WDR20	0.49	0.008	U

13531	GK	0.41	0.031	U
13551	COPA	0.42	0.024	U
13600	APPL2	0.38	0.046	U
13601	FAM189B	0.40	0.034	U
13620	HSF4	0.44	0.019	U
13629	SLC39A9	0.51	0.006	U
13678	VPREB1	0.49	0.008	U
13760	TMEM48	0.43	0.022	U
13811	PBLD	0.43	0.023	U
13831	WDR73	0.39	0.040	U
13860	GPR155	0.44	0.021	U
13871	CRIPAK	0.41	0.032	U
13943	ARFIP1	0.40	0.035	U
13971	AADAT	0.38	0.045	U
14092	CTAG2	0.40	0.033	U
14137	BOLA1	0.43	0.024	U
14172	FGF14	0.39	0.039	U
14208	MAST4	0.40	0.036	U
14218	HAX1	0.39	0.042	U
14242	SIM2	0.38	0.047	U
14320	LAIR1	0.45	0.017	U
14332		0.53	0.004	U
14345	CDK8	0.39	0.042	U
14353	BMP2	0.44	0.020	U
14401	AOC2	0.40	0.035	U
14405	IL24	0.38	0.045	U
14443	BMPR1A	0.54	0.003	U
14452	CERKL	0.39	0.041	U
14460	PIWIL1	0.41	0.030	U
14470	C1orf58	0.45	0.017	U
14494	CYS1	0.49	0.009	U
14515	NBR1	0.45	0.015	U
14549	KDELR3	0.39	0.040	U
14613	AKTIP	0.41	0.030	U
14664	TTC13	0.40	0.034	U
14699	C15orf26	0.42	0.026	U
14703	ZNF586	0.50	0.006	U
14711	GPR171	0.44	0.019	U

14756	LMLN	0.49	0.009	U
14762	C16orf75	0.40	0.035	U
14775	ANAPC11	0.46	0.013	U
14797	TSPYL2	0.52	0.004	U
14840	MANF	0.43	0.022	U
14880	DPP3	0.49	0.009	U
14905	GEM	0.41	0.030	U
14910	SLCO4A1	0.44	0.019	U
14911	MAP2K3	0.41	0.030	U
14934	MSR1	0.39	0.042	U
14968	HERPUD1	0.46	0.013	U
15138	ANGPTL4	0.52	0.004	U
15157	AMFR	0.42	0.025	U
15316	PLSCR2	0.39	0.041	U
15445	SRSF5	0.47	0.012	U
15582	GBA	0.60	0.001	U
15629	ZNF274	0.38	0.044	U
15645	ERO1L	0.39	0.042	U
15705	RNF207	0.52	0.005	U
15761	ZMAT1	0.40	0.035	U
15764	FAM20C	0.43	0.021	U
15777	PI4KB	0.38	0.044	U
15820	GMPPB	0.39	0.041	U
15940	ENTPD8	0.38	0.044	U
15944	PSEN1	0.55	0.003	U
15947	MBTPS2	0.49	0.008	U
15953	ZRANB3	0.49	0.008	U
15974	SLC35A2	0.40	0.035	U
16033	NEK9	0.40	0.035	U
16037	FAM20C	0.43	0.024	U
16060	ORAOV1	0.38	0.047	U
16077	OR5A2	0.38	0.043	U
16118	SPO11	0.42	0.027	U
16150	DUSP8	0.47	0.011	U
16179	SLC35A2	0.37	0.049	U
16187	HSF4	0.42	0.025	U
16188	HIST2H4A	0.42	0.026	U
16220		0.41	0.031	U

16256	MMEL1	0.48	0.009	U
16258	GPS2	0.40	0.034	U
16272	ZDHHC9	0.43	0.024	U
16273	HTR4	0.38	0.045	U
16460		0.54	0.003	U
16500	TULP4	0.44	0.019	U
16545	ATP2C1	0.45	0.017	U
16557	EPS8L1	0.42	0.028	U
16590	VWA5A	0.38	0.044	U
16694	GDF15	0.39	0.043	U
16752	KRTAP13-4	0.38	0.044	U
16772	PKD1L2	0.43	0.021	U
16815	NUDT9	0.39	0.041	U
16875	RBFOX1	0.38	0.045	U
16966	PIGO	0.44	0.019	U
17060	EMR3	0.41	0.032	U
17094	SLC30A8	0.45	0.016	U
17170	TTLL1	0.37	0.049	U
17182	SLC35B1	0.41	0.031	U
17193	NBPF1	0.43	0.024	U
17219	COG1	0.45	0.016	U
17229	LCMT2	0.39	0.038	U
17241	CRLF2	0.40	0.036	U
17328	CLDN14	0.42	0.025	U
17348	ITGA2B	0.42	0.026	U
17492	RORC	0.46	0.013	U
17564	GPR108	0.38	0.049	U
17613	ATF6	0.43	0.022	U
17654	FLG2	0.41	0.029	U
17719	ADAR	0.49	0.008	U
17724	CCDC62	0.39	0.041	U
17752	ENTPD8	0.45	0.016	U
17817	TMED3	0.41	0.032	U
17869	BTNL3	0.58	0.001	U
17918	EIF2C4	0.38	0.049	U
17920	FBXO44	0.41	0.028	U
17976	ITGBL1	0.39	0.042	U
18050	MUTYH	0.38	0.047	U

18098	SLC39A1	0.51	0.005	U
18151	TK2	0.38	0.048	U
18202	IRX3	0.45	0.015	U
18340	ZNF562	0.42	0.028	U
18341	TOM1L1	0.39	0.043	U
18343	COQ2	0.44	0.018	U
18392	GRID2	0.54	0.003	U
18424	ANKRD36	0.50	0.007	U
18474	PURG	0.37	0.050	U
18522	MYST4	0.42	0.025	U
18543	CHKB	0.50	0.007	U
18582	AGAP4	0.41	0.031	U
18599	FUT6	0.40	0.035	U
18627	C2CD4B	0.38	0.046	U
18669	DOK5	0.41	0.031	U
18802	PPP2R5A	0.43	0.024	U
18828	KIAA0913	0.47	0.013	U
18980	OTOA	0.41	0.032	U
18998	KIAA1530	0.43	0.024	U
19043	ANG	0.45	0.017	U
19159	C5orf25	0.37	0.049	U
19175	PSMD4	0.48	0.010	U
19188	LPPR1	0.41	0.029	U
19191	ZDHHC13	0.41	0.030	U
19229	MOBKL2C	0.46	0.013	U
19243	SELS	0.41	0.031	U
19264	CLK2P	0.38	0.046	U
19353	PDLIM5	0.54	0.003	U
19400	COQ6	0.47	0.011	U
19421	ZNF490	0.39	0.042	U
19422	AHR	0.46	0.015	U
19453	ST3GAL1	0.47	0.011	U
19531	PHF11	0.38	0.046	U
19558	AP3D1	0.41	0.030	U
19581	C20orf46	0.40	0.034	U
19655	KRTCAP2	0.61	0.001	U
19757	NFYA	0.39	0.041	U
19758	TLL2	0.39	0.039	U

19870	TTC13	0.38	0.049	U
20006	KRTAP12-4	0.38	0.047	U
20019	ZC3H14	0.39	0.038	U
20074	MPP5	0.41	0.032	U
20098	GPHN	0.46	0.015	U
20147	DMP1	0.49	0.008	U
20164	PCK1	0.38	0.049	U
20179		0.48	0.009	U
20182	TLX2	0.40	0.036	U
20198	MAP4K3	0.49	0.008	U
20214	FAM3B	0.48	0.011	U
20232	TPM3	0.42	0.028	U
20265	USF1	0.41	0.030	U
20277	BCL6	0.41	0.030	U
20327	RCE1	0.42	0.025	U
20390	DPAGT1	0.54	0.003	U
20478	ZNF672	0.41	0.032	U
20515	TNFRSF6B	0.39	0.038	U
20927	NDEL1	0.42	0.027	U
20931	FAM134B	0.41	0.032	U
20995	VPS53	0.39	0.042	U
20998	MCOLN1	0.57	0.002	U
21008	KCNH7	0.44	0.019	U
21013	BCAP31	0.41	0.032	U
21036	FBXW7	0.44	0.019	U
21049	CTAG2	0.43	0.024	U
21132	GPATCH2	0.43	0.021	U
21214	MTMR1	0.38	0.047	U
21283	MYOF	0.42	0.027	U
21370	USP53	0.55	0.003	U
21419	OR2T3	0.39	0.042	U
21432	C17orf77	0.45	0.015	U
21470	IGSF5	0.38	0.043	U
21537	GALNTL1	0.38	0.049	U
21547	TLE2	0.42	0.028	U
21557	SIL1	0.41	0.029	U
21641	PACRG	0.41	0.031	U
21658	MIA3	0.53	0.003	U

21726	PCDHGC3	0.40	0.033	U
21757	SRD5A3	0.41	0.032	U
21811	COQ6	0.45	0.016	U
22031	TRIM15	0.49	0.008	U
22080	SYTL2	0.40	0.034	U
22103	DPP3	0.39	0.040	U
22292	CTSA	0.38	0.046	U
22497	KITLG	0.39	0.038	U
22616	GNL3	0.45	0.017	U
22622	RHBDF2	0.44	0.019	U
22635	C16orf58	0.38	0.044	U
22707	ANXA11	0.45	0.016	U
22708	THSD4	0.43	0.024	U
22719	ZSCAN10	0.39	0.043	U
22801	CRCP	0.38	0.044	U
22967	ANG	0.39	0.042	U
23037	TNKS	0.46	0.014	U
23099	XPNPEP1	0.44	0.019	U
23346	SLC12A4	0.40	0.036	U
23370	MGST3	0.38	0.044	U
23379	EXD2	0.50	0.007	U
23410	MAP2K3	0.39	0.039	U
23446	SCAMP3	0.44	0.020	U
23501	INTS3	0.59	0.001	U
23546	RBM11	0.39	0.038	U
23557	GPR37	0.55	0.002	U
23560	GNPTG	0.43	0.023	U
23577	TMEM205	0.42	0.028	U
23600	NCSTN	0.59	0.001	U
23605	MFSD8	0.44	0.020	U
23661	DPM3	0.49	0.008	U
23791	PPM1B	0.38	0.048	U
23801	MCL1	0.50	0.006	U
23947	CTTN	0.51	0.005	U
23982	PTPRH	0.56	0.002	U
24083	TMEM161B	0.41	0.032	U
24309	NPC1	0.38	0.046	U
24328	SIAH1	0.47	0.012	U

24441	NLRP12	0.41	0.031	U
24444	MUC1	0.40	0.037	U
24459	LAMB2	0.48	0.010	U

APPENDIX D. 567 GENES THAT CORRELATE WITH SYNERGISM TO GEMCITABINE + CISPLATIN AND MET REQUIREMENTS FOR CLUSTERING.

Genes are listed as they appear in signature in Figure 3.3.

Symbol	Correl	Gene ID
CARS		106
BDNF	0.846	16094
ZEB2	0.803	16478
CLGN	0.782	21921
BNC2	0.770	23023
C1S	0.453	4309
BVES	0.851	23553
BDNF	0.550	23734
BCAT1	0.691	24503
AOX1	0.635	11905
SCG2	0.647	16299
IGF2BP1	0.186	3451
KIAA0368	0.690	20828
RBM24	0.496	5806
FBN2	0.765	11312
ROBO1	0.861	11823
EYA4	0.776	22152
CDKL3	0.588	11722
TRPC1	0.866	13590
HUWE1	0.662	22769
S1PR1	0.353	886
ANK2	0.897	15618
FBXO5	0.846	18085
FLJ35409	0.782	13192
ZNF23	0.766	14196
ELOVL2	0.682	15088
WDR11	0.783	17882
PIK3C3	0.574	21488
RTN4	0.444	2637

SNX24	0.820	13710
PKIA	0.752	19058
WNK3	0.710	12742
DCAF6	0.759	16591
TMEFF2	0.328	1055
KCNT2	0.742	10217
SCN9A	0.745	12092
C7orf69	0.881	16019
RECK	0.648	11059
GNAI1	0.736	14238
ATP5I	0.032	14856
FTCD	0.651	19885
FTCD	0.946	20228
ZBTB2	0.255	243
NDUFAF4	0.739	6260
FGF5	0.802	16498
SLC39A10	0.708	19122
HS2ST1	0.669	3683
PLOD2	0.762	15206
SGCB	0.625	3892
NME7	0.839	9603
FADS3	0.739	3977
HNRPDL	0.564	8442
AMN1	0.723	22463
AMZ2	0.486	1062
FAM49B	0.839	8687
NXT2	0.802	17033
OSBPL11	0.797	18148
EIF1AX	0.693	12652
HERPUD2	0.682	10962
DUSP11	0.853	13259
ARL6IP1	0.695	19121
LSM5	0.825	21894
PHF3	0.618	14356
LIN7C	0.816	21288
MCTS1	0.685	5550
C12orf11	0.829	17057
NKAP	0.732	19670

RPL23	0.558	1266
RPL9	0.938	20983
SUMO2	0.806	1661
TXNL1	0.935	3024
G3BP1	0.878	18357
PAPSS1	0.858	6083
OR52A5	0.686	4563
CDKN1B	0.690	3310
RTN3	0.913	8084
GOPC	0.778	4581
EXOSC10	0.789	2831
SRSF11	0.877	3145
C4orf46	0.843	15427
AMMECR1L	0.809	16306
PTMA	0.501	1512
SLBP	0.748	14355
HMGB2	0.769	18962
VHL	0.633	8116
BTG3	0.802	23587
MTF2	0.720	9316
TAF9	0.606	3140
IFT74	0.866	10375
TAF9	0.846	22995
LSM6	0.721	17770
RAP1B	0.683	21766
NAA50	0.774	21818
CCNH	0.547	6323
DNM1L	0.827	12597
ANP32A	0.521	4119
MRPL47	0.837	16743
HNRNPC	0.813	5083
MAK16	0.671	9913
MRPL52	0.754	22910
CCDC25	0.638	6530
PPP2CB	0.901	22295
SNX12	0.692	19496
LAS1L	0.516	959
C20orf27	0.727	9272

MRPL48	0.509	2416
RPL7	0.778	8916
TRUB2	0.871	18162
RPL14	0.734	7163
RPL13P5	0.859	22300
POLR1E	0.840	13055
CCDC77	0.681	12347
EMG1	0.745	15869
RPL9	0.655	15192
LIAS	0.829	19045
C12orf29	0.422	516
LARP4	0.814	12243
ATP2B1	0.716	14054
GPAM	0.730	12206
PPM1D	0.762	18218
EIF1B	0.800	19430
AKAP12	0.780	22614
SLC39A6	0.542	9903
UTP15	0.743	10156
NME1	0.917	24259
FAM72D	0.625	3658
PES1	0.812	5059
SSX2IP	0.804	4810
CHAC2	0.556	9506
FAM35A	0.851	10785
CD3EAP	0.691	16853
DPH5	0.717	14374
GGH	0.377	869
RAD1	0.688	7411
RPSA	0.635	7517
UBA2	0.807	14464
UTP18	0.815	15968
RPL21	0.798	16337
CPSF6	0.277	977
RABL5	0.725	17726
ZCRB1	0.764	6474
TRMT6	0.827	13226
DICER1	0.842	17532

ARID2	0.819	23125
ZNF331	0.065	1642
SMURF2	0.679	18898
PMS1	0.756	19153
TIMM10	0.617	10736
GPT	0.676	19735
FBXO10	0.352	19824
FLCN	0.413	3582
NOVA1	0.603	11946
NOL8	0.285	6977
BHLHB9	0.690	23579
ICOSLG	0.537	18222
GABARAPL2	-0.039	118
C11orf58	0.799	10160
NME1	0.815	15024
GLI1	0.637	4603
C19orf30	0.541	16120
IL16	0.852	16596
TDP2	0.658	10716
KPNA2	0.829	20113
H3F3A	0.397	7736
NACA2	0.639	8346
ZNF385D	0.739	20781
MCFD2	0.737	20480
UCHL1	0.570	15250
ISCA1	0.563	19111
MBLAC2	0.746	23855
OR4P4	0.211	1066
HAUS1	0.808	7350
SEPT7	0.617	1399
SMC3	0.806	12961
EIF3M	0.796	3025
FSD1	0.463	4877
FSD1	0.895	23612
NUDT11	0.815	24186
DACT1	0.469	5220
DACT1	0.962	11631

LRRC4C	0.847	9705
ZNF607	0.791	23189
SLITRK5	0.689	9275
ZNF804A	0.857	15114
NETO1	0.835	11037
DNAJC18	0.529	7215
RPL14	0.706	12618
TIPRL	0.786	15335
KIF5C	0.622	8447
THBS4	0.811	19874
METTL6	0.339	6350
BMP6	0.729	22736
STC1	0.629	8898
CLIP3	-0.020	2292
CD47	0.736	20155
CEP57	0.542	23191
RBBP4	0.802	23417
EYA4	0.527	4197
EYA4	0.957	7640
SCARF2	0.628	17567
LUC7L3	0.769	18915
C18orf32	0.558	9707
ATMIN	0.654	21853
MAP1LC3A	0.584	17687
NXPH2	0.406	2836
ZFPM2	0.802	10320
XAGE1D	0.780	8662
DCN	0.721	24470
PDE1A	0.603	13679
NRXN3	0.738	21861
ITLN1	0.768	24377
MAPKAP1	0.327	298
DCP1B	0.541	12066
RNF212	0.328	7090
KDELC1	0.101	813
ITSN1	0.702	15909
LYPD6B	0.573	10511

IPO8	0.368	1514
TRIM37	0.610	15226
ODZ3	0.654	23036
MPDZ	0.627	17034
ZNF673	0.487	2932
PHLPP2	0.823	21501
KDM3A	0.613	4133
KIF18A	0.715	8005
C10orf118	0.518	24362
ASAP1	0.428	3002
RBBP7	0.836	6912
ZDHHC2	0.603	8032
PHF23	0.415	22740
USP9X	0.444	14960
RPRD1A	0.223	1035
FADS1	0.752	7725
C18orf21	0.530	1380
ZNF271	0.804	10415
HSD11B1	-0.010	280
FOXS1	0.929	11713
PCDH10	0.870	19006
FPR1	0.550	3300
VCAM1	0.864	9635
EBF1	0.498	3740
CDH4	0.338	11885
MSC	0.779	24031
PRR5L	0.635	15165
CXCL5	0.395	1790
PAPPA	0.750	2490
SPECC1	0.587	9402
C1QTNF1	0.629	19833
CETP	0.701	23994
CALB2	0.570	14068
AGTRAP	0.700	15118
AGTRAP	0.921	16316
SAA1	0.498	621
POSTN	0.789	1585

KCTD12	0.865	9551
SPRR2F	0.822	7329
PTH2R	0.801	11622
RORB	0.792	7882
FAM101A	0.819	8348
C16orf73	0.322	9363
MRFAP1L1	0.648	17413
PNMAL1	0.488	21616
LAP3	0.147	10626
C6orf58	0.526	12492
STAT1	0.691	15683
TCP1	0.418	13993
BATF3	0.464	18927
FUBP1	0.290	136
RAB12	0.717	4090
MAP3K12	0.719	16369
KIF21A	0.645	5528
MPHOSPH6	0.747	7442
SCML2	0.455	405
CLCN5	0.661	16703
POU4F1	0.764	23961
TAF1B	0.431	12762
PIGL	0.627	19625
MOSPD2	0.604	4080
ANKRD19	0.776	8093
ATP6V1C1	0.785	17858
SLC35F1	0.608	6132
AGTPBP1	0.730	7577
TPTE	0.914	17335
CDO1	0.788	15249
LIN28B	0.830	13942
TBX18	0.632	7664
TBX18	0.646	13622
TRIM58	0.742	18829
SPG7	0.173	15692
ZNF442	0.793	24285
TOP3A	0.405	12590
C12orf24	0.402	2614

TMTC4	0.722	8342
ADPRH	0.756	17809
RAB6A	0.490	13130
SNX16	0.402	3017
ZFP1	0.801	6917
SRR	0.791	11142
PRKDC	0.743	11012
LOC728643	0.824	17545
HNRNPA1	0.934	23659
ZNF286A	0.597	3453
CDK5RAP2	0.766	18178
RPL7A	0.503	9253
PFAS	0.852	12217
CNTROB	0.605	14879
DYNC2H1	0.420	13909
LONRF1	0.702	16515
LOXL3	0.616	23497
PAQR3	0.558	22644
ZNF280A	0.123	3152
CDK4	0.832	23803
MYBBP1A	0.620	20042
METTL1	0.387	6438
MAP3K15	0.542	10476
CPNE7	0.688	19727
SLC6A15	0.482	20178
KCNJ8	0.191	322
FLCN	0.680	6351
ATP5G2	0.521	10584
IGDCC4	0.627	21097
ZCCHC3	0.364	6040
NSFL1C	0.875	23645
RASSF2	0.466	6294
RASSF2	0.924	17489
SLC7A7	0.639	15844
IGFL2	0.683	15442
FXYD7	0.831	20712
CYP26A1	0.864	24132
C12orf68	0.338	15881

ID2	0.320	5485
HDGFRP3	0.261	11528
PLXDC2	0.508	18964
S100A16	0.045	550
CD99	0.738	14390
SPINT2	0.587	4166
FAM83H	0.839	4317
MGMT	0.882	21165
SFN	0.840	11808
MGST2	0.759	5152
LGALS8	0.911	20193
ATP9A	0.757	21181
ZSCAN16	0.754	8038
APOBEC3B	0.624	10291
VAMP8	0.848	19012
STXBP2	0.904	22646
NUDT16P1	0.495	3894
BDH1	0.665	17735
WNT7B	0.238	5118
UBE2H	0.718	16325
PLEK2	0.583	17014
MID2	0.408	1414
EXOC5	0.654	14095
KDELR3	0.466	1756
KDELR3	0.940	10793
AES	0.787	19771
C19orf10	0.407	3326
GGA1	0.774	20087
XBP1	0.581	7933
XBP1	0.986	18154
BACE2	0.516	4097
BACE2	0.983	7355
ST3GAL1	0.716	4346
NOMO1	0.530	8805
FAM46C	0.716	22398
FAM133A	0.573	7896
TMEM8A	0.404	984
CHPF	0.673	14109

RPS6KA2	0.813	17439
MALL	0.588	2053
KIAA0513	0.814	18751
MST1R	0.842	23206
TRIOBP	0.537	17974
PTK6	0.753	20475
STAT6	0.434	5500
BHLHE40	0.918	8794
S100A6	0.826	9435
OCIAD2	0.942	20945
MSRB2	0.829	9178
DHRS3	0.847	23008
SH3PXD2A	0.671	11555
OPLAH	0.779	16490
TSC22D3	0.795	20553
TSC22D3	0.925	20569
VEGFA	0.371	9661
STK39	0.573	10900
NAV2	0.716	14003
PC	0.645	17684
PC	0.963	18865
ARSJ	0.372	8792
ITPR3	0.706	19765
TRIOBP	0.606	16091
MPG	0.797	18372
PXMP4	0.545	3709
CDCA7L	0.705	12090
CHST15	0.822	23610
SLC16A5	0.667	22362
KIAA1217	0.402	4937
GPRC5C	0.302	3820
GPRC5C	0.971	24063
CBR3	0.797	17933
BLVRA	0.721	9684
EPDR1	0.769	20803
IER3	0.594	3917
CD109	0.755	14014
HRCT1	0.460	2997

GMPR	0.735	12253
GRAMD3	0.604	16209
SGMS2	0.324	15246
UPP1	0.597	24345
CAPN13	-0.157	1461
SYTL2	0.816	2590
LGALS3	0.642	5533
ALS2CL	0.747	14984
PAX9	0.752	20510
CD6	0.761	21695
MYO5C	0.609	6324
MB	0.752	8495
MB	0.934	16398
LGMN	0.453	4328
LGMN	0.934	14844
FUT3	0.648	3040
SAMD10	0.751	19389
MCTP2	0.514	3120
CLSTN1	0.698	16066
RPS6KA2	0.249	5061
ACP6	0.799	15357
VWA1	0.638	6964
FOXA1	0.530	2689
FAM174B	0.864	12055
TMC6	0.794	14407
C11orf75	0.515	16326
GALNT12	0.665	16123
CCDC120	0.787	20568
MYO1D	0.642	4528
THNSL2	0.813	10487
MAL2	0.826	10359
LSR	0.899	15461
ENPP4	0.586	9924
RHOD	0.851	13617
AFTPH	0.790	6862
GADD45G	0.836	17975
CRELD2	0.722	21526

TMEM62	0.534	16512
ALG1L	0.545	4804
EVPL	0.764	22290
TMEM63A	0.421	5735
PKP3	0.805	9197
PTPN6	0.462	7416
S100A14	0.750	10703
TMPRSS13	0.856	11553
STARD10	0.877	17892
PPP1R14C	0.681	17720
ANK3	0.604	4930
GPR160	0.753	24028
PPP1R13B	0.620	11217
FAM189A2	0.711	6543
GPC4	0.807	20429
KLHDC9	0.588	12428
KLHDC9	0.939	23371
EHHADH	0.508	16102
ESYT2	0.016	1641
LDLRAP1	0.613	3360
CBX7	0.788	5146
ADCK5	0.575	8177
MBIP	0.727	17437
ATL1	0.564	17728
RNF208	0.433	1627
STEAP4	0.723	1749
TMEM61	0.802	2388
XKRX	0.724	12940
AKR1A1	0.668	17836
NPDC1	0.517	6179
AGPAT2	0.641	11682
AGPAT2	0.930	12361
TRAK1	0.668	10188
TRAK1	0.839	20162
LRP5	0.678	17284
TMEM134	0.575	2385
TMEM134	0.978	18231
C11orf80	0.735	18209

NDRG1	0.381	3973
CDK2AP2	0.784	6932
LGR4	0.617	14896
TPCN2	0.578	18873
DNAJC3	0.694	22902
PARM1	0.336	4074
RNF19A	0.703	5573
RNF19A	0.869	23312
GPAA1	0.683	8127
MGAT4A	0.804	20007
DGAT1	0.699	11700
SLC45A4	0.787	23309
NRTN	0.522	17253
TLR5	0.305	2743
RTN2	0.670	11542
SUN2	0.612	8756
STAP2	0.520	8053
STAP2	0.974	17206
STAP2	0.946	19081
ARHGEF5	0.713	13528
NET1	0.405	4734
NET1	0.874	9827
NET1	0.942	19606
GSTT1	0.654	23956
TAPBP	0.377	12756
LGALS9B	0.432	4765
ANXA11	0.638	18990
C20orf54	0.570	6818
FERMT1	0.670	18856
TRIM41	0.614	13347
STX10	0.737	19960
LRRC45	0.280	5057
LRRC45	0.801	11235
RNF39	0.570	6325
ALG11	0.653	17850
ADCK2	0.401	6005
RMND5B	0.619	13707
PEX6	0.529	11295

MT1H	0.237	591
MT1F	0.760	13965
MTSS1	0.729	10325
KCNK10	0.340	7828
CUL9	0.571	21630
WDR24	0.482	8992
TMEM198	0.751	19604
FBXL16	0.724	22310
ZNF688	0.638	10498
HDAC11	0.714	24171
FAM134B	0.065	983
COPE	0.729	3537
LONRF2	0.570	20270
ATG4A	0.532	2066
TBC1D8B	0.772	20705
PTPN3	0.654	5046
PVRL1	0.301	3087
SUSD4	0.699	19189
GAD1	0.378	2794
GAD1	0.976	4805
ITPKB	0.784	15791
GAD1	0.642	12232
APOOL	0.232	14105
RAB27A	0.643	14546
ARHGEF35	-0.050	3349
GCAT	0.466	24198
RORA	0.007	3695
RREB1	0.510	13215
FAM110C	0.674	20514
C11orf63	0.532	5714
ZNF654	0.554	13358
LOC399744	0.585	18058
SLC25A24	0.160	9619
ARTN	0.400	6145
PDZD2	0.618	11806
GPR172B	0.619	24040
OR2A9P	0.213	11791

MAX	0.515	15213
ZFP64	0.478	15315
OSM	0.652	24252
SHH	0.393	1114
CAMKK2	0.589	6488
INSIG1	0.412	6055
HYOU1	0.454	1668
KIAA1147	0.669	3375
CARD14	0.482	9939
LYST	0.741	23112
ACTR3B	0.271	9248

APPENDIX E. 387 GENES THAT CORRELATE WITH SYNERGY TO PACLITAXEL + CARBOPLATIN AND MET REQUIREMENTS FOR CLUSTERING.

Genes are listed as they are clustered in Figure 3.4

Symbol	Correlation	Gene ID
PHF7		3
CLEC2B	0.736	8207
C4orf38	0.517	22639
IMPA1	0.534	20539
GPR137B	0.278	4117
NBAS	0.765	6650
HSPC159	0.567	5785
CUL7	0.654	6660
ERCC1	0.299	4882
ERCC1	0.977	12210
TGFBR3	0.709	10541
KCNMA1	0.460	17823
FAM110B	0.514	12039
RERG	0.663	16079
LAIR2	0.042	218
CACNB4	0.873	7410
LAIR2	0.708	19836
HPCAL4	0.665	16870
ARHGAP21	0.316	4239
CEACAM1	0.622	17379
RGPD1	0.488	7267
ZNF580	0.678	17713
FUZ	0.682	18948
NEURL2	0.593	22946
PDE1B	0.436	601
SGK2	0.708	2602
HAVCR2	0.812	16811
MSMP	0.634	11425

KRT23	0.487	2141
VARS2	0.670	5147
C6orf81	0.470	13941
DDT	0.041	7788
TIFA	0.677	20968
C9orf24	0.527	21908
B3GNT2	0.241	1217
DNMT3A	0.571	4344
PDE9A	0.771	5006
LTB4R2	0.884	18503
QPRT	0.414	9716
DHTKD1	0.657	20043
SNRNP35	0.591	12297
MFSD9	0.599	16125
FAM69B	0.560	14395
KISS1R	0.405	13390
ZSCAN29	-0.065	1948
C14orf101	0.488	2927
ESCO1	0.686	7625
ARHGEF1	0.773	10490
SCYL3	0.658	6596
SEPHS2	0.219	6678
POMGNT1	0.775	9710
ZNF16	0.629	2418
MTF2	0.668	9316
PHTF2	0.273	2991
C1orf103	0.691	15110
PRTFDC1	0.549	3047
ARID4A	0.523	8561
NUPL1	0.761	14084
CAMKK2	0.396	21441
ZNF643	0.481	18663
CAND2	0.293	9791
PI4KA	0.842	16364
BRWD1	0.688	13745
ROCK1	0.464	21355
DCAF6	0.536	13310
UBE2V1	0.728	14501

NID1	0.670	15599
BEX4	0.499	3742
BEX4	0.941	14684
CCR10	0.345	4760
MFAP2	0.880	16687
DLX1	0.704	4880
SYT11	0.632	19061
CDNF	0.545	5163
ATP5S	0.540	6991
ATP5S	0.762	22546
PRRX1	0.109	1890
OR51B5	0.764	10263
HBA1	0.207	8733
RGS1	0.823	14683
C6orf162	0.436	17546
FDXR	0.376	4523
CSAG1	0.549	12132
NCRNA00115	0.435	12086
PLCG1	0.212	7380
ZNF335	0.750	21120
PTPN13	0.730	9942
ZNF320	0.509	9090
TERF1	0.500	544
ARNT	0.681	7173
PIK3C3	0.774	21488
C12orf23	0.599	10642
OSTC	0.678	15171
WSB2	0.791	21472
TMEM91	0.485	12833
ZNF428	0.497	6086
TMEM120A	0.620	20201
C2orf76	0.625	12666
SHOC2	0.681	15020
ATP5L	0.616	13354
SIRT4	0.661	14928
TRIM9	0.289	1481
B4GALT6	0.865	12971
YPEL5	0.651	8919

ELMO2	0.751	10424
ABAT	0.568	4043
CCDC8	0.845	9742
SEMA5A	0.895	11068
TRIM24	0.804	18484
SVOPL	0.780	23732
EGR2	0.700	19212
SERPING1	0.769	6623
ADAM10	0.836	10119
ARID3A	0.727	21265
COL3A1	0.725	6978
IGDCC3	0.866	16350
NDNL2	0.235	1833
NFATC1	0.770	3070
CHP	0.689	22095
USF2	0.701	23558
CCK	0.521	6659
CIB2	0.783	11190
ADCY6	0.682	7226
TOM1	0.595	7802
ENOSF1	0.323	9138
TMEM151A	0.724	15666
CHGB	0.785	20937
CAMP	0.551	18625
PCMTD1	0.101	10612
BTG1	0.741	15419
SLC35C2	0.637	19136
MRPL45	0.524	11888
RNF170	0.681	13117
MAP3K12	0.568	16369
RRAGB	0.708	22603
HIST1H2BG	-0.002	1350
HIST1H3D	0.683	7129
HIST1H2BC	0.721	1462
HIST1H1C	0.937	17994
HIST1H2BE	0.898	4911
HIST2H2AA3	0.740	6090
HIST2H2AC	0.989	19463

PPP1R1C	0.646	17913
TDRKH	0.517	9599
H2AFJ	0.738	17244
ABHD8	0.648	16086
LZTFL1	0.738	20058
C14orf4	0.676	17173
PDGFRA	0.657	22631
KDM3A	-0.055	4133
LSM6	0.675	17770
SPRR2F	0.395	7329
FRG1	0.588	8066
SH3YL1	0.166	8431
DPP4	0.699	15795
SLC2A10	0.560	21366
DUSP11	0.516	13259
PLIN2	-0.113	1493
DTX3	0.652	20045
ECSIT	0.368	2928
SCAMP5	0.791	24006
DOCK3	0.718	22748
PPAN	0.562	21224
TTC21A	0.033	1865
SLC12A5	0.722	6827
HSD17B14	0.560	7284
FGF11	0.696	18906
EGFL8	0.484	17319
TTLL1	0.356	3432
HCST	0.605	5356
FAM195B	0.771	21194
GLA	-0.387	368
CDC6	0.720	1606
ACER3	0.482	3966
POLR2L	0.697	19841
SLC6A8	0.456	5990
SLC6A10P	0.948	24425
KRT6A	0.466	12190
SLC7A5	0.235	988
DHRS4	0.714	4404

FAM125B	0.624	2282
HSD17B6	0.692	13044
NCAPG2	-0.049	6283
MAP6D1	0.726	8979
ERCC6L	0.647	10942
ERCC6L	0.849	16445
ZNF484	0.652	15752
PHLDB1	0.650	16718
CDH24	0.319	14869
IL17D	0.724	21259
TYRO3	0.565	18538
TELO2	0.382	7312
ABCB6	0.721	9443
ME3	0.815	12025
RGS12	0.518	13322
GAS6	0.046	479
GAS6	0.990	14358
UNKL	0.480	24344
SLC6A15	0.459	1138
RAB11FIP5	0.393	4199
PALLD	0.692	11899
LAMP2	0.660	12591
SLC25A43	0.649	6112
CHST3	0.743	12709
MICAL2	0.391	4700
RGS20	0.765	20855
CAV2	0.733	8672
MECP2	0.501	16709
MPP1	0.709	17261
RPS6KA4	0.799	19431
S100A2	0.652	9780
ANO1	0.700	20895
TSPAN7	0.200	1464
COL4A6	0.750	21154
CES1	0.596	8911
NOVA1	0.450	8690
TSC22D1	0.700	16989
AR	0.663	6562

PORCN	0.746	21216
CNTN1	0.447	12561
FPR1	0.167	3300
C1S	0.682	23974
CD99L2	0.626	5934
CD99L2	0.952	17615
HPD	0.158	2391
NQO1	0.732	2643
NEDD9	0.409	6894
CCL2	0.478	3308
DHDPSL	0.774	22043
PTGR1	0.598	21053
SLC11A1	0.424	2645
TSKU	0.672	2711
AKR1B10	0.731	17267
HSD11B1	0.517	18431
KRT81	0.269	1339
MID1	0.780	22602
KRT86	0.763	14363
CSRP1	0.387	20645
PCID2	0.511	2462
UBA1	0.732	9570
TMOD3	0.583	7104
GCNT2	0.683	10175
TENC1	0.494	2572
ALPK2	0.935	17064
SNRPN	0.447	5767
SNRPN	0.996	8128
EFHD2	0.147	3541
CDC42EP2	0.789	19781
PRR4	0.762	16222
MYH9	0.572	5213
C15orf52	0.747	7286
MFGE8	0.551	17870
CCDC136	0.599	23169
ARAP3	0.756	23827
CD151	0.552	6220
CD151	0.809	21423

PLSCR4	0.592	13379
PLCE1	0.510	20021
PARVA	0.432	6255
MAP1B	0.581	9165
MAP1B	0.970	18157
GABRE	0.658	16764
COL18A1	0.580	17110
FHOD3	0.227	4351
C9orf25	0.648	12379
STEAP3	0.378	4370
FOSL1	0.826	22679
MAP4	0.695	7579
VCL	0.699	9587
PITX1	0.356	6542
DIAPH2	0.793	17018
LRP8	0.691	15615
DDIT4	0.440	10516
MPP6	0.280	10925
TMEM100	0.621	13438
RGP1	0.694	15762
GLDN	0.336	18673
NOL3	0.278	449
RAB20	0.579	4112
CFI	0.401	5614
FAM113B	0.794	13752
GRB10	0.692	9472
GRB10	0.977	19171
FGFRL1	0.693	14595
SULT1A3	0.320	1014
SULT1A2	0.836	20836
KRT7	0.730	12011
MOCOS	0.626	15161
COBL	0.593	1959
ADAM15	0.705	6361
ADAM15	0.972	11353
ADAM15	0.969	21115
SEPX1	0.664	4773
NCS1	0.673	23331

NINJ1	0.740	23879
SEL1L3	0.132	5021
HSD3B7	0.804	5128
HTATIP2	0.781	15346
ITPR3	0.596	19765
DYNLT3	0.870	19783
LIMCH1	0.428	5922
MYO5C	0.715	6324
ASB9	0.416	594
ASB9	0.942	14582
GALNTL4	0.702	599
NAV2	0.760	14003
ABCC3	0.337	1048
EPHX1	0.801	22532
CYB5A	0.663	7085
CYB5A	0.976	18463
G6PD	0.570	1342
G6PD	0.965	13738
GPR126	0.357	2753
ME1	0.721	11033
SDPR	0.542	20320
C9orf84	0.573	1167
STBD1	0.885	19750
IDS	0.787	11723
MYLK	0.678	23360
FBXO32	0.474	6223
TRIM47	0.499	2855
PRKAR1B	0.424	2747
COL8A1	0.654	10850
C9orf140	0.423	3234
FBXL13	0.593	7020
C1orf61	0.811	16224
GCGR	0.761	19475
PRICKLE3	0.180	2880
PRSS3	0.728	16536
PLAC1	0.598	3445
HMGB3	0.767	24274
IL7R	0.575	12149

MALL	-0.002	2053
TNFAIP2	0.764	6930
HAPLN3	0.771	16250
CHST15	0.417	23610
MSN	0.440	2440
TSPO	0.799	3967
TSPO	0.986	22452
NQO1	0.832	17427
C9orf89	0.599	16633
SLC16A9	0.192	20324
RPL39L	0.677	22540
SLC16A3	-0.015	573
LAMB3	0.682	2401
PKP3	0.710	9197
SFN	0.789	11808
ELFN2	0.464	13154
SERPINB5	0.844	20386
TMEM187	0.607	16905
C9orf95	0.388	6316
PTK6	0.699	20475
KLK3	0.251	1492
PRSS23	0.834	7194
FLNB	0.699	16897
GPC1	0.732	23385
KLF10	0.467	7227
INF2	0.772	9947
INF2	0.941	16390
TUBB3	0.709	13095
CTSZ	0.233	13915
EFEMP1	0.518	20108
EFEMP1	0.951	22515
NAAA	0.228	16732
JAG2	0.657	21481
LCK	0.317	602
MAPK9	0.867	6060
C13orf15	0.590	818
TMEM156	0.804	6540
FAM129B	0.615	10393

FAM129B	0.879	13372
ADK	0.429	10130
COMMD10	0.733	21285
TRIM6	0.450	12585
PGM2L1	0.640	23522
TRIM6	0.638	19359
SLC9A3R2	-0.190	9832
KCTD5	0.661	24088
SH3RF2	0.534	18006
PDLIM3	0.638	20398
GPX3	0.576	17664
NOXO1	0.499	1870
NOXO1	0.920	13980
PILRB	0.707	15440
BCL9L	0.697	19138
HES2	0.635	23143
C8orf34	0.348	15072

APPENDIX F. 529 GENES THAT CORRELATE WITH SYNERGY TO PEMETREXED + CISPLATIN, AND MET REQUIREMENTS FOR CLUSTERING.

Genes are listed as they are shown in the cluster in Figure 3.5

Symbol	Correlation	Gene ID
CD164		15
H3F3A	0.759	7736
ZFP1	0.695	6917
RAD1	0.753	7411
SLC43A2	0.517	6024
FLOT2	0.630	7925
MYLIP	0.519	15815
NEDD9	0.649	19751
METTL7A	0.451	6017
DCAF6	0.626	16591
MFAP4	0.598	9910
CLEC1A	0.786	23649
PDGFRB	0.706	19090
SYMPK	0.180	533
PAK4	0.721	1476
CLASRP	0.842	8384
SIRT2	0.813	16155
SAMD4B	0.554	5942
C19orf12	0.773	20785
SUMO1	0.692	8612
ZBTB2	0.435	243
TXNL1	0.728	3024
SEPT7	0.640	1399
NNT	0.796	19256
BID	0.725	4748
PTMA	0.619	1512
SMAD7	0.756	12607
ANKRD27	0.473	18064
LSM5	0.776	21894

COL8A2	0.208	416
SH2B2	0.631	11757
NLK	0.634	19872
TMEM128	0.649	5596
ARFGEF1	0.695	11884
RRM2B	0.293	3348
C7orf11	0.718	9582
CYP2S1	0.180	2913
CYP2S1	0.793	22226
PNMAL1	0.609	21616
PRKD2	0.346	3099
PRKD2	0.826	21252
VASP	0.566	7497
DEDD2	0.404	12582
LRCH4	0.452	5153
ANXA4	0.651	11294
EGLN3	0.561	19725
C6orf120	0.342	17952
ACAP2	0.230	384
MRPL47	0.808	16743
DBR1	0.599	19151
TMEM8A	0.529	426
RPL23AP64	0.912	20197
TMEM199	0.744	7176
RPL23	0.649	1266
SUMO2	0.852	1661
RPL9	0.792	20983
HNRNPA1	0.857	23659
PABPC1	0.665	9868
ZNHIT3	0.731	21949
GPBP1	0.579	3656
POLR2J2	0.817	9271
DUSP11	0.684	13259
HIF1A	0.516	8999
C4orf41	0.686	13149
EXOSC10	0.456	2831
TATDN1	0.858	3694
RPL7	0.866	8916

ZFAND1	0.903	23880
RTCD1	0.678	23154
MTF2	0.718	9316
INTS8	0.783	22004
C14orf104	0.766	8244
XPO4	0.864	12083
UFM1	0.783	14795
SACM1L	0.778	8531
CTCFL	0.822	12830
ARPP19	0.697	21815
PAK1IP1	0.571	6467
PRR3	0.830	18111
SRSF11	0.645	3145
CUL4A	0.801	23421
PRKDC	0.747	11012
ELOVL5	0.476	13805
G3BP1	0.798	18357
RAP1B	0.850	21766
ACTR3	0.613	22574
CDKN1B	0.459	3310
PAPSS1	0.811	6083
YY1	0.918	22075
FAM103A1	0.847	12707
WRB	0.720	15016
FAM8A1	0.759	15658
ATXN1	0.462	16538
FGFR1OP2	0.585	4456
TM7SF3	0.806	6844
EHMT2	0.775	12489
ZNF226	0.583	22984
SPAST	0.184	1505
TTC35	0.707	7318
FAM49B	0.797	8687
DCAF13	0.587	9335
HRSP12	0.754	20371
USP8	0.504	22241
C6orf211	0.686	11859
FAM108B1	0.746	19806

RAD21	0.545	7425
SLBP	0.782	14355
HMGB2	0.848	18962
AHNAK	0.676	11853
KBTBD7	0.798	23547
TSC22D1	0.438	1277
FBXO30	0.805	17134
CCNH	0.667	6323
ISCA1	0.706	19111
TAF9	0.673	3140
PCGF6	0.789	5976
OSBPL8	0.757	12765
NAP1L1	0.868	21737
GNA13	0.898	21898
GMNN	0.702	15809
NDUFAF4	0.640	6260
WDR3	0.781	10920
PRR3	0.459	12712
C12orf11	0.714	17057
NOP2	0.635	22697
MRPL48	0.309	2416
NUP62	0.699	8326
C11orf73	0.756	12094
EED	0.762	17689
OVOS2	0.734	12050
SARS2	0.710	15389
FBL	0.870	16095
TGS1	0.725	6910
CAPN10	0.819	8285
C1orf212	0.719	22978
RPL14	0.608	7163
GSR	0.732	14800
RPL13	0.620	19452
RPL13P5	0.881	22300
TIPRL	0.495	15335
SLMO1	0.683	22793
USP25	0.129	2016
PDS5B	0.716	2912

BNIP3L	0.450	2043
HS2ST1	0.705	3683
ATP5S	0.727	6991
TMEM169	0.274	2321
NAGS	0.661	5617
C9orf82	0.109	1243
CCBL2	0.605	2568
TGIF2	0.702	4374
HNRNPUL1	0.727	6010
CXCR7	0.076	1429
GRK5	0.542	10523
KLK3	0.378	1492
RASL11B	0.560	10908
PPP2CB	0.663	22295
TUBB2B	0.461	23092
PTK2B	0.402	9473
DPYSL2	0.687	10681
PNMA2	0.782	15070
EMILIN2	0.110	3889
PDLIM1	0.620	4558
CARS	0.154	106
SLCO1A2	0.711	24433
MCTS1	0.436	5550
SOX30	0.480	4327
LGALS12	0.491	13628
ABCG1	0.633	18668
ABCG1	0.920	19425
RNF157	0.370	150
SORD	0.740	8126
C6orf162	0.683	17546
KRTAP19-6	0.599	2339
ABCD4	0.706	23429
OR52A5	0.422	4563
RBPJL	0.647	21426
SNCG	0.507	22905
TFAP4	0.402	8928
EXOSC5	0.743	9424
CALB2	0.559	14068

SLC2A6	0.616	19805
CCNB1IP1	0.416	1570
CCNB1IP1	0.966	21046
ORM1	0.694	2314
KIF21B	0.705	14667
TNFRSF9	0.620	18107
TOP1MT	0.395	18758
TOP1MT	0.762	19705
PFKM	0.743	23131
CORO1C	0.507	2303
C9orf21	0.768	5741
KATNAL1	0.589	8075
DSG4	0.759	16630
RPL7A	0.419	9253
MRPS12	0.752	22786
CCDC34	0.483	11446
TIMM8A	0.541	10812
SURF2	0.390	8532
C20orf27	0.609	9272
BEND4	0.305	18879
PPP1R14A	0.651	19242
RAET1G	0.482	21554
FBXO17	0.361	3465
SGK3	0.656	12768
SEPT4	0.597	15333
SLCO2B1	0.611	21622
UPF3A	0.084	393
SKP2	0.725	5671
CDK5RAP2	0.542	18178
CCDC25	0.516	6530
OTUD6B	0.666	17834
NAA35	0.520	17290
HSDL2	0.527	4388
MRPL52	0.742	22910
NUDT15	0.656	11439
KPNA2	0.710	20113
SMC2	0.520	10841
PSIP1	0.761	17281

PGBD1	0.581	12947
KIAA0368	0.542	20828
TRMT11	0.706	21901
C9orf9	0.301	18706
DENND1A	0.430	1891
SRPK2	0.443	7059
PUS7	0.717	12802
TRUB2	0.696	18162
MRPS28	0.790	21082
FKBP5	0.561	8741
KAT5	-0.009	4611
AP2A1	0.564	5456
N6AMT2	0.646	11480
CETP	0.497	23994
RASSF4	0.012	88
EML4	0.547	503
COL18A1	0.629	17110
MYO18A	0.488	982
TIAF1	0.933	11897
DYRK1B	0.758	5158
DYRK1B	0.846	15204
ICK	0.473	11160
TDRD7	0.643	17203
CDH24	0.399	14869
MED21	0.399	671
HECA	0.692	1986
XRN1	0.752	6458
LHFPL2	0.434	1157
C4orf33	0.043	6128
SPAG1	0.424	8983
SRD5A3	0.179	21757
CHRAC1	-0.225	1976
ZNF707	0.634	23908
PRMT2	0.382	8718
RBBP4	0.648	23417
TIMM10	0.164	10736
PTER	0.593	19709
STK33	0.182	2133

CPSF4	0.724	18360
RABL2A	0.565	23938
TSC22D2	0.372	7918
CASP6	0.704	17854
C7orf49	0.575	23253
KCNQ3	0.470	19130
KLF8	0.684	21310
TSPAN32	-0.043	2560
SSX5	0.736	8223
CEP68	0.413	3670
GPX1	0.546	18398
GRIK2	0.465	3297
PLCG1	0.565	3315
ITM2C	-0.363	3745
ITM2C	0.967	8903
BASP1	0.487	7079
CD3D	0.273	5402
ARRB1	0.619	8224
PIGX	0.541	16888
RAMP2	0.666	17923
LIMK1	0.320	6343
ST6GALNAC6	0.503	11973
HIST2H2BF	-0.210	112
ANKRD36B	0.538	780
ANKRD36	0.871	18424
CASC4	0.651	11102
ZDHHC9	0.817	16272
UNC5A	0.347	6373
ALS2CL	0.656	14984
CTTN	0.742	23947
XDH	0.449	8098
ARHGEF4	0.391	12353
PAOX	0.132	15918
FAM134B	0.535	983
FAM134B	0.947	20931
LDHD	0.663	10929
FAM134B	0.403	10477
VPS13C	0.397	3486

GALC	0.637	10859
GALC	0.871	11358
ANG	0.783	19043
ANG	0.920	22967
PHYH	0.467	9499
PHYH	0.896	13261
HERPUD1	0.674	14968
ROPN1B	0.518	1500
SLPI	0.712	7153
GNPTG	0.719	23560
CSTF1	0.320	4857
LAMB2	0.767	24459
XBP1	0.785	7933
XBP1	0.982	18154
AGR2	0.802	10248
C2CD4B	0.824	18627
C9orf86	0.655	11053
GDF15	0.299	16694
IRX3	0.590	18202
BCL6	0.666	20277
KDELR3	0.164	1756
KDELR3	0.826	14549
SOS2	0.513	1758
LGR4	0.725	14896
PHKB	0.667	4071
NOMO1	0.510	8805
MIA3	0.732	21658
ANGPTL4	0.683	15138
SUV420H1	0.357	8171
SLC39A9	0.723	13629
LMLN	0.744	14756
ATP5J	0.410	10145
ARFIP1	0.631	13943
TAOK2	0.109	1683
ATF7IP	0.641	8480
PC	0.729	18865
SYTL2	0.145	2590
PDXDC1	0.813	10432

RNF207	0.693	15705
KITLG	0.513	22497
C16orf93	0.523	13349
CMTM4	0.718	19409
CES3	0.531	5984
HIPK3	0.524	9956
ANXA11	0.739	22707
ZMAT1	0.493	15761
ECHDC2	0.329	7530
MUC1	0.791	24444
DUSP8	0.574	16150
LONRF2	0.296	20270
COG7	0.394	3311
FRAT1	0.624	11172
ENTPD8	0.703	15940
PIP	0.568	12965
FUT6	0.699	18599
DOK5	0.625	18669
SLC35A2	0.247	16179
ZSCAN10	0.743	22719
PTPRH	0.450	23982
ST3GAL1	0.459	4346
ST3GAL1	0.762	19453
NPDC1	0.583	6179
AKAP2	0.489	11896
FAM20C	0.656	15764
FAM20C	0.821	16037
ACADVL	0.427	1942
ACADVL	0.865	4141
AHR	0.716	19422
GPHN	0.446	3733
GPATCH2	0.814	21132
GPHN	0.563	20098
WDFY3	0.604	5391
PSEN1	0.738	15944
PATZ1	0.630	7513
CHKB	0.764	11143
SYNJ2BP	0.721	10411

EXD2	0.855	23379
TMED10	0.625	13295
ANKRD23	0.166	4349
LOC441268	0.640	11728
HSF4	0.751	13620
HSF4	0.733	16187
NBPF1	0.665	5234
NBPF1	0.956	17193
CRIPAK	0.563	13871
KIAA1530	0.874	18998
LPGAT1	-0.288	292
MAST4	0.626	14208
FAM46A	0.448	12734
DNASE1L1	0.558	13062
ABHD2	0.608	9808
CRLF2	0.656	17241
C9orf23	0.526	13397
MBTPS2	0.624	15947
PARD6A	0.193	1474
HIST2H2AC	0.755	19463
UHMK1	0.642	7616
FGF12	0.709	13314
RIMS2	0.517	11412
FBXO15	0.183	2497
C21orf119	0.736	11301
LRPAP1	0.624	8868
FAM110C	0.688	20514
THNSL2	0.383	10487
ZDHHC13	0.655	19191
THSD4	0.518	22708
PIGO	0.212	10748
TMEM205	0.764	23577
PIGO	0.530	16966
DOCK3	0.586	22748
TMEM134	0.367	2385
TMEM134	0.981	18231
C1orf228	0.755	4720
DPP3	0.495	14880

RCE1	0.752	20327
IFI6	0.592	3203
CORO1B	0.699	11955
FOXJ1	0.648	10311
MGST3	0.804	23370
ZNF586	0.659	14703
POLD4	0.262	3399
GSTO2	0.628	7444
TCEAL8	0.072	854
ARFGEF2	0.702	11777
BEX5	0.151	4870
EIF4E3	0.692	11020
TMSB15A	0.525	5770
NR1D2	0.517	8789
RBPMS	0.246	1991
KIAA0513	0.623	18751
C20orf46	0.600	19581
CYB5D2	0.559	8639
SYTL2	0.670	22080
GPR37	0.716	23557
SPINK1	0.422	7399
VWA5A	0.632	16590
ELMOD2	0.404	8140
ARMCX2	0.669	12642
CTSA	0.438	22292
TSPAN13	0.463	11240
TLE2	0.818	21547
EPS8L1	0.707	16557
MGAT4A	0.693	20007
C1orf58	-0.039	14470
IGSF5	0.634	21470
ERO1L	0.534	15645
RBM11	0.522	23546
OGDH	0.177	115
LIF	0.627	8852
SLCO4A1	0.723	14910
TK2	0.436	18151
FAM21C	0.466	3177

ZC3H14	0.582	20019
VPS53	0.585	20995
PBLD	0.318	13811
AMPH	0.420	1183
MAP2K3	0.583	23410
SRGAP1	0.363	8029
USP53	0.614	21370
MYPN	0.289	8742
IL24	0.688	14405
MSC	0.861	24031
GK	0.542	13531
SIM2	0.739	14242
C15orf48	0.252	3721
C15orf48	0.960	13373
GEM	0.421	14905
C11orf63	0.432	5714
MCOLN1	0.663	20998
UBASH3B	0.700	6272
SPHK1	0.706	8082
PPP2R5B	0.408	10643
MYOF	0.382	21283
CDC42BPA	0.504	10344
C5orf25	0.724	19159
CLCC1	0.406	11366
TCTN3	0.285	3185
OSBP2	0.617	11906
TYMP	0.482	7691
NPC1	0.623	24309
TOM1L1	0.595	18341
TNFRSF6B	0.388	20515
GPR89B	0.165	802
DPM3	0.632	9557
DPM3	0.945	23661
CASP9	0.451	7551
DPAGT1	0.708	8933
C9orf116	0.225	8070
HIST2H4A	0.657	16188
FAM91A2	0.636	12183

TMEM79	0.274	1669
C16orf75	0.609	14762
ARL5B	0.388	5731
SH3GL2	0.308	8568
RAPH1	0.789	10776
FAM3B	0.672	20214
MUTYH	0.075	1069
PMVK	0.601	4375
MAPT	0.741	8617
BOLA1	0.724	14137
HAX1	0.692	14218
RAG1AP1	0.610	5325
FAM189B	0.476	13601
COQ2	0.621	18343
PLEKHH1	0.093	8197
CYP27B1	0.647	9673
MT2A	0.583	1451
MT1G	0.728	3799
BMP2	0.548	14353
SETD3	0.169	934
CDK8	0.622	14345
RRM2	0.497	1635
TMEM48	0.743	13760
PPM1G	0.443	3006
UHRF1	0.639	5190
PDLIM5	0.483	12713
PDLIM5	0.770	19353
FSCN1	0.559	14863
GDA	0.808	14877
REEP1	-0.447	4395
GALNTL1	0.669	21537
H2AFY2	0.570	9581
DOCK5	0.502	10779
CTAG2	0.579	14092
CTAG2	0.945	21049
POGZ	0.249	5978
ZBTB25	0.600	6632
TRIP11	0.723	9304

TTC8	0.705	8591
KIAA0913	0.472	18828
SLC38A7	0.571	11187
CLCN5	0.610	16703
FGF12	0.309	13449
GNL3	0.670	22616

BIBLIOGRAPHY

Ahmedin, J., Rebecca, S., Jiaquan, X., & Elizabeth, W. (2010). Cancer Statistics, 2010. *CA A Cancer Journal for Clinicians*.

Amann, J., Kalyankrishna, S., Massion, P. P., Ohm, J. E., Girard, L., Shigematsu, H., . . . Carbone, D. P. (2005). Aberrant epidermal growth factor receptor signaling and enhanced sensitivity to EGFR inhibitors in lung cancer. *Cancer Res, 65*(1), 226-235.

Arriagada, R., Bergman, B., Dunant, A., Le Chevalier, T., Pignon, J., & Vansteenkiste, J. (2004). International Adjuvant Lung Cancer Trial Collaborative Group: Cisplatin-based adjuvant chemotherapy in patients with completely resected non-small-cell lung cancer. *N Engl J Med, 350*, 351 - 360.

Awasthi, N., Kirane, A., Schwarz, M., Toombs, J., Brekken, R., & Schwarz, R. (2011). Smac mimetic-derived augmentation of chemotherapeutic response in experimental pancreatic cancer. *BMC Cancer, 11*(1), 15.

Bai, L., Chen, W., Chen, W., Wang, X., Tang, H., & Lin, Y. (2009). IKKÎ²-mediated nuclear factor-ÎºB activation attenuates smac mimeticâ€“induced apoptosis in cancer cells. *Molecular Cancer Therapeutics, 8*(6), 1636-1645. doi: 10.1158/1535-7163.mct-09-0068

Baker, S. J., Markowitz, S., Fearon, E. R., Willson, J. K. V., & Vogelstein, B. (1990). Suppression of human colorectal carcinoma cell growth by wild-type p53. *Science, 249*(4971), 912-915.

Bank, A., Wang, P., Du, C., Yu, J., & Zhang, L. (2008). SMAC mimetics sensitize nonsteroidal anti-inflammatory drug-induced apoptosis by promoting caspase-3-mediated cytochrome c release. *Cancer Res, 68*(1), 276-284. doi: 68/1/276 [pii]
10.1158/0008-5472.CAN-07-5242

Benedettini, E., Sholl, L. M., Peyton, M., Reilly, J., Ware, C., Davis, L., . . . Loda, M. (2010). Met activation in non-small cell lung cancer is associated with de novo resistance to EGFR inhibitors and the development of brain metastasis. *The American Journal of Pathology, 177*(1), 415-423.

Beran, M., Cao, X., Estrov, Z., Jeha, S., Jin, G., O'Brien, S., . . . Kantarjian, H. (1998). Selective inhibition of cell proliferation and BCR-ABL phosphorylation in acute lymphoblastic leukemia cells expressing Mr 190,000 BCR-ABL protein by a tyrosine kinase inhibitor (CGP-57148). *Clin Cancer Res, 4*(7), 1661-1672.

Besse, B., & Le Chevalier, T. (2008). Adjuvant Chemotherapy for Non-Small-Cell Lung Cancer: A Fading Effect? *J Clin Oncol, 26*(31), 5014-5017. doi: 10.1200/jco.2008.18.1081

Bockbrader, K. M., Tan, M., & Sun, Y. (2005). A small molecule Smac-mimic compound induces apoptosis and sensitizes TRAIL- and etoposide-induced apoptosis in breast cancer cells. *Oncogene, 24*(49), 7381 - 7388.

Bonfil, R. D., Russo, D. M., Binda, M. M., Delgado, F. M., & Vincenti, M. (2002). Higher antitumor activity of vinflunine than vinorelbine against an orthotopic murine model of transitional cell carcinoma of the bladder. *Urologic Oncology, 7*(4), 159-166. doi: S1078143902001849 [pii]

Bos, J. L. (1989). ras Oncogenes in Human Cancer: A Review. *Cancer Research, 49*(17), 4682-4689.

Bourdon, J. C., Fernandes, K., Murray-Zmijewski, F., Liu, G., Diot, A., Xirodimas, D. P., . . . Lane, D. P. (2005). p53 isoforms can regulate p53 transcriptional activity. *Genes Dev, 19*(18), 2122-2137.

Boyce, M., & Yuan, J. (2006). Cellular response to endoplasmic reticulum stress: a matter of life or death. *Cell Death & Differentiation, 13*(3), 363-373. doi: 4401817 [pii]

10.1038/sj.cdd.4401817

Brose, M. S., Volpe, P., Feldman, M., Kumar, M., Rishi, I., Gerrero, R., . . . Weber, B. L. (2002). BRAF and RAS mutations in human lung cancer and melanoma. *Cancer Research, 62*(23), 6997-7000.

Brunton, L. L., Lazo, J. S., & Parker, K. L. (2006). *Goodman & Gilman's The Pharmacological Basis of Therapeutics* (Eleventh ed.). New York City, New York: McGraw - Hill Medical Publishing Division.

Buchdunger, E., Zimmermann, J., Mett, H., Meyer, T., Muller, M., Druker, B. J., & Lydon, N. B. (1996). Inhibition of the Abl Protein-Tyrosine Kinase in Vitro and in Vivo by a 2-Phenylaminopyrimidine Derivative. *Cancer Res, 56*(1), 100-104.

Carbone, D. P., & Minna, J. D. (1995). Chemotherapy for non-small cell lung cancer. *BMJ (Clinical research ed), 311*(7010), 889-890.

Cardenal, F., López-Cabrerizo, M. P., Antón, A., Alberola, V., Massuti, B., Carrato, A., . . . Rosell, R. (1999). Randomized Phase III Study of Gemcitabine-Cisplatin Versus Etoposide-Cisplatin in the Treatment of Locally Advanced or Metastatic Non–Small-Cell Lung Cancer. *Journal of Clinical Oncology, 17*(1), 12.

Cardenas, V. M., Thun, M. J., Austin, H., Lally, C. A., Clark, W. S., Greenberg, R. S., & Heath, C. W. (1997). Environmental tobacco smoke and lung cancer mortality in the American Cancer Society's Cancer Prevention Study II. *Cancer Causes and Control, 8*(1), 57-64. doi: 10.1023/a:1018483121625

Chabner, B. A., & Roberts, T. G. (2005). Chemotherapy and the war on cancer. [10.1038/nrc1529]. *Nat Rev Cancer, 5*(1), 65-72.

Checinska, A., Hoogeland, B., Rodriguez, J., Giaccone, G., & Kruyt, F. (2007). Role of XIAP in inhibiting cisplatin-induced caspase activation in non-small cell lung cancer cells: a small molecule Smac mimic sensitizes for chemotherapy-induced apoptosis by enhancing caspase-3 activation. *Exp Cell Res, 313*(6), 1215 - 1224.

Cheung, H. H., Lynn Kelly, N., Liston, P., & Korneluk, R. G. (2006). Involvement of caspase-2 and caspase-9 in endoplasmic reticulum stress-induced apoptosis: A role for the IAPs. *Experimental Cell Research, 312*(12), 2347-2357.

Chou, T. C.-., & Rideout, D. C. (1991) *Synergism and antagonism in chemotherapy* (pp. 61-102). San Deigo: Academic Press.

Chung, K. Y., Shia, J., Kemeny, N. E., Shah, M., Schwartz, G. K., Tse, A., . . . Saltz, L. B. (2005). Cetuximab Shows Activity in Colorectal Cancer Patients With Tumors That Do Not Express the Epidermal Growth Factor Receptor by Immunohistochemistry. *J Clin Oncol, 23*(9), 1803-1810. doi: 10.1200/jco.2005.08.037

Clarke, S., Abratt, R., Goedhals, L., Boyer, M., Millward, M., & Ackland, S. (2002). Phase II trial of Pemetrexed disodium (PEMETREXED, LY231514) in chemotherapy-naive patients with advanced non-small-cell lung cancer. *Ann Oncol, 13*, 737 - 741.

Danial, N. N., & Korsmeyer, S. J. (2004). Cell Death: Critical Control Points. *Cell, 116*(2), 205-219.

Davidson, B. L., & McCray, P. B. (2011). Current prospects for RNA interference-based therapies. [10.1038/nrg2968]. *Nat Rev Genet, 12*(5), 329-340.

Dean, E. J., Ward, T., Pinilla, C., Houghten, R., Welsh, K., Makin, G., . . . Dive, C. (2009). A small molecule inhibitor of XIAP induces apoptosis and synergises with vinorelbine and cisplatin in NSCLC. *British Journal of Cancer*.

Diamandopoulus, G. (1996). Cancer: An historical perspective. *Anticancer Res, 16*, 1595– 1602.

Dienstmann, R., Martinez, P., & Felip, E. (2011). *Personalizing Therapy with Targeted Agents in Non-Small Cell Lung Cancer* (Vol. 2).

Dineen, S. P., Roland, C. L., Greer, R., Carbon, J. G., Toombs, J. E., Gupta, P., . . . Brekken, R. A. (2010). Smac Mimetic Increases Chemotherapy Response and Improves Survival in Mice with Pancreatic Cancer. *Cancer Research, 70*(7), 2852-2861. doi: 10.1158/0008-5472.can-09-3892

Ding, L., Getz, G., Wheeler, D. A., Mardis, E. R., McLellan, M. D., Cibulskis, K., . . . Wilson, R. K. (2008). Somatic mutations affect key pathways in lung adenocarcinoma. [10.1038/nature07423]. *Nature, 455*(7216), 1069-1075. doi: http://www.nature.com/nature/journal/v455/n7216/suppinfo/nature07423_S1.html

Dittmer, D., Pati, S., Zambetti, G., Chu, S., Teresky, A. K., Moore, M., . . . Levine, A. J. (1993). Gain of Function Mutations in p53. *Nature Genetics, 4*(1), 42-45.

Druker, B. J., & Lydon, N. B. (2000). Lessons learned from the development of an Abl tyrosine kinase inhibitor for chronic myelogenous leukemia. *The Journal of Clinical Investigation, 105*(1), 3-7.

Du, C., Fang, M., Li, Y., Li, L., & Wang, X. (2000). Smac, a mitochondrial protein that promotes cytochrome c-dependent caspase activation by eliminating IAP inhibition. *Cell, 102*(1), 33 - 42.

Eckelman, B. P., & Salvesen, G. S. (2006). The Human Anti-apoptotic Proteins cIAP1 and cIAP2 Bind but Do Not Inhibit Caspases. *Journal of Biological Chemistry, 281*(6), 3254-3260. doi: 10.1074/jbc.M510863200

Ettinger, D. S. (2002). Is There a Preferred Combination Chemotherapy Regimen for Metastastic Non-Small Cell Lung Cancer? *The oncologist, 7*(3), 226-233. doi: 10.1634/theoncologist.7-3-226

Euhus, D., Hudd, C., LaRegina, M., & Johnson, F. (1986). Tumor measurement in the nude mouse. *J Surg Oncol, 31*, 229 - 234.

Fesik, S. W. (2005). Promoting apoptosis as a strategy for cancer drug discovery. *Nat Rev Cancer, 5*(11), 876-885. doi: nrc1736 [pii]
10.1038/nrc1736

Fischer, H., Koenig, U., Eckhart, L., & Tschachler, E. (2002). Human caspase 12 has acquired deleterious mutations. *Biochem Biophys Res Commun, 293*(2), 722-726. doi: 10.1016/S0006-291X(02)00289-9
S0006-291X(02)00289-9 [pii]
Flygare, J. A., & Fairbrother, W. J. (2010). Small-molecule pan-IAP antagonists: a patent review. *Expert Opinion on Therapeutic Patents, 20*(2), 251-267. doi: doi:10.1517/13543770903567077
Forgacs, E., Biesterveld, E. J., Sekido, Y., Fong, K., Muneer, S., Wistuba, I. I., . . . Minna, J. D. (1998). Mutation analysis of the PTEN/MMAC1 gene in lung cancer. *Oncogene, 17*(12), 1557-1565.
Gaither, A., Porter, D., Yao, Y., Borawski, J., Yang, G., Donovan, J., . . . Zawel, L. (2007). A Smac mimetic rescue screen reveals roles for inhibitor of apoptosis proteins in tumor necrosis factor-alpha signaling. *Cancer Res, 67*(24), 11493-11498. doi: 67/24/11493 [pii]
10.1158/0008-5472.CAN-07-5173
Gandhi, J., Zhang, J., Xie, Y., Soh, J., Shigematsu, H., Zhang, W., . . . Gazdar, A. F. (2009). Alterations in genes of the EGFR signaling pathway and their relationship to EGFR tyrosine kinase inhibitor sensitivity in lung cancer cell lines. *PLoS One, 4*(2), e4576.
Gao, Y., Ge, G., & Ji, H. (2011). LKB1 in lung cancerigenesis: a serine/threonine kinase as tumor suppressor. *Protein & Cell, 2*(2), 99-107. doi: 10.1007/s13238-011-1021-6
Gazdar, A. F., Gao, B., & Minna, J. D. (2010). Lung cancer cell lines: Useless artifacts or invaluable tools for medical science? *Lung cancer (Amsterdam, Netherlands), 68*(3), 309-318.
Gazdar, A. F., Girard, L., Lockwood, W. W., Lam, W. L., & Minna, J. D. (2010). Lung cancer cell lines as tools for biomedical discovery and research. *Journal of the National Cancer Institute, 102*(17), 1310-1321.
Gazdar, A. F., Kurvari, V., Virmani, A., Gollahon, L., Sakaguchi, M., Westerfield, M., . . . Shay, J. W. (1998). Characterization of paired tumor and non-tumor cell lines established from patients with breast cancer. *International Journal of Cancer, 78*(6), 766-774.
Gelderblom, H., Verweij, J., Nooter, K., & Sparreboom, A. (2001). Cremophor EL: the drawbacks and advantages of vehicle selection for drug formulation. *European Journal of Cancer, 37*(13), 1590-1598. doi: Doi: 10.1016/s0959-8049(01)00171-x
Gerber, D. E., & Minna, J. D. (2010). ALK inhibition for non-small cell lung cancer: from discovery to therapy in record time. *Cancer Cell, 18*(6), 548-551.
Goffin, J., Lacchetti, C., Ellis, P. M., Ung, Y. C., & Evans, W. K. (2010). First-Line Systemic Chemotherapy in the Treatment of Advanced Non-small Cell Lung Cancer: A Systematic Review. *Journal of thoracic oncology : official publication of the International Association for the Study of Lung Cancer, 5*(2), 260-274.
Goyette, M. C., Cho, K., Fasching, C. L., Levy, D. B., Kinzler, K. W., Paraskeva, C., . . . Stanbridge, E. J. (1992). Progression of colorectal cancer is associated with multiple tumor suppressor gene defects but inhibition of tumorigenicity is

accomplished by correction of any single defect via chromosome transfer. *Molecular and cellular biology*, *12*(3), 1387-1395.
Greene, F. L. (2004). TNM: Our Language of Cancer. *CA: A Cancer Journal for Clinicians*, *54*(3), 129-130. doi: 10.3322/canjclin.54.3.129
Hanahan, D., & Weinberg, Robert A. (2011). Hallmarks of Cancer: The Next Generation. *Cell*, *144*(5), 646-674. doi: 10.1016/j.cell.2011.02.013
Hecht, S. S. (1999). Tobacco Smoke Carcinogens and Lung Cancer. *Journal of the National Cancer Institute*, *91*(14), 1194-1210. doi: 10.1093/jnci/91.14.1194
Heinemann, V., Quietzsch, D., Gieseler, F., Gonnermann, M., Schonekas, H., Rost, A., . . . Heinrich, B. (2006). Randomized phase III trial of gemcitabine plus cisplatin compared with gemcitabine alone in advanced pancreatic cancer. *J Clin Oncol*, *24*(24), 3946 - 3952.
Hitomi, J., Katayama, T., Eguchi, Y., Kudo, T., Taniguchi, M., Koyama, Y., . . . Tohyama, M. (2004). Involvement of caspase-4 in endoplasmic reticulum stress-induced apoptosis and Aβ-induced cell death. *The Journal of Cell Biology*, *165*(3), 347-356. doi: 10.1083/jcb.200310015
Holcik, M., Gibson, H., & Korneluk, R. G. (2001). XIAP: apoptotic brake and promising therapeutic target. *Apoptosis*, *6*(4), 253 - 261.
Huarte, M., Guttman, M., Feldser, D., Garber, M., Koziol, M. J., Kenzelmann-Broz, D., . . . Rinn, J. L. (2010). A Large Intergenic Noncoding RNA Induced by p53 Mediates Global Gene Repression in the p53 Response. *Cell*, *142*(3), 409-419. doi: 10.1016/j.cell.2010.06.040
Identification and analysis of functional elements in 1% of the human genome by the ENCODE pilot project. (2007). [10.1038/nature05874]. *Nature*, *447*(7146), 799-816.
doi: http://www.nature.com/nature/journal/v447/n7146/suppinfo/nature05874_S1.html
Ihde, D. C., Cohen, M. H., Simms, E. B., Matthews, M. J., Bunn, P. A., & Minna, J. D. (1980). Evaluation of response to chemotherapy with fiberoptic bronchoscopy in non-small cell lung cancer. *Cancer*, *45*(7), 1693-1696.
Ihde, D. C., & Minna, J. D. (1991a). Non-small cell lung cancer. Part I: Biology, diagnosis, and staging. *Current problems in cancer*, *15*(2), 61-104.
Ihde, D. C., & Minna, J. D. (1991b). Non-small cell lung cancer. Part II: Treatment. *Current problems in cancer*, *15*(3), 105-154.
Janowski, B. A., Huffman, K. E., Schwartz, J. C., Ram, R., Hardy, D., Shames, D. S., . . . Corey, D. R. (2005). Inhibiting gene expression at transcription start sites in chromosomal DNA with antigene RNAs. *Nat Chem Biol*, *1*(4), 216-222.
Janowski, B. A., Huffman, K. E., Schwartz, J. C., Ram, R., Nordsell, R., Shames, D. S., . . . Corey, D. R. (2006). Involvement of AGO1 and AGO2 in mammalian transcriptional silencing. *Nat Struct Mol Biol*, *13*(9), 787-792. doi: nsmb1140 [pii]
10.1038/nsmb1140
Jemal, A., Siegel, R., Ward, E., Hao, Y., Xu, J., & Thun, M. (2009). Cancer statistics, 2009. *CA Cancer J Clin*, *59*(4), 225 - 249.

Karpozilos, A., & Pavlidis, N. (2004). The treatment of cancer in Greek antiquity. *European Journal of Cancer, 40*(14), 2033-2040.
Kerr, J. F., Wyllie, A. H., & Currie, A. R. (1972). Apoptosis: a basic biological phenomenon with wide-ranging implications in tissue kinetics. *Br J Cancer, 26*(4), 239-257.
Kieser, A. (2008). Pursuing different 'TRADDes': TRADD signaling induced by TNF-receptor 1 and the Epstein-Barr virus oncoprotein LMP1. *Biological Chemistry, 389*(10), 1261-1271. doi: 10.1515/bc.2008.144
Kimura, S., Ashihara, E., & Maekawa, T. (2010). New Tyrosine Kinase Inhibitors in the Treatment of Chronic Myeloid Leukemia. *Current Pharmaceutical Biotechnology, 7*(5), 371-379.
Kosmidis, P. (2002). Chemotherapy in NSCLC: historical review. *Lung Cancer, 38*(Supplement 3), 19-22. doi: Doi: 10.1016/s0169-5002(02)00261-1
Kostyal, D., Welt, R., Danko, J., Shay, T., Lanning, C., Horton, K., & Welt, S. (2011). Trastuzumab and lapatinib modulation of HER2 tyrosine/threonine phosphorylation and cell signaling. *Medical Oncology*, 1-9. doi: 10.1007/s12032-011-0025-7
Kreuter, M., Vansteenkiste, J., Griesinger, F., Hoffmann, H., Dienemann, H., De Leyn, P., & Thomas, M. (2007). Trial on Refinement of Early stage non-small cell lung cancer. Adjuvant chemotherapy with pemetrexed and cisplatin versus vinorelbine and cisplatin: The TREAT protocol. *BMC Cancer, 7*(1), 77.
Kuai, J., Nickbarg, E., Wooters, J., Qiu, Y., Wang, J., & Lin, L. L. (2003). Endogenous association of TRAF2, TRAF3, cIAP1, and Smac with lymphotoxin beta receptor reveals a novel mechanism of apoptosis. *J Biol Chem, 278*(16), 14363 - 14369.
Kuehbacher, A., Urbich, C., Zeiher, A. M., & Dimmeler, S. (2007). Role of Dicer and Drosha for Endothelial MicroRNA Expression and Angiogenesis. *Circ Res, 101*(1), 59-68. doi: 10.1161/circresaha.107.153916
LaCasse, E., Mahoney, D., Cheung, H., Plenchette, S., Baird, S., & Korneluk, R. (2008). IAP-targeted therapies for cancer. *Oncogene, 27*(48), 6252 - 6275.
Lamb, P., & Crawford, L. (1986). Characterization of the human p53 gene. *Mol. Cell. Biol., 6*(5), 1379-1385. doi: 10.1128/mcb.6.5.1379
Lavrik, I. N., & Krammer, P. H. (2009). Life and Death Decisions in the CD95 System: Main Pro-and Anti-Apoptotic Modulators. *Acta Naturae*
Lecis, D., Drago, C., Manzoni, L., Seneci, P., Scolastico, C., Mastrangelo, E., . . . Delia, D. (2010). Novel SMAC-mimetics synergistically stimulate melanoma cell death in combination with TRAIL and Bortezomib. *Br J Cancer, 102*(12), 1707-1716. doi: http://www.nature.com/bjc/journal/v102/n12/suppinfo/6605687s1.html
Leveque, D., & Jehl, F. (1996). Clinical pharmacokinetics of vinorelbine. *Clinical Pharmacokinetics, 31*(3), 184-197.
Li, J., Lee, B., & Lee, A. S. (2006). Endoplasmic reticulum stress-induced apoptosis: multiple pathways and activation of p53-up-regulated modulator of apoptosis (PUMA) and NOXA by p53. *J Biol Chem, 281*(11), 7260-7270. doi: M509868200 [pii]
10.1074/jbc.M509868200

Li, L., Thomas, R. M., Suzuki, H., De Brabander, J. K., Wang, X., & Harran, P. G. (2004). A Small Molecule Smac Mimic Potentiates TRAIL- and TNF[alpha]-Mediated Cell Death. *Science, 305*(5689), 1471-1474. doi: 10.1126/science.1098231

Li, P., Nijhawan, D., & Wang, X. (2004). Mitochondrial activation of apoptosis. *Cell, 116*(Supplement 2), S57-S61.

Liu, X., Sempere, L. F., Guo, Y., Korc, M., Kauppinen, S., Freemantle, S. J., & Dmitrovsky, E. (2011). Involvement of microRNAs in lung cancer biology and therapy. *Translational Research, 157*(4), 200-208. doi: 10.1016/j.trsl.2011.01.001

Liu, Z., Sun, C., Olejniczak, E. T., Meadows, R. P., Betz, S. F., Oost, T., . . . Fesik, S. W. (2000). Structural basis for binding of Smac/DIABLO to the XIAP BIR3 domain. *Nature, 408*(6815), 1004 - 1008.

Livak, K. J., & Schmittgen, T. D. (2001). Analysis of Relative Gene Expression Data Using Real-Time Quantitative PCR and the 2-[Delta][Delta]CT Method. *Methods, 25*(4), 402-408. doi: DOI: 10.1006/meth.2001.1262

Lowe, S., & Lin, A. (2000). Apoptosis in cancer. *Carcinogenesis, 21*(3), 485 - 495.

Lowe, S. W., Cepero, E., & Evan, G. (2004). Intrinsic tumour suppression. *Nature, 432*(7015), 307-315. doi: nature03098 [pii]
10.1038/nature03098

Lowery, A., & Han, Z. (2011). Assessment of tumor response to tyrosine kinase inhibitors. *Frontiers in Bioscience, 16*, 1996-2007. doi: http://dx.doi.org/10.2741/3836

. Lung. (2010). In S. B. Edge, D. R. Byrd & C. C. Compton (Eds.), *AJCC Cancer Staging Manual* (Vol. 7th edition, pp. 253-270). New York: Springer.

Mahmoudi, S., Henriksson, S., Corcoran, M., Mendez-Vidal, C., Wiman, K. G., & Farnebo, M. (2009). Wrap53, a natural p53 antisense transcript required for p53 induction upon DNA damage. *Mol Cell, 33*(4), 462-471. doi: S1097-2765(09)00073-2 [pii]
10.1016/j.molcel.2009.01.028

Manegold, C., Gatzemeier, U., von Pawel, J., Pirker, R., Malayeri, R., Blatter, J., & Krejcy, K. (2000). Front-line treatment of advanced non-small cell lung cancer with MTA and Cisplatin: a multicenter phase II trial. *Ann Oncol, 11*, 435 - 440.

Marciniak, S. J., & Ron, D. (2006). Endoplasmic Reticulum Stress Signaling in Disease. *Physiological Reviews, 86*(4), 1133-1149. doi: 10.1152/physrev.00015.2006

McAuliffe, G., Roberts, L., & Roberts, S. (2002). Paclitaxel administration and its effects on clinically relevant human cancer and non cancer cell lines. *Biotechnology Letters, 24*(12), 959-964. doi: 10.1023/a:1015629406774

McDermott, U., Iafrate, A. J., Gray, N. S., Shioda, T., Classon, M., Maheswaran, S., . . . Settleman, J. (2008). Genomic Alterations of Anaplastic Lymphoma Kinase May Sensitize Tumors to Anaplastic Lymphoma Kinase Inhibitors. *Cancer Res, 68*(9), 3389-3395. doi: 10.1158/0008-5472.can-07-6186

Minna, J. D., Fong, K., Zochbauer-Muller, S., & Gazdar, A. F. (2002). Molecular pathogenesis of lung cancer and potential translational applications. *Cancer journal (Sudbury, Mass), 8 Suppl 1*, S41-46.

Mitsudomi, T., Oyama, T., Gazdar, A. F., Minna, J. D., Okabayashi, K., & Shirakusa, T. (1992). [Mutations of ras and p53 genes in human non-small cell lung cancer cell lines and their clinical significance]. *Nihon Geka Gakkai zasshi, 93*(9), 944-947.

Mitsudomi, T., Steinberg, S. M., Nau, M. M., Carbone, D., D'Amico, D., Bodner, S., . . . et al. (1992). p53 gene mutations in non-small-cell lung cancer cell lines and their correlation with the presence of ras mutations and clinical features. *Oncogene, 7*(1), 171-180.

Moenner, M., Pluquet, O., Bouchecareilh, M., & Chevet, E. (2007). Integrated endoplasmic reticulum stress responses in cancer. *Cancer Res, 67*(22), 10631-10634. doi: 67/22/10631 [pii]

10.1158/0008-5472.CAN-07-1705

Nachmias, B., Ashhab, Y., & Ben-Yehuda, D. (2004). The inhibitor of apoptosis protein family (IAPs): an emerging therapeutic target in cancer. *Semin Cancer Biol, 14*(4), 231 - 243.

Non-small Cell Lung Cancer Collaborative, G. (1995). Chemotherapy in non-small cell lung cancer: a meta-analysis using updated data on individual patients from 52 randomised clinical trials. *BMJ, 311*(7010), 899-909.

O'Hare, T., Shakespeare, W. C., Zhu, X., Eide, C. A., Rivera, V. M., Wang, F., . . . Clackson, T. (2009). AP24534, a Pan-BCR-ABL Inhibitor for Chronic Myeloid Leukemia, Potently Inhibits the T315I Mutant and Overcomes Mutation-Based Resistance. *Cancer Cell, 16*(5), 401-412. doi: 10.1016/j.ccr.2009.09.028

Olivier, M., Eeles, R., Hollstein, M., Khan, M. A., Harris, C. C., & Hainaut, P. (2002). The IARC TP53 database: New online mutation analysis and recommendations to users. *Human mutation, 19*(6), 607-614. doi: 10.1002/humu.10081

Oltersdorf, T., Elmore, S., Shoemaker, A., Armstrong, R., Augeri, D., Belli, B., . . . Hajduk, P. (2005). An inhibitor of Bcl-2 family proteins induces regression of solid tumours. *Nature, 435*(7042), 677 - 681.

Oost, T. K., Sun, C., Armstrong, R. C., Al-Assaad, A.-S., Betz, S. F., Deckwerth, T. L., . . . Fesik, S. W. (2004). Discovery of Potent Antagonists of the Antiapoptotic Protein XIAP for the Treatment of Cancer. *Journal of Medicinal Chemistry, 47*(18), 4417-4426. doi: 10.1021/jm040037k

Owens, J. (2007). Determining druggability. [10.1038/nrd2275]. *Nat Rev Drug Discov, 6*(3), 187-187.

Pallis, A., Briasoulis, E., Linardou, H., Papadimitriou, C., Bafaloukos, D., Kosmidis, P., & Murray, S. (2011). Mechanisms of resistance to epidermal growth factor receptor tyrosine kinase inhibitors in patients with advanced non-small-cell lung cancer: clinical and molecular considerations. *Curr Med Chem, 18*(11), 1613-1628. doi: BSP/CMC/E-Pub/2011/ 108 [pii]

Pao, W., Miller, V., Zakowski, M., Doherty, J., Politi, K., Sarkaria, I., . . . Varmus, H. (2004). EGF receptor gene mutations are common in lung cancers from “never smokers” and are associated with sensitivity of tumors to gefitinib and erlotinib. *Proceedings of the National Academy of Sciences of the United States of America, 101*(36), 13306-13311. doi: 10.1073/pnas.0405220101

Park, S.-J., Wu, C.-H., Gordon, J. D., Zhong, X., Emami, A., & Safa, A. R. (2004). Taxol Induces Caspase-10-dependent Apoptosis. *J. Biol. Chem., 279*(49), 51057-51067. doi: 10.1074/jbc.M406543200

Parkin, D. M., Bray, F., Ferlay, J., & Pisani, P. (2005). Global Cancer Statistics, 2002. *CA: A Cancer Journal for Clinicians, 55*(2), 74-108. doi: 10.3322/canjclin.55.2.74

Pass, H. I., Carbone, D. P., Johnson, D. H., Minna, J. D., Scagliotti, G. V., & Turrisi, A. T. (2010). *Principles and Practice of Lung Cancer*: Lippincott Williams & Wilkins.

Pass, H. I., Pogrebniak, H. W., Steinberg, S. M., Mulshine, J., & Minna, J. (1992). Randomized trial of neoadjuvant therapy for lung cancer: interim analysis. *The Annals of thoracic surgery, 53*(6), 992-998.

Pei-Chun Liao, S.-K. T. C.-H. L. H.-K. J. (2008). Involvement of endoplasmic reticulum in paclitaxel-induced apoptosis. *Journal of Cellular Biochemistry, 104*(4), 1509-1523.

Petersen, S. L., Wang, L., Yalcin-Chin, A., Li, L., Peyton, M., Minna, J., . . . Wang, X. (2007). Autocrine TNF[alpha] Signaling Renders Human Cancer Cells Susceptible to Smac-Mimetic-Induced Apoptosis. *Cancer Cell, 12*(5), 445-456.

Phelps, R. M., Johnson, B. E., Ihde, D. C., Gazdar, A. F., Carbone, D. P., McClintock, P. R., . . . Mulshine, J. L. (1996). NCI-Navy Medical Oncology Branch cell line data base. *J Cell Biochem Suppl, 24*, 32-91.

Pietras, K., & Hanahan, D. (2005). A Multitargeted, Metronomic, and Maximum-Tolerated Dose "Chemo-Switch" Regimen is Antiangiogenic, Producing Objective Responses and Survival Benefit in a Mouse Model of Cancer. *J Clin Oncol, 23*(5), 939-952. doi: 10.1200/jco.2005.07.093

Printz, C. (2010). BATTLE to personalize lung cancer treatment. *Cancer, 116*(14), 3307-3308. doi: 10.1002/cncr.25493

Probst, B. L., Liu, L., Ramesh, V., Li, L., Sun, H., Minna, J. D., & Wang, L. (2010). Smac mimetics increase cancer cell response to chemotherapeutics in a TNF-alpha-dependent manner. *Cell Death & Differentiation*. doi: cdd201044 [pii]
10.1038/cdd.2010.44

Ramirez, R. D., Sheridan, S., Girard, L., Sato, M., Kim, Y., Pollack, J., . . . Minna, J. D. (2004). Immortalization of human bronchial epithelial cells in the absence of viral oncoproteins. *Cancer Research, 64*(24), 9027-9034.

Richter, B. W., & Duckett, C. S. (2000). The IAP proteins: caspase inhibitors and beyond. *Science Signaling, 2000*(44), 1-4. doi: 10.1126/stke.2000.44.pe1
2000/44/pe1 [pii]

Rohaly, G., Chemnitz, J., Dehde, S., Nunez, A. M., Heukeshoven, J., Deppert, W., & Dornreiter, I. (2005). A Novel Human p53 Isoform Is an Essential Element of the ATR-Intra-S Phase Checkpoint. *Cell, 122*(1), 21-32. doi: 10.1016/j.cell.2005.04.032

Rowinsky, E. K., Jiroutek, M., Bonomi, P., Johnson, D., & Baker, S. D. (1999). Paclitaxel Steady-State Plasma Concentration as a Determinant of Disease Outcome and Toxicity in Lung Cancer Patients Treated with Paclitaxel and Cisplatin. *Clinical Cancer Research, 5*(4), 767-774.

Rudin, C. M., Avila-Tang, E., Harris, C. C., Herman, J. G., Hirsch, F. R., Pao, W., . . . Samet, J. M. (2009). Lung Cancer in Never Smokers: Molecular Profiles and Therapeutic Implications. *Clinical Cancer Research, 15*(18), 5646-5661. doi: 10.1158/1078-0432.ccr-09-0377

Sabbatini, P., Korenchuk, S., Rowand, J. L., Groy, A., Liu, Q., Leperi, D., . . . Kumar, R. (2009). GSK1838705A inhibits the insulin-like growth factor-1 receptor and anaplastic lymphoma kinase and shows antitumor activity in experimental models of human cancers. *Molecular Cancer Therapeutics, 8*(10), 2811-2820. doi: 10.1158/1535-7163.mct-09-0423

Salvesen, G. S., & Duckett, C. S. (2002). IAP proteins: blocking the road to death's door. *Nature Reviews Molecular Cell Biology, 3*(6), 401-410. doi: 10.1038/nrm830
nrm830 [pii]

Samuel, T., Welsh, K., Lober, T., Togo, S. H., Zapata, J. M., & Reed, J. C. (2006). Distinct BIR domains of cIAP1 mediate binding to and ubiquitination of tumor necrosis factor receptor-associated factor 2 and second mitochondrial activator of caspases. *J Biol Chem, 281*(2), 1080-1090. doi: M509381200 [pii]
10.1074/jbc.M509381200

Sato, M., Vaughan, M. B., Girard, L., Peyton, M., Lee, W., Shames, D. S., . . . Minna, J. D. (2006). Multiple Oncogenic Changes (K-RASV12, p53 Knockdown, Mutant EGFRs, p16 Bypass, Telomerase) Are Not Sufficient to Confer a Full Malignant Phenotype on Human Bronchial Epithelial Cells. *Cancer Res, 66*(4), 2116-2128. doi: 10.1158/0008-5472.can-05-2521

Scheffler, M., Di Gion, P., Doroshyenko, O., Wolf, J., & Fuhr, U. (2011). Clinical Pharmacokinetics of Tyrosine Kinase Inhibitors: Focus on 4-Anilinoquinazolines. *Clinical Pharmacokinetics, 50*(6), 371-403 310.2165/11587020-000000000-000000000.

Schimmer, A. D., Welsh, K., Pinilla, C., Wang, Z., Krajewska, M., Bonneau, M. J., . . . Reed, J. C. (2004). Small-molecule antagonists of apoptosis suppressor XIAP exhibit broad antitumor activity. *Cancer Cell, 5*(1), 25 - 35.

Schwartz, J. C., Younger, S. T., Nguyen, N. B., Hardy, D. B., Monia, B. P., Corey, D. R., & Janowski, B. A. (2008). Antisense transcripts are targets for activating small RNAs. *Nat Struct Mol Biol, 15*(8), 842-848. doi: nsmb.1444 [pii]
10.1038/nsmb.1444

Servida, F., Lecis, D., Scavullo, C., Drago, C., Seneci, P., Carlo-Stella, C., . . . Onida, F. (2010). Novel second mitochondria-derived activator of caspases (Smac) mimetic compounds sensitize human leukemic cell lines to conventional chemotherapeutic drug-induced and death receptor-mediated apoptosis. *Investigational New Drugs*, 1-12. doi: 10.1007/s10637-010-9475-6

Settleman, J. (2009). Cell Culture Modeling of Genotype-Directed Sensitivity to Selective Kinase Inhibitors: Targeting the Anaplastic Lymphoma Kinase (ALK). *Seminars in Oncology, 36*(Supplement 1), S36-S41.

Sharma, S., Straub, C., & Zawel, L. (2006). Development of Peptidomimetics Targeting IAPs. *International Journal of Peptide Research and Therapeutics, 12*(1), 21-32.

Sharma, S. V., Lee, D. Y., Li, B., Quinlan, M. P., Takahashi, F., Maheswaran, S., . . . Settleman, J. (2010). A Chromatin-Mediated Reversible Drug-Tolerant State in Cancer Cell Subpopulations. *Cell, 141*(1), 69-80. doi: 10.1016/j.cell.2010.02.027

Shi, Y. (2004). Caspase activation, inhibition, and reactivation: a mechanistic view. *Protein Sci, 13*(8), 1979-1987. doi: 10.1110/ps.04789804
13/8/1979 [pii]

Siegel, R., Ward, E., Brawley, O., & Jemal, A. (2011). Cancer statistics, 2011. *CA: A Cancer Journal for Clinicians, 61*(4), 212-236. doi: 10.3322/caac.20121

Sieren, J. C., Ohno, Y., Koyama, H., Sugimura, K., & McLennan, G. (2010). Recent technological and application developments in computed tomography and magnetic resonance imaging for improved pulmonary nodule detection and lung cancer staging. *Journal of Magnetic Resonance Imaging, 32*(6), 1353-1369. doi: 10.1002/jmri.22383

Sledz, C. A., Holko, M., de Veer, M. J., Silverman, R. H., & Williams, B. R. G. (2003). Activation of the interferon system by short-interfering RNAs. *Nat Cell Biol, 5*(9), 834-839.

Spurgers, K. B., Gold, D. L., Coombes, K. R., Bohnenstiehl, N. L., Mullins, B., Meyn, R. E., . . . McDonnell, T. J. (2006). Identification of cell cycle regulatory genes as principal targets of p53-mediated transcriptional repression. *J Biol Chem, 281*(35), 25134-25142. doi: M513901200 [pii]
10.1074/jbc.M513901200

Srinivasula, S. M., & Ashwell, J. D. (2008). IAPs: what's in a name? *Molecular Cell, 30*(2), 123-135. doi: S1097-2765(08)00208-6 [pii]
10.1016/j.molcel.2008.03.008

Staquet, M., Rozencweig, M., Duarte-Karim, M., & Kenis, Y. (1977). Pharmacokinetics of adriamycin and adriamycin--DNA complex in L1210 mice and men. *European Journal of Cancer, 13*(4-5), 433-435.

Strano, S., Dell'Orso, S., Di Agostino, S., Fontemaggi, G., Sacchi, A., & Blandino, G. (2007). Mutant p53: an oncogenic transcription factor. *Oncogene, 26*(15), 2212-2219. doi: 1210296 [pii]
10.1038/sj.onc.1210296

Sun, H., Nikolovska-Coleska, Z., Lu, J., Qiu, S., Yang, C. Y., Gao, W., . . . Wang, S. (2006). Design, synthesis, and evaluation of a potent, cell-permeable, conformationally constrained second mitochondria derived activator of caspase (Smac) mimetic. *Journal of Medicinal Chemistry, 49*(26), 7916 - 7920.

Sun, H., Nikolovska-Coleska, Z., Yang, C.-Y., Xu, L., Liu, M., Tomita, Y., . . . Wang, S. (2004). Structure-Based Design of Potent, Conformationally Constrained Smac Mimetics. *Journal of the American Chemical Society, 126*(51), 16686-16687. doi: 10.1021/ja047438+

Sun, H., Nikolovska-Coleska, Z., Yang, C. Y., Xu, L., Liu, M., Tomita, Y., . . . Wang, S. (2004). Structure-based design of potent, conformationally constrained Smac mimetics. *J Am Chem Soc, 126*(51), 16686 - 16687.

Sun, H., Nikolovska-Coleska, Z., Yang, C. Y., Xu, L., Tomita, Y., Krajewski, K., . . . Wang, S. (2004). Structure-based design, synthesis, and evaluation of conformationally constrained mimetics of the second mitochondria-derived

activator of caspase that target the X-linked inhibitor of apoptosis protein/caspase-9 interaction site. *Journal of Medicinal Chemistry, 47*(17), 4147 - 4150.

Sun, Q., Zheng, X., Zhang, L., & Yu, J. Smac Modulates Chemosensitivity in Head and Neck Cancer Cells through the Mitochondrial Apoptotic Pathway. *Clinical Cancer Research*. doi: 10.1158/1078-0432.ccr-10-2262

Sun, S., Schiller, J. H., & Gazdar, A. F. (2007). Lung cancer in never smokers [mdash] a different disease. *Nat Rev Cancer, 7*(10), 778-790.

Suzuki, M., Shigematsu, H., Iizasa, T., Hiroshima, K., Nakatani, Y., Minna, J. D., . . . Fujisawa, T. (2006). Exclusive mutation in epidermal growth factor receptor gene, HER-2, and KRAS, and synchronous methylation of nonsmall cell lung cancer. *Cancer, 106*(10), 2200-2207.

Szegezdi, E., Logue, S. E., Gorman, A. M., & Samali, A. (2006). Mediators of endoplasmic reticulum stress-induced apoptosis. *EMBO Rep, 7*(9), 880-885. doi: 7400779 [pii]

10.1038/sj.embor.7400779

Tam, I. Y. S., Chung, L. P., Suen, W. S., Wang, E., Wong, M. C. M., Ho, K. K., . . . Wong, M. P. (2006). Distinct epidermal growth factor receptor and KRAS mutation patterns in non-small cell lung cancer patients with different tobacco exposure and clinicopathologic features. *Clinical cancer research : an official journal of the American Association for Cancer Research, 12*(5), 1647-1653.

Team, N. L. S. T. R. The National Lung Screening Trial: Overview and Study Design. *Radiology*. doi: 10.1148/radiol.10091808

Ting, A. H., Schuebel, K. E., Herman, J. G., & Baylin, S. B. (2005). Short double-stranded RNA induces transcriptional gene silencing in human cancer cells in the absence of DNA methylation. *Nat Genet, 37*(8), 906-910.

Toyooka, S., Maruyama, R., Toyooka, K. O., McLerran, D., Feng, Z., Fukuyama, Y., . . . Gazdar, A. F. (2003). Smoke exposure, histologic type and geography-related differences in the methylation profiles of non-small cell lung cancer. *International journal of cancer Journal international du cancer, 103*(2), 153-160.

Triano, L. R., Deshpande, H., & Gettinger, S. N. (2010). Management of Patients with Advanced Non-Small Cell Lung Cancer: Current and Emerging Options. *Drugs, 70*(2), 167-179 110.2165/11532200-000000000-000000000.

Van Cruchten, S., & Van den Broeck, W. (2002). Morphological and Biochemical Aspects of Apoptosis, Oncosis and Necrosis. *Anatomia, Histologia, Embryologia, 31*(4), 214-223. doi: 10.1046/j.1439-0264.2002.00398.x

Van Dyke, T. (2007). p53 and tumor suppression. *N Engl J Med, 356*(1), 79-81. doi: 356/1/79 [pii]

10.1056/NEJMcibr066301

Varfolomeev, E., Blankenship, J. W., Wayson, S. M., Fedorova, A. V., Kayagaki, N., Garg, P., . . . Vucic, D. (2007). IAP Antagonists Induce Autoubiquitination of c-IAPs, NF-[kappa]B Activation, and TNF[alpha]-Dependent Apoptosis. *Cell, 131*(4), 669-681.

Vikis, H., Sato, M., James, M., Wang, D., Wang, Y., Wang, M., . . . You, M. (2007). EGFR-T790M is a rare lung cancer susceptibility allele with enhanced kinase activity. *Cancer Research, 67*(10), 4665-4670.

Vince, J. E., Wong, W. W.-L., Khan, N., Feltham, R., Chau, D., Ahmed, A. U., . . . Silke, J. (2007). IAP Antagonists Target cIAP1 to Induce TNF[alpha]-Dependent Apoptosis. *Cell, 131*(4), 682-693.

Wang, C.-Y., Mayo, M. W., Korneluk, R. G., Goeddel, D. V., & Baldwin, A. S., Jr. (1998). NF-B Antiapoptosis: Induction of TRAF1 and TRAF2 and c-IAP1 and c-IAP2 to Suppress Caspase-8 Activation. *Science, 281*(5383), 1680-1683. doi: 10.1126/science.281.5383.1680

Warburg, O. (1956). On the origin of cancer cells. *Science, 123*(3191), 309-314.

Wei, M. C., Zong, W.-X., Cheng, E. H.-Y., Lindsten, T., Panoutsakopoulou, V., Ross, A. J., . . . Korsmeyer, S. J. (2001). Proapoptotic BAX and BAK: A Requisite Gateway to Mitochondrial Dysfunction and Death. *Science, 292*(5517), 727-730. doi: 10.1126/science.1059108

Wei, Y., Fan, T., & Yu, M. (2008). Inhibitor of apoptosis proteins and apoptosis. *Acta Biochim Biophys Sin (Shanghai), 40*(4), 278-288.

Weisz, L., Oren, M., & Rotter, V. (2007). Transcription regulation by mutant p53. *Oncogene, 26*(15), 2202-2211.

Wennerberg, K., Rossman, K. L., & Der, C. J. (2005). The Ras superfamily at a glance. *Journal of Cell Science, 118*(5), 843-846. doi: 10.1242/jcs.01660

Whitehead, K. A., Langer, R., & Anderson, D. G. (2009). Knocking down barriers: advances in siRNA delivery. [10.1038/nrd2742]. *Nat Rev Drug Discov, 8*(2), 129-138.

Whitehurst, A. W., Bodemann, B. O., Cardenas, J., Ferguson, D., Girard, L., Peyton, M., . . . White, M. A. (2007). Synthetic lethal screen identification of chemosensitizer loci in cancer cells. *Nature, 446*(7137), 815-819.

Williams, N. S., Burgett, A. W. G., Atkins, A. S., Wang, X., Harran, P. G., & McKnight, S. L. (2007). Therapeutic anticancer efficacy of a synthetic diazonamide analog in the absence of overt toxicity. *Proceedings of the National Academy of Sciences, 104*(7), 2074-2079. doi: 10.1073/pnas.0611340104

Wu, X., Ye, Y., Rosell, R., Amos, C. I., Stewart, D. J., Hildebrandt, M. A. T., . . . Yang, P. (2011). Genome-wide association study of survival in non-small cell lung cancer patients receiving platinum-based chemotherapy. *Journal of the National Cancer Institute, 103*(10), 817-825.

Yigong, S. (2004). Caspase activation, inhibition, and reactivation: A mechanistic view. *Protein Science, 13*(8), 1979-1987.

Yu, J., & Zhang, L. (2005). The transcriptional targets of p53 in apoptosis control. *Biochemical and Biophysical Research Communications, 331*(3), 851-858. doi: 10.1016/j.bbrc.2005.03.189

Yuan, J. (2006). Divergence from a dedicated cellular suicide mechanism: exploring the evolution of cell death. *Molecular Cell, 23*(1), 1-12. doi: S1097-2765(06)00414-X [pii]

10.1016/j.molcel.2006.06.008

Yuan, J., Shaham, S., Ledoux, S., Ellis, H. M., & Horvitz, H. R. (1993). The C. elegans cell death gene ced-3 encodes a protein similar to mammalian interleukin-1 beta-converting enzyme. *Cell, 75*(4), 641-652. doi: 0092-8674(93)90485-9 [pii]

Zhang, D., Qiu, L., Jin, X., Guo, Z., & Guo, C. (2009). Nuclear factor-kappaB inhibition by parthenolide potentiates the efficacy of Taxol in non-small cell lung cancer in vitro and in vivo. *Mol Cancer Res, 7*(7), 1139-1149. doi: 1541-7786.MCR-08-0410 [pii]

10.1158/1541-7786.MCR-08-0410

Zobel, K., Wang, L., Varfolomeev, E., Franklin, M. C., Elliott, L. O., Wallweber, H. J. A., . . . Deshayes, K. (2006). Design, Synthesis, and Biological Activity of a Potent Smac Mimetic That Sensitizes Cancer Cells to Apoptosis by Antagonizing IAPs. *ACS Chemical Biology, 1*(8), 525-533. doi: 10.1021/cb600276q